SOME PROBLEMS IN LINEAR WATER WAVE THEORY

by

C.M. SMITH

A dissertation submitted for the degree of Doctor of Philosophy in the Department of Applied Mathematics, University of Bristol.

April, 1983.

ACKNOWLEDGEMENTS

I should like to thank Dr. D.V. Evans for his suggestion of the subject matter of this thesis, and for his constant help, guidance and encouragement during its preparation.

I should also like to thank Miss G. Bartlett for the excellent typing of this dissertation, Dr. P. McIver for his valuable assistance in the drawing of the diagrams and the Science and Engineering Research Council for a maintenance grant.

Finally, thanks are due to both my husband, Andrew, and my parents for their forbearance and continual support throughout the course of this work.

MEMORANDUM

The work in this dissertation was carried out in the Department of Mathematics, University of Bristol, and has not been submitted for any other degree or diploma of any examining body. All the work is the original work of the author, except where otherwise acknowledged in the text.

cmsmith

C.M. SMITH

SUMMARY

This thesis is based on the classical linear theory for water waves as described in, for instance, Wehausen and Laitone (1960). Thus the fluid is assumed to be of constant density, inviscid, incompressible and in irrotational motion, and the governing equations and boundary conditions are derived from the linear term in a perturbation expansion in terms of a small, dimensionless parameter (usually taken to be the wave slope).

Over the years numerous linear wave theory problems have been investigated. A brief account of this development is presented in Chapter 1. The theory used to solve such problems, including the effect of surface tension, is given in Chapter 2 where some general relations are also derived. This theory is used in the following chapter to study the small, simple harmonic oscillations of a totally submerged circular cylinder.

In the subsequent chapters the effect of surface tension is taken to be negligible. Chapter 4 examines the scattering of waves by a barrier, fixed in a vertical position in a fluid of finite depth. The forces and moments acting on the barrier are calculated and an approximate solution for a long barrier is found.

The transient motion of a rolling barrier hinged at its submerged end, and of a circular pendulum bob is studied in Chapters 5 and 6 respectively. In both cases the ultimate decaying behaviour is found to be algebraic in time.

Finally, the theory of wave energy absorption by oscillating surface pressure distributions is applied to different configurations in Chapter 7. Two idealized situations of a narrow duct with unequal length sides, and of a pressure patch against a vertical barrier are considered before examining the two-dimensional harbour problem. This consists of a fixed barrier placed in front of the harbour end. In addition to the full solution to this problem, the limiting cases of a shallow barrier and of a narrow duct are also studied and compared to the full solution.

The thesis concludes with a short summary of its contents in Chapter 8.

CONTENTS

CHAPTER 1

INTRODUCTION

An everyday occurrence that is readily observed and familiar to most is the interaction of water waves on obstacles. Usually this behaviour is appreciated in a descriptive way without any technical knowledge. On the other hand the subject has been extensively studied by specialists from several fields, particularly by mathematicians and marine engineers. The theoretical, mathematical approach began over a century ago, although it is only within the last fifty years that there has been a renewed and inspired interest in the subject. To complement this growth many experimental observations have been carried out, usually performed by hydraulic engineers.

It is scarcely surprising that this area of work should receive a good deal of attention for the motion of waves in the presence of some special configuration is of great significance to oceanographers, ship designers and engineers. Unfortunately even the simplest problems have proved too difficult to solve completely, and in order to make any progress assumptions have had to be made both about the property of the fluid and the nature of the generated motion. One theory which results is a linear theory, based on an inviscid, incompressible fluid in irrotational motion when the amplitude of the wave is small compared to its wavelength. This linear theory has been used to solve a wide range of problems within the area of diffraction of waves by bodies, and consequently there is comprehensive literature on the subject. Nevertheless, the topic grew from an examination of the behaviour of waves in the presence of simple,

two-dimensional obstacles.

The configuration that proved to provide the starting block was that of an infinitely long thin barrier, fixed in a vertical position in a fluid of infinite depth with the assumption that gravity was the only restoring force on the free surface. This was solved by Dean (1945) for the case of a barrier extending from the depths of the fluid up to a point beneath the free surface, and by Ursell (1947) for a finite barrier intersecting the free surface. In both cases the incident wave crests were parallel to the barrier.

Ursell (1948) quickly extended his work to consider the forced rolling motion of a barrier in an otherwise still fluid; a behaviour relevant to the rolling of a thin ship. From there, other bodies of regular shape such as the half-immersed and totally submerged cylinder and sphere were examined. Further work then progressed to include more than one body, a fluid with depth, the unsteady motions that arise from an initial disturbance and the effect of surface tension, to name but a few areas. A complete list of all the accomplished extensions would be too lengthy.

Through these investigations it was soon noticeable that the majority of linear wave theory problems do not, in general, possess explicit solutions. Indeed some cases reduced to situations which were too difficult to even contemplate solving. This encouraged certain configurations to be solved in an approximate manner. An example of such a case occurs when the distance between two or more bodies is large compared to the wavelength. It is then permissible to assume that local interaction effects are negligible, and that the only interaction that takes place is due to travelling waves which pass between the bodies. This is known as a wide-spacing approximation and has been used by Newman (1977a) and Srokosz and Evans (1979). On the other hand, if the bodies are close together the corresponding narrow gap approximation of

matched asymptotic expansions can be exploited. This approach requires solving the problem in a neighbourhood of the area of interest and at a large distance from it. The two solutions are then matched in an overlap region where both expressions are valid. A full explanation of this method is found in Tuck (1975). Other, much exploited approximate techniques reduce the problem to an integral equation to which a variational method can be applied.

As before, these approaches were originally investigated on a two-dimensional problem. However, it may be regarded that two-dimensional, or infinitely long body problems are not appropriate to the real world. Nevertheless, they provide a useful stepping-stone to understanding the more complicated, three-dimensional, obstacle-wave interaction since they are more amenable to mathematical analysis. Further, many of the early experimental investigations were performed in narrow tanks where the obstacle spanned the width of the tank. Thus two-dimensional theory was applicable in predicting and confirming these experimental results.

It has already been suggested how two-dimensional "strip" theory can be used to describe the motion of ships. Indeed, a consideration of this and other physical problems such as breakwaters, harbours and docks, and oil-rig platforms, have motivated many of the researched areas. One such field which has recently been rejuvenated is that of wave-energy.

The concept of harnessing the ocean waves to provide an alternative source of energy was first recorded by Stahl (1892). The idea then lay virtually dormant until it was harshly awoken by the rise of the oil crisis and the growing fears that more traditional energy supplies of oil, coal and nuclear fuels were dwindling. This turning point occurred a decade ago, and since then a multitude of wave-absorbing devices have been proposed. The first potential, full-scale device was the Salter Duck.

The fundamental principle on which this device is based is that the incoming waves cause the body to oscillate, generating a motion which can be converted into a useful form of power by some mechanical means. Other devices operating on the same basis include the floating, articulated, Cockerell raft and the submerged Bristol Cylinder.

An alternative mode of operation which underlies the design of another group of devices is an oscillating column of water. In this collection of systems the device is held fixed, allowing the oscillatory wave motion to drive the column of water back and forth. In response to this action, the air flow created above the water column is driven through a turbine, which in turn generates power.

Prior to the wave-energy explosion Masuda had already exploited this idea on a small scale to self-power navigational buoys. Since then large scale devices have been developed, including the C.E.G.B. device which consists of a forward rectangular duct and a rigid rear portion resembling an inverted, drawn-out matchbox. Other devices currently under development include the moored, partly submerged, spherical buoy of Queen's University, Belfast, and the Japanese Kaimei project. This latter device consists of a converted ship housing a number of oscillating water columns in its hull.

Fuller descriptions of most of these devices can be found in Quarrell (1978), together with details of several other promising wave-power absorbers not mentioned here. One device which is not included in this book is the Kværner multiresonant oscillating water column, a novel device invented by the Norwegians. This device incorporates an oscillating column of water within the shelter of two parallel walls extending throughout the depth of the water. The purpose of these protrusions is to increase the efficiency of the system by including additional harbour

resonance effects. Both a theoretical model of this device and a summary of the experimental investigations are given in Ambli et al. (1982).

A review of linear wave-power absorption theory appropriate for studying idealized versions of these devices is given in Evans' (1981) article, "Power from Water Waves". However, before applying this theory to the oscillating water column devices it is first necessary to model the movement of the column of water by enclosing a light piston attached to a linear spring-damper system. This approach makes no allowance for the variation of the trapped free surface and is therefore not a strictly correct way of describing the true problem. Thus a more suitable theory has recently been developed by Evans (1982a) to take account of this effect by modelling the free surface by a uniform pressure distribution. Evans (1982b) has since extended the method for specific application to the multiresonant device.

From this brief resumé of the study of water waves on bodies it is evident that even within the bounds of linear theory the subject covers a wide variety of areas. A selection of some of these topics are presented in the subsequent chapters to illustrate several of the mathematical techniques that can be employed in this field.

Each chapter is aimed to be a complete and self-contained unit, with consistent notation throughout the whole thesis. However, to avoid repeating the basic equations of motion, these are presented in Chapter 2 for a two-dimensional fluid acting under the influence of gravity and surface tension when the usual assumptions of small amplitude linearized wave theory are applied. Also in this chapter, some of the theorems and fundamental definitions, originally derived when surface tension was considered negligible are extended to include this effect. These equations are then applied in Chapter 3 to examine the forced oscillations of a submerged circular cylinder.

The following chapters proceed under the assumption that surface tension is negligible, a condition which is automatically assumed whenever reference is made to Chapters 2 and 3. To be specific, the problems of the next three chapters are described by equations identical to those obtained in the second chapter when the surface tension term is put equal to zero.

Chapter 4 examines the diffraction of waves by a thin barrier, fixed in a vertical position such that it intersects the free surface of a fluid of finite depth. The solution is then applied to obtain the first-order oscillatory and second-order steady forces and moments acting on the barrier. A limiting case of this problem is when the barrier is such that only a small gap remains at the bottom; a situation which is solved using the approximate method of matched asymptotic expansions.

A study of the transient motion of a rolling barrier pivoted at its submerged end point, and of a circular pendulum bob is made in Chapters 5 and 6 respectively. In the former, the motion following an initial disturbance by a force and a displacement is treated, whilst the latter chapter contains only that problem which can be compared to the classical, oscillatory motion of a simple pendulum in air - the initial displacement problem. In conclusion to these transient body problems, a comment is made about the general case of an arbitrary, totally submerged body, surging in a fluid of infinite depth.

Finally, Chapter 7 applies Evans' (1982a) surface pressure distribution theory to three different oscillating water column wave-energy devices. Two of these configurations yield simple, straightforward solutions, whilst a fuller analysis is made of the third. This device is the two-dimensional side view of the Kværner multiresonant oscillating water column, which gives rise to interesting limiting cases. Some of these are studied. To conclude, brief remarks

and comments about the contents of the thesis are summarized in Chapter 8.

The work of Chapter 5 has already appeared in Smith (1982).

CHAPTER 2

SOME GENERAL RELATIONS ALLOWING FOR THE EFFECT OF SURFACE TENSION

2.1 Introduction

"Surface tension acts like a stretched membrane on the surface of a fluid." (Whitham, 1974).

Apparently Kelvin was the first person to introduce the phenomenon of surface tension acting on a fluid into the theory of waves in 1871. Through his research he explained many of the essential features that had previously been discovered through observation by Russell and others. An account of this classical work and also that of Rayleigh, is described in Lamb (1932).

The main modification necessary when surface tension is included is a more complicated free surface condition which involves the third derivative of the velocity potential. Further difficulties arise when an obstacle intersects the free surface, for an additional boundary condition at the intersection is required. The nature of this condition is uncertain, but it is accepted that it involves the angle of contact the free surface makes with the immersed boundary. This concept has been emphasized in Wehausen and Laitone (1960), and Evans (1968 a,b), and will not be discussed here for only submerged bodies are considered.

It can be shown (see for example Lighthill, 1979) that surface tension becomes important for "ripples"; short waves of wavelength less than 0·1 m. Furthermore, when water waves have wavelength less than 4 mm, surface tension is the dominant restoring force. Such waves are

called "capillary waves".

Owing to this very restricted range of influence, the effect of surface tension has usually been neglected in linear wave theory and many of the established results have been derived for waves under the action of gravity alone. Thus Haskind, Newman and others have obtained relationships between various quantities of hydrodynamic interest.

In this introductory chapter the effect of surface tension is allowed for. The equations of motion are presented in §2.2; and in §2.3 and §2.4, the general theorems of Haskind and Newman are extended, together with the definitions of the added mass and damping coefficients. Throughout all this work it can be seen that the well known results, previously derived without surface tension, are readily obtained.

2.2 Equations of motion

Consider the two-dimensional motion of an ideal fluid of constant density ρ under the action of gravity and surface tension. Cartesian co-ordinates (x,y) are chosen such that $y = 0$ is the undisturbed free surface with y measured vertically downwards and x to the right. The fluid occupies the region $0 < y < d$ where d may be either finite or, for the case of very deep fluid, infinity. Under the usual assumptions of linearized inviscid flow the fluid motion is described by a velocity potential $\Phi(x,y,t)$ which satisfies

$$\frac{\partial^2\Phi}{\partial x^2} + \frac{\partial^2\Phi}{\partial y^2} = 0 \qquad \text{in the fluid} \tag{2.1}$$

and

$$\frac{\partial\Phi}{\partial y} = 0 \qquad \text{on } y = d\ . \tag{2.2a}$$

If the fluid is of infinite depth, this condition is modified to

$$\frac{\partial\Phi}{\partial x}\ ,\ \frac{\partial\Phi}{\partial y} \to 0 \qquad \text{as } y \to \infty\ . \tag{2.2b}$$

The linearized equation relating the surface elevation of the free surface $\eta(x,t)$ to the velocity potential is

$$\frac{\partial \eta}{\partial t} = \frac{\partial \Phi}{\partial y} \qquad \text{on} \quad y = 0 \ . \tag{2.3}$$

It is known that the effect of surface tension is to produce a jump in pressure across the free surface which is proportional to the radius of curvature, R_1, of the surface. This can be written as

$$p_1 - p_2 = \frac{T_s}{R_1} \tag{2.4}$$

where the pressure of the fluid p_1 is greater than the atmospheric pressure p_2, and T_s is the coefficient of surface tension, a constant dependent on the fluid and its temperature. An alternative representation for R_1 is

$$\frac{1}{R_1} = \frac{\partial^2 \eta}{\partial x^2} \Big/ \left\{1 + \left(\frac{\partial \eta}{\partial x}\right)^2\right\}^{\frac{1}{2}}$$

which on linearization gives

$$\frac{1}{R_1} = \frac{\partial^2 \eta}{\partial x^2} \ . \tag{2.5}$$

Again using linear theory, the pressure of the fluid just below the free surface is given by Bernoulli's equation as

$$\frac{p_1}{\rho} = g\eta - \frac{\partial \phi}{\partial t} \ . \tag{2.6}$$

Hence, using (2.5), (2.6) and taking $p_2 = 0$, (2.4) becomes

$$g\eta - \frac{\partial \Phi}{\partial t} = \frac{T_s}{\rho} \frac{\partial^2 \eta}{\partial x^2} \ . \tag{2.7}$$

Eliminating η between (2.3) and (2.7) gives the free surface condition

$$\frac{\partial^2\Phi}{\partial t^2} = g\frac{\partial\Phi}{\partial y} - \frac{T_s}{\rho}\frac{\partial^3\Phi}{\partial x^2\partial y} \quad \text{on } y = 0 . \tag{2.8}$$

If the motion is assumed to be steady and simple harmonic in time with frequency ω then

$$\frac{\partial^2\Phi}{\partial t^2} + \omega^2\Phi = 0$$

and it is convenient to introduce a time-independent velocity potential $\phi(x,y)$ such that

$$\Phi(x,y,t) = \text{Re}\{\phi(x,y)e^{-i\omega t}\}. \tag{2.9}$$

Then from equations (2.1), (2.2) and (2.8), $\phi(x,y)$ must satisfy

$$\frac{\partial^2\phi}{\partial x^2} + \frac{\partial^2\phi}{\partial y^2} = 0 \quad \text{in the fluid,} \tag{2.10}$$

$$K\phi + \frac{\partial\phi}{\partial y} + M\frac{\partial^3\phi}{\partial y^3} = 0 \quad \text{on } y = 0 , \tag{2.11}$$

where $$K = \frac{\omega^2}{g} , \quad M = \frac{T_s}{\rho g}$$

and either $$\frac{\partial\phi}{\partial y} = 0 \quad \text{on } y = d \tag{2.12a}$$

or $$\frac{\partial\phi}{\partial x} , \frac{\partial\phi}{\partial y} \to 0 \quad \text{as } y \to \infty . \tag{2.12b}$$

A solution to equation (2.10), satisfying (2.11) and (2.12a) is the incident wave potential from $x = +\infty$,

$$\phi_I(x,y) = -\frac{igA}{\omega}\frac{\cosh\kappa(d-y)}{\cosh\kappa d}e^{-i\kappa x} \tag{2.13}$$

where κ is the real, positive wavenumber with surface tension, satisfying the dispersion relation

$$K = k(1 + Mk^2)\tanh kd. \tag{2.14}$$

This corresponds to a wave elevation

$$\eta = \mathrm{Re}\{Ae^{-i(\kappa x + \omega t)}\} .$$

Similarly, a solution of Laplace's equation satisfying (2.11) and the infinite depth condition (2.12b) is

$$\phi_I(x,y) = -\frac{igA}{\omega} e^{-i\kappa_o x - \kappa_o y} \tag{2.15}$$

corresponding to a wave elevation

$$\eta = \mathrm{Re}\{Ae^{-i(\kappa_o x + \omega t)}\}$$

where κ_o is the real positive root of

$$K = k(1 + Mk^2) . \tag{2.16}$$

A full derivation of these linearized equations with surface tension can be found in Wehausen and Laitone (1960).

The general problem to be considered is that of the behaviour of a body in the fluid. Suppose a totally submerged body of wetted surface S_o is introduced into the fluid and is constrained to make small amplitude oscillations about its equilibrium position in response to an incident wave from $x = +\infty$. As the problem is linear, these oscillations may be expressed as a combination of the independent modes sway, heave and roll, corresponding respectively to the horizontal and vertical displacements of the centre of mass of the body, and the angular displacement about its point of rotation (see Wehausen, 1971). Let

$$\zeta_j(t) = \mathrm{Re}\{\xi_j e^{-i\omega t}\} , \quad j = 1,2,3, \tag{2.17}$$

describe these displacements where j = 1,2 refers to sway and heave motions and j = 3 to roll motions. Then the linearized condition on the equilibrium position of the body, imposed by the condition that the component of the body velocity normal to itself is equal to the normal velocity of the fluid at that point, is

$$\frac{\partial \Phi}{\partial n} = \sum_{j=1}^{3} \dot{\zeta}_j n_j \qquad \text{on } S_o \tag{2.18}$$

where $\frac{\partial}{\partial n}$ denotes differentiation with respect to the normal, $\underline{n} = (n_1, n_2)$ is the unit normal vector directed outwardly from the body and $n_3 = (x - x_s)n_2 - (y - y_s)n_1$, where (x_s, y_s) represents the point about which the body is rotating. In terms of the time-independent quantities, this becomes

$$\frac{\partial \phi}{\partial n} = - i\omega \sum_{j=1}^{3} \xi_j n_j \, . \tag{2.19}$$

The response of the body to the incident wave train is to diffract the wave from the body, scattering it in all directions, and to set the body in motion which in turn generates more outward radiating waves. As linear theory is applicable this reaction can also be described linearly by decomposing the velocity potential into the sum of two parts, Φ_s, Φ_R, representing the scattered and radiated solutions respectively. The scattered problem is one where the body is held fixed in the presence of an incoming wave, and the radiation problem is one where the body is forced to oscillate in the absence of any incident wave train.

Equivalently this may be written in time-independent quantities as

$$\phi = I\phi_s - i\omega \sum_{j=1}^{3} \xi_j \phi_j \tag{2.20}$$

where

$$I = \frac{-igA}{\omega \cosh \kappa d} \quad \text{or} \quad \frac{-igA}{\omega}$$

for a fluid of finite or infinite depth respectively. In this decomposition ϕ_s is the scattered potential in the presence of an incident wave of unit amplitude and the second term is the radiation potential, ϕ_R.

The potentials $\phi_s(x,y)$, $\phi_j(x,y)$ satisfy (2.10), (2.11) and (2.12) with

$$\frac{\partial \phi_s}{\partial n} = 0 \qquad \text{on } S_o \tag{2.21}$$

and

$$\frac{\partial \phi_j}{\partial n} = n_j \qquad \text{on } S_o \, . \tag{2.22}$$

To completely specify both of these problems, the radiation condition that at large distances waves are travelling outwards must be imposed. However before applying this condition to the scattered potential it is first necessary to exclude the incident wave by writing

$$\phi_s = \frac{1}{I} (\phi_I + \phi_D) \tag{2.23}$$

where ϕ_I is defined by (2.13) or (2.15) and $\phi_D(x,y)$ represents outward radiating waves. Then the appropriate radiation conditions for a fluid of finite depth are

$$\phi_s \sim (e^{-i\kappa x} + Re^{i\kappa x}) \cosh \kappa(d-y) \qquad \text{as } x \to \infty, \tag{2.24}$$

$$\phi_s \sim Te^{-i\kappa x} \cosh \kappa(d-y) \qquad \text{as } x \to -\infty, \tag{2.25}$$

$$\phi_R \sim A^{\pm} e^{\pm i\kappa x} \cosh \kappa(d-y) \qquad \text{as } x \to \pm\infty, \tag{2.26}$$

and, for the case of infinite depth,

$$\phi_s \sim (e^{-i\kappa_o x} + Re^{i\kappa_o x}) e^{-\kappa_o y} \qquad \text{as } x \to \infty, \tag{2.27}$$

$$\phi_s \sim Te^{-i\kappa_o x - \kappa_o y} \qquad \text{as } x \to -\infty, \tag{2.28}$$

$$\phi_R \sim A^{\pm} e^{\pm i\kappa_o x - \kappa_o y} \qquad \text{as } x \to \pm\infty. \tag{2.29}$$

Here $|R|$, $|T|$ are respectively the complex reflection and transmission coefficients, and $A^{\pm}$ are complex constants.

2.3 Extension of the Newman relations

In order to derive these relations, Green's second identity for any two harmonic functions ψ_1, ψ_2 in a region bounded by a surface S is required. This gives

$$\int_S \left(\psi_1 \frac{\partial \psi_2}{\partial n} - \psi_2 \frac{\partial \psi_1}{\partial n} \right) dS = 0 , \tag{2.30}$$

and is applied to the functions ϕ_s and $\psi = \phi_R - \overline{\phi}_R$, where a bar denotes complex conjugate. The control surface S is taken to be the closed contour consisting of the free surface, the body surface, the fluid bottom at $y = \infty$ and the two vertical lines at $x = \pm X_o$ where the asymptotic forms are valid. Note that only the case of a totally submerged body in a fluid of infinite depth is treated here.

On the body surface

$$\frac{\partial \psi}{\partial n} = \frac{\partial \phi_R}{\partial n} - \frac{\partial \overline{\phi}_R}{\partial n} = 0, \quad \text{from (2.22) as } n_j \text{ is real.}$$

This result in conjunction with equation (2.21), and equation (2.12b) shows that there is no contribution to the integral in (2.30) from the body surface and the fluid bottom. The only contributions arise from the free surface and the lines at $x = \pm X_o$. By combining equations (2.10), (2.11) and integrating by parts, the contribution from the free surface is

$$\frac{M}{K} \left[\phi_{sxy} \psi_y - \psi_{xy} \phi_{sy} \right]_{x=-\infty}^{x=+\infty} . \tag{2.31}$$

On using the asymptotic forms given in (2.27)-(2.29), this becomes

$$\frac{-2iM\kappa_o^3}{K} \left[A^+ + \overline{A^+} R + \overline{A^-} T \right]$$

Similarly, the contribution from the vertical lines at $x = \pm X_o$ as $X_o \to \infty$ is

$$-i\left[A^+ + \overline{A^+}\, R + \overline{A^-}\, T\right] .$$

Therefore the identity (2.30) yields

$$-\left(i + \frac{i2M\kappa_o^3}{K}\right)\left[A^+ + \overline{A^+}\, R + \overline{A^-}\, T\right] = 0 .$$

Since

$$1 + \frac{2M\kappa_o^3}{K} = \frac{1 + 3M\kappa_o^2}{1 + M\kappa_o^2} > 0 , \quad \text{as} \quad M > 0 ,$$

the usual Newman relation relating the far field amplitudes to the reflection and transmission coefficients,

$$A^+ + \overline{A^+}\, R + \overline{A^-}\, T = 0 \tag{2.32}$$

is again obtained for a totally submerged body in the presence of surface tension.

2.4 Forces on the body

The total first-order hydrodynamic force on the body is given by

$$F = \mathrm{Re}\{Xe^{-i\omega t}\} \tag{2.33}$$

which can be separated into two parts corresponding to the linear decomposition of ϕ by writing

$$F = F_s + F_R \tag{2.34}$$

and

$$X = X_s + X_R \ . \tag{2.35}$$

These forces can be calculated by integrating the pressure over the body surface as follows:

(a) Added mass and damping coefficients

The radiation force in the ξ_k direction is

$$F_R^k = -\int_{S_o} p n_k \, dS$$

$$= \mathrm{Re}\left\{-\rho\omega^2 e^{-i\omega t} \sum_{j=1}^{3} \xi_j \int_{S_o} \phi_j n_k dS\right\}$$

on using Bernoulli's Theorem, (2.9) and (2.20). With equation (2.7) this becomes

$$F_R^k = -\sum_{j=1}^{3} \{a_{kj}\ddot{\zeta}_j + b_{kj}\dot{\zeta}_j\} \tag{2.36}$$

where

$$-\rho\omega^2 \int_{S_o} \phi_j n_k dS = \omega^2 a_{kj} + i\omega b_{kj} \tag{2.37}$$

and a_{kj}, b_{kj} are the added mass and damping coefficients, respectively. From equation (2.36) it is clear that a_{kj} is in phase with the acceleration of the body and describes the apparent increase in inertia of the body due to the fluid, whilst b_{kj} is in phase with the body velocity, providing a measure of the energy radiated away from the body due to its forced oscillation.

(b) Extension of the Haskind relation

The scattered force in the ξ_k direction is similarly defined as

$$F_s^k = \int_{S_o} \rho \frac{\partial \phi_s}{\partial t} n_k \, dS$$

$$= \mathrm{Re}\left\{-i\omega\rho e^{-i\omega t} \int_{S_o} (\phi_I + \phi_D) \frac{\partial \phi_k}{\partial n} dS\right\},$$

by (2.9), (2.20) (2.22) and (2.23). This can be reduced further by applying the relation (2.30) to ϕ_D and ϕ_k. Since both potentials represent

outward travelling waves there is no contribution to the integral from the lines at $x = \pm X_o$ and from the free surface. There is also no contribution from the fluid bottom. Therefore with the aid of (2.21) and (2.23), the identity (2.30) gives

$$\int_{S_o} \left(\phi_k \frac{\partial \phi_D}{\partial n} - \phi_D \frac{\partial \phi_k}{\partial n} \right) dS = - \int_{S_o} \left(\phi_k \frac{\partial \phi_I}{\partial n} + \phi_D \frac{\partial \phi_k}{\partial n} \right) dS = 0 .$$

Hence

$$\begin{aligned} F_s^k &= \mathrm{Re} \left\{ -i\omega\rho e^{-i\omega t} \int_{S_o} \left(\phi_I \frac{\partial \phi_k}{\partial n} - \phi_k \frac{\partial \phi_I}{\partial n} \right) dS \right\} \\ &= \mathrm{Re} \left\{ i\omega\rho e^{-i\omega t} \int_{s=\pm X_o} \left(\phi_I \frac{\partial \phi_k}{\partial n} - \phi_k \frac{\partial \phi_I}{\partial n} \right) dS \right\} , \text{ by (2.30)} \\ &= \mathrm{Re} \left\{ -i\rho g A A^+ e^{-i\omega t} \right\} . \end{aligned} \tag{2.38}$$

That is, the Haskind relation continues to hold when $M \neq 0$, and so the exciting force on the body due to an incident wave is proportional to the far field complex amplitude of the radiation problem in the direction from which the waves are incident.

(c) Relation between the damping coefficient and the far-field radiated amplitudes

Here Green's second identity (2.30) is applied to ϕ_i and $\bar{\phi}_i$, which with the equations (2.11), (2.12b), (2.22) and (2.37) enables the expression

$$b_{ii} = \frac{\rho\omega}{2} \left(\frac{1 + 3M\kappa_o^2}{1 + M\kappa_o^2} \right) (|A_i^+|^2 + |A_i^-|^2) \tag{2.39}$$

to be obtained. This provides an alternative method for evaluating the damping coefficient.

Some of the essential definitions and results of linear theory have now been established for a fluid acting under the influence of gravity and surface tension. In the next chapter they are combined to solve

the radiation problem for a submerged circular cylinder, and in the following three chapters they are used to study problems when the surface tension force is neglected.

CHAPTER 3

THE EFFECT OF SURFACE TENSION ON THE FORCED OSCILLATIONS OF A SUBMERGED CIRCULAR CYLINDER IN DEEP WATER

3.1 Introduction

Several of the well known problems of linear wave theory originally solved without accounting for the presence of surface tension, have been re-investigated to include this effect. In particular Evans (1968 a,b) has examined the reflection of waves by a fixed vertical barrier, either partially immersed or totally submerged in a deep fluid; and the forced waves due to the heaving motion of a half-immersed circular cylinder. Following this Rhodes-Robinson (1970,1971) studied the fundamental singularities of waves with surface tension and extended Havelock's (1929) classical wave-maker theory. He continued by investigating the reflection of waves by a vertical wall and the forced three-dimensional waves in a channel (1974), before developing a reduction method for immersed vertical boundaries in 1979.

In this chapter the effect of surface tension is likewise allowed for to study the forced surface waves due to a submerged circular cylinder. This classical problem was originally solved by Ursell (1950a) by putting Dean's work (1948) of waves passing over a submerged cylinder on a rigorous basis. Ursell developed a form for the solution by placing a series of multipoles of unknown strengths at the centre of the cylinder. These strengths were found to be determined by a well-behaved infinite system of linear simultaneous equations which permitted reasonable calculations to be computed. Ursell (1950b) also supplied a uniqueness proof.

This theory was widely extended by Ogilvie (1963) to treat several specific problems, namely the first-order oscillatory and second-order steady forces for circular cylinders which were either fixed, undergoing forced oscillations, or freely-floating and neutrally bouyant. In the course of his work Ogilvie showed that if the centre of the cylinder moves uniformly in a circle of small radius, the waves produced on the free surface above the cylinder travelled away in one direction only. This result motivated Evans to consider the submerged cylinder as a possible wave energy device, for it follows that by reversing the time co-ordinate, a circular motion of the cylinder exists which completely absorbs an incident wave train. The original two-dimensional theory for this device is explained in Evans et al. (1979), where both experimental and theoretical results are presented. The forced motion of the cylinder is also considered in the appendix, and Ogilvie's results are re-derived.

In this chapter the method of Evans is followed closely. Hence the solution is expressed as a sum of multipole expansions, this choice being justified in §3.6. The problem is formulated in §3.2 and solved in §3.4 using the singularity expressions obtained in §3.3. Dean's result that an incident wave is totally transmitted is recovered in §3.5, where it is also seen that the submerged cylinder continues to be an attractive wave-energy device when the presence of surface tension is included. Results for the added mass and damping coefficients, and for the amplitude and phase of the heaving motion are presented in §3.7, with final conclusions being made in §3.8.

3.2 Formulation of the problem

A circular cylinder of radius a is located under the free surface of an infinitely deep fluid with its centre at $(0,h)$, $h > a$. In the absence of an incident wave the cylinder is forced to make small, simple harmonic

horizontal and vertical oscillations of frequency ω about its equilibrium position with a displacement described by equation (2.17). Since the cylinder is symmetric, this motion can be represented by a linear combination of heave and surge motions. Thus in the notation of the preceding chapter, j = 1 and 2 only.

Under the usual assumptions of linear theory the velocity potential of the fluid, Φ satisfies equations (2.1), (2.2b), (2.8) and (2.18). It is further assumed that the sinusoidal motion of the cylinder generates waves of the same frequency, and so Φ can be written in terms of the time-independent velocity potential given by (2.20) with $\phi_s = 0$ as

$$\phi(x,y) = - i\omega \sum_{j=1}^{2} \xi_j \phi_j(x,y) \quad . \tag{3.1}$$

ϕ has been separated into asymmetric (ϕ_1) and symmetric (ϕ_2) potentials where each ϕ_j satisfies Laplace's equation (2.10), the free surface condition with surface tension (2.11) and, from (2.22)

$$\frac{\partial \phi_j}{\partial n} = n_j \qquad \text{on} \quad r = a. \tag{3.2}$$

Here co-ordinates defined by $x = r\sin\theta$, $y - h = r\cos\theta$ have been introduced such that $r^2 = x^2 + (y-h)^2$. Note that for a circular cylinder $n_1 = \sin\theta$ and $n_2 = \cos\theta$. It is also assumed that the radiation condition representing outward travelling waves is given by

$$\phi_j \sim A_j^{\pm} e^{\pm i\kappa_o x - \kappa_o y} \qquad \text{as} \quad x \to \pm\infty \tag{3.3}$$

where κ_o satisfies the dispersion relation (2.16). By symmetry

$$A_1^+ = - A_1^- \qquad \text{and} \qquad A_2^+ = A_2^- \quad . \tag{3.4}$$

The potentials ϕ_1 and ϕ_2 satisfying the conditions stated above are required. If the fluid extended to infinity in all directions a solution

would be sought in terms of the basic singular potentials, log r, $r^{-n}\cos n\theta$, $r^{-n}\sin n\theta$ $(n = 1,2,\ldots)$. However the presence of the free surface suggests that these basic singular potentials need to be modified to satisfy the free surface condition. That is, the appropriate multipole expansions are needed.

3.3 Multipole expansions

We require the two-dimensional motions produced by line singularities which may be asymmetric (horizontal) and symmetric (vertical) multipoles. In each case the singularity can be described by a complex-valued harmonic potential function ϕ_{1n}, ϕ_{2n} respectively, in which the time dependence is suppressed in the usual way. These potentials satisfy Laplace's equation (2.10) in the fluid except at the singularity, the free surface boundary condition (2.11) and $\nabla\phi \to 0$ as $y \to \infty$. Also imposed are the conditions that ϕ behaves like a typical singular harmonic function near the singularity, and represents outgoing waves in the far field. This last condition ensures uniqueness.

Firstly, consider the asymmetric potential by writing

$$\phi_{1n} = \frac{\sin n\theta}{r^n} + \int_0^\infty a(k)e^{-ky}\sin kx\, dk + Ce^{-\kappa_0 y}\sin \kappa_0 x \qquad (3.5)$$

where the last two terms are odd in x and a(k),C are to be determined from the free surface condition and the behaviour for large $|x|$ respectively. Using the representation

$$\frac{\sin n\theta}{r^n} = \frac{(-1)^{n-1}}{(n-1)!}\int_0^\infty k^{n-1}e^{-k(h-y)}\sin kx\, dk \text{ , valid for } h > y \text{ ,} \qquad (3.6)$$

the free surface condition gives

$$a(k) = \frac{(-1)^{n-1}}{(n-1)!}\, k^{n-1}\, \frac{[k(1+Mk^2)+K]}{k(1+Mk^2)-K}\, e^{-kh} \text{ .} \qquad (3.7)$$

Therefore

$$\phi_{in} = \frac{\sin n\theta}{r^n} + \frac{(-1)^{n-1}}{(n-1)!}\int_0^\infty k^{n-1}\,\frac{[k(1+Mk^2)+K]}{k(1+Mk^2)-K}\,e^{-k(y+h)}\sin kx\,dk + Ce^{-\kappa_o y}\sin\kappa_o x \tag{3.8}$$

where the Cauchy principal value of the integral is assumed. This integral can be written as

$$\mathrm{Im}\int_0^\infty k^{n-1}\,\frac{[k(1+Mk^2)+K]}{k(1+Mk^2)-K}\,e^{-k(y+h)+ikx}\,dk$$

$$= \mathrm{Im}\left\{\int_0^\infty i^n k^n\,\frac{[ik(1-Mk^2)+K]}{ik(1-Mk^2)-K}\,e^{-ik(y+h)-kx}\,dk\right\} + 2\pi\cos\kappa_o x\;\kappa_o^n\,\frac{(1+M\kappa_o^2)}{1+3M\kappa_o^2}\,e^{-\kappa_o(y+h)}$$

for $x > 0$, where the path of integration has been rotated through 90°.

Thus

$$\phi_{1n} \sim \frac{(-1)^{n-1}}{(n-1)!}\,2\pi\,\kappa_o^n\,\frac{(1+M\kappa_o^2)}{1+3M\kappa_o^2}\,e^{-\kappa_o(y+h)+i\kappa_o x} \qquad \text{as } x\to\infty$$

if

$$C = \frac{(-1)^{n-1}}{(n-1)!}\,2\pi i\kappa_o^n\,\frac{(1+M\kappa_o^2)}{1+3M\kappa_o^2}\,e^{-\kappa_o h} \quad . \tag{3.9}$$

Hence

$$\phi_{1n} = \frac{\sin n\theta}{r^n} + \frac{(-1)^{n-1}}{(n-1)!}\int_0^\infty k^{n-1}\,\frac{[k(1+Mk^2)+K]}{k(1+Mk^2)-K}\,e^{-k(y+h)}\sin kx\,dk + \frac{(-1)^{n-1}}{(n-1)!}\,2\pi i\kappa_o^n\,\frac{(1+M\kappa_o^2)}{1+3M\kappa_o^2}\,e^{-\kappa_o(y+h)}\sin\kappa_o x \tag{3.10}$$

and

$$\phi_{1n} \sim \mathrm{sgn}x\,\frac{(-1)^{n-1}}{(n-1)!}\,2\pi\kappa_o^n\,\frac{(1+M\kappa_o^2)}{1+3M\kappa_o^2}\,e^{-\kappa_o(y+h)+i\kappa_o|x|} \qquad \text{as } |x|\to\infty\,, \tag{3.11}$$

Similarly the even multipole potentials can be written as

$$\phi_{2n} = \frac{\cos n\theta}{r^n} + \frac{(-1)^n}{(n-1)!}\int_0^\infty k^{n-1}\,\frac{[k(1+Mk^2)+K]}{k(1+Mk^2)-K}\,e^{-k(y+h)}\cos kx\,dk$$

$$+ \frac{(-1)^n}{(n-1)!}\,2\pi i\kappa_o^n\,\frac{(1+M\kappa_o^2)}{1+3M\kappa_o^2}\,e^{-\kappa_o(y+h)}\cos\kappa_o x \qquad (3.12)$$

$$\sim \frac{(-1)^n}{(n-1)!}\,2\pi i\kappa_o^n\,\frac{(1+M\kappa_o^2)}{1+3M\kappa_o^2}\,e^{-\kappa_o(y+h)+i\kappa_o|x|} \qquad \text{as } |x|\to\infty\,. \qquad (3.13)$$

These derivations are essentially those of Rhodes-Robinson (1970).

Using

$$e^{-ky-ikx} = e^{-kre^{i\theta}-kh} = e^{-kh}\sum_{m=o}^{\infty}\frac{(-1)^m r^m k^m e^{mi\theta}}{m!}\,, \qquad (3.14)$$

which is valid for $0 < r < 2h$, these potentials can be expanded as

$$\phi_{1n} = \frac{\sin n\theta}{r^n} + \sum_{m=o}^{\infty} B_{mn}\,r^m \sin m\theta\,, \qquad (3.15)$$

$$\phi_{2n} = \frac{\cos n\theta}{r^n} + \sum_{m=o}^{\infty} B_{mn}\,r^m \cos m\theta\,, \qquad (3.16)$$

where

$$B_{mn} = \frac{(-1)^{m+n-1}}{(n-1)!m!}\left\{\int_0^\infty k^{m+n-1}\,\frac{[k(1+Mk^2)+K]}{K-k(1+Mk^2)}\,e^{-2kh}\,dk - 2\pi i\kappa_o^{m+n}\,\frac{(1+M\kappa_o^2)}{1+3M\kappa_o^2}\,e^{-2\kappa_o h}\right\}. \qquad (3.17)$$

By employing (2.16), this integral can be re-written as

$$\kappa_o^{m+n}\int_0^\infty t^{m+n-1}\,\frac{[1+t+M\kappa_o^2(1+t^3)]}{1-t+M\kappa_o^2(1-t^3)}\,e^{-2\kappa_o th}\,dt$$

$$= \kappa_o^{m+n}\int_0^\infty t^{m+n-1}\left[1+\frac{2t(1+M\kappa_o^2t^2)}{1-t+M\kappa_o^2(1-t^3)}\right]e^{-2\kappa_o th}\,dt\,.$$

Hence, using Gradshteyn and Ryzhik (1980), equation (3.351.3),

$$B_{mn} = (-1)^{m+n-1}\kappa_o^{m+n}\,\frac{(m+n)!}{(n-1)!m!}\,[a_{m+n}-ib_{m+n}] \qquad (3.18)$$

where, for $n > 1$,

$$a_n = \frac{2}{n!}\int_0^\infty \frac{(1+M\kappa_o^2t^2)t^n e^{-2\kappa_o th}}{[1-t+M\kappa_o^2(1-t^3)]}\,dt + \frac{1}{n(2\kappa_o h)^n} \qquad (3.19)$$

and

$$b_n = \frac{2\pi}{n!}\,e^{-2\kappa_o h}\,\frac{(1+M\kappa_o^2)}{1+3M\kappa_o^2} \quad . \qquad (3.20)$$

An alternative approach

These multipole expansions can also be obtained by considering the time-independent complex potential

$$w(z) = \phi(x,y) + j\psi(x,y)$$

for a submerged pulsating source. Here $z = x + jy$ where $j = \sqrt{-1}$, and it is important to remember that

$$\phi(x,y) = \mathrm{Re}_j\{w(z)\}$$

whilst

$$\Phi(x,y,t) = \mathrm{Re}_i\{\phi(x,y)e^{-i\omega t}\} \quad .$$

In a manner analogous to the above it can be shown that

$$w = \log\frac{z-jh}{z+jh} + 2\int_0^\infty \frac{(1+Mk^2)e^{jk(z+jh)}}{K-k(1+Mk^2)}\,dk - 2\pi i\,\frac{(1+M\kappa_o^2)}{1+3M\kappa_o^2}\,e^{j\kappa_o(z+jh)} \quad . \qquad (3.21)$$

Following Ursell (1950a), this can be written as

$$w = \log\kappa_o(z-jh) + G[\kappa_o(h-jz)] \qquad (3.22)$$

where $G[\kappa_o(h-jz)]$ is regular in the region $x > 0$, $y > 0$. For any $h' < h$, $G[\kappa_o(h-jz)]$ is bounded in the region $x > 0$, $y > -h'$; and since $G[\kappa_o(h-jz)]$ is real on the imaginary axis it may be continued by reflection over the whole region $y > -h$. It is therefore bounded in $y > -h' > -h$.

Near $z = jh$ the integral in (3.21) can be written as

$$\int_o^\infty \frac{(1+Mk^2)e^{jk(z-jh)-2kh}}{K-k(1+Mk^2)}\,dk = \int_o^\infty \frac{(1+M\kappa_o^2t^2)}{1-t+M\kappa_o^2(1-t^3)}\,e^{j\kappa_o t(z-jh)-2\kappa_o th}\,dt$$

$$= \int_o^\infty \frac{(1+M\kappa_o^2t^2)e^{-2\kappa_o th}}{1-t+M\kappa_o^2(1-t^3)} \sum_{m=o}^{\infty} \frac{[j\kappa_o t(z-jh)]^m}{m!}\,dt\ ,$$

whilst

$$\log \kappa_o(z+jh) = \log\,(2\kappa_o hj) - \sum_{m=1}^{\infty} \frac{[j\kappa_o(z-jh)]^m}{m\,(2\kappa_o h)^m}\ .$$

Thus near $z = jh$,

$$w = \log \kappa_o(z-jh) + \sum_{m=o}^{\infty} (a_m - ib_m)[j\kappa_o(z-jh)]^m \qquad (3.23)$$

where a_m, b_m are as in (3.19) and (3.20) for $m \geq 1$, with

$$a_o = 2\int_o^\infty \frac{(1+M\kappa_o^2t^2)e^{-2\kappa_o th}}{1-t+M\kappa_o^2(1-t^3)}\,dt - \log(2\kappa_o hj)\ ,$$

and

$$b_o = 2\pi e^{-2\kappa_o h}\,\frac{(1+M\kappa_o^2)}{1+3M\kappa_o^2}\ .$$

From (3.23) it is possible to derive by differentiation poles of any assigned order at $z = jh$. The differentiation is simplified by noting that

$$\frac{\partial G}{\partial h} = j\frac{\partial G}{\partial z}\ .$$

Consider the symmetric oscillations first. Then

$$\phi_{2n} + j\psi_{2n} = \frac{(-1)}{(n-1)!}\left(\frac{\partial w}{\partial h}\right)^n$$

$$= \frac{(-1)^n}{[j(z-jh)]^n} + \kappa_o^n \sum_{m=n}^{\infty} \frac{(-1)^{n-1}\,m!}{(m-n)!(n-1)!}\,(a_m - ib_m)[j\kappa_o(z-jh)]^{m-n}$$

yielding

$$\phi_{2n} = \frac{\cos n\theta}{r^n} + \sum_{m=0}^{\infty} (-1)^{m+n-1} \frac{(m+n)!}{m!(n-1)!} (a_{m+n} - ib_{m+n}) r^m \cos m\theta \kappa_o^{m+n} ,$$

in agreement with (3.16).

Similarly for the asymmetric multipoles,

$$\phi_{1n} + j\psi_{1n} = \frac{1}{(n-1)!} \frac{\partial}{\partial z} \left(\frac{\partial w}{\partial h}\right)^{n-1}$$

$$= \frac{j(-1)^{n+1}}{[j(z-jh)]^n} + (-1)^{n+1} j\kappa_o^n \sum_{m=n}^{\infty} (a_m - ib_m) [j\kappa_o (z-jh)]^{m-n} \frac{m!}{(m-n)!(n-1)!}$$

giving

$$\phi_{1n} = \frac{\sin n\theta}{r^n} + \sum_{m=0}^{\infty} (-1)^{m+n-1} \frac{(m+n)!}{m!(n-1)!} (a_{m+n} - ib_{m+n}) r^m \sin m\theta \kappa_o^{m+n}$$

as in (3.15).

3.4 Solution for $\phi_i(x,y)$

We can now proceed to determine $\phi_i(x,y)$. From the boundary condition on the cylinder (3.2), it is clear that ϕ_i need only be expressed as a sum of multipoles for ϕ_{in}. Thus a solution for ϕ_i is posed as the sum of multipole potentials with unknown strengths p_{in}, in the form

$$\phi_i = \sum_{n=1}^{\infty} \frac{a^{n+1}}{n} p_{in} \phi_{in}(x,y) . \qquad (3.24)$$

Since each of the functions ϕ_{in} satisfies Laplace's equation, the free surface condition and represents outgoing waves at infinity, it remains to satisfy the condition on the cylinder and so determine the unknown constants.

Applying this condition (3.2) to ϕ_1 implies

$$\left.\frac{\partial \phi_1}{\partial r}\right|_{r=a} = \sin\theta = -\sum_{n=1}^{\infty} p_{1n}\left\{ \sin n\theta - \sum_{m=1}^{\infty} \frac{m}{n}\, a^{m+n} B_{mn} \sin m\theta \right\}$$

which gives on equating the coefficients of $\sin m\theta$, $m=1,2,\ldots$, the infinite system of equations

$$p_{1m} - \sum_{n=1}^{\infty} \frac{m}{n}\, a^{m+n} B_{mn} p_{1n} = -\delta_{1m} \,. \tag{3.25}$$

An identical system for p_{2m} is also obtained by applying condition (3.2) to $\phi_2(x,y)$. It therefore follows that if equation (3.25) has a solution, $p_{1m} = p_{2m} = p_m$, say $(m=1,2,\ldots)$.

Equations of this type were also obtained by Ursell (1950a), Evans (1968b), Srokosz (1979) and Thomas (1981a), and have been studied by H. von Koch. He showed that the more general system

$$\mu_n = k_n + \sum_{m=1}^{\infty} C_{mn} k_m$$

could be solved by infinite determinants under the conditions

$$\sum_{n=1}^{\infty} |\mu_n| < \infty \quad \text{and} \quad \sum_{m=1}^{\infty} \sum_{n=1}^{\infty} |C_{mn}| < \infty \quad ;$$

provided that the determinant of the system does not vanish.

Clearly

$$\sum_{n} |\delta_{1n}| = 1 < \infty \,,$$

and from (3.18)

$$\left| \frac{m}{n}\, a^{m+n} B_{mn} \right| = \left| (\kappa_o a)^{m+n} \frac{(m+n)!}{n!\,(m-1)!} \left(a_{m+n} - i b_{m+n}\right) \right| \,. \tag{3.26}$$

Since equation (3.23) is valid near $z = ih$, a number h' can be taken such that $a < h' < h$. Then, when $|z-ih| = 2h'$, the series (3.23)

converges so that

$$|a_n|(2\kappa_o h')^n < M_1(\kappa_o h') \quad ,$$

$$|b_n|(2\kappa_o h')^n < M_2(\kappa_o h') \quad ,$$

and therefore from (3.26)

$$\left|\frac{m}{n}\, a^{m+n} B_{mn}\right| < \frac{M_3(\kappa_o h')}{(2\kappa_o h')^{m+n}} (\kappa_o a)^{m+n} \frac{(m+n)!}{n!(m-1)!}$$

where M_1, M_2 and M_3 depend only on $\kappa_o h'$. Thus

$$\sum_{m=1}^{\infty} \sum_{n=1}^{\infty} \left|\frac{m}{n}\, a^{m+n} B_{mn}\right| < M_3(\kappa_o h') \sum_{m=1}^{\infty} \sum_{n=1}^{\infty} \frac{(m+n)!}{n!(m-1)!} \left(\frac{a}{2h'}\right)^{m+n}$$

$$= M_3(\kappa_o h') \sum_{n=1}^{\infty} n! \left(\frac{a}{2h'}\right)^n \sum_{m=o}^{n-1} \frac{1}{m!(n-m-1)!}$$

$$= M_3(\kappa_o h') \sum_{n=1}^{\infty} n! \left(\frac{a}{2h'}\right)^n \frac{2^{n-1}}{(n-1)!}$$

$$= \frac{M_3(\kappa_o h')}{2} \sum_{n=1}^{\infty} n \left(\frac{a}{h'}\right)^n$$

$$< \infty \quad \text{since} \quad a < h' \ .$$

Hence provided the infinite determinant of the system does not vanish, which is equivalent to assuming that the system

$$p_m - \sum_{n=1}^{\infty} \frac{m}{n}\, a^{m+n} B_{mn} p_n = 0 \qquad (3.27)$$

possesses the trivial solution $p_n = 0$, equation (3.25) has a unique solution p_n such that $\sum_{n=1}^{\infty} |p_n| < \infty$.

Once these constants have been determined, the full solution for $\phi_i(x,y)$ is known. However in its present form the complex system of

simultaneous equations (3.25) is not convenient for computation. It can be reduced to two real systems, suitable for numerical evaluation by writing

$$\frac{(-1)^m(\kappa_o a)^m p_m}{m} = q_m - ir_m \ . \tag{3.28}$$

Using this in (3.25) with (3.17), and equating real and imaginary parts gives

$$q_m + \sum_{n=1}^{\infty} \beta_{mn} q_n = - \frac{(-1)^m(\kappa_o a)^m}{m} \delta_{1m} + \frac{(\kappa_o a)^{2m}}{m!} S_r \tag{3.29}$$

$$r_m + \sum_{n=1}^{\infty} \beta_{mn} r_n = - \frac{(\kappa_o a)^{2m}}{m!} S_q \tag{3.30}$$

where

$$S_x = 2\pi e^{-2\kappa_o h} \frac{(1+M\kappa_o^2)}{1+3M\kappa_o^2} \sum_{n=1}^{\infty} \frac{x_n}{(n-1)!} \tag{3.31}$$

and

$$\beta_{mn} = - \frac{\kappa_o^{m-n} a^{2m}}{(n-1)!m!} \int_0^{\infty} k^{m+n-1} \frac{[k(1+Mk^2)+K]}{k(1+Mk^2)-K} e^{-2kh} \, dk \ . \tag{3.32}$$

As in Ursell (1950a), let ε_n, γ_n satisfy

$$\varepsilon_m + \sum_{n=1}^{\infty} \beta_{mn} \varepsilon_n = \frac{(\kappa_o a)^{2m}}{m!} \tag{3.33}$$

$$\gamma_m + \sum_{n=1}^{\infty} \beta_{mn} \gamma_n = \delta_{1m} \ . \tag{3.34}$$

Then after some algebra,

$$q_n = \kappa_o a \gamma_n + \varepsilon_n S_r \tag{3.35}$$

$$r_n = - S_q \varepsilon_m \tag{3.36}$$

$$S_q = \frac{\kappa_o a \, S_\gamma}{1+S_\varepsilon^2} \tag{3.37}$$

and $$S_r = -\kappa_o a \frac{S_\gamma S_\varepsilon}{1+S_\varepsilon^2} \quad . \tag{3.38}$$

Hence it can be seen that the solution for q_m and r_m, and therefore for the complex constants p_m, is given in terms of the real infinite systems (3.33) and (3.34), which are readily solved on a computer by a standard numerical procedure after truncating each system to a finite number of terms. This method of solution is discussed in §3.7.

For computational purposes it is also convenient to re-write β_{mn}. Rhodes-Robinson (1971) has proved that the dispersion relation (2.16) has one real root κ_o say, and two complex roots κ_1, κ_2 lying in the second and third quadrants respectively, such that $\kappa_2 = \overline{\kappa_1}$. Therefore the integrand in equation (3.32) can be split into partial fractions, and by using integrals such as

$$\int_o^\infty \frac{x^n}{x+\beta} e^{-\mu x}\, dx = (-1)^{n-1} \beta^n e^{\beta\mu} Ei(\beta\mu) + \sum_{k=1}^{n} \frac{(k-1)!}{\mu^k} (-\beta)^{n-k} ,$$

[Gradshteyn and Rhyzik, equation (3.353.5)], β_{mn} reduces to

$$\beta_{mn} = \frac{(\kappa_o a)^{2m}}{(n-1)!m!} \left\{ -\frac{(m+n-1)!}{(2\kappa_o h)^{m+n}} + 2\frac{(1+M\kappa_o^2)}{1+3M\kappa_o^2} \left[e^{-2\kappa_o h} Ei(2\kappa_o h) - \sum_{k=o}^{m+n-2} \frac{k!}{(2\kappa_o h)^{k+1}} \right.\right.$$

$$\left.\left. + 2Re\left(\kappa_1'^{m+n-1} \frac{(\kappa_1'+2)}{\kappa_1'-\kappa_2'} \left[-e^{-2\kappa_1 h} Ei(2\kappa_1 h) + \sum_{k=o}^{m+n-2} \frac{k!}{(2\kappa_1 h)^{k+1}} \right] \right) \right] \right\} \tag{3.39}$$

where

$$\kappa_1 = \kappa_o \kappa_1' \quad \text{and} \quad \kappa_2 = \kappa_o \kappa_2' .$$

This alternative expression for β_{mn} enables the limit as $M \to 0$ to be examined. From the properties of the roots of a quadratic equation, it can be shown that

$$\kappa_1 + \overline{\kappa_1} = -\kappa_o \quad \text{and} \quad \kappa_1\overline{\kappa_1} = \frac{1+M\kappa_o^2}{M} ,$$

which combine to yield

$$\kappa_1 = \frac{-\kappa_o}{2} + \frac{i}{2}\sqrt{\frac{4+3M\kappa_o^2}{M}} \quad .$$

Also, the exponential integral functions of real and complex arguments can be expanded as

$$Ei(2\kappa_o h) = \ell n(2\kappa_o h) + \gamma + \sum_{n=1}^{\infty} \frac{(2\kappa_o h)^n}{n.n!} \tag{3.40}$$

and

$$Ei(2\kappa_1 h) = \ell n(-2\kappa_1 h) + \gamma + \sum_{n=1}^{\infty} \frac{(2\kappa_1 h)^n}{n.n!} \tag{3.41}$$

respectively, where γ is Euler's constant. Therefore for small M,

$$\beta_{mn} = \frac{(\kappa_o a)^{2m}}{(n-1)!m!} \left\{ - \frac{(m+n-1)!}{(2\kappa_o h)^{m+n}} + 2\left[e^{-2\kappa_o h} Ei(2\kappa_o h) - \sum_{k=o}^{m+n-2} \frac{k!}{(2\kappa_o h)^{k+1}} \right] \right\} + O\left(\log \frac{1}{M}\right) \tag{3.42}$$

where the first term is identical to that obtained by putting M = 0 in the original expression (3.39).

Note on uniqueness. It remains to show that the homogeneous infinite system (3.27) has only the trivial solution and therefore that the solution for ϕ is unique. A sufficient condition for this to be true is

$$\sum_{m=1}^{\infty} \sum_{n=1}^{\infty} \left| \frac{m}{n} a^{m+n} B_{mn} \right| = \rho < 1 \quad .$$

In this way Ursell (1950b) has given a proof for the corresponding problem when surface tension is neglected, by considering the complex potential for large $|z|$, applying a conformal transformation and constructing a third-order homogeneous difference equation. Following this method to include the effect of surface tension leads to a seventh-order difference equation which is more difficult to solve and has not

been done.

3.5 Applications

(a) Far-field behaviour

From equations (3.11), (3.13) and (3.24) the far-field radiated behaviour for ϕ_i is given for $|x| \to \infty$ by

$$\phi_1(x,y) \sim -2\pi a \, \mathrm{sgn}x \, \frac{(1+M\kappa_o^2)}{1+3M\kappa_o^2} \sum_{n=1}^{\infty} \frac{(-1)^n(\kappa_o a)^n p_n}{n!} e^{-\kappa_o(y+h)+i\kappa_o|x|}$$

and

$$\phi_2(x,y) \sim 2\pi i a \, \frac{(1+M\kappa_o^2)}{1+3M\kappa_o^2} \sum_{n=1}^{\infty} \frac{(-1)^n(\kappa_o a)^n p_n}{n!} e^{-\kappa_o(y+h)+i\kappa_o|x|} \, .$$

Comparing these with equation (3.3) gives

$$A_1^+ = -ae^{\kappa_o h} S \tag{3.43}$$

and

$$A_2^+ = iae^{\kappa_o h} S \tag{3.44}$$

where

$$S = 2\pi \, \frac{(1+M\kappa_o^2)}{1+3M\kappa_o^2} \, e^{-2\kappa_o h} \sum_{n=1}^{\infty} \frac{(-1)^n(\kappa_o a)^n p_n}{n!}$$

$$= S_q - iS_r \qquad \text{(by (3.28) and (3.31))}. \tag{3.45}$$

Therefore

$$A_1^+ = iA_2^+ \, , \tag{3.46}$$

indicating that the waves radiated away from the cylinder due to horizontal and vertical oscillations are equal in amplitude and 90° out of phase with each other.

Now, from equations (2.9) and (3.1)

$$\Phi(x,y,t) = \mathrm{Re}\{-i\omega \sum_{j=1}^{2} \phi_j \xi_j \, e^{-i\omega t}\} \quad ,$$

and using (3.3), (3.4), and (3.46), it follows that

$$\begin{aligned} \Phi(x,y,t) &\sim \mathrm{Re}\{-i\omega(\xi_1 A_1^{\pm} + \xi_2 A_2^{\pm})e^{-i\omega t}\} \quad \text{as } x \to \pm\infty \\ &= \mathrm{Re}\{-i\omega A_1^{+}(\pm\xi_1 - i\xi_2)e^{-i\omega t}\} \quad \text{by (3.46)} \; . \end{aligned} \tag{3.47}$$

Suppose that the centre of the cylinder describes a circle of radius δ in a clockwise direction. Then $\zeta_1 = \delta\cos\omega t$ and $\zeta_2 = \delta\sin\omega t$ so that $\xi_1 = \delta$, $\xi_2 = i\delta$ and from equation (3.47),

$$\Phi(x,y,t) \to \mathrm{Re}\{-2i\omega A_1^{+}\delta e^{-i\omega t}\} \quad \text{as } x \to \infty$$

and

$$\Phi(x,y,t) \to 0 \quad \text{as } x \to -\infty \quad ,$$

showing that waves are radiated away from the cylinder on one side only. Similarly, if the cylinder rotates in an anticlockwise direction ($\xi_1 = \delta$, $\xi_2 = -i\delta$) waves are radiated to $x = -\infty$ only. This is the same result as derived by Ogilvie for the case when $M = 0$.

(b) Transmission of an incident wave

Dean (1948) discovered that when $M = 0$, an incident wave passing over a fixed submerged circular cylinder undergoes no reflection, only a phase shift. By making use of the Newman relations (2.32),

$$A_i^{+} + A_i^{+}R + A_i^{-}T = 0 \; , \qquad i = 1,2 \; . \tag{3.48}$$

similar results can be obtained for the case when $M \neq 0$. For from the symmetry relations (3.4), equation (3.48) becomes

$$R + T = -\frac{A_1^{+}}{\overline{A_1^{+}}} \; , \qquad R - T = -\frac{A_2^{+}}{\overline{A_2^{+}}}$$

and by (3.44), (3.46)

$$R = 0$$

$$T = \frac{-S}{\bar{S}} \quad \text{giving } |T| = 1 \quad .$$

S is defined by (3.45), and substituting for S_q, S_r by equations (3.37) and (3.38),

$$S = \kappa_o a \, S_\gamma \, \frac{(1+iS_\varepsilon)}{1+S_\varepsilon^2} \quad .$$

Hence

$$T = - \frac{(1+iS_\varepsilon)}{1-iS_\varepsilon}$$

$$= -e^{i\psi_1}$$

where

$$\psi_1 = \tan^{-1} \frac{2S_\varepsilon}{1-S_\varepsilon^2} \tag{3.49}$$

is the transmission phase shift. Thus the results of Dean are again obtained when the presence of surface tension is accounted for.

(c) Added mass and damping coefficients

From equation (2.37) the added mass and damping coefficients are given by

$$\omega^2 a_{jk} + i\omega b_{jk} = -\rho\omega^2 \int_{S_o} \phi_k \frac{\partial \phi_j}{\partial n} \, dS \, , \qquad j,k = 1,2$$

where a_{jk}, $b_{jk} = 0$ for $j \neq k$ by symmetry. Using (3.24) with (3.15) and (3.25) gives

$$\phi_1(x,y) = \sum_{n=1}^{\infty} \frac{a^{n+1} p_n}{n} \left\{ \frac{\sin n\theta}{r^n} + \sum_{m=o}^{\infty} B_{mn} r^m \sin m\theta \right\}$$

$$= \sum_{n=1}^{\infty} \frac{a p_n}{n} \sin n\theta \left\{ \left(\frac{a}{r}\right)^n + \left(\frac{r}{a}\right)^n \right\} + r\sin\theta \, .$$

Therefore

$$\omega^2 a_{11} + i\omega b_{11} = -\rho\omega^2 a \int_{-\pi}^{\pi} \phi_1 \Big|_{r=a} \sin\theta \, d\theta$$

$$= -\rho\omega^2 a^2 \pi (1+2p_1)$$

and hence by equations (3.28), (3.35) and (3.36), this becomes

$$\omega^2 a_{11} + i\omega b_{11} = -\rho\omega^2 a^2 \pi \left[1 - 2 \frac{(\kappa_o a \gamma_1 + \varepsilon_1 S_r + i S_q \varepsilon_1)}{\kappa_o a}\right] .$$

On equating real and imaginary parts, non-dimensionalizing by putting

$$a_{11} = \rho a^2 \pi \mu \quad , \quad b_{11} = \omega \rho a^2 \pi \lambda \quad , \tag{3.50}$$

and using (3.37), (3.38) we obtain

$$\mu = 2\gamma_1 - 1 - \frac{2\varepsilon_1 S_\gamma S_\varepsilon}{1+S_\varepsilon^2} \tag{3.51}$$

and

$$\lambda = \frac{2S_\gamma \varepsilon_1}{1+S_\varepsilon^2} \quad . \tag{3.52}$$

In a similar manner it can be shown that

$$\phi_2(x,y) = \sum_{n=1}^{\infty} \frac{a p_n}{n} \cos n\theta \left\{ \left(\frac{a}{r}\right)^n + \left(\frac{r}{a}\right)^n \right\} + r\cos\theta$$

and hence that

$$a_{22} = a_{11} \quad \text{and} \quad b_{22} = b_{11} \, .$$

(d) <u>Phase and amplitude of the heaving motion</u>

From (3.44) and (3.45),

$$A_2^+ = a e^{\kappa_o h} \sqrt{S_q^2 + S_r^2} \, e^{i\psi_2}$$

where

$$\psi_2 = \tan^{-1}\left(\frac{S_q}{S_r}\right)$$

$$= \frac{\psi_1}{2} \quad , \tag{3.53}$$

giving the amplitude and phase of the heaving cylinder as

$$|A_2^+| = ae^{\kappa_o h}\sqrt{S_q^2 + S_r^2} \tag{3.54}$$

and

$$\delta_2 = \psi_2 \ . \tag{3.55}$$

Alternatively, $|A_2^+|$ can be determined from equation (2.39) which with (3.4) and (3.50) gives

$$\frac{|A_2^+|^2}{a^2} = \lambda\pi\left(\frac{1+M\kappa_o^2}{1+3M\kappa_o^2}\right) \ . \tag{3.56}$$

This relation may be used to check the consistency of the numerical results obtained by solving the infinite system of equations. From Haskind's relation, equation (2.38), δ_2 is also the phase of the exciting force on the body, agreeing with Ogilvie's results when M = 0.

When the cylinder is forced to oscillate, outward travelling waves are produced which satisfy the free surface elevation given by equation (2.3). For motion restricted to that of heave, (3.1) reduces with (2.9) to give

$$\phi(x,y,t) = \mathrm{Re}\{-i\omega\xi_2\phi_2(x,y)e^{-i\omega t}\} \ .$$

Thus by (2.3)

$$\eta(x,t) = \mathrm{Re}\left\{\xi_2\frac{\partial\phi_2}{\partial y}(x,0)e^{-i\omega t}\right\}$$

within an additive constant. Using (3.3)

$$\eta(x,t) \sim \mathrm{Re}\left\{-\kappa_o A_2^{\pm}\xi_2 e^{\pm i\kappa_o x - i\omega t}\right\} \quad \text{as } x \to \pm\infty \ . \tag{3.57}$$

Therefore the wavemaker amplitudes at $x = \pm\infty$ are $\kappa_o|A_2^{\pm}|\xi_2$, and hence the relative amplitude, A_R, of the cylinder motion is

$$A_R = \frac{\text{amplitude of wavemaker}}{\text{sum of amplitudes at } x = \pm\infty}$$

$$= \frac{1}{2\kappa_o|A_2^{\mp}|} \ , \tag{3.58}$$

with a phase lag of $\pi + \delta_2$.

3.6 Justification of choice of solution for $\phi_i(x,y)$

The heaving motion of a circular cylinder with its axis in the free surface in the presence of surface tension was solved by Evans (1968b) using a modification of Ursell's (1950b) work for a submerged cylinder without surface tension. This method is now applied to a heaving submerged cylinder when surface tension is allowed for. Thus a complex potential $w(z)$ is introduced where $w(z) = \phi(x,y) + j\psi(x,y)$ and $z = x + jy$, as before.

Consider the function

$$F(z) = Kw + j\frac{dw}{dz} - jM\frac{d^3w}{dz^3} \ , \tag{3.59}$$

By the free-surface condition (2.11)

$$\mathrm{Re}_j\{F(z)\} = 0 \qquad \text{on } y = 0 \ . \tag{3.60}$$

Hence $F(z)$ may be continued by Schwarz's reflection principle into a regular single-valued function outside the circles $|z \pm jh| = a$. Further, a value of w may be determined by integrating along a path from the real

axis to any point in the half-plane $y < 0$, the same value being obtained for any two paths provided a singularity is not enclosed. Indeed continuation along a closed path surrounding the circle $|z + jh| = a$ is unclear and may not lead to a one-valued function. Therefore a cut is introduced from $-j(a+h)$ to $-j\infty$ across which analytic continuation is not permitted. The function $F(z)$ is continuous across the cut, so that

$$\left(K + \frac{\partial}{\partial y} + M \frac{\partial^3}{\partial y^3}\right) [w] = 0 \quad , \tag{3.61}$$

where [ ] denotes the discontinuity across the cut. Thus

$$[w] = j \sum_{s=0}^{2} A_s e^{-\kappa_s y} \tag{3.62}$$

where κ_s $(s = 0,1,2)$ are the roots of $K = k(1+Mk^2)$, κ_0 real and positive and $\kappa_2 = \overline{\kappa_1}$. Since $\phi(x,y)$ is symmetric about $x = 0$, it is continuous across the cut, and so A_0 is real and $A_2 = \overline{A_1}$.

Let w_{2n} denote the even submerged complex multipole potentials satisfying (3.60) and producing outgoing waves at infinity. Then in $x > 0$, $y > -h$

$$w_{2n} = \frac{e^{j(n+1)\theta}}{r^{n+1}} + \frac{(-1)^{n+1}}{n!} \int_0^\infty k^n \frac{[k(1+Mk^2)+K]}{k(1+Mk^2)-K} e^{-k(y+h)+jkx} \, dk$$

$$+ \frac{(-1)^{n+1}}{n!} 2\pi i \kappa_0^{n+1} \left(\frac{1+M\kappa_0^2}{1+3M\kappa_0^2}\right) e^{-\kappa_0(y+h)+j\kappa_0 x} \quad , \; n=0,1,2,\ldots \tag{3.63}$$

It can be shown that w_{2n} may be continued in to the z-plane cut from $z = -j(a+h)$ to $z = -j\infty$, and that

$$[w_{2n}] = -j4\pi \frac{(-1)^n}{n!} \sum_{s=0}^{2} \frac{(1+M\kappa_s^2)}{1+3M\kappa_s^2} \kappa_s^{n-1} e^{-\kappa_s(y+h)} \quad . \tag{3.64}$$

It is now possible to define a function $W(z)$ with real constants α_n, $n = 0,1,2$ by

$$W(z) = w(z) - \sum_{n=0}^{2} \alpha_n w_{2n}(z)$$

such that W is continuous across the cut. This requires

$$[w(z)] - \sum_{n=0}^{2} \alpha_n [w_{2n}(z)] = 0 \ ,$$

yielding the system

$$\begin{pmatrix} 1 & \kappa_0 & \kappa_0^2 \\ 1 & \kappa_1 & \kappa_1^2 \\ 1 & \kappa_2 & \kappa_2^2 \end{pmatrix} \begin{pmatrix} \alpha_0 \\ \alpha_1 \\ \alpha_2 \end{pmatrix} = \frac{(-1)^{n+1} n!}{4\pi} \begin{pmatrix} \frac{A_0}{\kappa_0} \left(\frac{1+3M\kappa_0^2}{1+M\kappa_0^2}\right) e^{\kappa_0 h} \\ \frac{A_1}{\kappa_1} \left(\frac{1+3M\kappa_1^2}{1+M\kappa_1^2}\right) e^{\kappa_0 h} \\ \frac{A_2}{\kappa_2} \left(\frac{1+3M\kappa_2^2}{1+M\kappa_2^2}\right) e^{\kappa_0 h} \end{pmatrix} .$$

The determinant of this system is non-zero and so the α_n (n=0,1,2) exist and are unique. Hence W(z) is a regular single-valued function outside $|z \pm jh| = a$, and a Laurent expansion exists in the form

$$W(z) = \sum_{n=0}^{\infty} a_n (jz)^n + \sum_{n=1}^{\infty} b_n (jz)^{-n}$$

$$= F_1(z) + F_2(z) \qquad (3.65)$$

for $|z| > h + a$, where a_n, b_n are real since ϕ is even.

The function $F_1(z)$ converges for all $|z| > h + a$ and hence for all z. Apply the operator $L \equiv K + j \frac{d}{dz} - jM \frac{d^3}{dz^3}$ to $w_{2n}(z)$. Then

$$Lw_{2n}(z) = \frac{(-1)^n}{n!} \left\{K \frac{n!}{(h-iz)^{n+1}} + \frac{(n+1)!}{(h-iz)^{n+2}} + M \frac{(n+3)!}{(h-iz)^{n+4}}\right\}$$

$$+ \frac{(-1)^{n+1}}{n!} \left\{K \frac{n!}{(h+iz)^{n+1}} + \frac{(n+1)!}{(h+iz)^{n+2}} + M \frac{(n+3)!}{(h+iz)^{n+4}}\right\} ,$$

where

$$\frac{e^{j(n+1)\theta}}{r^{n+1}} = \frac{1}{n!} \int_0^{\infty} k^n e^{-k(y-h)+jkx} \, dk \qquad \text{for } y > h \ , \qquad (3.66)$$

has been used. Therefore Lw_{2n} is bounded for $|z| > h + 2a$. Also $LF_2(z)$ is bounded for $|z| > h + 2a$, and $Lw(z) = o(z)$ since $dw/dz = o(1)$ as $y \to \infty$. Thus

$$LF_1(z) = o(z) = jB \quad , \qquad |z| > h + 2a \ ,$$

and

$$LF_1(z) = O(1) \quad , \qquad |z| < h + 2a$$

where B is a real constant from (3.60), whence

$$F_1(z) = \frac{jB}{K} + De^{j\kappa_o z}$$

where D is real from symmetry. Hence

$$w(z) = \sum_{n=o}^{2} \alpha_n w_{2n}(z) + \frac{jB}{K} + De^{j\kappa_o z} + \sum_{n=1}^{\infty} \frac{b_n}{(jz)^n} \ .$$

Since $\phi(x,y)$ represents outgoing waves at infinity, D = 0, and this gives

$$\phi(x,y) = \sum_{n=o}^{2} \alpha_n \phi_{2n}(x,y) + \sum_{n=1}^{\infty} \mathrm{Re}\left\{\frac{b_n}{(jz)^n}\right\} \quad \text{for large } |z| \ . \tag{3.67}$$

That is, as $|z| \to \infty$, ϕ can be written in terms of the first three even multipole expansions plus terms that decay to zero.

Returning to equation (3.24), we have posed a solution for ϕ_2 in the form

$$\phi_2(x,y) = \sum_{n=o}^{\infty} \frac{a^{n+2}}{n+1} p_{n+1} \phi_{2n}(x,y) \tag{3.68}$$

where p_n are complex constants determined from equation (3.25), and the ϕ_{2n} are given by equation (3.12) with n replaced by n+1. Alternatively these can be written as

$$\phi_{2n}(x,y) = \frac{\cos(n+1)\theta}{r^{n+1}} + \frac{(-1)^{n+1}}{n!} \int_o^{\infty} k^n \frac{[k(1+Mk^2)+K]}{k(1+Mk^2)-K} e^{-k(y+h)} \cos kx \, dk$$

where the integral is along the real axis indented around the pole at $k = \kappa_o$.

Applying the theorem:

If Φ is a harmonic potential function which is zero on $y = 0$, then

$$\phi = K\Phi - \frac{\partial \Phi}{\partial y} - M \frac{\partial^3 \Phi}{\partial y^3} \tag{3.69}$$

is a harmonic potential function which satisfies the free surface condition with surface tension.

given in Rhodes-Robinson (1970), to

$$\Phi = \frac{(-1)^n}{n!} \int_o^\infty k^n e^{-k(y+h)} \cos kx \, dk + \frac{\cos(n+1)\theta}{r^{n+1}} \quad ,$$

and using

$$\frac{\cos(n+1)\theta}{r^{n+1}} = \frac{(-1)^{n+1}}{n!} \int_o^\infty k^n e^{-k(h-y)} \cos kx \, dk \qquad \text{for } h > y \ ,$$

the wave-free potentials, ϕ_{2n}^F , for these multipole expansions are found to be

$$\phi_{2n}^F = \frac{(-1)^n}{n!} \int_o^\infty k^n [K+k(1+Mk^2)] e^{-k(y+h)} \cos kx \, dk$$

$$+ K \frac{\cos(n+1)\theta}{r^{n+1}} + (n+1) \frac{\cos(n+2)\theta}{r^{n+2}} + (n+1)(n+2)(n+3)M \frac{\cos(n+4)\theta}{r^{n+4}} \ . \tag{3.70}$$

By induction it can be proved that for $n = 3,4,5,\ldots$, ϕ_{2n} can be written in terms of the first three expressions, $n = 0,1,2$, plus wave-free potentials. Thus (3.68) becomes

$$\phi_2(x,y) = \sum_{n=o}^{2} C_{2n} \phi_{2n}(x,y) + \sum_{n=o}^{\infty} C_{2n}^F \phi_{2n}^F \tag{3.71}$$

where C_{2n}, C_{2n}^F are constants.

Now from (3.66) and using Gradsteyn and Ryzhik equation (3.351.3),

$$\frac{\cos(n+1)\theta}{r^{n+1}} = \mathrm{Re}\left(\frac{e^{i\theta}}{r}\right)^{n+1} = \mathrm{Re}\left(\frac{-1}{h+iz}\right)^{n+1} ,$$

and

$$\int_0^\infty k^n e^{-k(y+h)} \cos kx \, dk = \mathrm{Re}\left[\frac{n!}{(h-iz)^{n+1}}\right] \qquad \text{for } y > -h .$$

Thus it is clear from (3.70) that for large $|z|$ and constants d_n, d_n^* ,

$$\phi_{2n}^F = \mathrm{Re}\left[\sum_{n=1}^{\infty} \frac{d_n}{(iz)^n}\right]$$

and therefore

$$\phi(x,y) = \sum_{n=0}^{2} C_{2n}\phi_{2n}(x,y) + \sum_{n=1}^{\infty} \mathrm{Re}\left[\frac{d_n^*}{(iz)^n}\right] \qquad \text{as } |z| \to \infty .$$

Comparing this with equation (3.67) justifies our assumed form of solution.

3.7 Results

Experiments performed by Evans et al. (1979) on a submerged circular cylinder of radius 5 cm were carried out in a wave tank 10 cm long, 30 cm wide and 60 cm deep. There they found that when the axis of the cylinder was submerged to a depth h = 6.25 cm and h = 7.5 cm the deep water theory was sufficient over most of the wavelength range considered. Although no experimental work has been attempted to account for the effect of surface tension these values have been borne in mind here in order that the infinite depth expressions may still be valid. Thus, computations have been performed for cylinders of radii 2,2.5,4 and 5 cms at various depths of submergence such that the cylinder is never greater than 12.5 cm away from the free surface.

These calculations require the solution of two infinite systems of

real equations. This is achieved by truncating the systems after a finite number of terms and solving the resultant finite systems by a standard numerical procedure. This involves only one matrix inversion since both systems possess the same left-hand side. Solutions were computed with 10, 15 and 20 terms, and results in general agreed to 4 or 5 significant figures. For small $Ka < .1$ and $h/a < 1.25$, agreement was less good.

It is assumed that water occupies the tank so that

$$T_s = 74 \text{ dyn}|\text{cm} = 74 \times 10^{-3} \text{ N}|\text{m}.$$

Therefore, taking $\rho = 1 \text{ Kg}|\text{m}^3$ and $g = 10 \text{ ms}^{-2}$,

$$M = 74 \times 10^{-4} \text{ m}^2 .$$

This quantity can suitably be non-dimensionalized by writing

$$\gamma = \frac{M}{a^2} .$$

Thus $\gamma = 18.5, 11.84, 4.625, 2.96$ corresponding respectively to the cylinder radii given above.

Various curves for the quantities obtained in the previous sections are now presented as a function of the wave-number $\kappa_o a$ or $\kappa_o h$ for a selection of the parameter values γ and h/a. It is worth noting that for the curves of constant submergence-cylinder radius ratio, the case when $M = 0$ has been plotted for comparison even though in the context of the graph this corresponds to an infinitely large cylinder.

Figures (3.1) and (3.2) show the added mass parameter for varying h/a when $a = 4$ and 2 cm respectively. It can be seen that as the depth of submergence is increased μ approaches one. This is to be expected

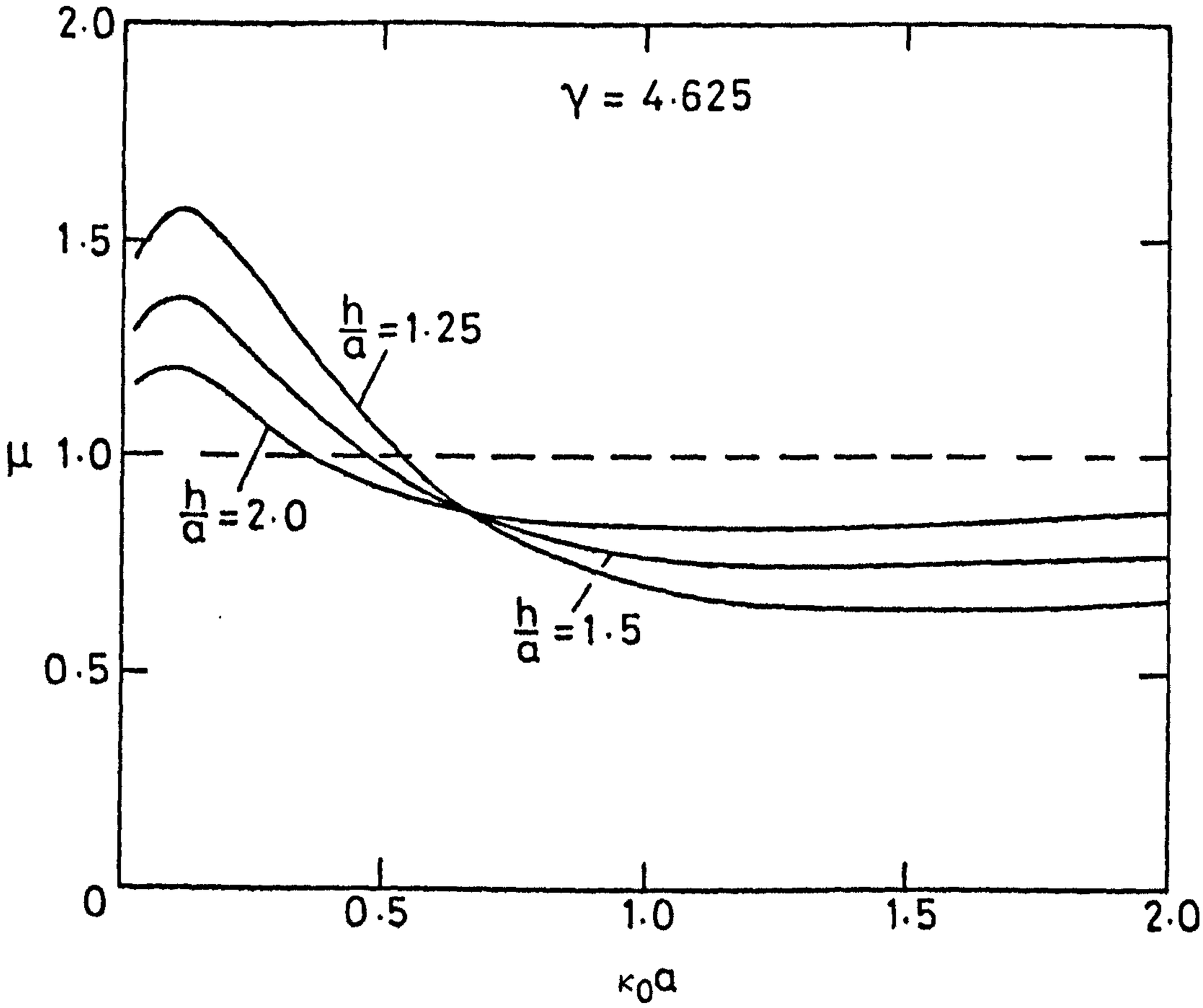
γ = 4.625
h/a = 1.25
h/a = 2.0
h/a = 1.5
μ
κ0a
2.0
1.5
1.0
0.5
0
0.5
1.0
1.5
2.0

FIG. (3.1)

γ = 18.5
h/a = 1.25
h/a = 2.0
h/a = 1.5
μ
κ0a
2.0
1.5
1.0
0.5
0
0.5
1.0
1.5
2.0

FIG. (3.2)

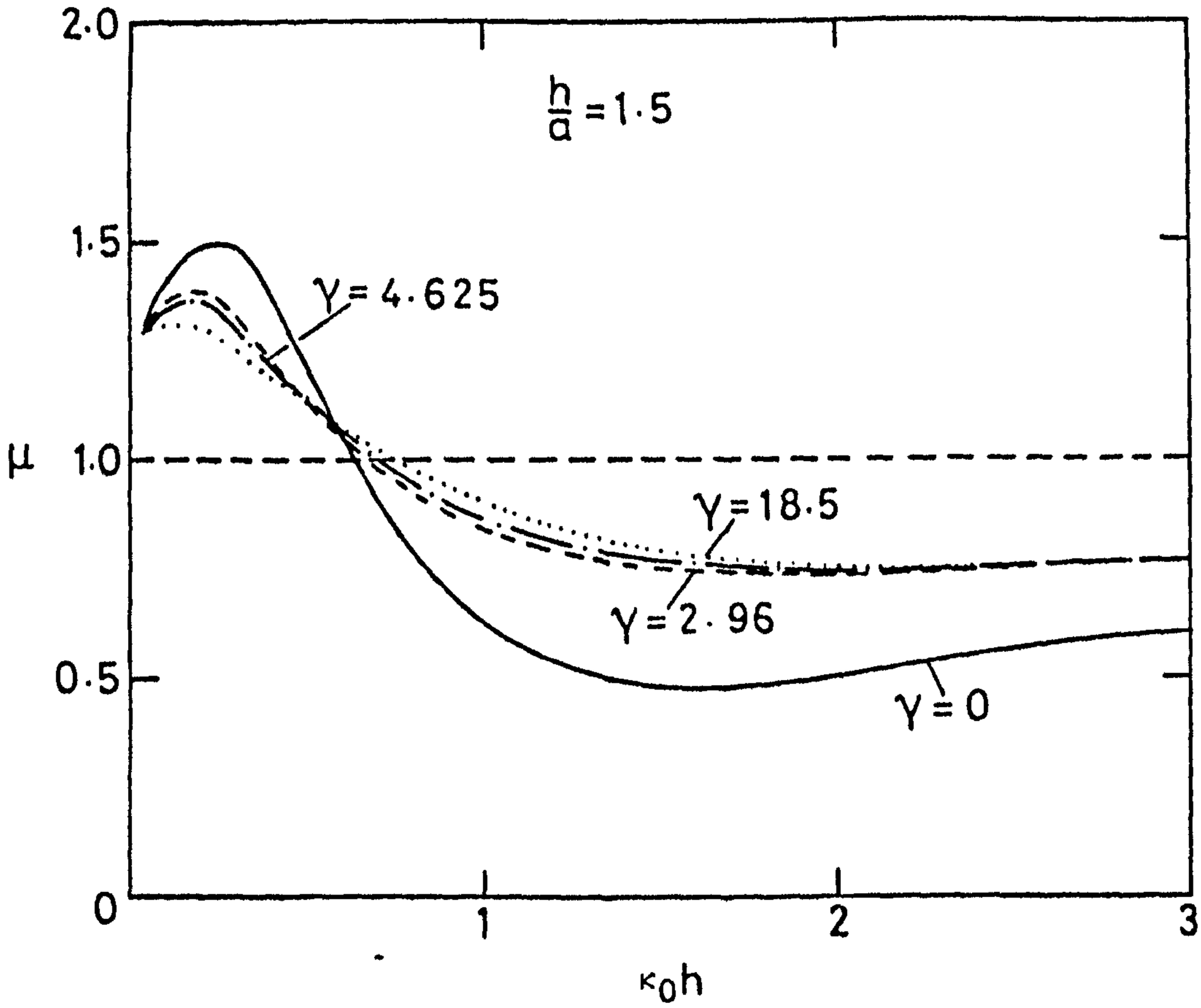

FIG. (3.3)

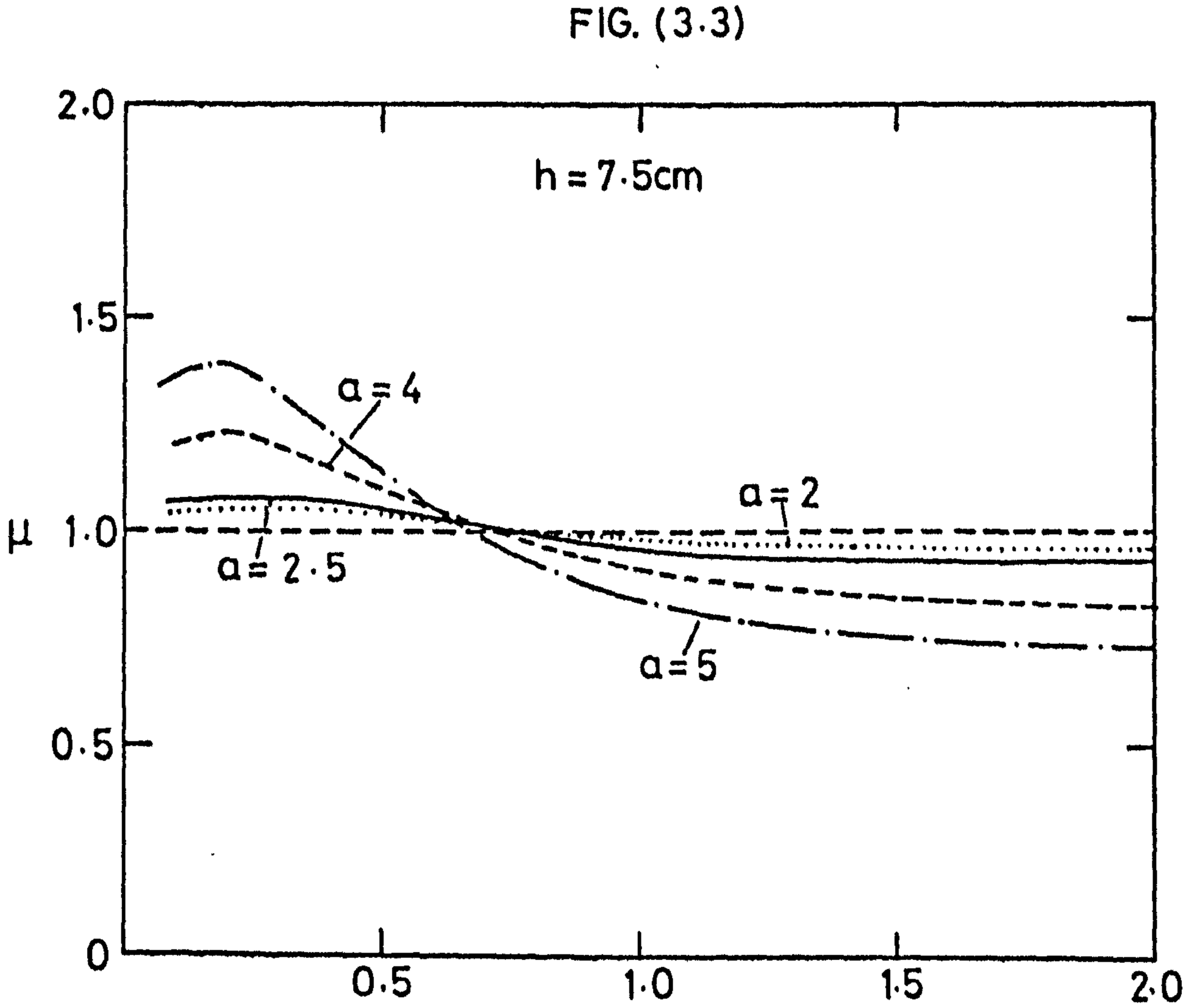

FIG. (3.4)

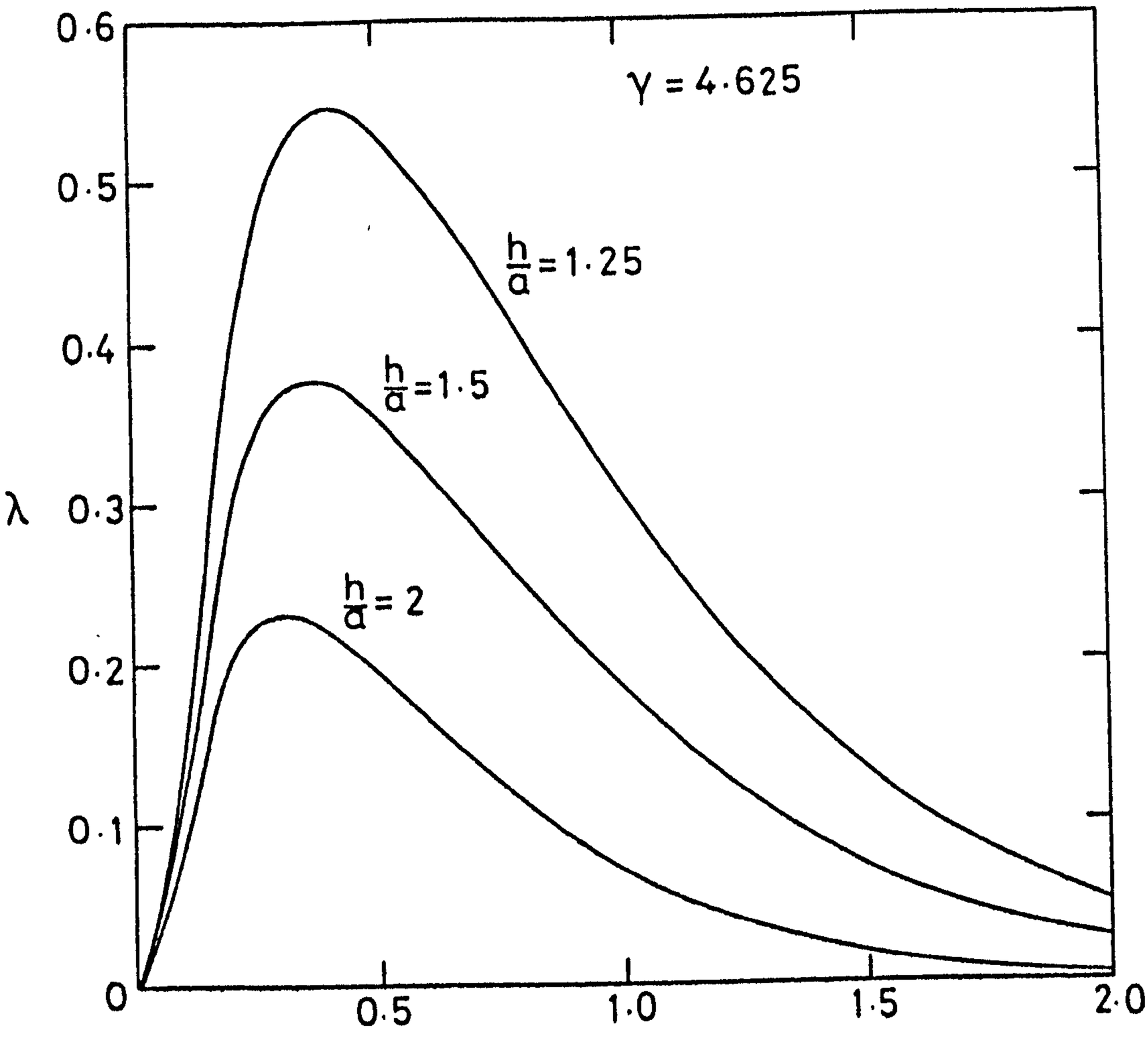
γ = 4·625
h/a = 1·25
h/a = 1·5
h/a = 2
λ
0·6
0·5
0·4
0·3
0·2
0·1
0
0·5
1·0
1·5
2·0
κ0a

FIG. (3·5)

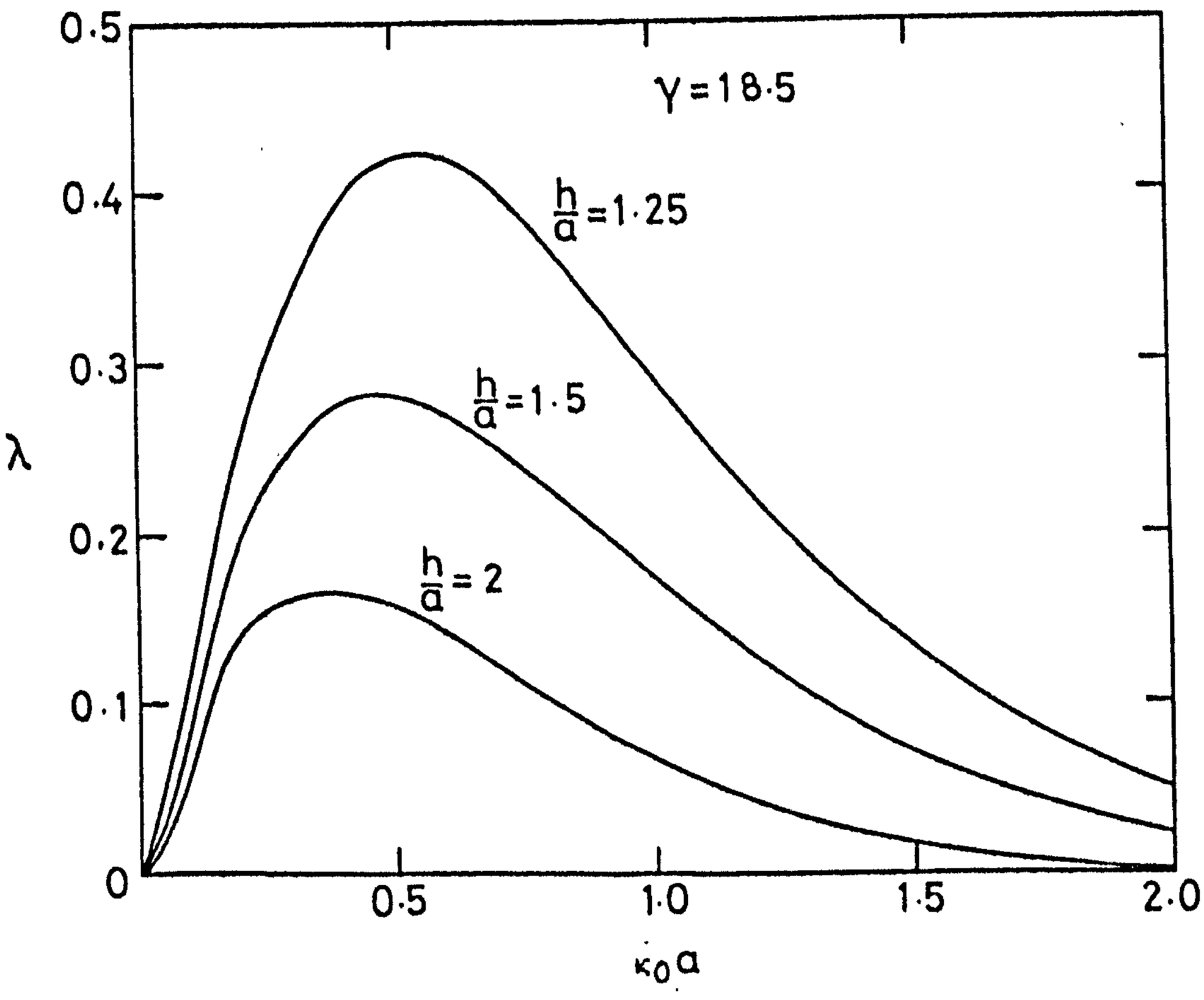
γ = 18·5
h/a = 1·25
h/a = 1·5
h/a = 2
λ
0·5
0·4
0·3
0·2
0·1
0
0·5
1·0
1·5
2·0
κ0a

FIG. (3·6)

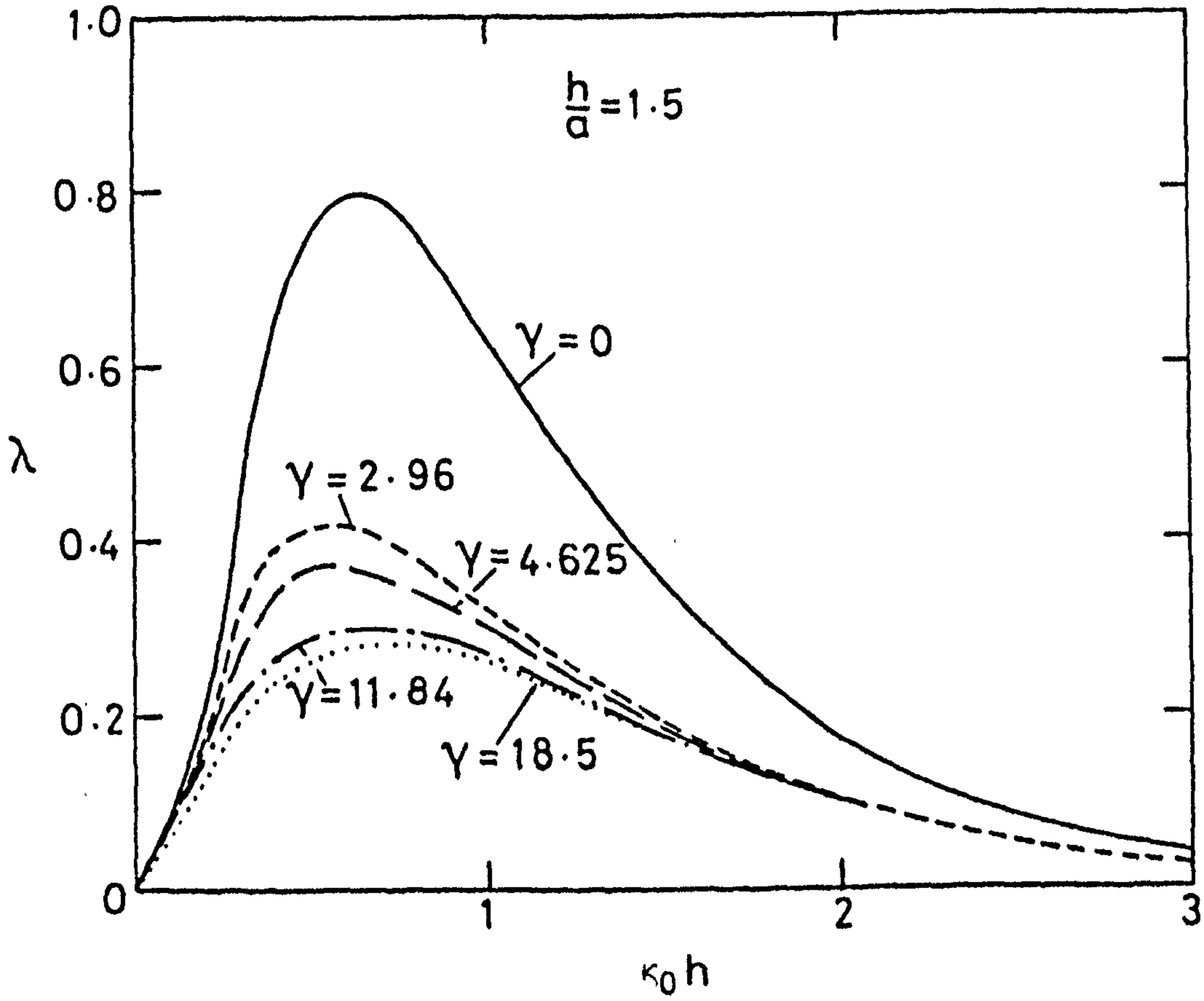
h/a = 1·5
γ = 0
γ = 2·96
γ = 4·625
γ = 11·84
γ = 18·5
λ
κ0 h
1·0
0·8
0·6
0·4
0·2
0
1
2
3

FIG. (3·7)

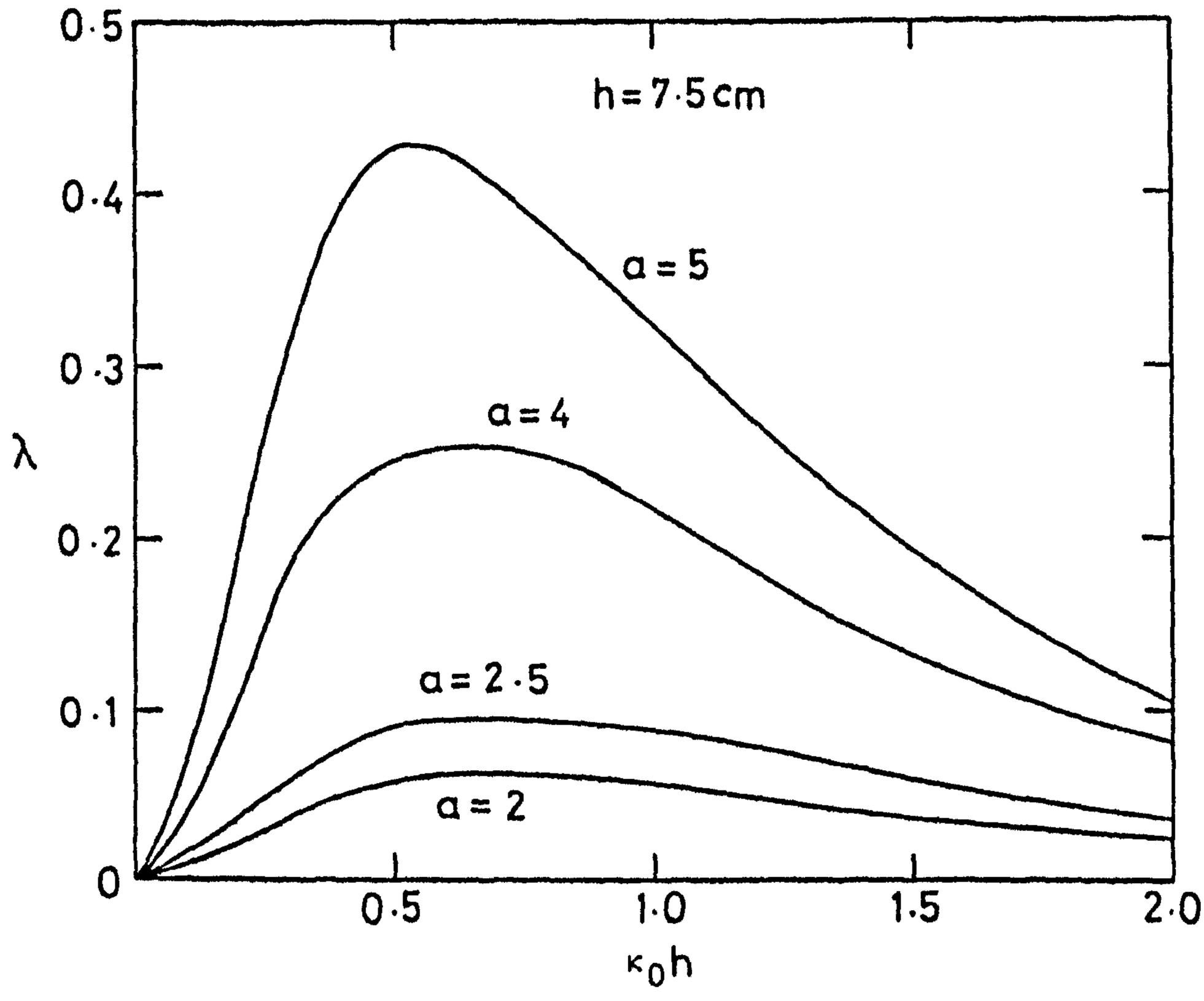
h = 7·5 cm
a = 5
a = 4
a = 2·5
a = 2
λ
κ0 h
0·5
0·4
0·3
0·2
0·1
0
0·5
1·0
1·5
2·0

FIG. (3·8)

because as the cylinder becomes deeply submerged the effect of the free surface is minimal and so the non-dimensional added mass tends to the added mass of a cylinder oscillating in an infinite fluid with no free surface; that is, unity. The effect of cylinder radii on μ for constant h/a at 1.5, is seen in fig. (3.3) to be very insignificant, except when surface tension is neglected. In this case there is a noticeable increase throughout the considered range. By keeping h constant and varying a, the results for the added mass are more varied, as displayed in fig. (3.4). Clearly the smaller cylinder is more deeply submerged, and so μ does not deviate from one as much as the cylinder with a larger radius.

In figs. (3.5) and (3.6) curves of λ are plotted for a specific cylinder as h/a varies. Since the damping coefficient and the amplitude of the radiated waves at infinity are related, it is not surprising that as the cylinder becomes more deeply submerged, the damping coefficient decreases. This corresponds to the wave-making capability of any oscillating body vanishing as depth becomes very large. It is noticeable that the maximum value of λ occurs very close to the point where μ crosses the line $\mu = 1$. The damping parameter for different cylinder radii when the cylinder is submerged to a depth-to-radius ratio of 1.5 is shown in fig. (3.7). For $.3 < \kappa_o h < 1.5$ there is more damping for the larger cylinder, but as $\kappa_o h$ increases the damping becomes the same for all cylinders. Again there is a significant difference between the cylinder of radius 2 cm with surface tension accounted for, and the result when this term is neglected. The final graph of λ in fig. (3.8) shows the effect of the value h remaining constant. As expected, there is less damping on the smallest cylinder.

Results for ψ_2, the phase lag of both the heaving and the forced oscillatory motions are presented in figs. (3.9)-(3.12). These curves are also equivalent to half the transmitted phase lag. The first two graphs show that the phase lags more and more as the cylinder is considered to be closer to the surface. A physical interpretation for this is given

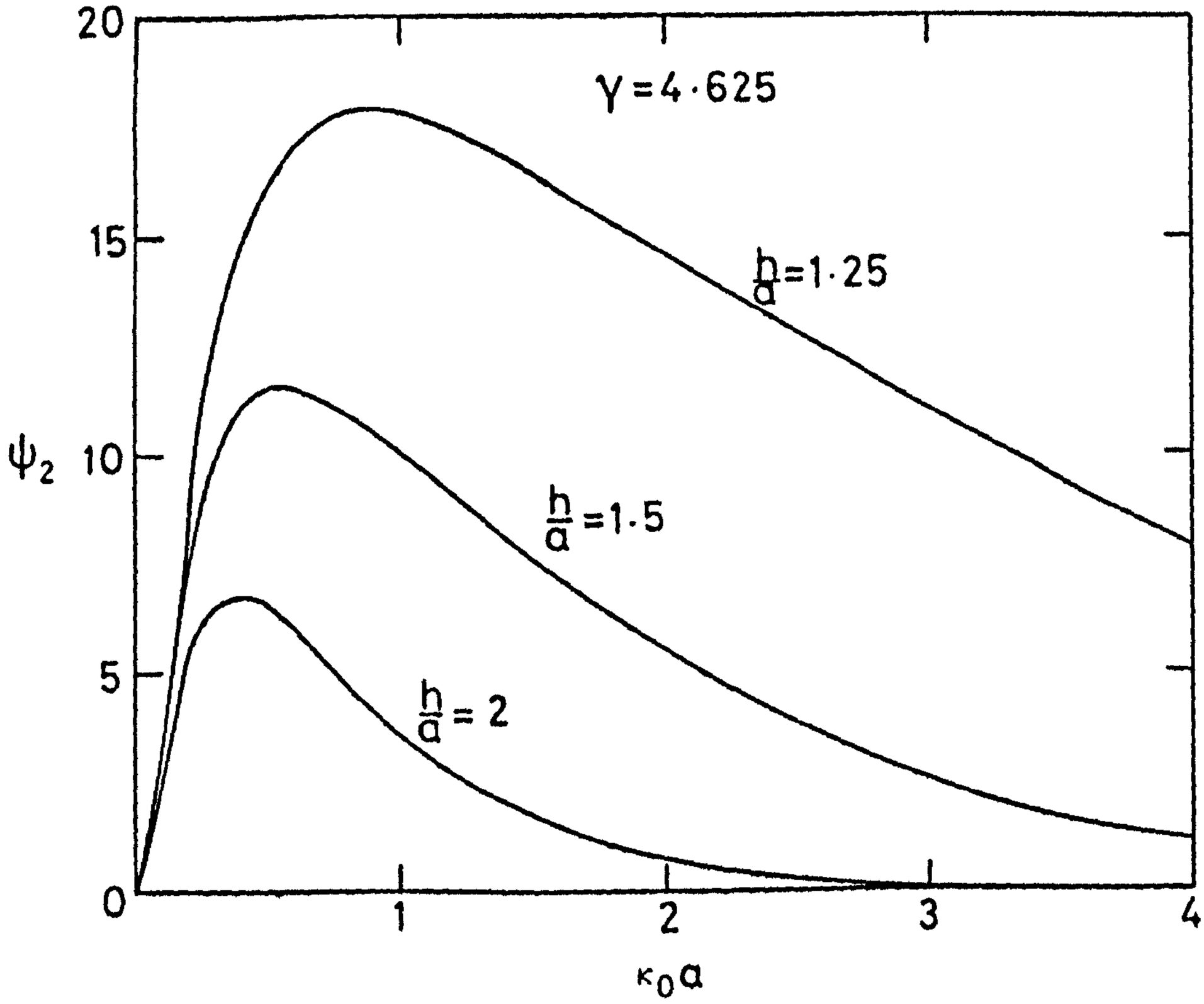

FIG. (3·9)

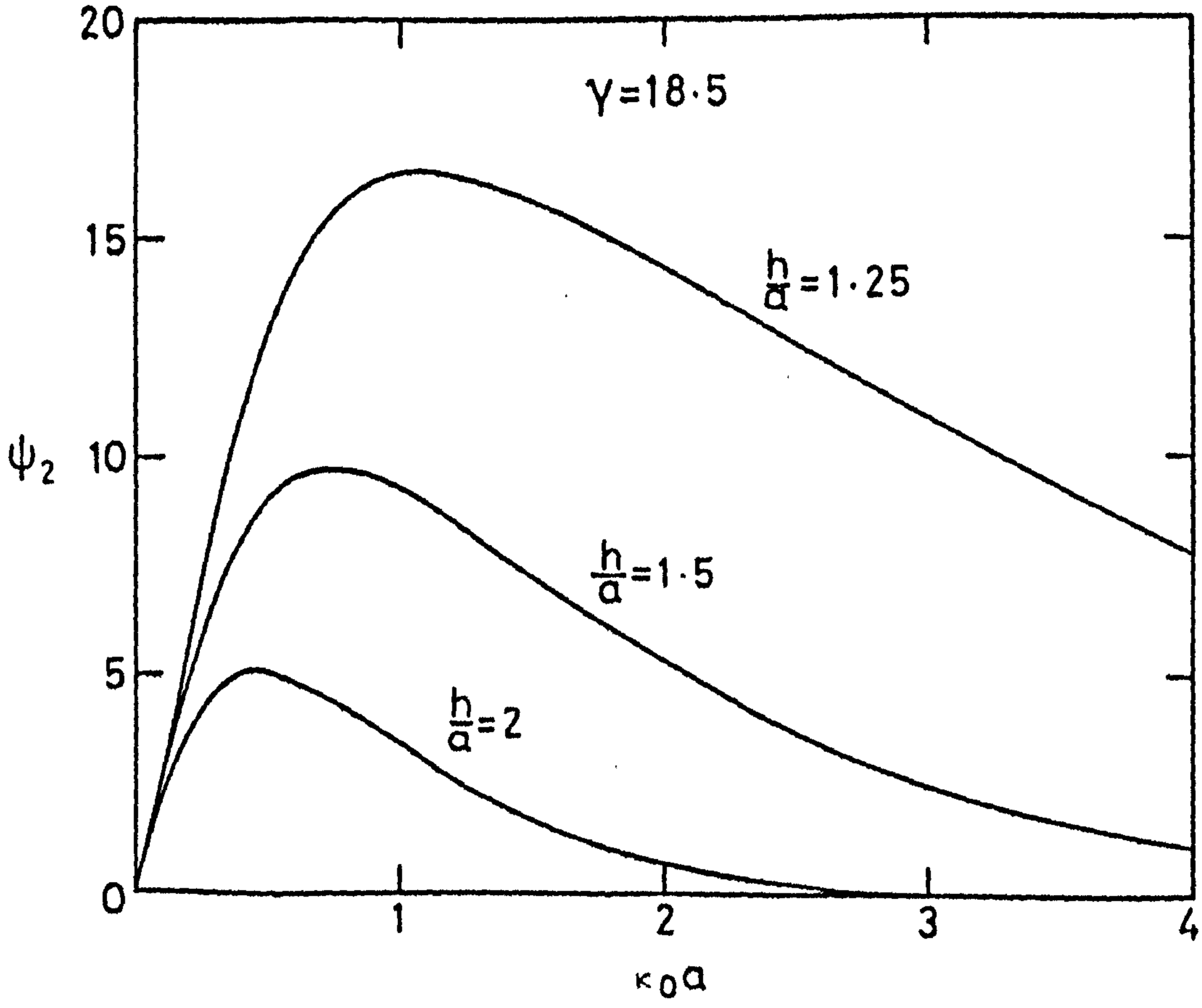

FIG. (3·10)

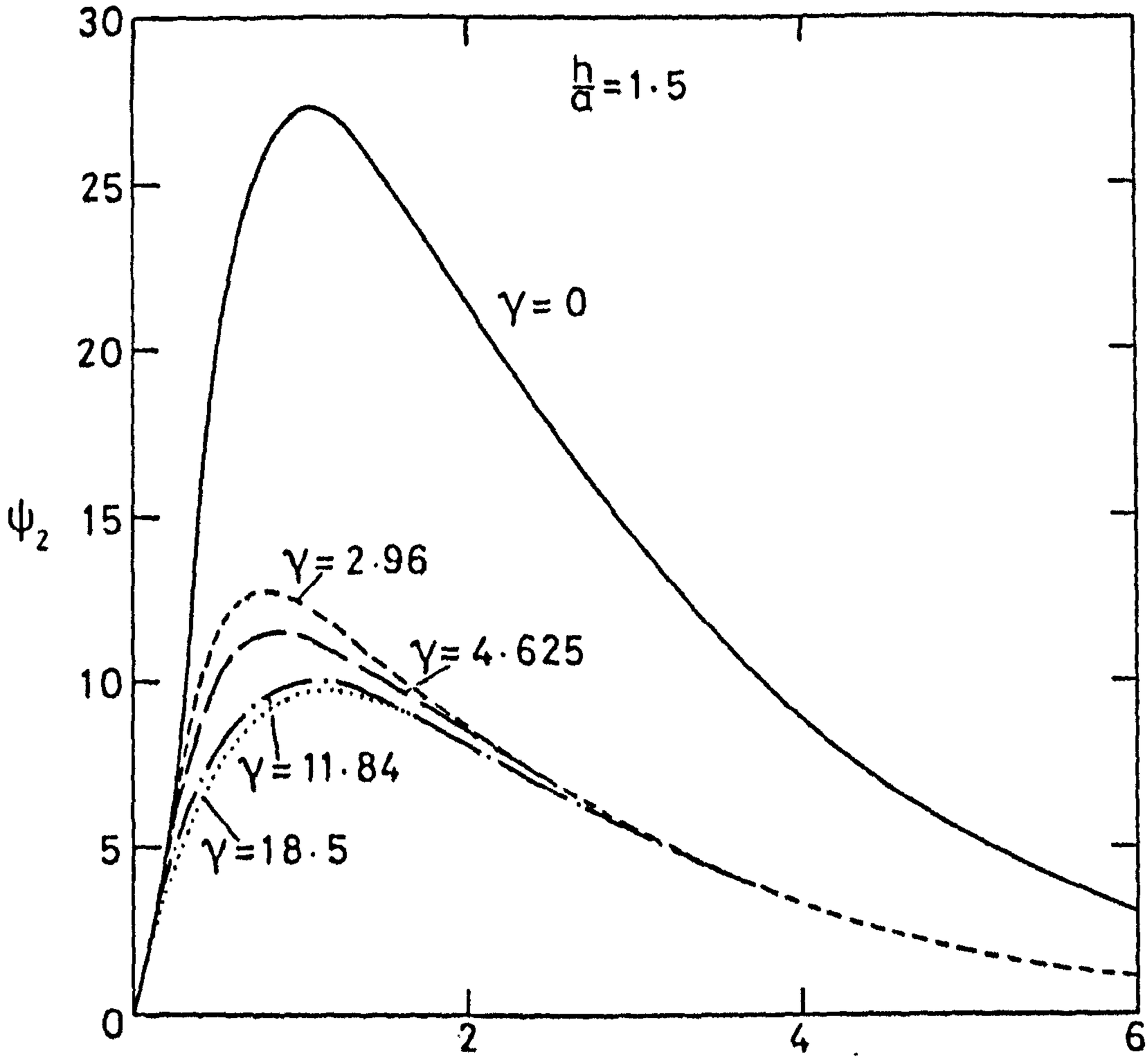

FIG. (3·11)

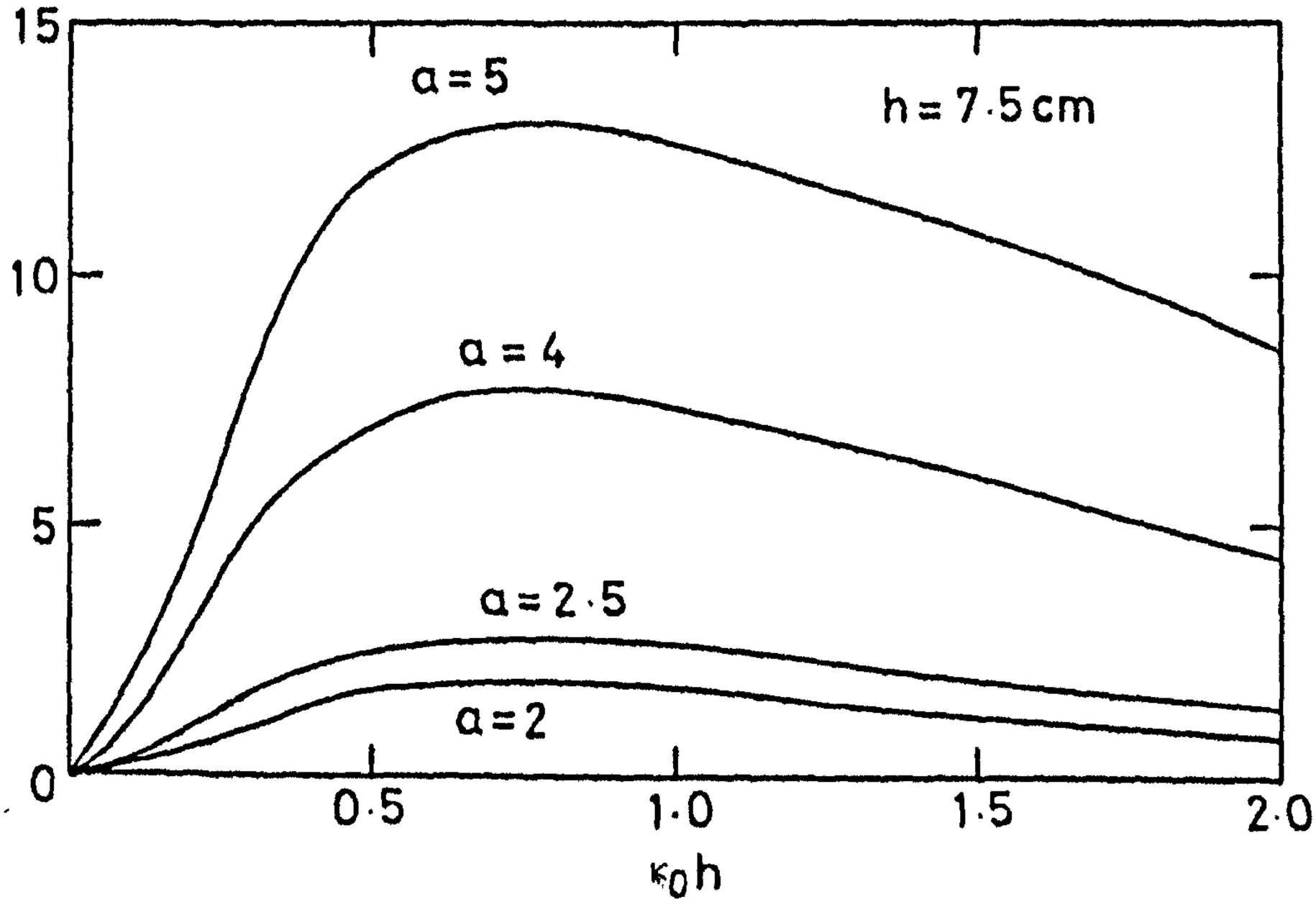

FIG. (3·12)

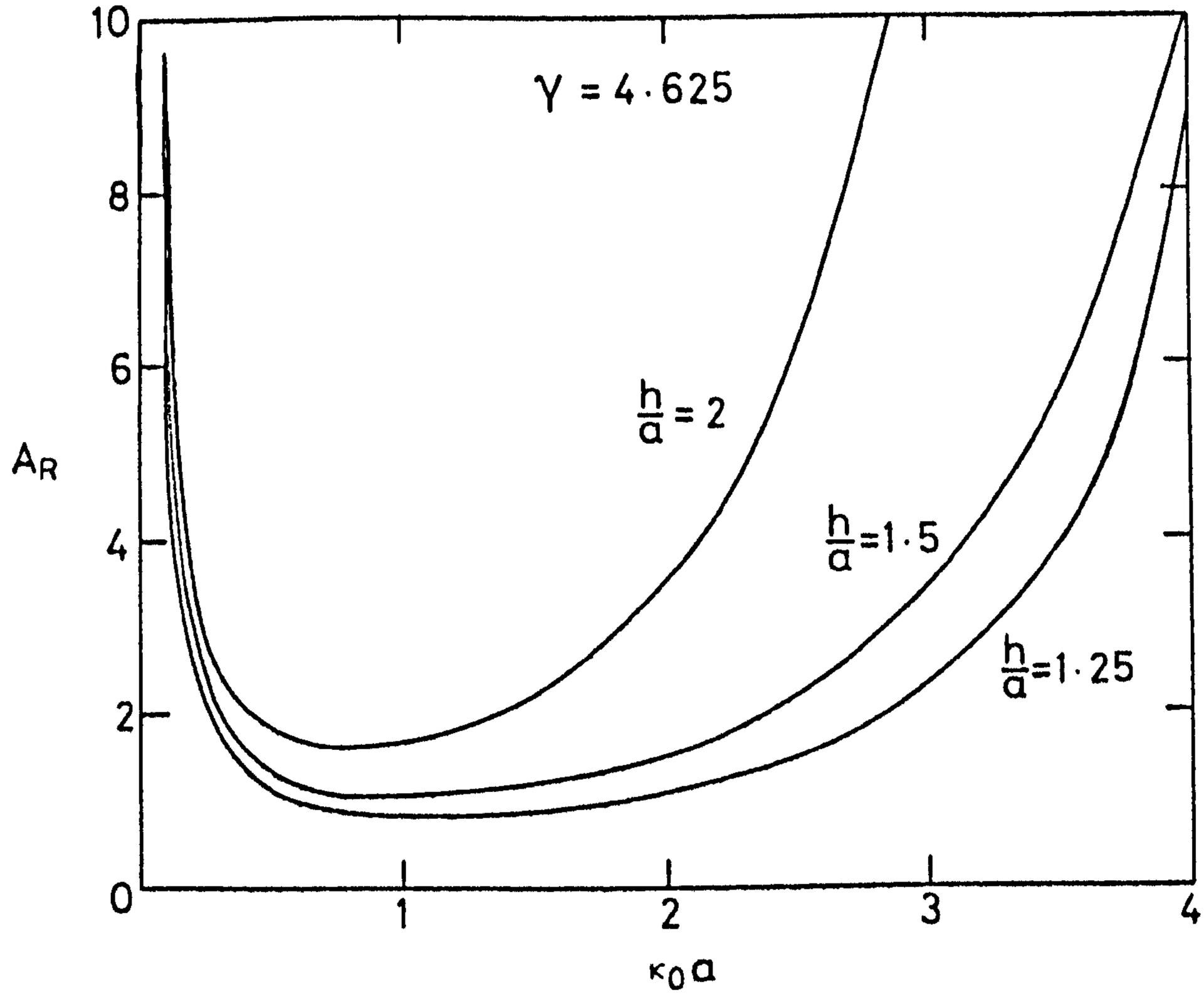

FIG. (3·13)

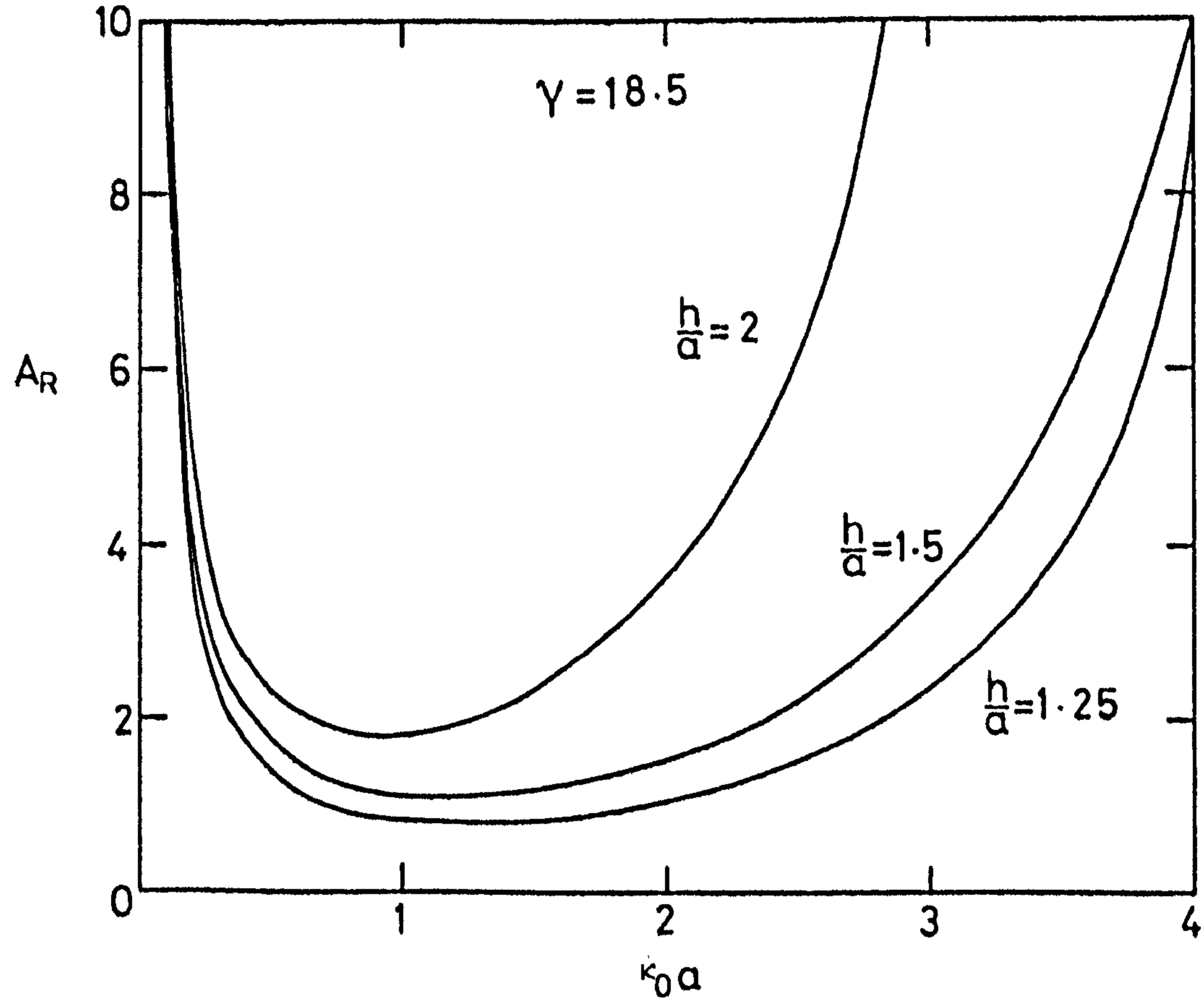

FIG. (3·14)

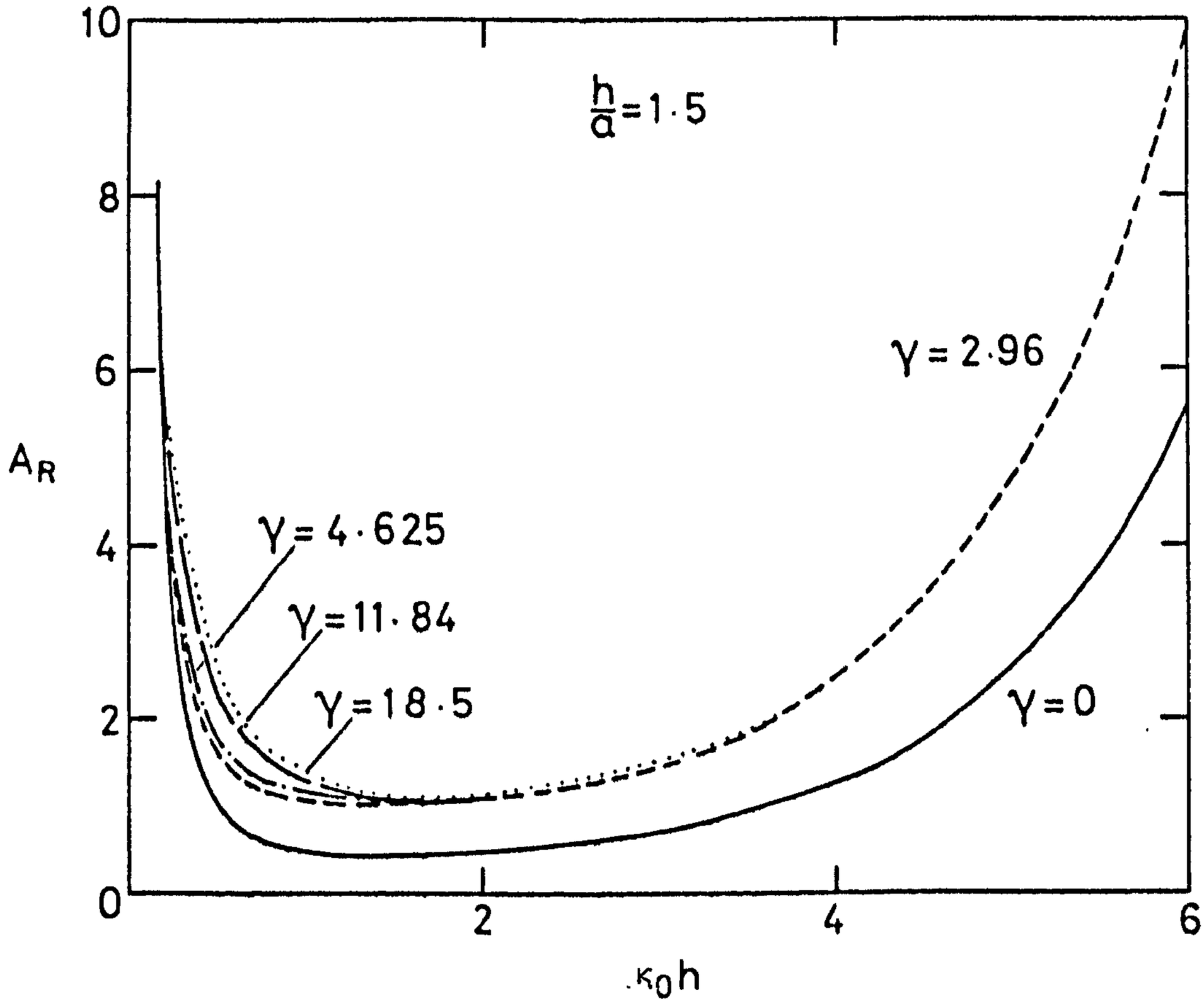

FIG. (3·15)

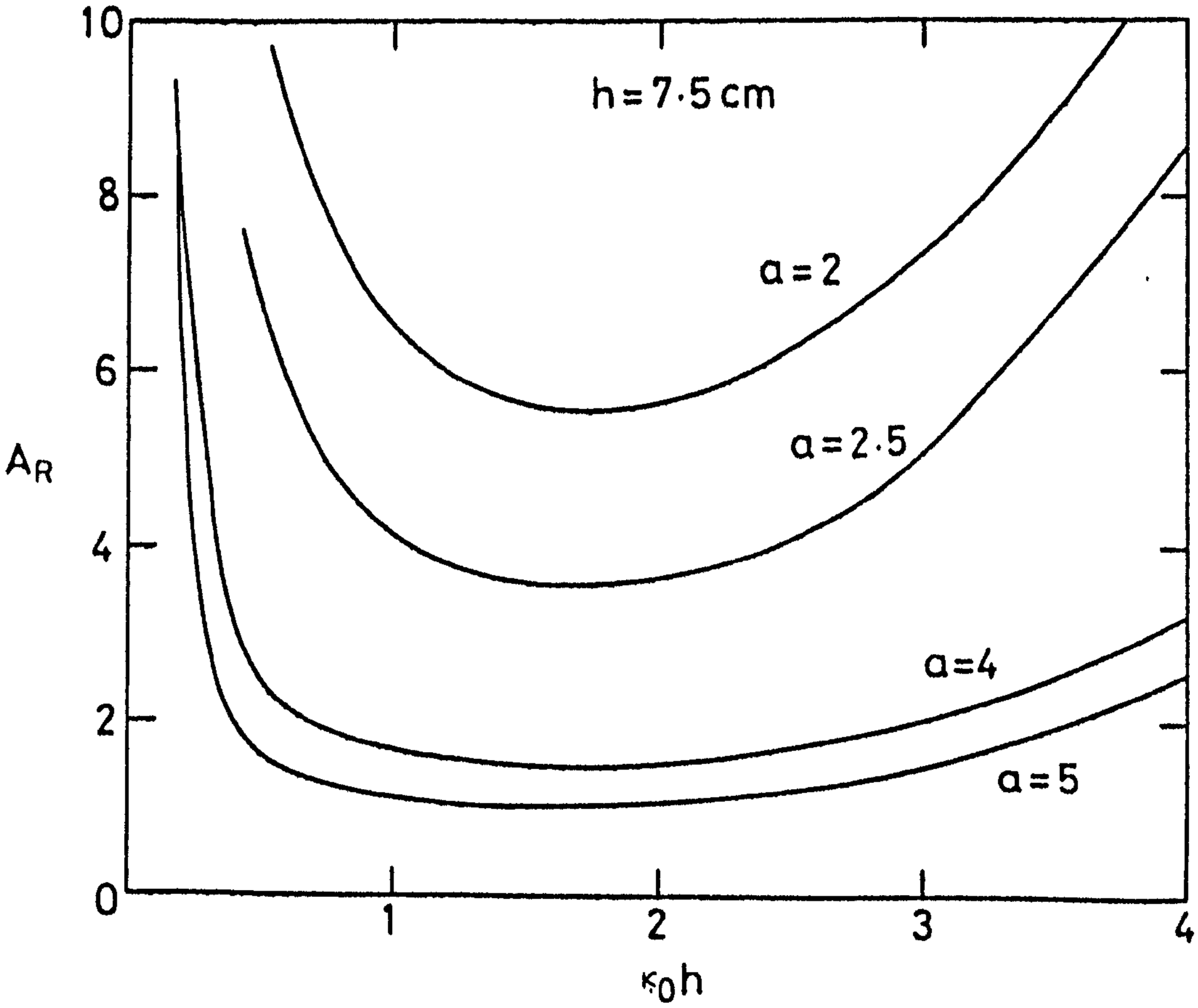

FIG. (3·16)

in Ogilvie (1963) and proceeds as follows. When a wave is incident on a submerged cylinder essentially all of the wave energy passes above the cylinder regardless of its depth of submergence. Thus the situation is similar to that of a wave entering shallow water, so that when the wave emerges on the other side its phase speed is reduced and it exhibits a phase lag. The closer the cylinder is to the surface, the greater this lag will be. Further, because of the geometrical symmetry of the cylinder, if it can be supposed that half of the lag occurs before the wave reaches the origin, and the other half afterwards, then it is reasonable that the oscillatory forces should show a phase lag of one-half of the total transmission lag. In a sense the force depends on the average of the passing wave.

Fig. (3.11) presents results of ψ_2 for cylinders submerged to the same submergence-radius ratio. In contrast to this fig. (3.12) displays curves when h = 7.5 cm and a varies. In both cases the phase is less for smaller cylinders.

Finally curves for the relative amplitude are presented. Since A_R is related to the damping coefficient by equation (3.56), these curves are as expected. Hence for a given cylinder, figs. (3.13) and (3.14) show that A_R is greater when it is more deeply submerged. However, if h/a is kept constant and the radius of the cylinder changes, then the smaller cylinder produces a slightly smaller relative amplitude, as seen in fig. (3.15) when $.15 \prec \kappa_o h \prec 3$. At this upper value of $\kappa_o h$, the graphs merge together and so the radius of the cylinder has no effect. A greater difference between results is displayed in fig. (3.16) when h is taken to be 7.5 cm for all cylinder radii.

3.8 Conclusion

The velocity potential for the forced oscillation of a submerged circular cylinder in the presence of surface tension has been determined

in terms of a convergent infinite system. From this it has been possible to show that when the cylinder moves uniformly in a circle of small radius waves are radiated outwards in one direction only and that an incident wave undergoes no reflection on encountering a fixed circular cylinder, only a phase change. This phase shift, along with the added mass and damping coefficients have been computed and results presented.

Perhaps the most striking feature of these curves is the difference between the behaviour for small M and the results when surface tension is neglected. This discrepancy stems from the mathematical behaviour of the solutions as $M \to 0$. It can be seen in §3.4 and §3.5 that all the computed quantities depend on β_{mn}, a function which differs for the limiting case by a term of order log M as $M \to 0$ (equation (3.42)). It is the presence of this factor that causes the curves for small M to reluctantly approach the $M = 0$ value. In spite of this, it is evident that by putting $M = 0$, the known results in the absence of surface tension are obtained.

CHAPTER 4

DIFFRACTION OF SURFACE WAVES BY A FIXED VERTICAL BARRIER IN A FLUID OF FINITE DEPTH

4.1 Introduction

This and subsequent chapters proceed under the assumption that the effect of surface tension is negligible and that gravity is the sole restoring force on the free surface. In particular this implies that $\kappa_o = K$, and to avoid confusion with the result when surface tension is included, κ is re-written as k. All other definitions and results previously derived remain the same and are used as required.

It is well known that linear potential theory does not, in general, permit an explicit solution to describe the diffraction of waves by obstacles. Indeed, most of the exact solutions are for thin vertical plates in a fluid of infinite depth. The first such solution was found by Dean (1945) who solved the problem of a fixed, submerged, semi-infinite plate extending up to a finite depth beneath the free surface. Then Ursell (1947) considered the scattering of waves by a fixed plate intersecting the free surface. Further aspects of a single, surface-piercing barrier have been treated in Ursell (1948), Haskind (1948, 1959) and Levine and Rodemich (1958). Evans (1970) solved the problem of a single submerged oscillating barrier and Porter (1972) investigated the transmission of waves through a gap in a semi-infinite barrier. The more general problem of scattering by an arbitrary number of vertical barriers has been considered by Lewin (1963), Mei (1966) and Porter (1974), where the known results of Dean (1945) and Ursell (1947) are re-derived as special cases. Numerous authors have re-investigated some of these

problems to exploit an alternative technique and others have extended the field to include obliquely incident waves and barriers in parallel. Thus there has been a thorough investigation of infinite depth problems involving thin vertical barriers.

However, the case of barriers in finite depth has not been examined so fully for exact solutions are not obtained. Ogilvie (1960) examines the case of a thin vertical barrier situated on the fluid bed by applying a general procedure specifically developed for a fluid of non-constant depth. This method results in an asymptotic expansion for the reflection coefficient which is evaluated and presented for various parameter values.

Mei and Black (1969) apply a variational method to determine the scattering properties for bottom and surface rectangular obstacles, and, as a limiting case present numerical solutions for a thin barrier. Black, Mei and Bray (1971) extend this problem and consider the radiation problem when the cylinder is forced to oscillate. The approximate far-field amplitudes are obtained and hence, using Haskind's relations, the forces on a stationary body are determined. Again, results for the limiting case of a thin barrier are shown.

In contrast to the above, Morris (1970) deals directly with the thin barrier problem and includes the general case of obliquely incident waves. However the variational technique is adopted and so only approximate results are obtained.

Another comparable investigation to a thin barrier problem in finite depth has been made by Stiassnie and Dagan (1973) in examining the first-order problem of an elliptical cylinder under the influence of an incident wave. They assume that the cylinder's cross-section is a thin ellipse and apply boundary conditions on the major axis of the cylinder. Their results are comparable with the thin barrier case of Black, Mei and Bray (1971).

Throughout all this work there is an absence of any full solution. In the light of this, the case of a barrier intersecting the free surface in a fluid of finite depth is treated herein. The formulation of §4.2 and §4.3 follows closely that of Mei and Black (1969) and Morris (1970), and the method of solution is due to Garrett (1970, 1971), which is also used in Thomas (1981a). The problem is then reduced to the solution of an infinite system of equations well suited to numerical computation. Expressions are obtained for the reflection and transmission coefficients and in §4.4, for the first- and second-order forces and moments acting on the barrier.

A special case of this problem is when the barrier is such that only a small gap remains at the bottom. Similar problems have drawn the attention of Tuck (1971, 1975), Guiney, Noye and Tuck (1972) and Packham and Williams (1972) in studying the flow of fluid through a small aperture in a wall, and Evans (1975, 1977), in flow through gaps in two, and an arbitrary number of walls, respectively.

One technique used to solve such problems is that of matched asymptotic expansions. This method was first used by Tuck (1971) to yield an approximate formula for the transmission coefficient when an incident wave impinges on a thin wall with a small slit in a fluid of infinite depth. It has since been extended to include barriers with thickness (Guiney et al. (1972), Evans (1977)),and also finite depth (Tuck (1975), Guiney et al. (1972)). The approach is now applied in §4.5 to the case when only one barrier is present.

The method involves solving the problem in a "short-sighted" region in the neighbourhood of the gap and in a "long-sighted" way at a distance from the hole. The two solutions are then matched in an intermediate region so that they represent the same flow, that is, the inner limit of

the outer solution must agree with the outer limit of the inner solution. This technique is more fully described in Tuck (1975).

Another approach is used by Packham and Williams (1972) to extend Tuck's original problem (1971) to flow through a gap in a wall in a fluid of finite and infinite depth in two and three dimensions. This method sets up the exact solution to the problem in terms of an integral equation, and then solves this equation approximately for small holes. In fact the result given for the transmission coefficient in the limiting case as the bottom barrier becomes negligible provides a check for the problem in hand. This technique was also employed by Evans (1975) for gaps in two vertical barriers.

Results for both the full and approximate solutions are presented and discussed in §4.6. Also shown are the exact solutions of Ursell's problem (1947) for an infinitely deep fluid given, for example, in Evans (1970). Finally conclusions are drawn in §4.7.

4.2 Formulation

A train of small amplitude surface waves travelling from $x = +\infty$ are incident on a thin barrier which is held fixed in a fluid of finite depth. The barrier occupies the interval $x = 0$, $0 < y < \ell$ and will partially reflect and partially transmit the incoming wave.

The time-independent velocity potential $\phi(x,y)$ describing the fluid motion satisfies Laplace's equation (2.10), the free-surface condition (2.11), and the fluid bed condition (2.12a). On the barrier

$$\frac{\partial \phi}{\partial x} = 0 , \qquad x = 0,\ 0 < y < \ell \tag{4.1}$$

whilst beneath it, continuity of the horizontal velocity and the pressure requires that ϕ and its first derivatives must be continuous across $x = 0$, $\ell < y < d$. Finally, the appropriate radiation condition is

$$\left.\begin{aligned} \phi &\to Ie^{-ikx}\cosh k(d-y) + R'e^{ikx}\cosh k(d-y) \quad \text{as } x \to \infty \\ \phi &\to T'e^{-ikx}\cosh k(d-y) \quad \text{as } x \to -\infty \end{aligned}\right\} \tag{4.2}$$

where

$$I = \frac{-igA}{\omega \cosh kd}$$

in accordance with equation (2.13), and k satisfies the dispersion relation given by (2.14) as

$$K = k\tanh kd \ .$$

4.3 The full solution

It can be shown (see Havelock, 1942) that the set of functions $\{f_n\}$ defined in the notation of Miles and Gilbert (1968) as

$$f_o = N_o^{-\frac{1}{2}} \cosh k(d-y) \quad \text{where} \quad N_o = \frac{1}{2}\left[1 + \frac{\sinh 2kd}{2kd}\right] \tag{4.3}$$

and

$$f_n = N_n^{-\frac{1}{2}} \cos k_n(d-y) \quad \text{where} \quad N_n = \frac{1}{2}\left[1 + \frac{\sin 2k_n d}{2k_n d}\right] \ , \ n \geq 1$$

in which k_n are the real positive roots of

$$K = -k_n \tan k_n d \quad \text{with} \quad k_n < k_{n+1} \quad (n \geq 1) \ , \tag{4.4}$$

form a complete orthogonal set in [0,d]. Since each f_n satisfies the free surface condition and the bottom condition, solutions for ϕ defined by $\phi^+(x,y)$ in $x > 0$ and by $\phi^-(x,y)$ in $x < 0$ can be constructed in the form

$$\left.\begin{aligned} \phi^+(x,y) &= [e^{-ikx} + Re^{ikx}]\, B_o f_o + \sum_{n=1}^{\infty} B_n^+ e^{-k_n x} f_n \\ \text{and} \qquad \phi^-(x,y) &= Te^{-ikx} f_o + \sum_{n=1}^{\infty} B_n^- e^{k_n x} f_n \end{aligned}\right\} . \tag{4.5}$$

Here $|R|$, $|T|$ are the complex reflection and transmission coefficients respectively, $B_n^{\pm}$ are complex constants, and $B_o = IN_o^{\frac{1}{2}}$ to satisfy (4.2) as the wave tends to infinity.

It only remains for ϕ to satisfy the continuity conditions across $x = 0$. In order to do this the function $U(y)$ defined by

$$\frac{\partial \phi^+}{\partial x} = \frac{\partial \phi^-}{\partial x} = U(y) , \quad x = 0, \; 0 < y < d \tag{4.6}$$

is introduced where, from (4.1),

$$U(y) = 0 , \quad 0 < y < \ell . \tag{4.7}$$

Now the $\{f_n\}$ form a complete set, so $U(y)$ may be expanded over $0 < y < d$ as

$$U(y) = \sum_{n=0}^{\infty} \mathscr{U}_n f_n(y) \tag{4.8}$$

where

$$\mathscr{U}_n = \frac{1}{d} \int_{\ell}^{d} f_n(y) U(y) \, dy . \tag{4.9}$$

Then, using (4.6) and (4.8) in (4.5) we find that

$$\left.\begin{aligned} -ik[1 - R]B_o &= -ikT = \mathscr{U}_o \\ \text{and} \qquad -k_n B_n^+ &= k_n B_n^- = \mathscr{U}_n , \quad n > 1 . \end{aligned}\right\} \tag{4.10}$$

The representation for ϕ therefore becomes on substituting (4.10) in (4.5),

$$\left.\begin{aligned} \phi^+(x,y) &= \left[e^{-ikx} + \left(1 + \frac{\mathscr{U}_o}{ikB_o}\right) e^{ikx}\right] f_o B_o - \sum_{n=1}^{\infty} \frac{\mathscr{U}_n f_n}{k_n} e^{-k_n x} \\ \phi^-(x,y) &= -\frac{\mathscr{U}_o f_o}{ik} e^{-ikx} + \sum_{n=1}^{\infty} \frac{\mathscr{U}_n f_n}{k_n} e^{k_n x} \end{aligned}\right\} . \tag{4.11}$$

Finally, matching ϕ across $x = 0$, $\ell < y < d$ gives

$$\frac{f_o B_o}{d} = \sum_{n=0}^{\infty} \mathscr{U}_n f_n R_n \tag{4.12}$$

where

$$R_n = \frac{1}{k_n d} \tag{4.13}$$

and $k_o = -ik$ has been used. Further, from (4.7) and (4.8),

$$\sum_{n=0}^{\infty} \mathcal{A}_n f_n = 0 , \quad 0 < y < \ell . \tag{4.14}$$

Equations (4.12) and (4.14) are two infinite systems of equations for the unknown constants $\mathcal{A}_n$. They can be combined into one system by multiplying each equation by $\frac{f_m}{d}$, integrating over the appropriate region of validity and then adding. This gives rise to the complex matrix equation

$$\sum_{n=0}^{\infty} E_{mn} \mathcal{A}_n = C_m \tag{4.15}$$

where

$$E_{mn} = (R_n - 1)D_{mn} + \delta_{mn} , \tag{4.16}$$

$$D_{mn} = \frac{1}{d}\int_{\ell}^{d} f_m(y) f_n(y)\, dy , \tag{4.17}$$

and

$$C_m = \frac{o}{d} D_{mo} = \frac{m}{d} . \tag{4.18}$$

Carrying out the integration in (4.17) gives

$$\left.\begin{aligned}
&D_{mn} = (N_m N_n)^{-\frac{1}{2}} \left[\frac{k_n d \sin k_n h \cos k_m h - k_m d \sin k_m h \cos k_n h}{k_n^2 d^2 - k_m^2 d^2}\right] \text{ for } n \neq m;\ m,n \geq 1;\\
&D_{mn} = \frac{1}{2N_m}\left[\frac{h}{d} + \frac{\sin 2k_m h}{2k_m d}\right] , \qquad m \geq 1 ;\\
&D_{on} = D_{no} = (N_o N_n)^{-\frac{1}{2}} \left[\frac{kd \sinh kh \cos k_n h + k_n d \sin k_n h \cosh kh}{k_n^2 d^2 + k^2 d^2}\right] , \ n \geq 1
\end{aligned}\right\} \tag{4.19}$$

and

$$D_{oo} = \frac{h}{2dN_o}\left[1 + \frac{\sinh 2kh}{2kh}\right].$$

It is clear from (4.13) and (4.16) that E_{mn} is real except for $n = 0$. Therefore it is convenient to define real constants $a_n, b_n, B_{or}, B_{oi}, \alpha_m, \beta_m$ such that

$$d\,\mathcal{A}_n = a_n + ib_n , \tag{4.20}$$

$$B_o = B_{or} + iB_{oi} \quad , \tag{4.21}$$

and
$$E_{mo} = \alpha_m + i\beta_m \tag{4.22}$$

where
$$\alpha_m = -D_{mo} \tag{4.23}$$

and
$$\beta_m = \frac{D_{mo}}{kd} \quad . \tag{4.24}$$

Using (4.18)-(4.22) and (4.24) in (4.15) gives

$$(\alpha_m + i\beta_m)(a_o + ib_o) + \sum_{n=1}^{\infty} E_{mn}(a_n + ib_n) = (B_{or} + iB_{oi})kd\beta_m$$

which on equating real and imaginary parts reduces to the two real systems of equations,

$$\alpha_m a_o + \sum_{n=1}^{\infty} E_{mn} a_n = (B_{or} kd + b_o)\beta_m \quad , \tag{4.25}$$

and
$$\alpha_m b_o + \sum_{n=1}^{\infty} E_{mn} b_n = (B_{oi} kd - a_o)\beta_m \quad . \tag{4.26}$$

Now, if S_n satisfies

$$\alpha_m S_o + \sum_{n=1}^{\infty} E_{mn} S_n = \beta_m \quad , \tag{4.27}$$

then (4.25) and (4.26) give

$$\left.\begin{aligned} a_n &= (B_{or} kd + b_o)S_n \quad , \\ \text{and} \qquad b_n &= (B_{oi} kd - a_o)S_n \quad . \end{aligned}\right\} \tag{4.28}$$

Combining these yield

$$a_o = (B_{or} + B_{oi}\, S_o)\, \frac{kdS_o}{1+S_o^2} \quad ,$$

$$b_o = (B_{oi} - B_{or}\, S_o)\, \frac{kdS_o}{1+S_o^2}$$

and substituting for a_n, b_n in (4.20) implies

$$\mathcal{U}_n = \frac{B_o kdS_n}{d(1+iS_o)} \quad . \tag{4.29}$$

Thus, once the system of equations (4.27) has been solved the $\mathscr{C}_n$'s are determined from (4.29), and therefore by (4.11), the full solution for $\phi(x,y)$ is known.

In particular, on the plate

$$\phi^{+}(0,y) = \left(1 + \frac{1}{1+iS_o}\right) B_o f_o(y) - \sum_{n=1}^{\infty} \frac{kS_n}{k_n(1+iS_o)} f_n(y)$$

and

$$\phi^{-}(0,y) = \left(1 - \frac{1}{1+iS_o}\right) B_o f_o(y) + \sum_{n=1}^{\infty} \frac{kS_n}{k_n(1+iS_o)} f_n(y) \ .$$

That is,

$$\phi^{\pm}(0,y) = \phi_I(0,y) \pm \gamma(y) \tag{4.30}$$

where $\phi_I(x,y)$ is given by (2.13) and

$$\gamma(y) = \frac{B_o f_o(y)}{1+iS_o} - \sum_{n=1}^{\infty} \frac{kS_n}{k_n(1+iS_o)} f_n(y) \ . \tag{4.31}$$

Clearly the quantities of prime interest are immediately available. From (4.10) and (4.29) the reflection coefficient is given by

$$|R| = \left|\frac{1}{1+iS_o}\right| \ , \tag{4.32}$$

and similarly the transmission coefficient is

$$|T| = \left|\frac{iS_o}{1+iS_o}\right| \tag{4.33}$$

showing, incidentally, that

$$|R|^2 + |T^2| = 1$$

as is required by conservation of energy flux.

4.4 The forces and moments acting on the barrier

The first-order force and moment acting on the barrier are found by integrating the linearized expression for the pressure,

$$p(x,y,t) = -\rho \frac{\partial \phi}{\partial t}(x,y,t) + \rho g y \ , \tag{4.34}$$

around the boundary of the plate. Thus, the force per unit width acting on the barrier is

$$\begin{aligned} X^{(1)}(t) &= \int_0^{\ell} \{p^-(0,y,t) - p^+(0,y,t)\}\, dy \\ &= \mathrm{Re}\{i\omega\rho e^{-i\omega t} \int_0^{\ell} [\phi^-(0,y,t) - \phi^+(0,y,t)]\, dy\} \\ &= \mathrm{Re}\{-2i\omega\rho e^{-i\omega t} \int_0^{\ell} \gamma(y)\, dy\} \\ &= \mathrm{Re}\left\{\frac{-2\rho g A \ell e^{-i\omega t}}{N_o^{-\frac{1}{2}} \cosh kd\,(1+iS_o)} \left[\frac{N_o^{-\frac{1}{2}}}{k\ell}(\sinh kd - \sinh kh) \right.\right. \\ &\qquad \left.\left. - \sum_{n=1}^{\infty} \frac{kdS_n N_n^{-\frac{1}{2}}}{k_n d k_n \ell}(\sin k_n d - \sin k_n h)\right]\right\} . \end{aligned} \tag{4.35}$$

Similarly, the first-order moment per unit width about the origin is

$$\begin{aligned} M^{(1)}(t) &= \int_0^{\ell} y\{p^-(0,y,t) - p^+(0,y,t)\}\, dy \\ &= \mathrm{Re}\{-2i\omega\rho e^{-i\omega t} \int_0^{\ell} y\gamma(y)\, dy\} \\ &= \mathrm{Re}\left\{\frac{-2\rho g A \ell^2 e^{-i\omega t}}{N_o^{-\frac{1}{2}} \cosh kd\,(1+iS_o)} \left[\frac{N_o^{-\frac{1}{2}}}{k^2\ell^2}(\cosh kd - \cosh kh - k\ell \sinh kh) \right.\right. \\ &\qquad \left.\left. - \sum_{n=1}^{\infty} \frac{kdS_n N_n^{-\frac{1}{2}}}{k_n d (k_n \ell)^2}(\cos k_n h - \cos k_n d - k_n \ell \sin k_n h)\right]\right\} . \end{aligned} \tag{4.36}$$

Therefore the centre of pressure, $C_p^{(1)}$, of the first-order force as a fraction of the barrier length, measured from the top edge downwards is

$$C_p^{(1)} = -\frac{M^{(1)}(t)}{\ell X^{(1)}(t)} \tag{4.37}$$

where $M^{(1)}(t)$ and $X^{(1)}(t)$ are given by the above expressions (4.35) and (4.36).

It has been shown (Haskind (1948), Ogilvie (1963)) that the mean values of the second-order hydrodynamic forces and moments acting on an oscillating body can be determined from the first-order velocity potential. For this, the exact expression for the pressure

$$p(x,y,t) = -\rho\frac{\partial\Phi_{ex}}{\partial t} + \rho g y - \frac{1}{2}\rho|\nabla\Phi_{ex}|^2 \ ,$$

where Φ_{ex} is the exact velocity potential, is needed.

Following Haskind (1959), the total force and moment acting on the barrier is

$$X(t) = \int_{\eta^-}^{\ell} p^-(0,y,t)dy - \int_{\eta^+}^{\ell} p^+(0,y,t)dy \ , \tag{4.38}$$

and

$$M(t) = \int_{\eta^-}^{\ell} yp^-(0,y,t)dy - \int_{\eta^+}^{\ell} yp^+(0,y,t)dy \ , \tag{4.39}$$

where $\eta^{\pm}$ is the increase in height of the fluid on the sides $x \gtrless 0$ respectively. Since we are concerned with the second-order problem and the integrals within the limits $\eta^{\pm}$ to zero give terms of the third-order for M, equations (4.38) and (4.39) can be written as

$$X = X_1 + X_2$$

with

$$X_1 = \int_0^{\ell} (p^- - p^+)\ dy \ ,$$

$$X_2 = \int_0^{\eta^+} p^+\ dy - \int_0^{\eta^-} p^-\ dy \ ,$$

and

$$M = \int_0^{\ell} y(p^- - p^+)\ dy \ .$$

Similarly, as X_2 gives second-order terms, it is sufficient to use the expression (4.34) for the linearized pressure to evaluate this quantity. Indeed, within the limits of integration, $\phi^{\pm}(0,y)$ can be replaced by their values at $y = 0$, and so, with equation (2.7)

$$X_2 = \frac{\rho}{2g}\left[\left(\frac{\partial\phi^-}{\partial t}\right)^2 - \left(\frac{\partial\phi^+}{\partial t}\right)^2\right] .$$

Let the notation

$$U^* = \frac{\omega}{2\pi} \int_t^{t+\frac{2\pi}{\omega}} U(t)\, dt$$

denote a time averaged quantity over a period of oscillation.

Now Haskind (1959) has shown that the mean second-order horizontal force and moment per unit width are given by

$$X^{(2)*} = \frac{\rho}{4} \int_0^{\ell} (|\nabla\phi^+|^2 - |\nabla\phi^-|^2)dy + X_2^* \tag{4.40}$$

and

$$M^{(2)*} = \frac{\rho}{4} \int_0^{\ell} y(|\nabla\phi^+|^2 - |\nabla\phi^-|^2)dy \tag{4.41}$$

where $\Phi(x,y,t)$ is the first-order velocity potential satisfying (2.9).

Using

$$(uv)^* = \frac{1}{2} \mathrm{Re}\ (u\bar{v})$$

with (4.1) and (4.30), (4.40) and (4.41) reduce to

$$X^{(2)*} = \frac{\rho g A k}{\omega \cosh kd}\ \mathrm{Im} \int_0^{\ell} \sinh k(d-y)\ \frac{d\gamma}{dy}\ (y)\ dy + \rho\omega A\ \mathrm{Im}\ \gamma(0)$$

$$M^{(2)*} = \frac{\rho g A k}{\omega \cosh kd}\ \mathrm{Im} \int_0^{\ell} y \sinh k(d-y)\ \frac{d\gamma}{dy}\ (y)\ dy\ .$$

Then after some manipulation,

$$X^{(2)*} = -\frac{1}{2}\rho g A^2 |R|^2 \left(1 + \frac{2kd}{\sinh 2kd}\right) \tag{4.42}$$

and

$$M^{(2)*} = \frac{-2\rho g A^2 \ell}{\sinh 2kd\ N_o^{-\frac{1}{2}}(1+S_o^2)} \left\{ \frac{N_o^{-\frac{1}{2}}}{4} \left(kd+kh - \frac{1}{2k\ell}\ [\cosh 2kd - \cosh 2kh] \right) \right.$$

$$+k\ell \sum_{n=1}^{\infty} \frac{S_n N_n^{-\frac{1}{2}}}{(k^2\ell^2+k_n^2\ell^2)^2} \left[2k\ell k_n \ell (\cosh kd\ \cos k_n d - \cos k_n h\ \cosh kh) \right.$$

$$\left. \left. +(k_n^2\ell^2 - k^2\ell^2)(\sinh kd\ \sin k_n d - \sin k_n h\ \sinh kh) \right] \right\} \tag{4.43}$$

where the result

$$(kd)^2 \sum_{n=1}^{\infty} \frac{S_n N_n^{-\frac{1}{2}}}{k_n d} \frac{\{k_n d \cosh kh \sin k_n h + kd \sinh kh \cos k_n h\}}{k_n^2 d^2 + k^2 d^2} = \frac{N_o^{-\frac{1}{2}}}{4} (\sinh 2kh + 2kh)$$

has been used. This relation corresponds to the zero, mean second-order horizontal force across the gap beneath the barrier. The expression (4.42) is in agreement with that obtained by Longuet-Higgins (1977).

The corresponding centre of pressure is

$$C_p^{(2)} = \frac{M^{(2)*}}{\ell X^{(2)*}} \tag{4.44}$$

All the determined expressions defining various properties of a fixed barrier in a fluid of finite depth require the solution of the infinite set of equations (4.27). As in Chapter 3 this is accomplished by truncating the system to a finite number of terms, N, and applying a standard numerical procedure. In this case the convergence is much slower, and the required limit as $N \to \infty$ must be studied. This is achieved by regarding the solution as functions of N, plotting them against N^{-1}, and then extrapolating back to zero. In this way it is seen that the convergence is almost linearly dependent on N^{-1} for large N. Using this linear extrapolation through N = 70, 80 and N = 90, 100, agreement was generally found to 3 or 4 significant figures. However, for smaller values of ℓ/d and certain values of kd, N needed to be larger to maintain the accuracy. The results of this method are presented in §4.6.

4.5 The narrow gap approximation

Here we consider the situation when the length of the barrier ℓ is such that only a small gap of width $h = 2\varepsilon$ remains. This instance is very similar to the work of Packham and Williams (1972) and Tuck (1975), of flow through a small aperture in a thin wall when only the upper wall is present. However in this case the symmetry of flow about a horizontal line through the mid-point of the gap is lost and therefore slight modifications have to be made to their work. Following Tuck (1971), the problem is solved by matching the inner solution valid in the neighbourhood of the gap, with the

outer solution valid at large distances from the barrier, in the overlap region where both expansions are assumed to be valid.

In the outer region, $2\varepsilon/\ell$ is assumed to be small, so an observer on the left-hand side of the barrier at a distance $O(\ell)$ from it will be unable to distinguish the flow from that of an oscillating source on the bottom of the fluid. At the same time a distant observer on the other side of the barrier will see,by continuity, the flow due to a sink of the same strength as the source. Therefore, for $x < 0$,

$$\phi(x,y) = mG(x,y;0,d) \tag{4.45}$$

where m is the half strength of the source whose velocity potential at $(0,d)$, $G(x,y;0,d)$, is given by Thorne (1953) as

$$G(x,y;0,d) = \log \frac{r}{r'} + 2 \int_0^\infty \left[\frac{\cosh t(d-y)}{\cosh td(K\cosh td - t\sinh td)} - e^{-td} \frac{\sinh td \sinh ty}{t \cosh td} \right] \cos tx \, dt$$

$$- 4\pi i \frac{\cosh k(d-y)\cos kx}{2kd+\sinh 2kd}$$

with

$$r^2 = x^2 + (y-d)^2 \quad \text{and} \quad (r')^2 = x^2 + (y+d)^2,$$

and where the integral takes its Cauchy principal value.

Similarly for $x > 0$,

$$\phi(x,y) = -mG(x,y;0,d) + (A_r + iA_i) \cosh k(d-y)\cos kx \tag{4.46}$$

where a standing wave of arbitrary amplitude has been introduced to account for an incident and a reflected wave, and A_r, A_i are real constants.

Now, as $|x| \to \infty$ it is clear that

$$G(x,y;0,d) \to - \frac{4\pi i \cosh k(d-y)}{2kd+\sinh 2kd} e^{ik|x|}$$

which from (4.45) and (4.46) gives

$$\phi(x,y) \to \left\{\left(\frac{A_r+iA_i}{2} + \frac{4\pi im}{2kd+\sinh 2kd}\right)e^{ikx} + \frac{(A_r+iA_i)}{2}e^{-ikx}\right\}\cosh k(d-y), \text{ as } x \to \infty,$$

and, as $x \to -\infty$,

$$\phi(x,y) \to -\frac{4\pi im \cosh k(d-y)}{2kd+\sinh 2kd}e^{-ikx} .$$

It therefore follows from (4.2) that the reflection coefficient

$$R = \frac{R'}{I} = 1 + \frac{8\pi im}{(2kd+\sinh 2kd)(A_r+iA_i)}$$

and the transmission coefficient

$$T = \frac{T'}{I} = \frac{-8\pi im}{(2kd+\sinh 2kd)(A_r+iA_i)} . \qquad (4.47)$$

All that remains is to determine the unknown constants A_r, A_i which requires a closer examination of the behaviour of the flow near the gap. In this region $r \to 0$ and

$$G(x,y;0,d) \to \log\frac{r}{2d} + 2\int_0^\infty \left[\frac{1}{\cosh td(K\cosh td - t\sinh td)} - \frac{e^{-td}\sinh^2 td}{t\cosh td}\right]dt$$

$$- \frac{4\pi i}{2kd+\sinh 2kd}$$

$$= \log r + \alpha_r + i\alpha_i + o(1)$$

where

$$\alpha_r = -\log 2d + 2\int_0^\infty \left[\frac{1}{\cosh td(K\cosh td - t\sinh td)} - \frac{e^{-td}\sinh^2 td}{t\cosh td}\right]dt$$

and $$\alpha_i = \frac{-4\pi}{2kd+\sinh 2kd} .$$

Hence as $z \to 0^+ + id$,

$$\phi \to -m[\log r + \alpha_r + i\alpha_i] + A_r + iA_i$$

giving

$$\Phi \to (-m[\log r + \alpha_r] + A_r)\cos \omega t - (m\alpha_i - A_i)\sin \omega t . \qquad (4.48)$$

Similarly as $z \to 0^- - id$,

$$\phi \to m[\log r + \alpha_r + i\alpha_i]$$

yielding

$$\Phi \to m[\log r + \alpha_r]\cos \omega t + m\alpha_i \sin \omega t \ . \qquad (4.49)$$

In the vicinity of the gap an observer positioned on the bottom of the fluid directly beneath the barrier will not feel the presence of the free surface. Rather he will see flow past a vertical, semi-infinite plate extending away from him bounded below by a rigid wall, as illustrated in fig. (4.1). To obtain the velocity potential for this motion use is made of the Schwarz-Christoffel transformation,

$$x + j(y-d) = \frac{h\zeta}{[h^2-\zeta^2]^{\frac{1}{2}}} \qquad (4.50)$$

which maps the z-plane onto the upper half ζ-plane with a correspondence between points as shown in fig. (4.2). The transformed flow is now represented by a source of strength m_ζ, say, at $\zeta = h$, and a sink of the same strength at $\zeta = -h$. Hence the complex potential, w, describing this flow is given by

$$w = m_\zeta \log \left(\frac{\zeta + h}{\zeta - h}\right) + C \ , \qquad (4.51)$$

where C is any constant.

It can be seen that this potential does indeed give the correct behaviour in the z-plane. In the neighbourhood of $\zeta = h$, corresponding to the quarter circle as $x \to \infty$ in the z-plane,

$$\zeta - h \to \frac{-h^3}{2r^2} \ , \quad \text{from (4.50)} \ .$$

So, as $x \to \infty$,

$$\begin{aligned} w &\to m_\zeta \log \left(\frac{-4r^2}{h^2}\right) + C \\ &= 2m_\zeta \log r + m_\zeta \log \left(-\frac{4}{h^2}\right) + C \ , \end{aligned} \qquad (4.52)$$

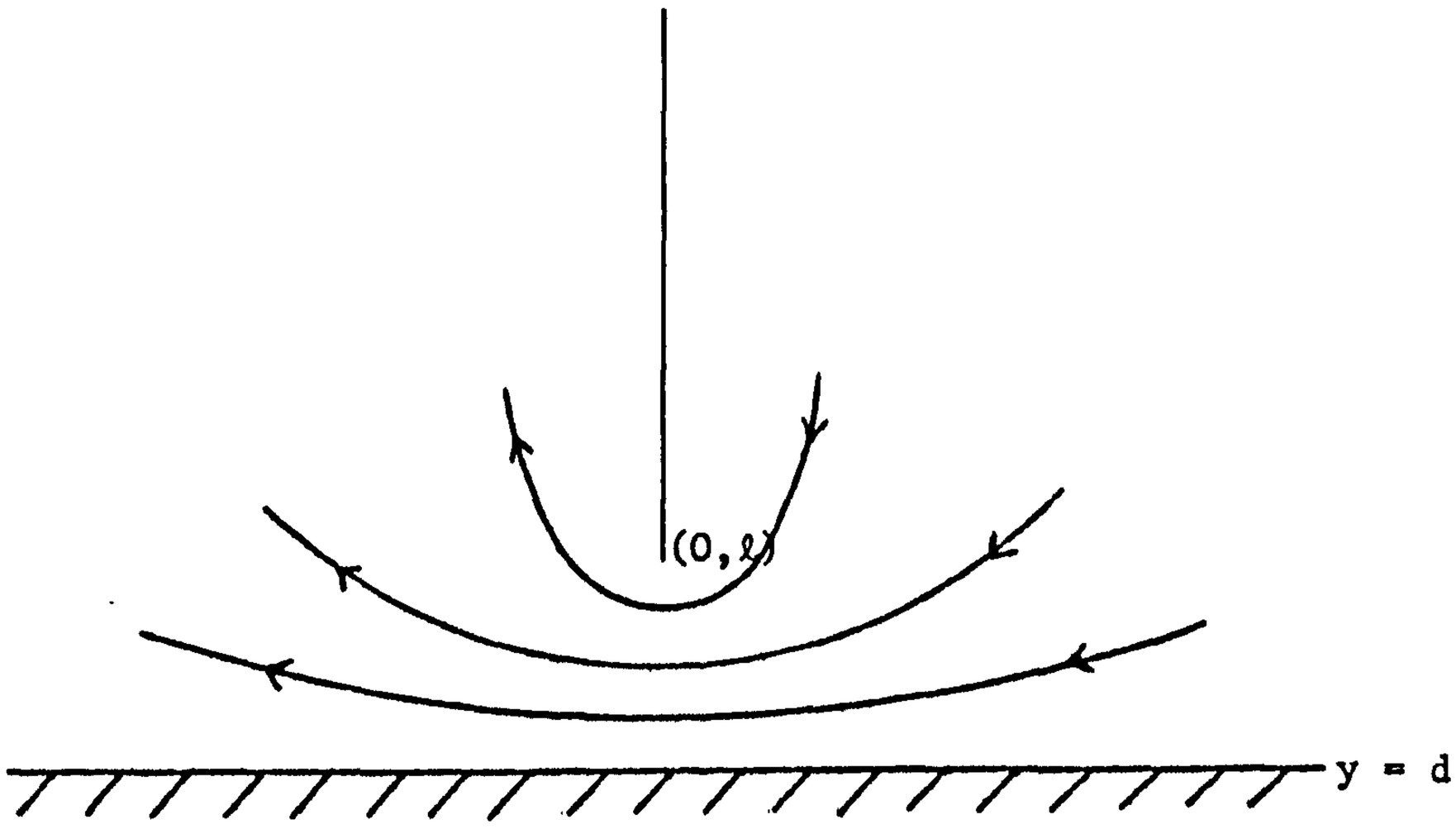

FIG. (4.1)

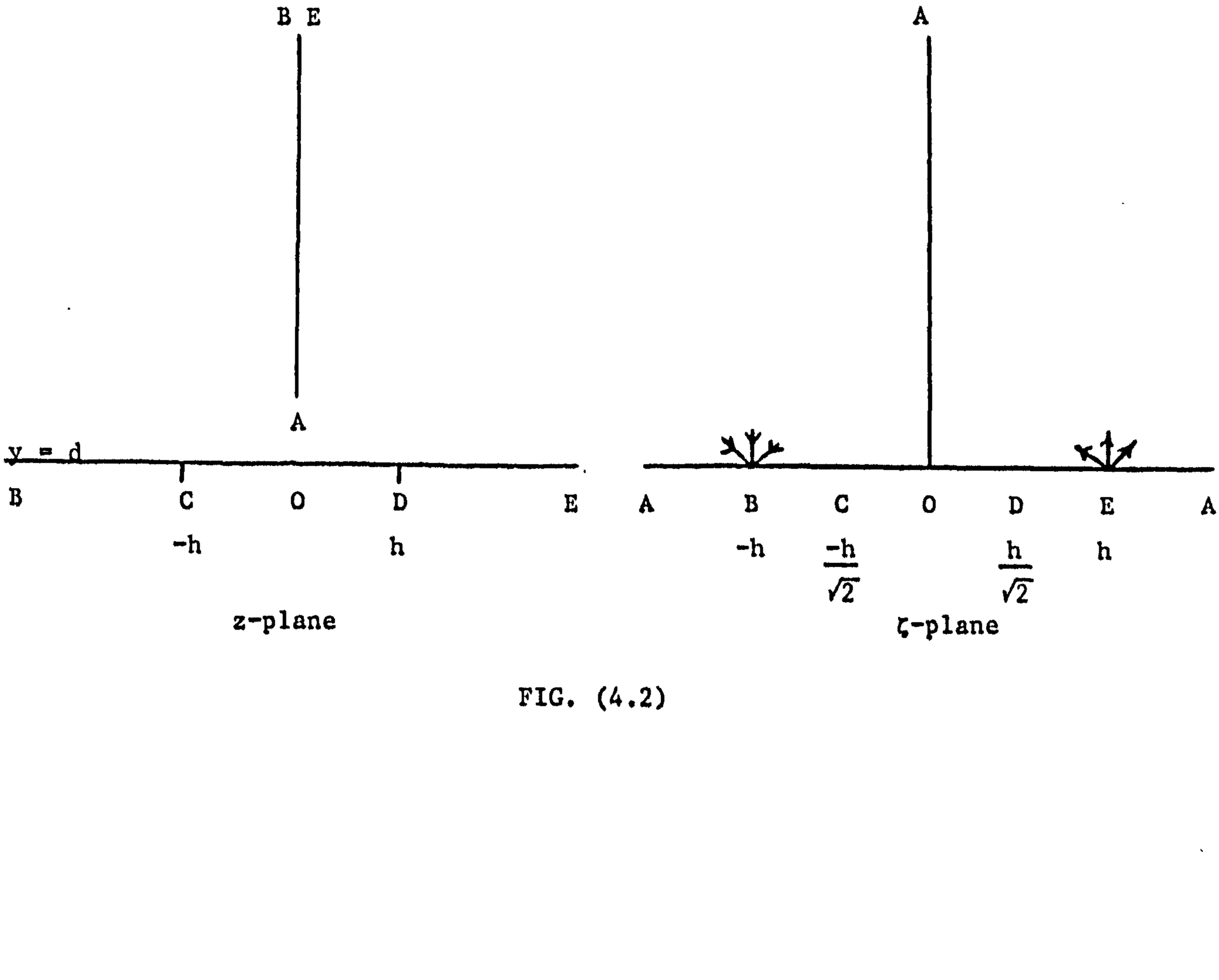

FIG. (4.2)

a flow due to a sink at x = 0, y = d. Similarly, in the neighbourhood of $\zeta = -h$ or the left-hand quarter circle in the z-plane,

$$\zeta + h \to \frac{h^3}{2r^2}$$

giving

$$w \to -2m_\zeta \log r - m_\zeta \log\left(-\frac{4}{h^2}\right) + C \ , \quad \text{as } x \to -\infty \ . \tag{4.53}$$

This represents a source like flow away from x = 0, y = d. The real part of (4.52) and (4.53) gives the velocity potential as

$$\phi(x,y,t) \to 2m_\zeta \log r + m_\zeta \log\left(\frac{4}{h^2}\right) + C_r \ , \quad \text{as } x \to \infty \tag{4.54}$$

and

$$\phi(x,y,t) \to -2m_\zeta \log r - m_\zeta \log\left(\frac{4}{h^2}\right) + C_r \ , \text{ as } x \to -\infty \ , \tag{4.55}$$

where C_r is the real part of the constant C.

The inner behaviour of the outer solution given by equations (4.48) and (4.49) must now be matched with equations (4.54) and (4.55) respectively, which provide the outer limit of the inner solution. Thus

$$2m_\zeta = -m \cos \omega t \ , \tag{4.56}$$

$$(A_r - m\alpha_r) \cos \omega t + (A_i - m\alpha_i) \sin \omega t = m_\zeta \log\left(\frac{4}{h^2}\right) + C_r \tag{4.57}$$

and

$$m\alpha_r \cos \omega t + m\alpha_i \sin \omega t = -m_\zeta \log\left(\frac{4}{h^2}\right) + C_r \ . \tag{4.58}$$

Eliminating C_r from (4.57) and (4.58), substituting m_ζ from (4.56) and equating coefficients of cos ωt, sin ωt gives

$$A_r = 2m\alpha_i \ ,$$

$$A_i = 2m\alpha_r - m \log\left(\frac{4}{h^2}\right) \ .$$

Therefore from (4.47) the transmission coefficient is

$$|T|^{-2} = 1 + \left[\frac{(2kd+\sinh 2kd)}{2\pi} \left\{ \int_0^\infty \left[\frac{1}{\cosh td(K\cosh td - t\sinh td)} - \frac{e^{-td}\sinh^2 td}{t\cosh td} \right] dt + \frac{1}{2} \log\left(\frac{h}{4d}\right) \right\} \right]^2 .$$

This expression is in agreement with those given by Packham and Williams (1972) and Tuck (1975) when the fluid bottom is taken to pass through the centre of the gap in the barriers.

4.6 Results and discussion

Curves for the reflection and transmission coefficients and their arguments are shown below in figs. (4.3)-(4.6). Firstly, as a check on the numerical procedure involved, results are presented for a deep fluid so that comparison can be made with the infinite depth results of Ursell (1947), namely,

$$|R| = \frac{\pi I_1(K\ell)}{\pi^2 I_1^2(K\ell) + K_1^2(K\ell)} , \qquad |T| = \frac{K_1(K\ell)}{\pi^2 I_1^2(K\ell) + K_1^2(K\ell)} ,$$

$$\arg(R) = \tan^{-1}\left(\frac{-K_1(K\ell)}{\pi I_1(K\ell)}\right) , \quad \arg(T) = \tan^{-1}\left(\frac{\pi I_1(K\ell)}{K_1(K\ell)}\right) .$$

Figures (4.3) and (4.4) show that this agreement is very good, for the case $\ell/d = 1/10$ is indistinguishable from the infinite depth results. In addition to this, the following physical consideration of the problem justifies the shape of the curves.

When k is small, the wavelength of the wave is so large that the wave does not sense the presence of the plate. Therefore the amount of reflection is small. As the wave number increases, the wavelength becomes comparable with the dimensions of the plate and more of the wave is reflected. Ultimately, when the wavelength diminishes completely, all of the wave is reflected. The description of the "argument" curves follows as a logical consequence,for when the incident wave undergoes no reflection, the transmitted wave is exactly in phase with the incoming wave. However, as an increasing proportion of the wave gets reflected,

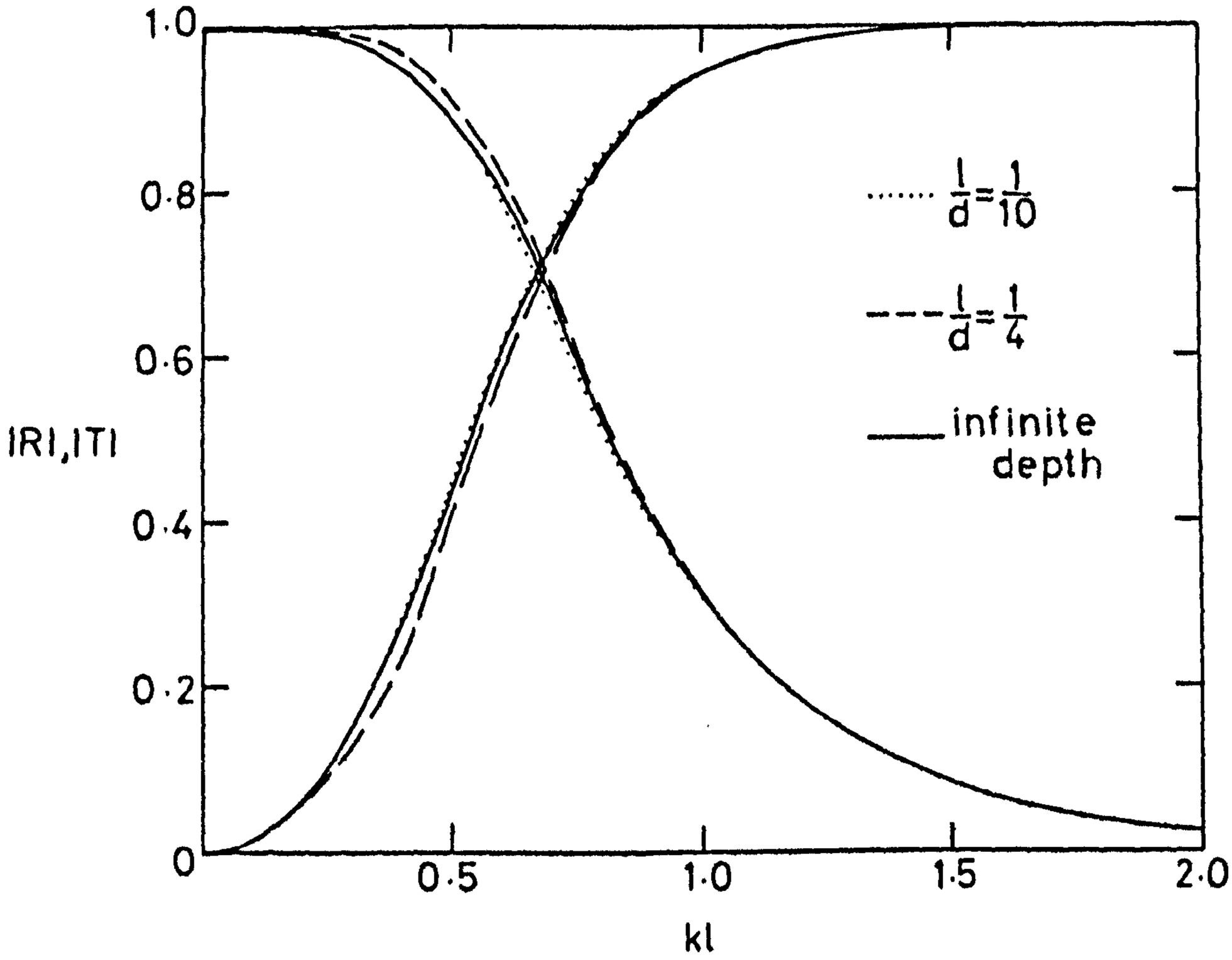
1·0
0·8
0·6
0·4
0·2
0
IRI,ITI
0·5
1·0
1·5
2·0
kl
$\frac{1}{d}=\frac{1}{10}$
$\frac{1}{d}=\frac{1}{4}$
infinite depth

FIG. (4·3)

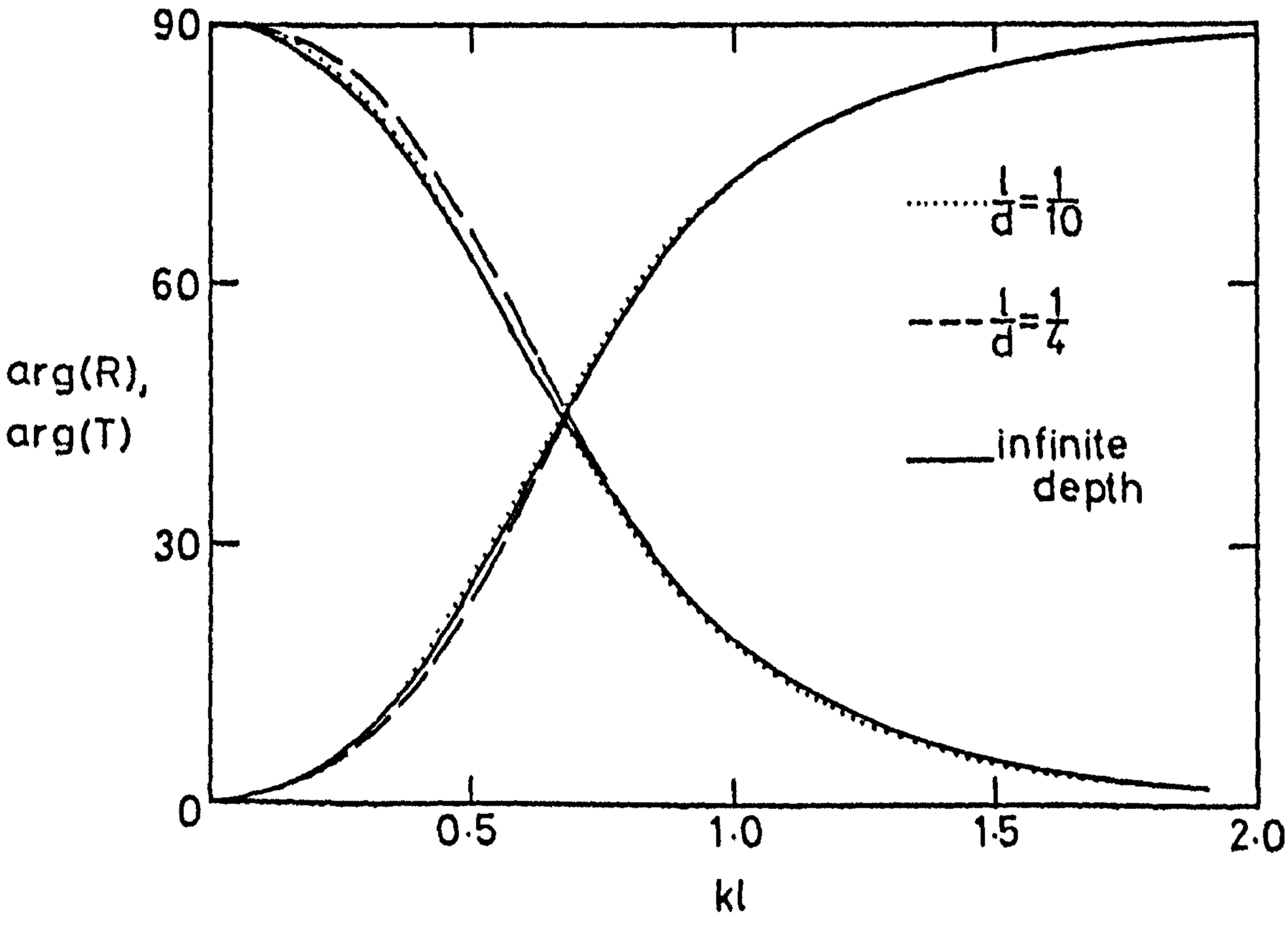
90
60
30
0
arg(R),
arg(T)
0·5
1·0
1·5
2·0
kl
$\frac{1}{d}=\frac{1}{10}$
$\frac{1}{d}=\frac{1}{4}$
infinite depth

FIG. (4·4)

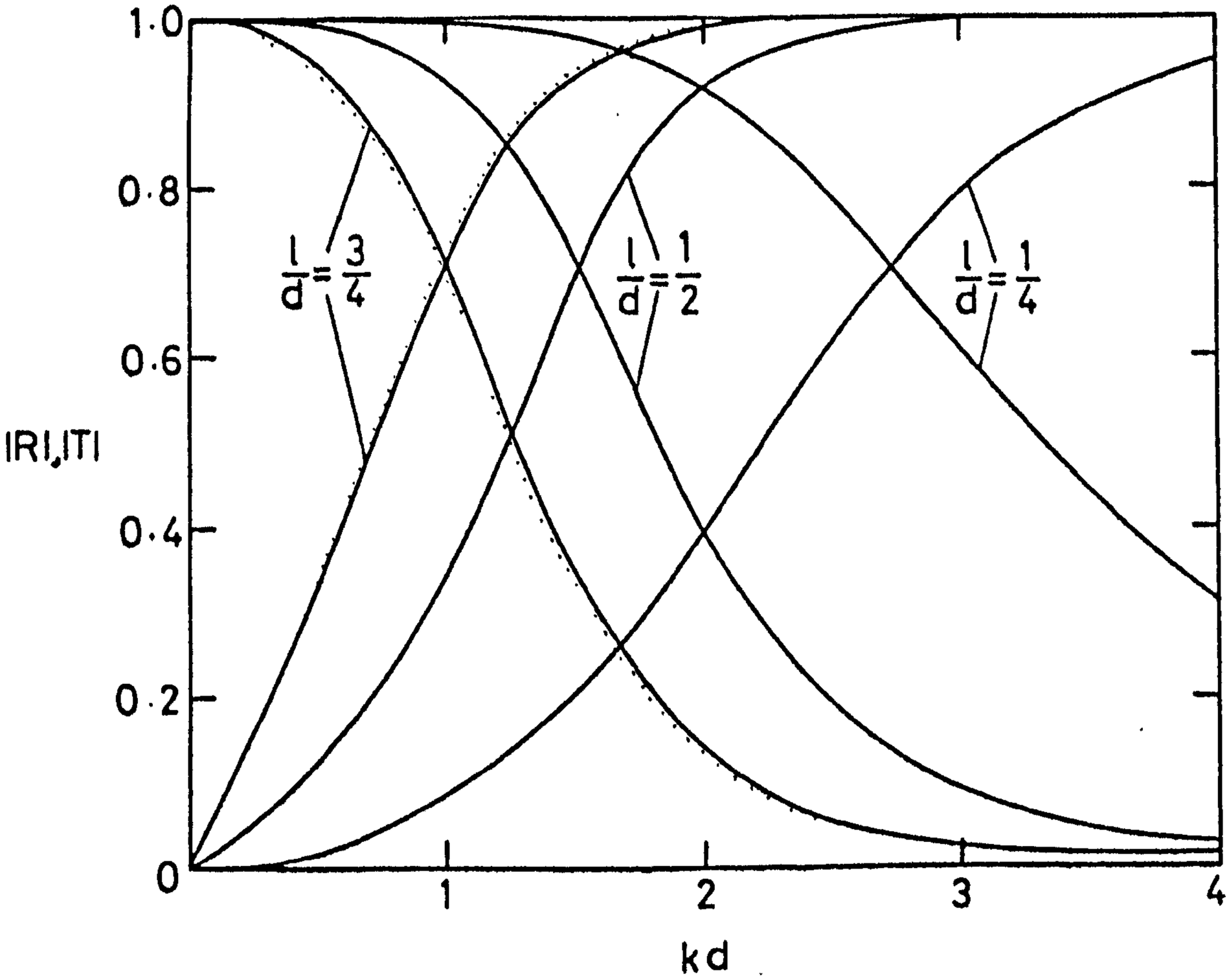
1·0
0·8
0·6
0·4
0·2
0
|R|,|T|
l/d = 3/4
l/d = 1/2
l/d = 1/4
1
2
3
4
kd

FIG. (4·5)

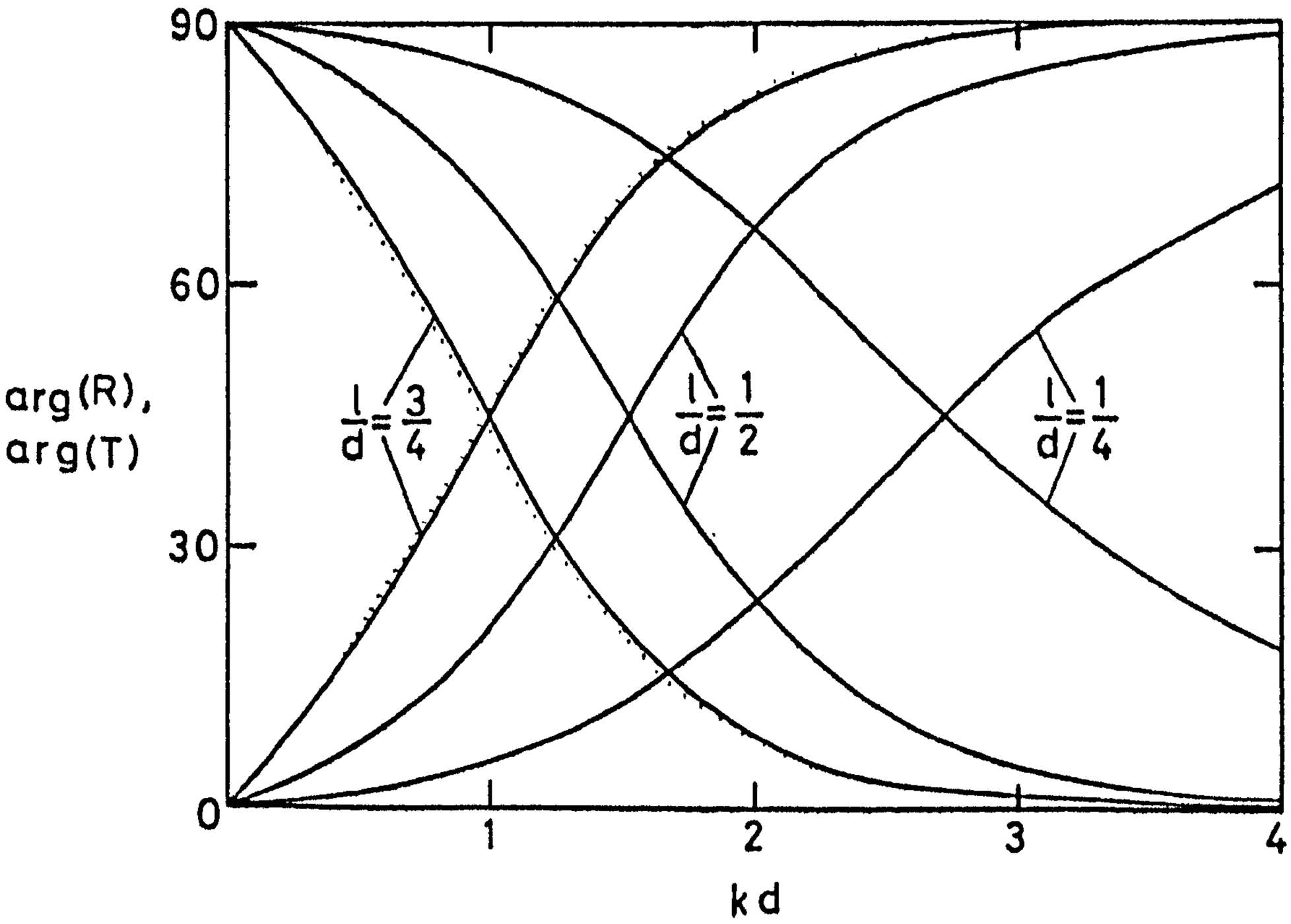
90
60
30
0
arg(R),
arg(T)
l/d = 3/4
l/d = 1/2
l/d = 1/4
1
2
3
4
kd

FIG. (4·6)

the transmitted wave suffers a growing phase shift until finally it leads by 90°. This occurs when the incident wave is completely reflected. Since the reflected wave travels in the opposite direction to the incident wave its corresponding phase undergoes a lag in a complementary manner to the transmitted argument. Thus, when the waves are very large it begins with a maximum lag of 90° which decreases as the wavelength decreases until eventually the reflection is in phase with the incoming wave.

This explanation is pronounced in figs. (4.5) and (4.6) where the effect of the barrier length is emphasized. As expected, a short barrier provides little resistance to the majority of incident waves, except those whose wavelength is very small. Hence the amount of reflection increases slowly over the wavenumber range considered. In contrast to this a long barrier produces the opposite effect with a greater proportion of the wave being reflected. Similarly, the argument curves are also in accordance with the physical results.

The dotted curves on these figures display the approximate results derived in §4.5 for the extreme case of a very long barrier. There is a slight discrepancy between the two curves when $\ell/d = 3/4$, but it is seen that as the gap gets smaller these differences decrease. Indeed, when $\ell/d = \cdot 9$, the two curves are indistinguishable. Finally, the reflection curves for $\ell/d = 1/2$ compare well with the results of the variational technique presented in Mei and Black (1969).

As in Black, Mei and Bray (1971), the horizontal force and moment expressions are normalized with respect to the characteristic hydrostatic force due to the incident wave. Thus curves are presented for

$$\frac{|X^{(1)}(t)|}{2\rho g A \ell}, \quad \frac{|M^{(1)}(t)|}{2\rho g A \ell^2}, \quad \frac{-X^{(2)*}}{\frac{1}{2}\rho g A^2}, \quad \frac{M^{(2)*}}{\frac{1}{2}\rho g A^2 \ell}$$

and $C_p^{(1)}$, $C_p^{(2)}$.

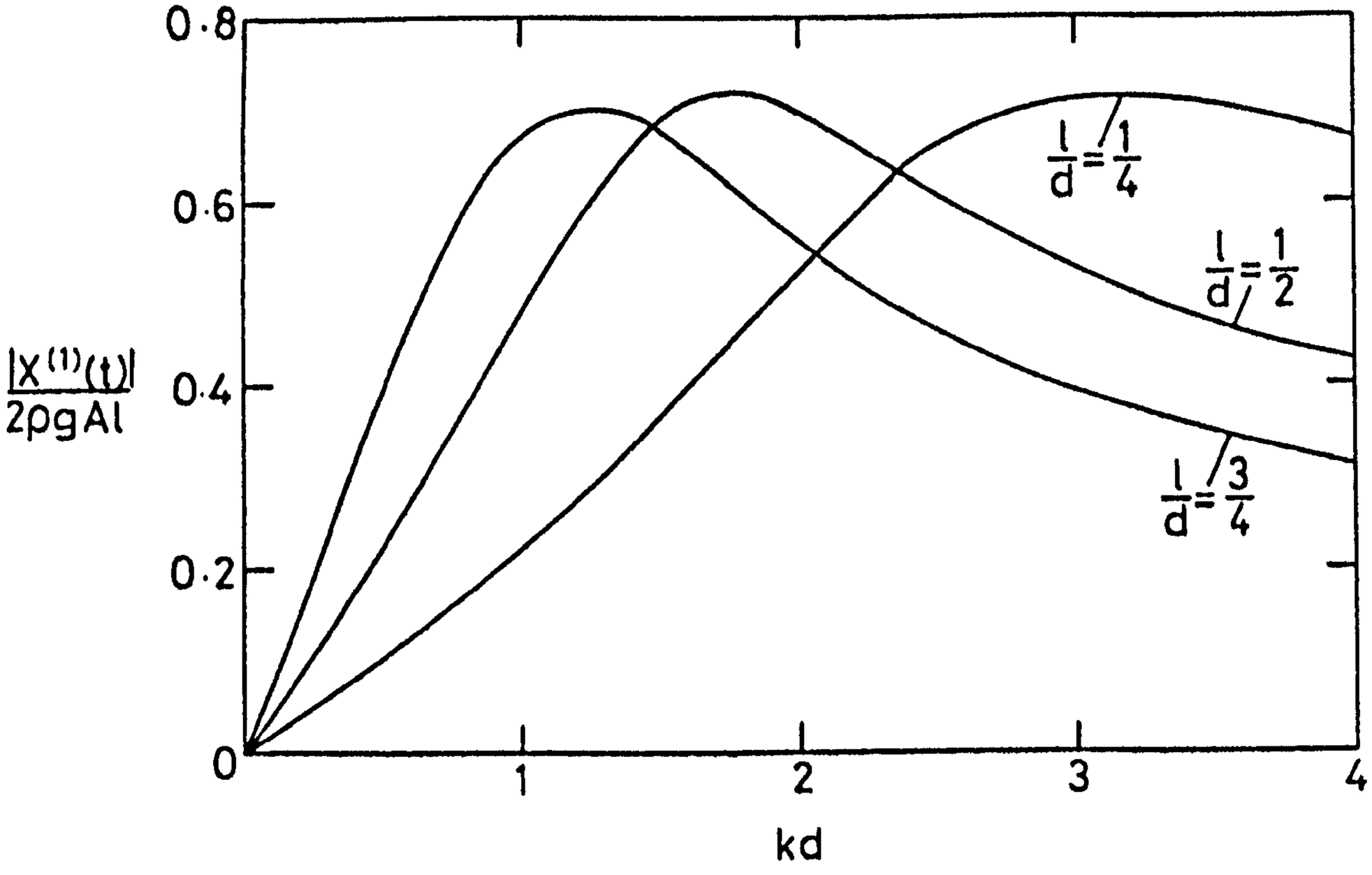
0·8
0·6
0·4
0·2
0
1
2
3
4
kd
$\frac{|X^{(1)}(t)|}{2\rho g A l}$
$\frac{l}{d}=\frac{1}{4}$
$\frac{l}{d}=\frac{1}{2}$
$\frac{l}{d}=\frac{3}{4}$

FIG. (4·7)

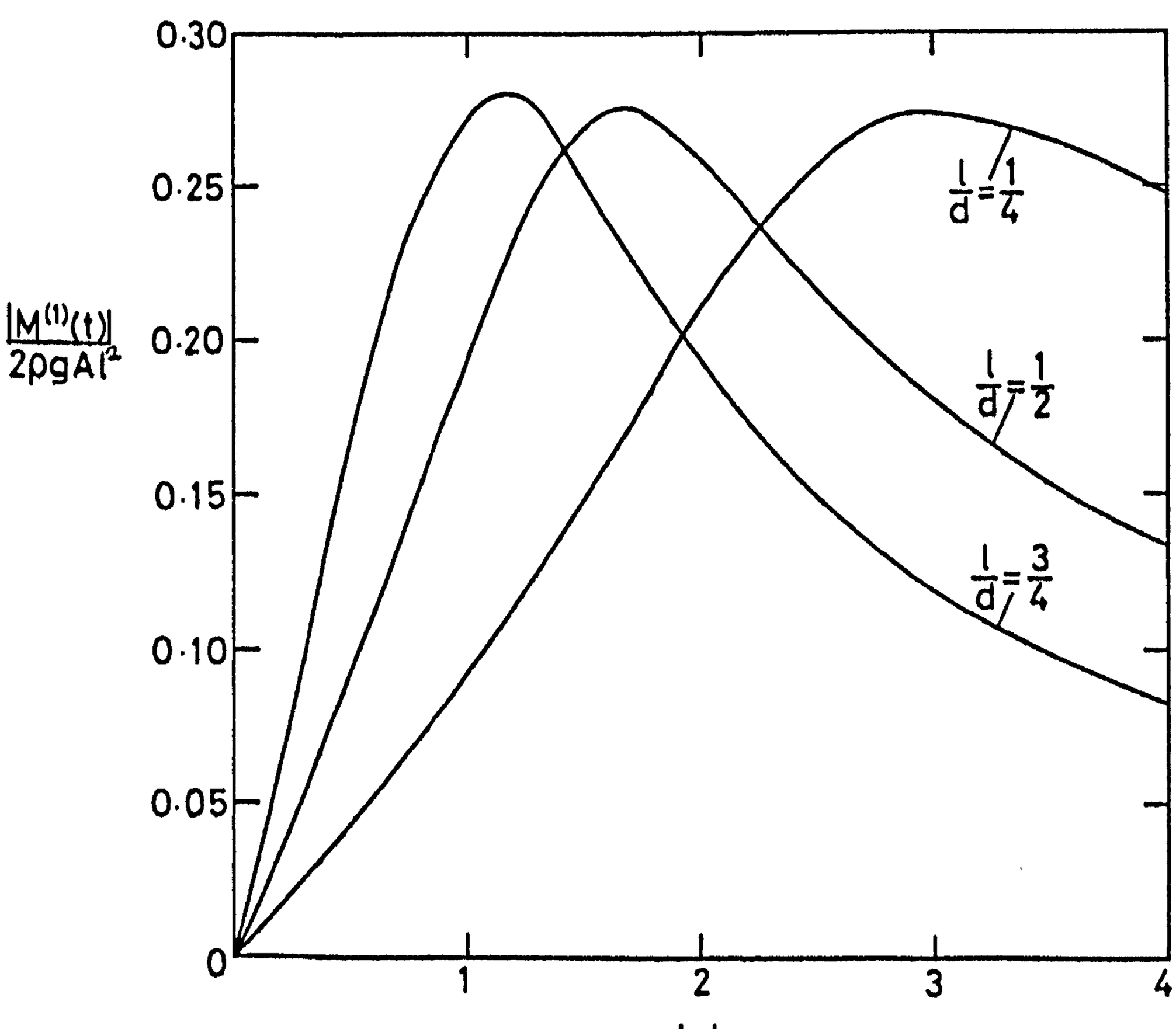
0·30
0·25
0·20
0·15
0·10
0·05
0
1
2
3
4
kd
$\frac{|M^{(1)}(t)|}{2\rho g A l^2}$
$\frac{l}{d}=\frac{1}{4}$
$\frac{l}{d}=\frac{1}{2}$
$\frac{l}{d}=\frac{3}{4}$

FIG. (4·8)

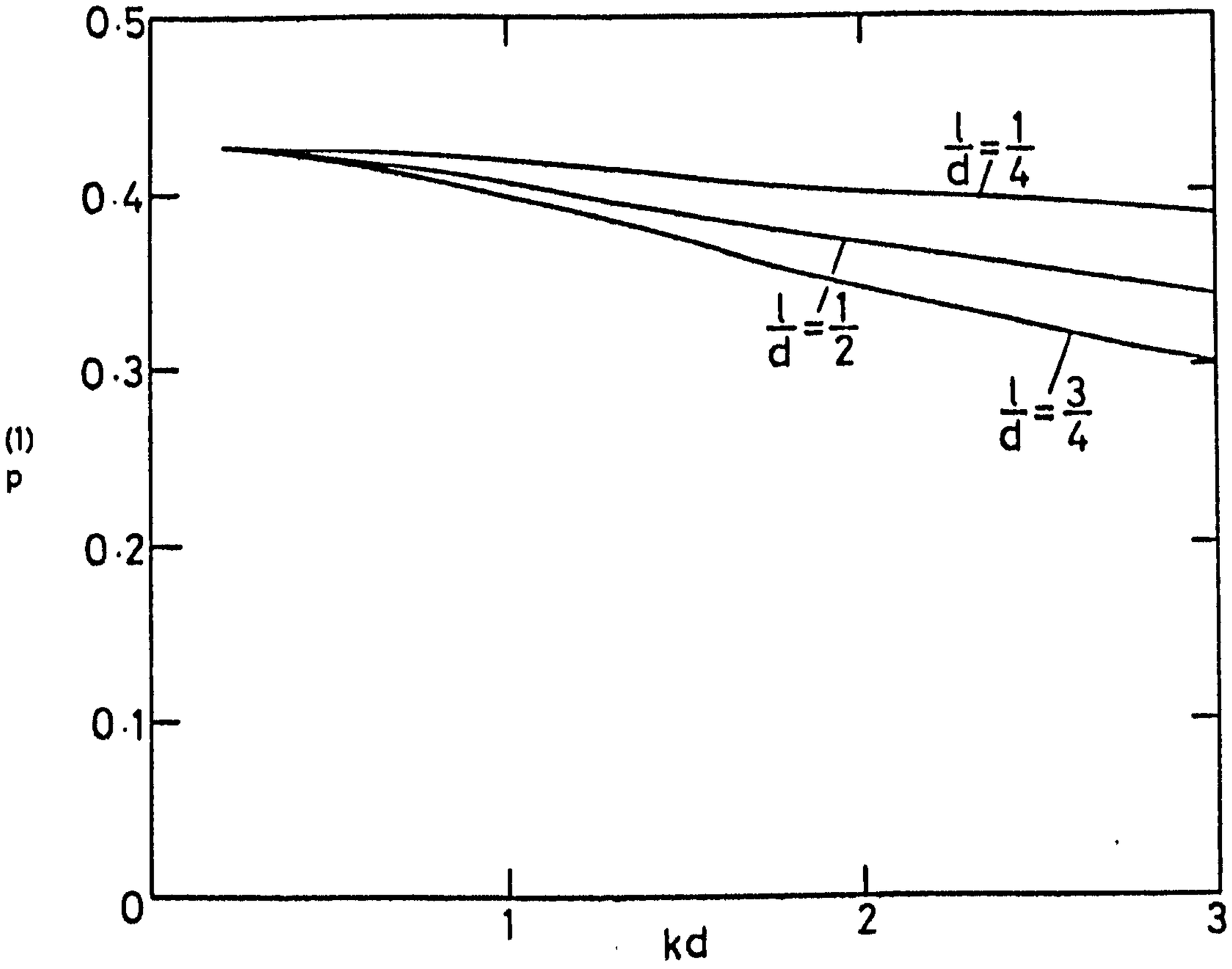

FIG. (4·9)

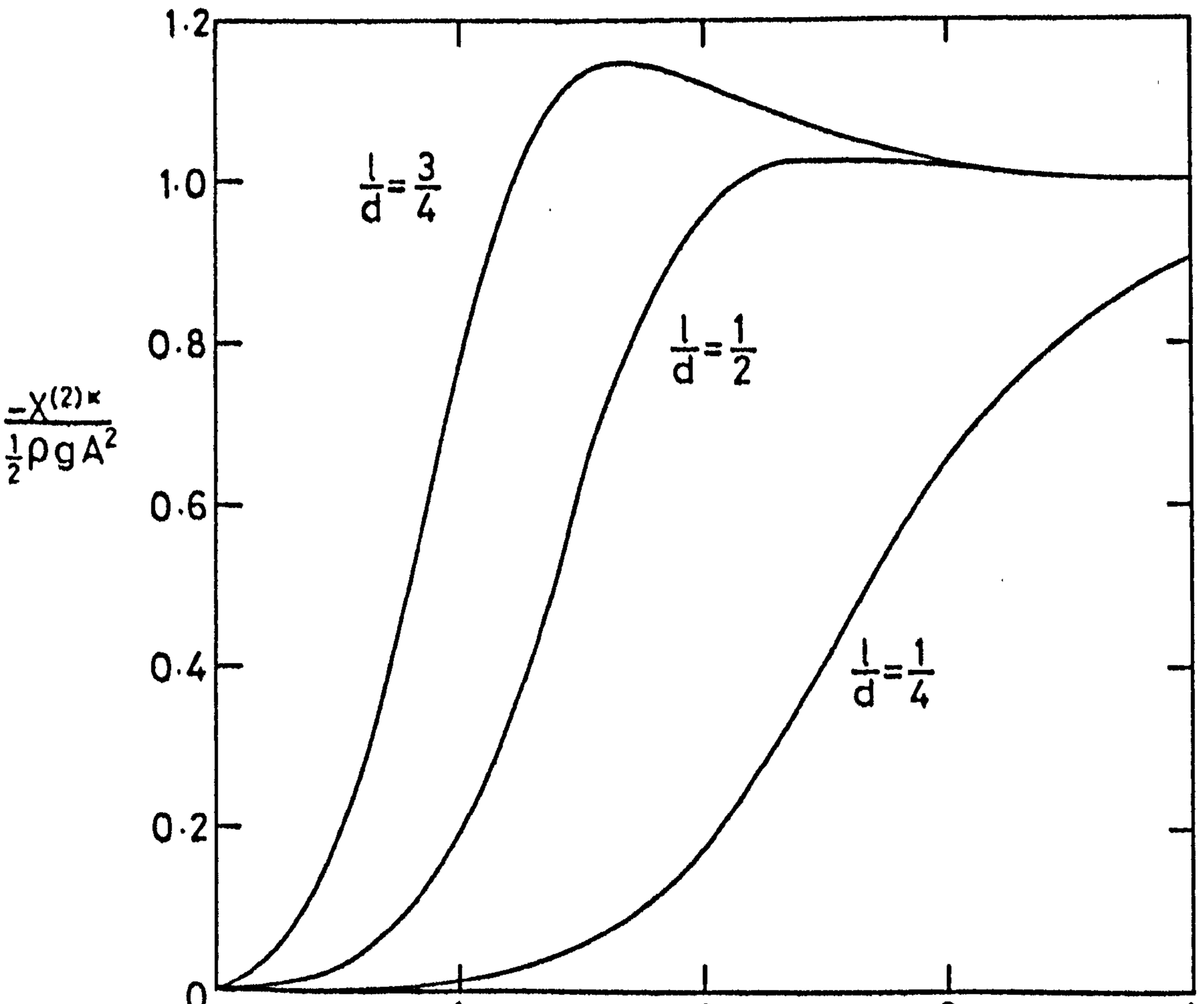

FIG. (4·10)

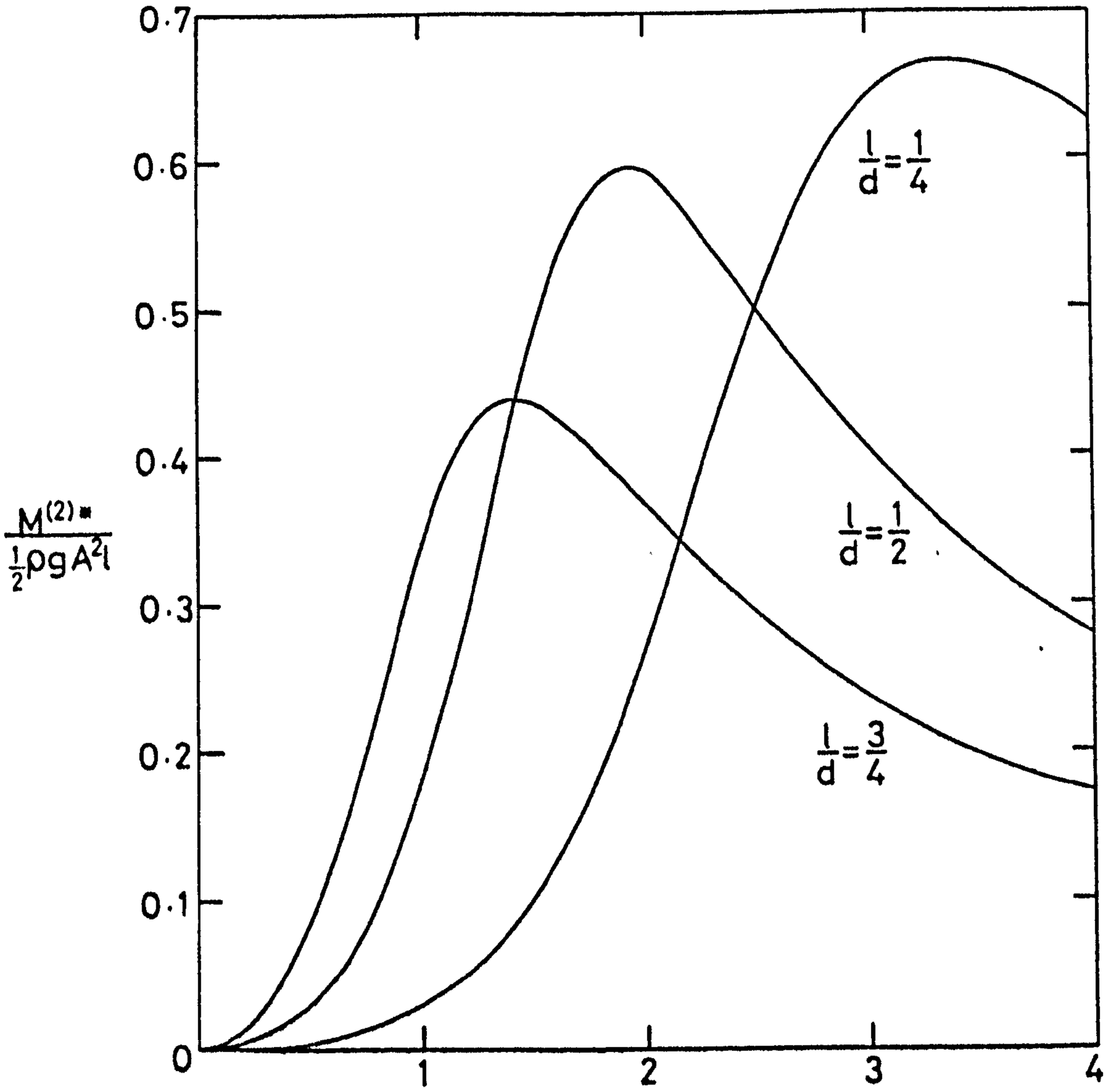

FIG. (4·11)

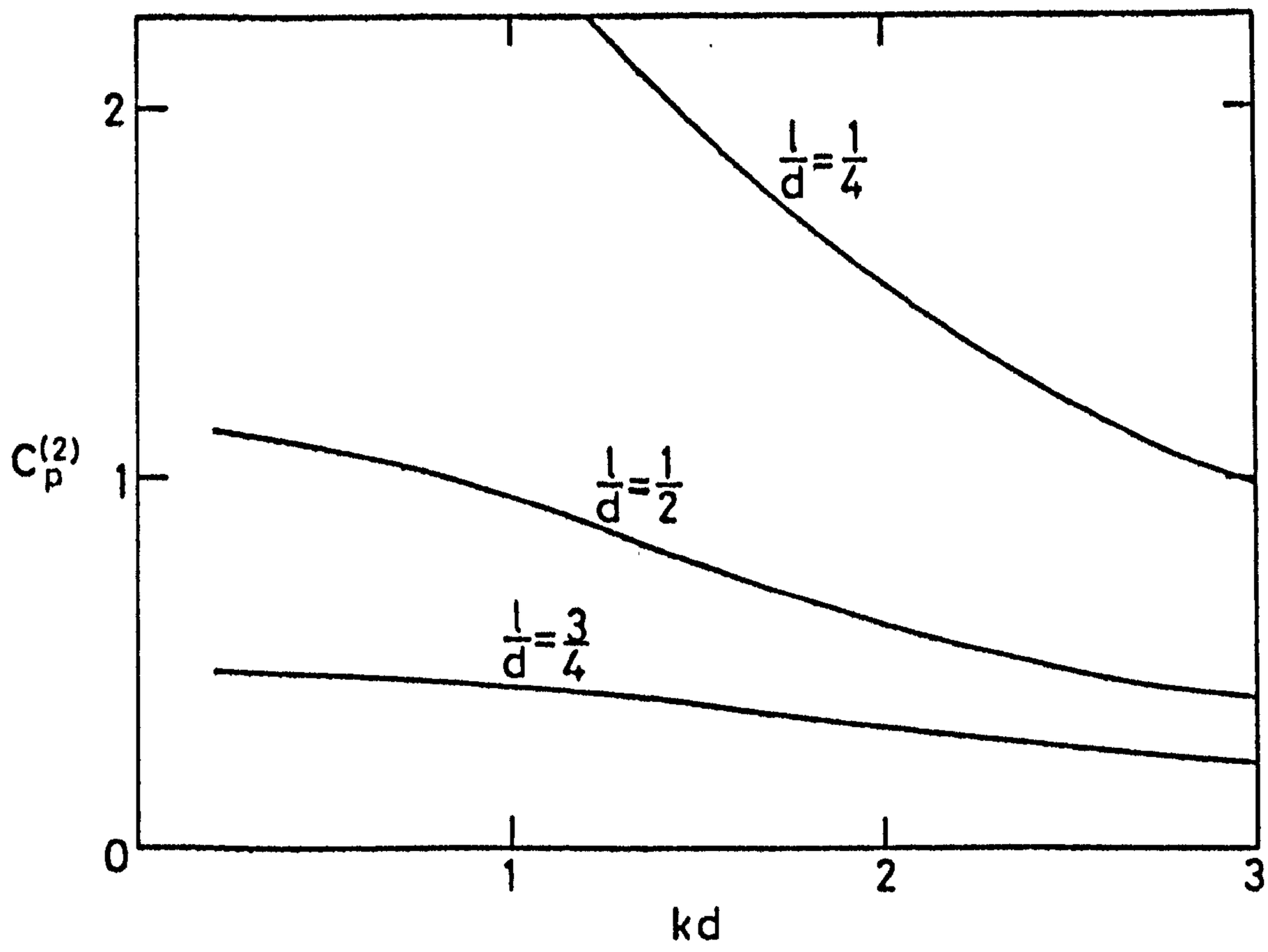

FIG. (4·12)

The amplitude of the normalized first-order horizontal force and moment acting on the plate is shown in figs. (4.7) and (4.8) respectively, where the case $\ell/d = 1/2$ is in very good agreement with the results published in Black, Mei and Bray, obtained by exploiting the approximate variational method. As the plate gets longer both the force and the moment reaches its maximum at a smaller value of the wavelength and subsequently dies away more rapidly. The corresponding centre of pressure of this horizontal, oscillatory force as a fraction of the plate length is displayed in fig. (4.9). For large kd or short waves, the force will act at a point very close to the top edge of the plate. Hence the curves tend asymptotically to zero as $kd \to \infty$. This decay is slower for a shorter barrier, since then the force is more uniformly distributed over its length.

In conclusion, figs. (4.10) and (4.11) show the variation of the average second-order horizontal force and moment, whilst the point of action of this force is presented in fig. (4.12). In contrast to the centre of the first-order force which acts through a point on the plate, this force acts through a point lying above the free surface since $C_p^{(2)}$ is negative. There is also a greater fluctuation over the wavelength range.

4.7 Conclusion

A study has been made of the diffraction of waves by a fixed vertical barrier in a fluid of finite depth. In particular, results are presented for the reflection and transmission coefficients and the first- and mean second-order forces. In the limiting case of a very deep fluid, these computations are in agreement with the exact solution of Ursell (1947), whilst in the extreme case of a very long barrier, an approximate solution compares very favourably with the full solution.

CHAPTER 5

THE TRANSIENT MOTION OF A PARTIALLY IMMERSED ROLLING STRIP IN WATER

5.1 Introduction

When a body floating on, or submerged in a fluid is initially disturbed from its hydrostatic equilibrium position, the subsequent motion consists of a motion of the body and the wave motion of the fluid. If the fluid is unbounded horizontally, energy is continually transferred away from the body, into the fluid, and out to infinity. The amplitude of the body motion decays until finally both the body and the fluid return to their equilibrium state.

This general problem has been investigated by several authors. Wehausen and Laitone (1960) present a general theory for an initially displaced body which reduces the solution to a pair of integro-differential equations. They then describe the work of Sretenskii (1937) who simplifies the problem to obtain a single integro-differential equation which is solved numerically for a thin wedge.

Ursell (1964) discusses a Fourier transform method applicable to bodies of arbitrary shape in two and three dimensions and considers in detail the small amplitude heaving motion of a half-immersed, long, horizontal circular cylinder in deep water. The cylinder is set in motion either by an applied force or by an initial displacement, in each case the cylinder's subsequent vertical displacement being described in the form of a Fourier integral. This integral involves a force coefficient term which represents the force acting on the body when it is undergoing forced time-harmonic oscillations, and can be determined

for any one value of the frequency by solving an infinite system of equations. Thus this term is not known in closed form and therefore the displacement expressions are not explicit. However Ursell found that the oscillatory behaviour eventually becomes exponentially small and that ultimately the decay is algebraic, like t^{-3} or t^{-2} for the motion generated by an initial force or an initial displacement respectively. A numerical study of this problem is made in Maskell and Ursell (1970) where the infinite system of equations is truncated in order to compute the behaviour of the motion. Furthermore, an experimental observation of a heaving sphere has been made by Bailey, Griffiths and Maskell (1976).

A similar method is used by Kotik and Lurye (1967) in looking at the heaving motion produced by an initial displacement on a half-submerged circular cylinder and sphere. This time the force term is evaluated by use of the so called Hi-Fi approximation (a computational method for evaluating heave damping parameters which are asymptotically valid at high and low frequencies and are quite accurate at all frequencies) and the Kramers-Kronig relations (Kotik and Mangulis, 1962) relating the added mass and damping coefficients. However another approach is utilized in Kotik and Lurye (1964) to examine the asymptotic behaviour of this motion. Here expressions of the added mass and damping parameters for small frequencies lead to the asymptotic result that for an arbitrary, surface-piercing body, a three-dimensional body approaches equilibrium faster than a two-dimensional one by a factor proportional to t^{-2}. Indeed the asymptotic decay of t^{-2} for a circular cylinder is in agreement with Ursell's (1964) result.

In all of the above work viscosity and surface tension have been neglected and the equations of motion linearized. Warren (1968) develops the theory to include the effect of viscosity by looking at

vertically symmetric bodies whose thicknesses are small compared with their lateral dimensions and constrained to heaving motion. For this body shape damping is less and viscosity more important than for fatter bodies. The specific case of a disc is taken and it is found that superimposed on the oscillations is a small displacement which decays like t^{-4} or t^{-5}, corresponding to the motion following an initial displacement or an initial force.

In this chapter we revert to the original conditions of neglecting viscosity and surface tension, and use Ursell's approach to look at the two-dimensional rolling motion of an initially disturbed vertical strip in deep water which is pivoted along its submerged end and subject to a linear restoring force. (Even though the equations of motion are linearized this could be relevant to the rolling of a thin ship if the angle of roll is small and the effect of the beam is neglected.) Under the Fourier transform to the frequency domain the motion can be regarded as simple harmonic forced rolling motion. Thus the force coefficient describing the hydrodynamic force is known explicitly, for Mei (1976) using Ursell's (1948) theory, derives the added inertia and damping coefficients. This damping parameter had previously been deduced by Kotik (1963), from which he calculated the added inertia by numerically integrating the Kramers-Kronig relation. Meanwhile in the addendum a reviewer (J.N. Newman) quotes the analytic expression for this parameter when the barrier rolls about a fixed point in the free surface. Although numerical computations for these coefficients have been presented, with a discussion of Kotik's accuracy appearing in Porter (1965), there has been no published working of the techniques involved to obtain the explicit expressions. Therefore, in Appendix A these results are derived, using a method due to Porter (1974).

The problem is formulated in §5.2. The motion following the

disturbance caused by an applied force on the strip is considered in §5.3, and in §5.4 the strip is displaced, the fluid allowed to come to rest and then the motion following the strip's release is found. In both cases the displacement is obtained in terms of a Fourier integral which involves two parameters. A comment on the corresponding behaviour in an undamped system is added before examining these integrals in §5.5 both analytically and numerically. The computed results are plotted and discussed, with final conclusions being drawn in §5.8.

5.2 Formulation

A strip is hinged in deep water at the fixed point (0,a) such that its equilibrium position is $x = 0$, $0 < y < a$. The angular displacement of the strip from this position is to be found.

Under the usual assumptions of two-dimensional linearized inviscid flow the fluid motion is described by a velocity potential $\phi(x,y,t)$ which satisfies equations (2.1), (2.2b), (2.8) and the radiation condition at infinity that waves exist which travel away from the strip. As in problems of this type the fluid velocity will necessarily possess a square root singularity at the edge of the strip. The roll amplitude of the strip is assumed small so that its normal velocity is given by

$$\frac{\partial \phi}{\partial x} = (a-y)\ \Theta_o(t) \qquad x = 0,\ 0 < y < a\ . \tag{5.1}$$

Finally, the equation of motion of the strip is

$$I_o\ \ddot{\Theta}_o(t) = -\ k_s\ \Theta_o(t) - \int_{s_o} [p](a-y)dy + F_o(t)$$

where [ ] denotes the jump across the strip and $I_o = \frac{1}{3}\rho s h a^3$, is the moment of inertia per unit length of the plate about the bottom edge where s is the specific gravity of the strip and h is its small thickness.

On the right-hand side of this equation the first term is the restoring force due to an external spring of stiffness k_s, the second is the resultant of the hydrodynamic pressures, and the third term is the applied rotational force. On using Bernoulli's theorem, this equation becomes

$$I_o \ddot{\Theta}_o(t) = - k_s \Theta_o(t) + \rho \int_o^a (a-y)\left[\frac{\partial \Phi}{\partial t}(0,y,t)\right]dy + F_o(t) \quad . \tag{5.2}$$

The Fourier transform is applied to these equations, supposing that there is no motion when $t < 0$ and by writing

$$\phi(x,y,\omega) = \int_o^\infty e^{i\omega t}\phi(x,y,t)dt \quad , \tag{5.3}$$

$$\theta_o(\omega) = \int_o^\infty e^{i\omega t}\ \Theta_o(t)dt \quad , \tag{5.4}$$

$$f_o(\omega) = \int_o^\infty e^{i\omega t}F_o(t)dt \ .$$

The corresponding inversion formulae are

$$\phi(x,y,t) = \frac{1}{2\pi}\int_{-\infty}^\infty e^{-i\omega t}\phi(x,y,\omega)d\omega \quad , \tag{5.5}$$

$$\Theta_o(t) = \frac{1}{2\pi}\int_{-\infty}^\infty e^{-i\omega t}\theta_o(\omega)d\omega \quad . \tag{5.6}$$

Clearly, if the total energy of the motion is finite then the potential energy of the body must remain bounded. Thus $\Theta_o(t)$ is bounded and therefore $\theta_o(\omega)$ is regular in the upper half complex ω-plane.

5.3 Motion by an applied force

Here we consider the problem where the system is left to respond to a prescribed rotational force $F_o(t)$ acting on the strip for a finite time. Initially $\Phi = \dot{\Phi} = 0$ on the free surface to account for the zero impulsive pressure and zero elevation. Also imposed are the conditions

$$\Theta_1(0) = \dot{\Theta}_1(0) = 0.$$

Applying the Fourier transform to the equations of motion and using these initial conditions it follows that

$$\left(\frac{\partial^2}{\partial x^2} + \frac{\partial^2}{\partial y^2}\right)\phi(x,y,\omega) = 0 \quad \text{in the fluid,} \tag{5.7}$$

$$\left(\omega^2 + g\frac{\partial}{\partial y}\right)\phi(x,y,\omega) = 0 \quad \text{on } y = 0, \tag{5.8}$$

$$\frac{\partial \phi}{\partial x} = -(a-y)i\omega\theta_1(\omega) \quad \text{on } x = 0,\ 0 < y < a\ , \tag{5.9}$$

$$-I_o\omega^2\theta_1(\omega) = -k_s\theta_1(\omega) - 2\rho i\omega \int_o^a \phi(0,y,\omega)(a-y)dy + f_o(\omega)\ . \tag{5.10}$$

In (5.10) the fact that on physical grounds ϕ is an odd function of x has been used. There is also the radiation condition for ϕ that at large distances waves travel away from the plate. Equations (5.7)-(5.9) are identical (except for a normalizing constant) for real ω with equations describing the fluid motion of a rolling plate due to periodic motion with time factor $e^{-i\omega t}$ and amplitude $\theta_1(\omega)$. Thus for positive ω, $\phi(x,y,\omega)$ is proportional to the potential obtained by Ursell (1948) and to its complex conjugate for negative ω. The hydrodynamic force term can therefore be expressed using equation (2.37) as

$$2\omega i\rho \int_o^a \phi(0,y,\omega)(a-y)dy = -\omega^2\left[a_{33} \pm \frac{i}{\omega}b_{33}\right]\theta_1(\omega), \quad \omega \gtrless 0 \tag{5.11}$$

where a_{33}, b_{33} are the added inertia and damping coefficients for a rolling barrier, published in Mei (1976) as

$$a_{33} = \frac{\pi\rho a^4}{(Ka)^4 I_1}\left\{\frac{K_1}{\pi^2 I_1^2 + K_1^2}\left[\frac{Ka}{2} - (1-Ka)(I_1 + L_1)\right]^2 - \frac{(Ka)^3}{4} I_o\right.$$

$$- \frac{2}{\pi} I_1(1-Ka)^2 \int_o^{Ka} xL_1(x)dx + Ka(1-Ka)[(1-Ka)L_1 - Ka][I_1L_o - L_1I_o]$$

$$\left. + (Ka)^2 I_1\left[\frac{1}{2} + \frac{2Ka}{3\pi}(1-Ka) + \frac{(Ka)^2}{16}\right]\right\},$$

and

$$b_{33} = \frac{\pi^2 \rho \omega a^4}{(Ka)^2} \frac{1}{\pi^2 I_1^2 + K_1^2} \left[\frac{1}{2} - \frac{(1-Ka)}{Ka}(I_1 + L_1) \right]^2$$

where the modified Bessel functions I_o, I_1, K_1 and the modified Struve functions L_o, L_1 are of argument Ka. A derivation of these results is given in Appendix A.

It now follows from (5.10), (5.11) that

$$\theta_1(\omega) = \frac{f_o(\omega)}{k_s - \omega^2(I_o + a_{33}) \mp i\omega b_{33}} \quad , \quad \omega \gtrless 0 \quad . \tag{5.12}$$

It is convenient to non-dimensionalize by writing

$$a_{33} = I_M \mu_{33} \ , \ b_{33} = I_M \omega \lambda_{33} \quad \text{and} \quad k_s = I_o \omega_o^2 \ ,$$

where $I_M = \frac{1}{4} \pi \rho a^4$ is the moment of inertia per unit length of fluid displaced by a semi-circular cylinder of radius a around its axis, and ω_o is the natural frequency of the motion for the undamped system.

Then (5.12) becomes

$$\theta_1(\omega) = \frac{f_o(\omega)}{I_M[I' \omega_o^2 - \omega^2(I' + \Lambda)]}$$

where

$$\Lambda = \mu_{33} \pm i\lambda_{33} \ , \qquad \omega \gtrless 0 \ ,$$

is the non-dimensionalized force coefficient and

$$I' = \frac{I_o}{I_M} \ .$$

In general I' is small enough for the inertia of the plate I_o to be neglected.

By an application of the inversion formula (5.6),

$$\Theta_1(t) = \frac{1}{2\pi I_M}\int_{-\infty}^{\infty} \frac{f_o(\omega)e^{-i\omega t}d\omega}{I'\omega_o^2 - \omega^2(I'+\Lambda)} \,. \tag{5.13}$$

Then, introducing a normalized frequency, $u = \omega\left(\frac{a}{g}\right)^{\frac{1}{2}}$, we have by the convolution theorem,

$$\Theta_1(t) = \frac{1}{I_M}\left(\frac{a}{g}\right)^{\frac{1}{2}}\int_o^t F_o(t')h_1\left[(t-t')\left(\frac{g}{a}\right)^{\frac{1}{2}}\right]dt' \tag{5.14}$$

where

$$h_1(\tau) = \frac{1}{2\pi}\int_{-\infty}^{\infty} \frac{e^{-iu\tau}\,du}{k' - u^2(I'+\Lambda)} \,, \qquad \tau > 0 \tag{5.15}$$

$$= 0 \,, \qquad \tau < 0$$

and $$k' = \frac{I'\omega_o^2 a}{g} \,.$$

Equations (5.13) and (5.14) solve the problem for any given force $F_o(t)$ in terms of a Fourier integral.

When the motion is started impulsively at $t = 0$, then

$$\Theta_1(t) = \frac{1}{I_M}\left(\frac{a}{g}\right)^{\frac{1}{2}}\mathcal{I}h_1\left(t\left(\frac{g}{a}\right)^{\frac{1}{2}}\right) \tag{5.16}$$

where $\mathcal{I} = \int_o^{\infty} f_o(t')dt'$, is the total impulse per unit width and the integration in fact extends over a short time. Equation (5.16) gives a physical meaning to $h_1(\tau)$ which is shown to be related to the initial velocity in §5.8.

If the problem is repeated with the same initial conditions but this time in a system where the fluid is replaced by air, the pressure term in (5.2) is neglected. The corresponding non-dimensional motion is described by the function

$$h_1^v(\tau) = \frac{1}{2\pi}\int_{-\infty}^{\infty} \frac{e^{-iu\tau}\,du}{k' - u^2 I'}$$

where the path of integration is deformed to pass over the poles of the integrand at $u = \pm\left(\frac{k'}{I'}\right)^{\frac{1}{2}}$. It follows that

$$\begin{aligned} h_1^v(\tau) &= \frac{1}{(k'I')^{\frac{1}{2}}} \sin\left[\left(\frac{k'}{I'}\right)^{\frac{1}{2}}\tau\right] \quad , \quad \tau > 0 \\ &= 0 \quad , \quad \tau < 0 \, , \end{aligned} \tag{5.17}$$

which represents undamped oscillatory motion.

5.4 Strip slightly displaced from equilibrium

In this section the strip is given an initial displacement $\Theta_2(0)$. Once the fluid has again come to rest the strip is released at time $t = 0$ with zero velocity. Proceeding in a similar manner to the previous section the Fourier transform of equations (2.1) and (2.8) remain as in (5.7), (5.8) while equations (5.1) and (5.2) transform respectively to

$$\frac{\partial \phi}{\partial x} = [-i\omega\theta_2(\omega) - \Theta_2(0)](a-y) \quad \text{on} \quad x = 0, \; 0<y<a \tag{5.18}$$

and

$$I_o[-\omega^2\theta_2(\omega) + i\omega\,\Theta_2(0)] = -k_s\theta_2(\omega) - 2\rho i\omega \int_o^a \phi(0,y,\omega)(a-y)dy \, . \tag{5.19}$$

There is also the radiation condition that waves travel outwards.

Since equations (5.7) and (5.8) hold in both problems and only the coefficients in (5.18) and (5.9) differ, it follows that

$$2\rho i\omega \int_o^a \phi(0,y,\omega)(a-y)dy = i\omega\left[a_{33} \pm \frac{i}{\omega} b_{33}\right][i\omega\theta_2(\omega) + \Theta_2(0)] \, , \; \omega \gtrless 0 \, . \tag{5.20}$$

Substituting (5.20) in (5.19), non-dimensionalizing as in §5.3, and applying (5.6) to the resulting expression for $\theta_2(\omega)$ gives the solution,

$$\Theta_2(t) = \Theta_2(0)h_2(\tau) \tag{5.21}$$

where

$$h_2(\tau) = \frac{-i}{2\pi}\int_{-\infty}^{\infty} \frac{(I' + \Lambda)ue^{-iu\tau}}{k' - u^2(I' + \Lambda)}\,du \quad , \qquad \tau > 0$$
$$= 0 \qquad , \qquad \tau < 0 \tag{5.22}$$

and $$\tau = \left(\frac{g}{a}\right)^{\frac{1}{2}} t \ .$$

Note that from (5.15) and (5.22),

$$k'h_1(\tau) + h_2'(\tau) = 0 \quad \text{for} \quad \tau > 0 \ .$$

Equation (5.21) gives $h_2(\tau) \to 1$ as $\tau \to 0$ through positive values, therefore

$$h_2'(\tau) = -k'h_1(\tau) \tag{5.23}$$

and

$$h_2(\tau) = \int_{\tau}^{\infty} k'h_1(\tau')d\tau' \tag{5.24}$$

showing that $h_1(\tau)$ and $h_2(\tau)$ are related.

Also note that the corresponding behaviour of $h_2(\tau)$ for motion in an undamped system is given by

$$h_2^v(\tau) = \cos\left[\left(\frac{k'}{I'}\right)^{\frac{1}{2}}\tau\right] \ . \tag{5.25}$$

5.5 The functions $h_1(\tau)$ and $h_2(\tau)$

As in Ursell (1964), $h_1(\tau)$ and $h_2(\tau)$ can be examined analytically to derive approximate expressions as $\tau \to 0$ and ∞. The same methods are involved, but for entirety the main details are repeated below.

The function $\Lambda(u)$ is originally defined for real u, but its definition, and therefore that of the integrand of $h_1(\tau)$ can be extended to the whole complex u-plane cut along the negative imaginary axis

(see Appendix A). Correspondingly, the variable $\omega = u\left(\frac{g}{a}\right)^{\frac{1}{2}}$ is regarded as a complex variable and the integral as a contour of integration. The integrand in general has singularities in the lower half plane, those lying on or nearest to the real ω-axis being the logarithmic branch point at $\omega = 0$ and possibly the points $\omega = \pm\infty$ on the real axis. It is these singular points that dominate the asymptotic behaviour of $h_1(\tau)$ as $\tau \to \infty$ (Carslaw and Jaeger, 1947). The integral of (5.15) is therefore deformed from along the real axis into a contour AC^-OC^+B as shown in fig. (5.1). It is chosen to pass above the singularity at the origin and is such that all the singularities lie below it. For large τ, Watson's lemma is used to find the contribution to $h_1(\tau)$ from

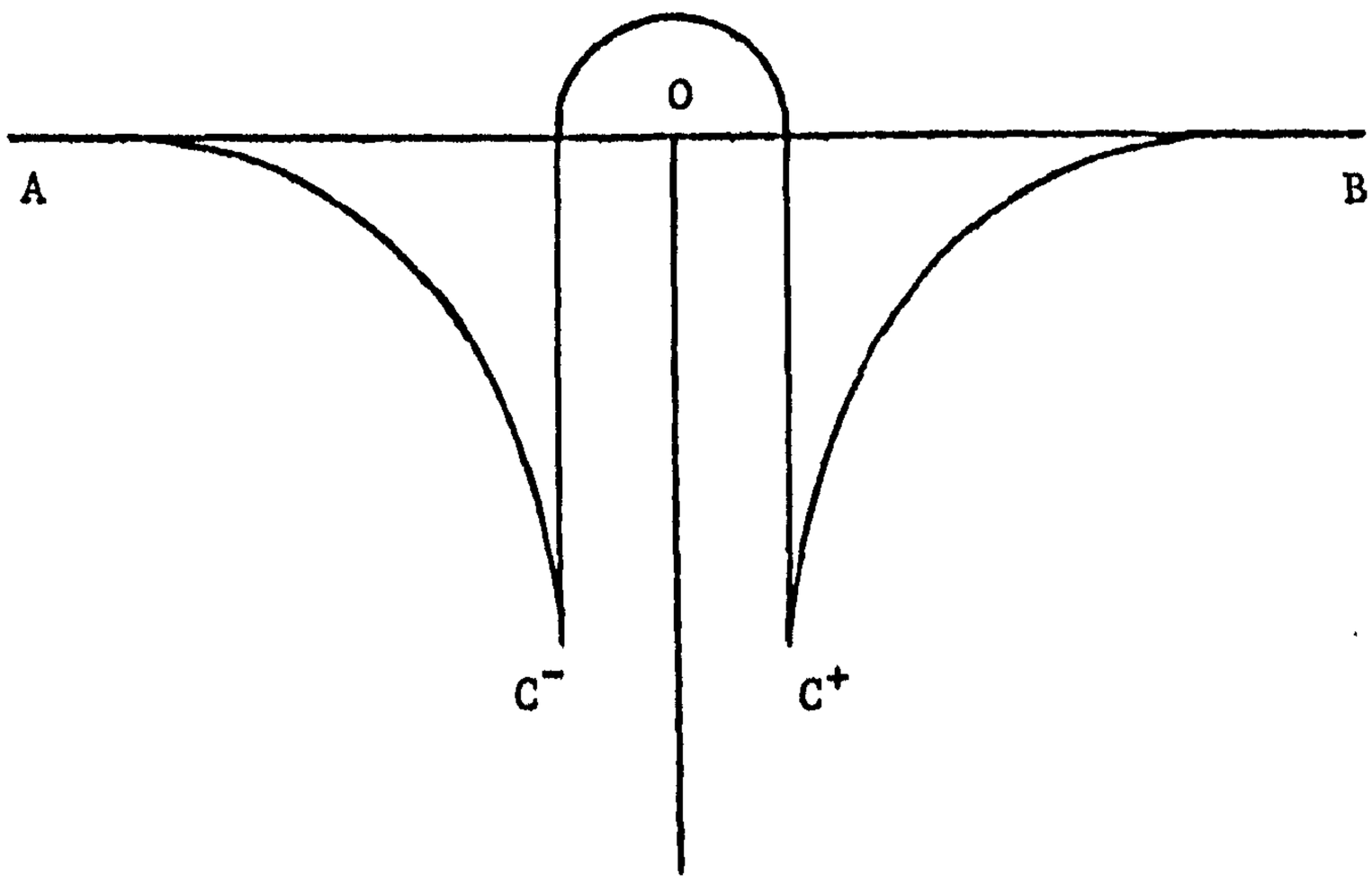

FIG. (5.1)

C^-OC^+, for which the expansion of the integrand in (5.15) for small u is needed. This is given by equation (A21), and therefore

$$[k' - u^2(I' + \Lambda)]^{-1} = \frac{1}{k'}\left[1 + \frac{u^2 I'}{k'} + \frac{u^2}{k'}\left\{2 - \frac{16}{3\pi} + \frac{4}{\pi^2} - 4u^2\left(\frac{1}{2} - \frac{2}{3\pi}\right)^2\left(\ln\frac{u^2}{2} - i\pi\right)\right\}\right]$$

$$+ \text{ smaller terms.}$$

Integrating along $OC^+\left(\text{argu} = -\frac{\pi i}{2}\right)$ and $OC^-\left(\text{argu} = \frac{3\pi i}{2}\right)$ gives

$$\frac{1}{2\pi}\left(\int_{OC^+} - \int_{OC^-}\right) \frac{e^{-iu\tau}}{k' - u^2(I' + \Lambda)}\, du \sim -\frac{8}{k'^2}\left(\frac{1}{2} - \frac{2}{3\pi}\right)^2 \int_0^\infty |u|^6 e^{-|u|\tau_d|u|}$$

$$\sim -\frac{8}{k'^2}\left(\frac{1}{2} - \frac{2}{3\pi}\right)^2 \frac{6!}{\tau^7} \quad . \tag{5.26}$$

The contribution from AC^- and C^+B is found from considering the asymptotic expansion of $h_1(\tau)$ for large u. Use of the appropriate asymptotic expansions of the modified Bessel and Struve functions (see for example Watson, 1940) shows that

$$\Lambda(u) \sim \frac{1}{4} - \frac{8}{3\pi} + \frac{8}{\pi^2} + \frac{1}{u^2}\left(\frac{32}{3\pi} - \frac{32}{\pi^2} - 1\right) + \ldots. \tag{5.27}$$

as $u \to \infty$, provided $|\arg(u)| < \frac{\pi}{4}$. This may be differentiated any number of times (Erdélyi, 1956) and so the derivatives of $\Lambda(u)$ do not oscillate rapidly for large u. The method of integration of parts can therefore be applied. Now equation (5.27) is valid throughout the sector $-\frac{\pi}{4} < \text{argu} < 0$ of the complex u-plane, and since $\Lambda(\bar{u}) = \overline{\Lambda(u)}$ it also holds in $\pi < \text{argu} < \frac{5\pi}{4}$. Therefore the paths AC^-, C^+B of the Fourier integral can be deformed into the lower half u-plane so as to make an angle with the real u-axis for large $|u|$. Hence the contribution to $h_1(\tau)$ is exponentially small. Thus

$$h_1(\tau) \sim -\frac{8}{k'^2}\left(\frac{1}{2} - \frac{2}{3\pi}\right)^2 \frac{6!}{\tau^7} \qquad \text{as} \quad \tau \to \infty \, . \tag{5.28}$$

To determine the corresponding behaviour of $h_2(\tau)$ for large τ, this method could be repeated. Alternatively use of (5.24) gives

$$h_2(\tau) \sim -\frac{8}{k'^2}\left(\frac{1}{2} - \frac{2}{3\pi}\right)^2 \int_\tau^\infty \frac{6!}{\tau'^7}\, d\tau'$$

$$= -\frac{8}{k'^2}\left(\frac{1}{2} - \frac{2}{3\pi}\right)^2 \frac{5!}{\tau^6} \qquad \text{as} \quad \tau \to \infty \, . \tag{5.29}$$

In both problems the final decay of the motion is clearly algebraic.

The nature of $h_i(\tau), i = 1,2$, for small τ can be inferred from the behaviour of the integrands for large u. Using (5.27) we see that by defining

$$a' = \frac{1}{4} - \frac{8}{3\pi} + \frac{8}{\pi^2} \quad , \qquad b' = \frac{32}{3\pi} - \frac{32}{\pi^2} - 1 \quad ,$$

then

$$\frac{1}{k' - u^2(I' + \Lambda)} \sim -\frac{1}{u^2(I' + a')} - \frac{(k'-b')}{u^4(I' + a')^2} + \cdots\cdots \qquad (5.30)$$

and

$$\frac{u(I' + \Lambda)}{k' - u^2(I' + \Lambda)} = -\frac{1}{u} + \frac{k'}{u[k' - u^2(I' + \Lambda)]}$$

$$\sim -\frac{1}{u} - \frac{k'}{u^3(I' + a')} - \frac{k'(k' - b')}{u^5(I' + a')^2} \quad . \qquad (5.31)$$

By the energy consideration following equation (5.6), the functions on the left of (5.30) and (5.31) are regular in the upper half u-plane. The asymptotic behaviour for small τ is then found by term by term integration. Hence

$$h_1(\tau) \sim \frac{1}{2\pi} \int_{-\infty}^{\infty} e^{-iu\tau} \left[\frac{-1}{u^2(I' + a')} - \frac{(k' - b')}{u^4(I' + a')^2} \right] du$$

$$= \frac{\tau}{I' + a'} - \frac{(k' - b')}{(I' + a')^2} \frac{\tau^3}{6} \qquad (5.32)$$

and similarly

$$h_2(\tau) = 1 - \frac{k'}{I' + a'} \frac{\tau^2}{2} + \frac{k'(k' - b')}{(I' + a')^2} \frac{\tau^4}{24} \qquad (5.33)$$

for small τ.

So far we have used the definitions of $h_1(\tau)$ and $h_2(\tau)$ as originally derived. Using $\Lambda(\bar{u}) = \overline{\Lambda(u)}$, (5.15) and (5.22) become

$$h_1(\tau) = \frac{1}{\pi} \mathrm{Re} \left\{ \int_0^{\infty} \frac{e^{-iu\tau}\, du}{k' - u^2(I' + \Lambda)} \right\} \qquad (5.34)$$

and

$$h_2(\tau) = \frac{1}{\pi}\mathrm{Re}\left\{\int_0^\infty \frac{-iue^{-iu\tau}\,du}{k' - u^2(I' + \Lambda)}\right\} \quad . \tag{5.35}$$

Further, exploiting the condition that $h_i(\tau) = 0$, $i = 1,2$, for $\tau < 0$ gives

$$h_1(\tau) = \frac{2}{\pi}\int_0^\infty \frac{u^2\lambda_{33}\sin u\tau\,du}{[k' - u^2(I' + \mu_{33})]^2 + u^4\lambda_{33}^2} \tag{5.36}$$

and

$$h_2(\tau) = \frac{2}{\pi}\int_0^\infty \frac{k'u\lambda_{33}\cos u\tau\,du}{[k' - u^2(I' + \mu_{33})]^2 + u^4\lambda_{33}^2} \quad . \tag{5.37}$$

As in Kotik and Lurye (1967) equations (5.36) and (5.37) are in convenient form for computation for the integrands are of the order $\frac{\sin u\tau}{u^6}$ and $\frac{\cos u\tau}{u^5}$ respectively for large u. Since they involve two parameters k', I' only a few cases are considered. However the overall motion for various pairs of the parameters are so similar that the values chosen are sufficient to get an idea of the general transient behaviour. Combinations of results for $k' = 2,3,4$ with $I' = 0.05$, 0.1 and 0.15 are presented below in figs. (5.2)-(5.13). For small τ the computed values of $h_1(\tau)$ and $h_2(\tau)$ are in good agreement with the series expansions (5.32) and (5.33).

For further analysis of these functions use is made of the definitions of $h_i(\tau)$, $i = 1,2$, given by (5.34) and (5.35). The integral is deformed from along the real axis into a contour C which extends from 0 to ∞ such that it lies entirely in the region $-\frac{\pi}{4} < \arg u < 0$, and a large circular arc closing the gap at infinity. In this region equation (5.27) is valid, so by use of Cauchy's Theorem and Jordan's lemma

$$\int_0^\infty = \int_C - 2\pi i \sum \text{residue of the poles} \tag{5.38}$$

where the integral on the right-hand side represents the integral along the contour C. Let the contribution to $h_i(\tau)$, $i = 1,2$, from this

component be the integral component, $\hat{h}_i(\tau)$, and the contribution from the second term the polar component, $h_i^p(\tau)$.

In order to find these contributions the contour C must be specified. This was done by first looking for the zeros of $F(u) = k' - u^2(I' + \Lambda)$ in the region $-\frac{\pi}{4} < \arg u < 0$. For the pairs of parameter values considered two zeros were readily found and so C was set along a ray such that it passed below both of them, the ray $\arg u = -\frac{\pi}{6}$ being a suitable choice. $\Lambda(u)$ was then found to have a pole within the sector bounded by this line and the ray $\arg u = 0$. These are all the singularities, as was verified computationally by use of the argument principle, and later by the results obtained.

Thus $h_i(\tau)$, $i = 1,2$, has been split into two parts, the sum of which is an alternative representation for these functions.

The polar component can be considered as follows:

Suppose that there is a pole at $u = u_i = a_i + b_i$. Then the contribution to $h_1^p(\tau)$ is

$$2\rho_i e^{b_i\tau} \sin(a_i\tau + \phi_i)$$

where

$$\rho_i = \left\{\left[\mathrm{Re}(F'(u_i))\right]^2 + \left[\mathrm{Im}(F'(u_i))\right]^2\right\}^{-\frac{1}{2}},$$

$$\phi_i = \tan^{-1}\left[\frac{\mathrm{Im}(F'(u_i))}{\mathrm{Re}(F'(u_i))}\right].$$

Summing over all the poles,

$$h_1^p(\tau) = 2\sum_i \rho_i e^{b_i\tau} \sin(a_i\tau + \phi_i), \qquad (5.39)$$

with a similar expression for $h_2^p(\tau)$.

For the cases under consideration in this chapter, the contribution from the dominant pole is shown in figs. (5.8)-(5.11). The integral

component, evaluated along argu = $-\frac{\pi}{6}$, is plotted in figs. (5.12) and (5.13) where the results agree with (5.28) and (5.29) for large τ.

5.6 Notes on computation

The integrals (5.36) and (5.37) defining $h_1(\tau)$ and $h_2(\tau)$ are evaluated for all values of τ using a doubly adaptive Clenshaw-Curtis quadrature method put forward by Oliver (1972). The same routine is used to compute the integral components where the expressions (5.34) and (5.35), integrated along argu = $-\frac{\pi}{6}$ are used. For small values of τ these last two integrals converge very slowly, like $u^{-2}e^{-iu\tau}$ and $u^{-1}e^{-iu\tau}$ respectively, and it is necessary to subtract known standard integrals, as in Maskell and Ursell (1970).

The behaviour of $f(u) = [k' - u^2(I' + \Lambda)]^{-1} = [F(u)]^{-1}$ for large u is given by equation (5.30). By choosing constants A_1, B_1 such that

$$\frac{A_1}{(1+u^2)} + \frac{B_1}{(1+u^2)^2} \sim \frac{1}{u^2(I' + a')} + \frac{(k' - b')}{u^4(I' + a')^2} ,$$

it follows that

$$\frac{A_1}{u^2}\left(1 - \frac{1}{u^2}\right) + \frac{B_1}{u^4} \sim \frac{1}{u^2(I' + a')} + \frac{(k' - b')}{u^4(I' + a')^2} ,$$

whence

$$A_1 = \frac{1}{I' + a'} \quad \text{and} \quad B_1 = \frac{1}{I' + a'} + \frac{(k' - b')}{(I' + a')^2} .$$

Therefore

$$\hat{h}_1(\tau) = \frac{1}{\pi} \mathrm{Re}\left\{\int_0^\infty \left[\frac{1}{k' - u^2(I' + \Lambda)} + \frac{A_1}{1+u^2} + \frac{B_1}{(1+u^2)^2}\right] e^{-iu\tau}\, du\right\} \quad (5.40)$$

$$- \frac{A_1}{2\pi}\int_{-\infty}^{\infty} \frac{e^{-iu\tau}}{1+u^2}\, du - \frac{B_1}{2\pi}\int_{-\infty}^{\infty} \frac{e^{-iu\tau}}{(1+u^2)^2}\, du .$$

The integrand in (5.40) decreases faster than u^{-4} and thus makes numerical integration possible, whilst the two definite integrals are

known functions:

$$\int_{-\infty}^{\infty} \frac{e^{-iu\tau}}{1+u^2}\,du = \pi e^{-\tau}, \quad \int_{-\infty}^{\infty} \frac{e^{-iu\tau}}{(1+u^2)^2}\,du = \frac{\pi}{2}(1+\tau)e^{-\tau}.$$

Similarly it can be shown that

$$\hat{h}_2(\tau) = \frac{1}{\pi}\,\mathrm{Re}\left\{ -i \int_0^{\infty}\left[\frac{u(I'+\Lambda)}{k'-u^2(I'+\Lambda)} + \frac{A_2 u}{1+u^2} + \frac{B_2 u}{(1+u^2)^2} + \frac{C_2 u}{(1+u^2)^3}\right] e^{-iu\tau}\,du \right\}$$

$$+ \frac{iA_2}{2\pi}\int_{-\infty}^{\infty}\frac{ue^{-iu\tau}}{1+u^2}\,du + \frac{iB_2}{2\pi}\int_{-\infty}^{\infty}\frac{ue^{-iu\tau}}{(1+u^2)^2}\,du + \frac{iC_2}{2\pi}\int_{-\infty}^{\infty}\frac{ue^{-iu\tau}}{(1+u^2)^3}\,du$$

where

$$A_2 = 1\ ,\ B_2 = 1 + \frac{k'}{I'+a'} \quad \text{and} \quad C_2 = 1 + \frac{2k'}{I'+a'} + \frac{k'(k'-b')}{(I'+a')^2}\ .$$

Again the definite integrals are known functions:

$$\int_{-\infty}^{\infty}\frac{ue^{-iu\tau}}{(1+u^2)}\,du = -\pi i e^{-\tau}\ , \quad \int_{-\infty}^{\infty}\frac{ue^{-iu\tau}}{(1+u^2)^2}\,du = -\frac{\pi i}{2}\ \tau e^{-\tau},$$

$$\int_{-\infty}^{\infty}\frac{ue^{-iu\tau}}{(1+u^2)^3}\,du = -\frac{\pi i}{8}\,\tau(1+\tau)e^{-\tau}\ .$$

Checks were applied near $\tau = 0$ to test the accuracy of the computed values of $\hat{h}_i(\tau)$, $i = 1,2$. As seen in the tables of values displayed in the next section, agreement was found to be very satisfactory.

It remains to find the poles of F(u) in order to compute the polar component. These were found directly by applying the downhill method to $F(u) = 0$ using a routine written by Bach (1969). To provide a check on these single precision complex results, a hybrid method due to Powell, given in Rabinowitz (1970) was applied to the real and imaginary parts of F(u). As in Maskell and Ursell (1970), one starting value for these methods was obtained by using the following tangent approximation method. The zero, $u = u_1$, say, of $\mathrm{Re}[F(u)] = k' - u^2(I' + \mu_{33})$ was found. Then, using accurate values of $F(u_1)$ and $F'(u_1)$ the

approximate value

$$u_{12} = u_1 - \frac{F(u_1)}{F'(u_1)}$$

was calculated. This value u_{12} was seen to be comparable with the exact value of the dominant pole. Other poles were found by trying various starting values to test for further zeros closer to the origin. All the zeros determined gave $|F(u)| < 10^{-5}$.

5.7 Discussion of results

On physical grounds one would expect a system with a constant inertia parameter, moving under the initial application of a force to originally move further away from its equilibrium position when there is less spring force resistance. This is verified on comparing our results in figs. (5.2) and (5.3) for $I' = \cdot 1$ with $k' = 2,3$ and 4. The motion then diminishes more rapidly and with fewer oscillations for smaller values of k'. The general behaviour of $h_2(\tau)$ is similar to that of $h_1(\tau)$ where again the strip oscillates more frequently and with greater amplitudes for the larger value of k'. If I' is now allowed to vary, k' remaining constant, the results are also as anticipated, as seen in figs. (5.4) and (5.5). That is, the smaller the inertia parameter, the larger the amplitudes of motion with more oscillatory behaviour. It is worthwhile to note that for $h_2(\tau)$ the first two troughs are of approximately equal amplitude, allowing the system to adjust to the initial displacement. Thereafter there is a regular decay of the amplitudes. Computations have been continued as far as $\tau = 40$ where oscillatory motions still exist. This is shown in figs. (5.6) and (5.7) for $I' = \cdot 1$ with $k' = 4$.

After the first one and a half cycles it is clear from figs. (5.8) and (5.9) that the behaviour of $h_1(\tau)$ is approximated well by the

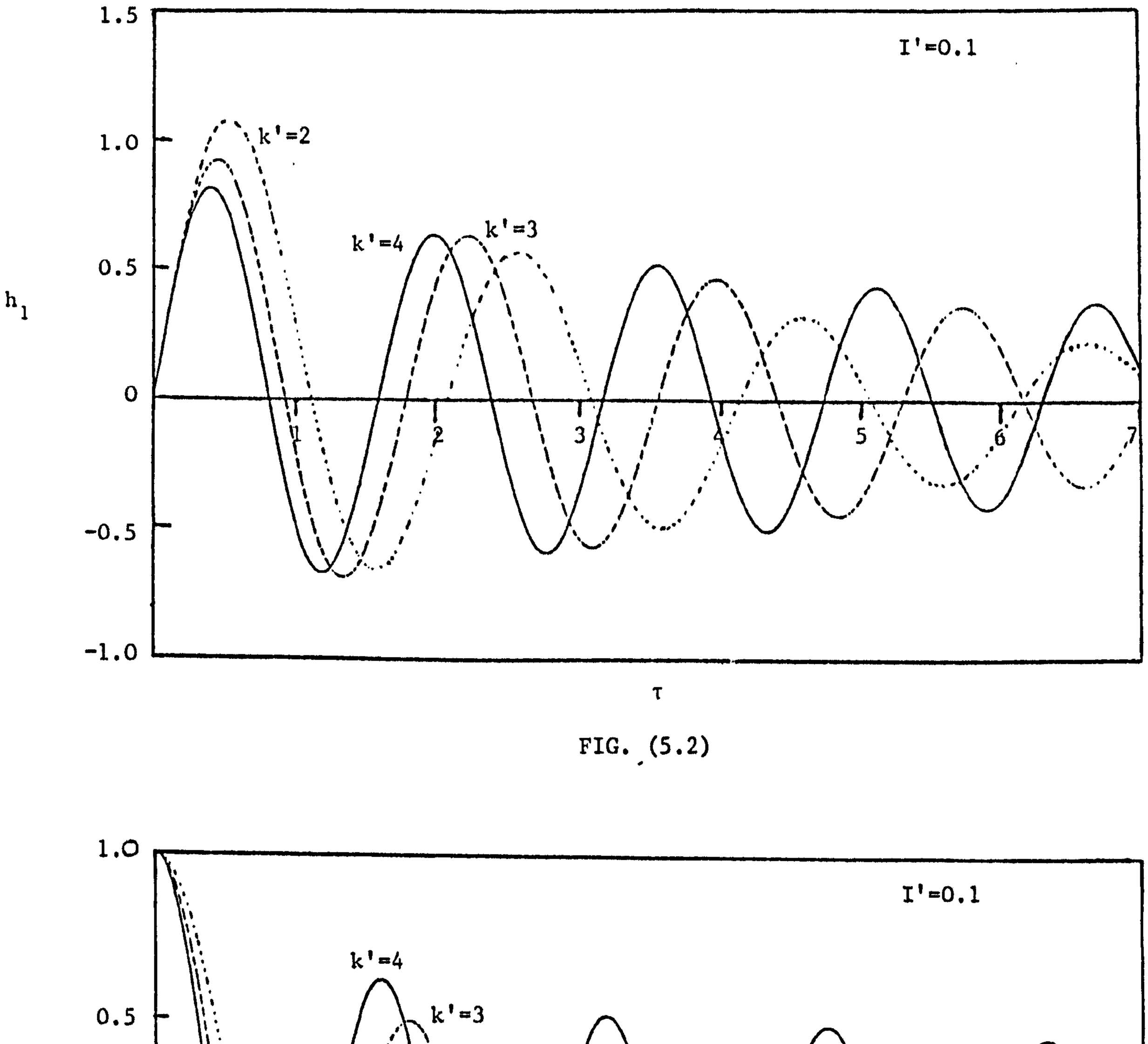
1.5
1.0
0.5
0
-0.5
-1.0
I'=0.1
k'=2
k'=3
k'=4
1
2
3
4
5
6
7
τ
h1

FIG. (5.2)

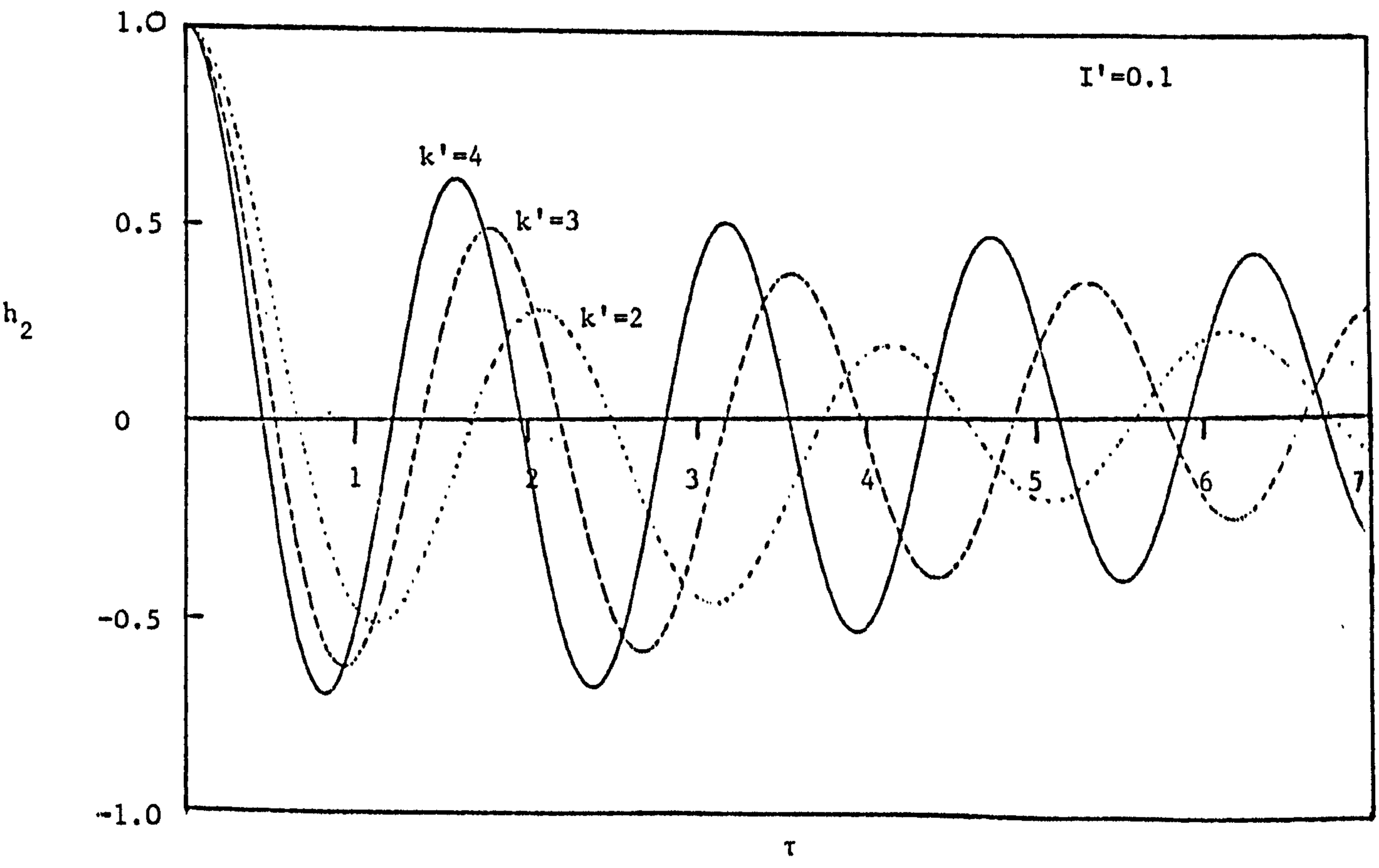
1.0
0.5
0
-0.5
-1.0
I'=0.1
k'=4
k'=3
k'=2
1
2
3
4
5
6
7
τ
h2

FIG. (5.3)

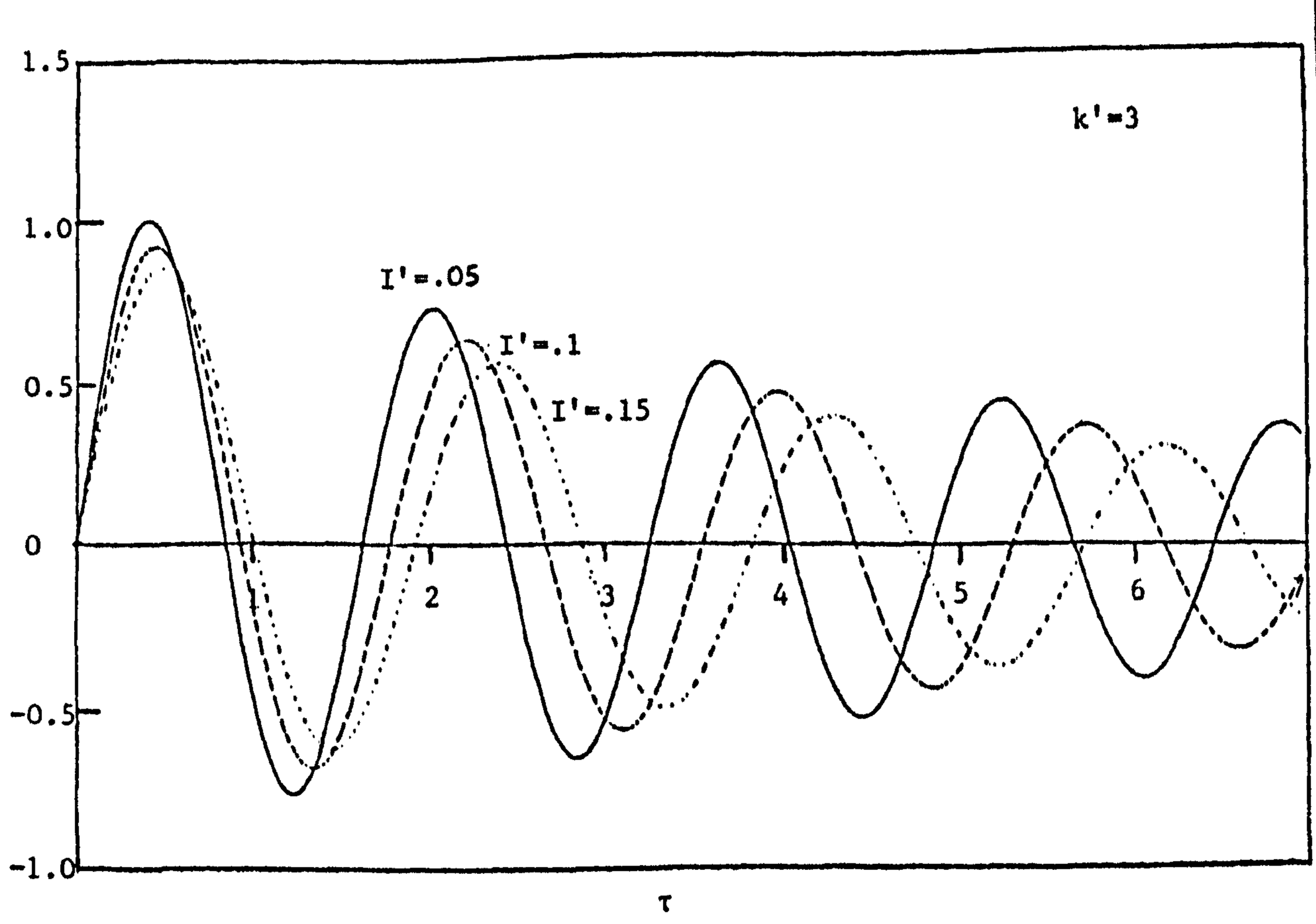
1.5
1.0
0.5
0
-0.5
-1.0
k'=3
I'=.05
I'=.1
I'=.15
1
2
3
4
5
6
7
h1
τ

FIG. (5.4)

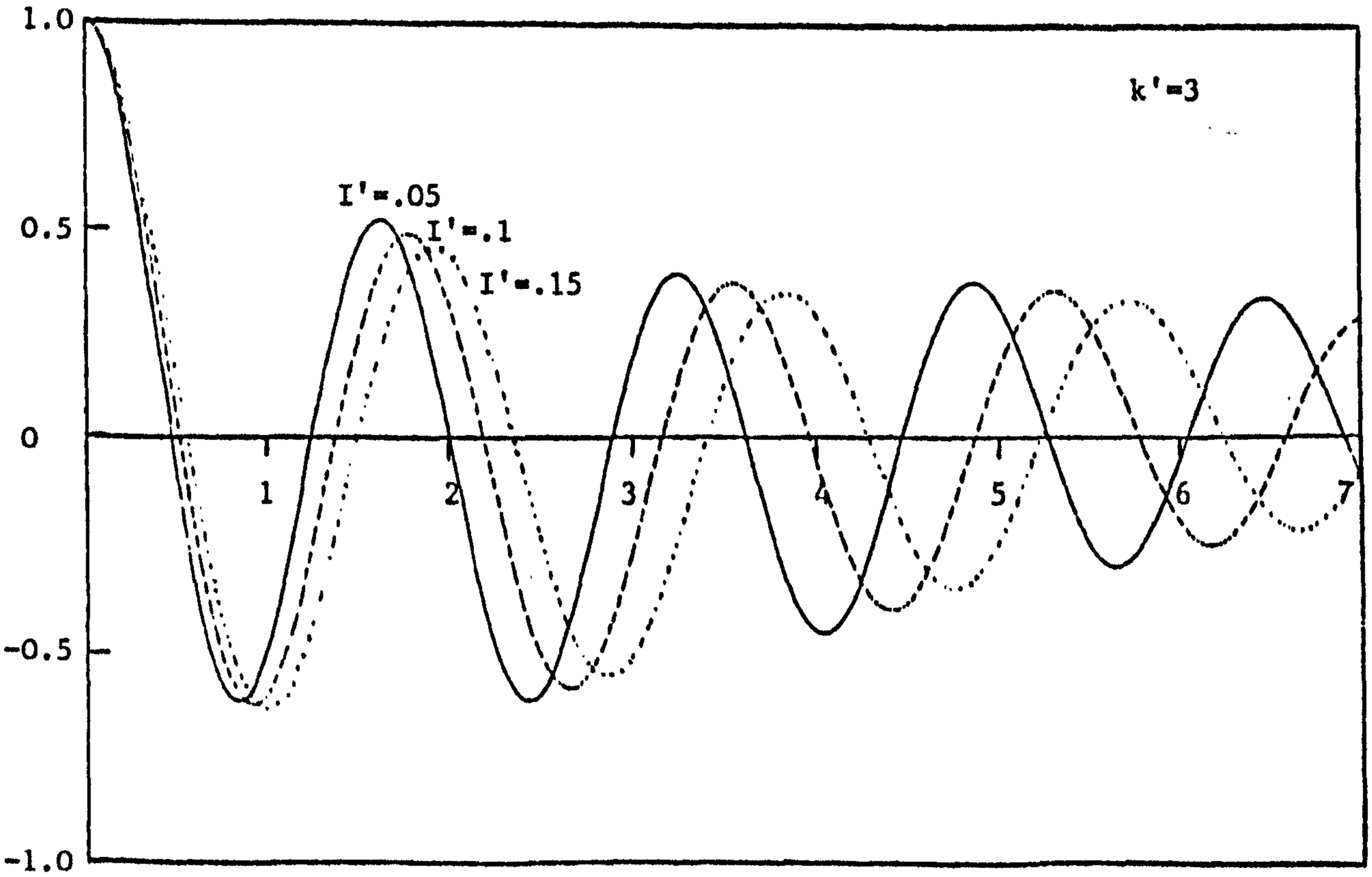
1.0
0.5
0
-0.5
-1.0
k'=3
I'=.05
I'=.1
I'=.15
1
2
3
4
5
6
7
h2
τ

FIG. (5.5)

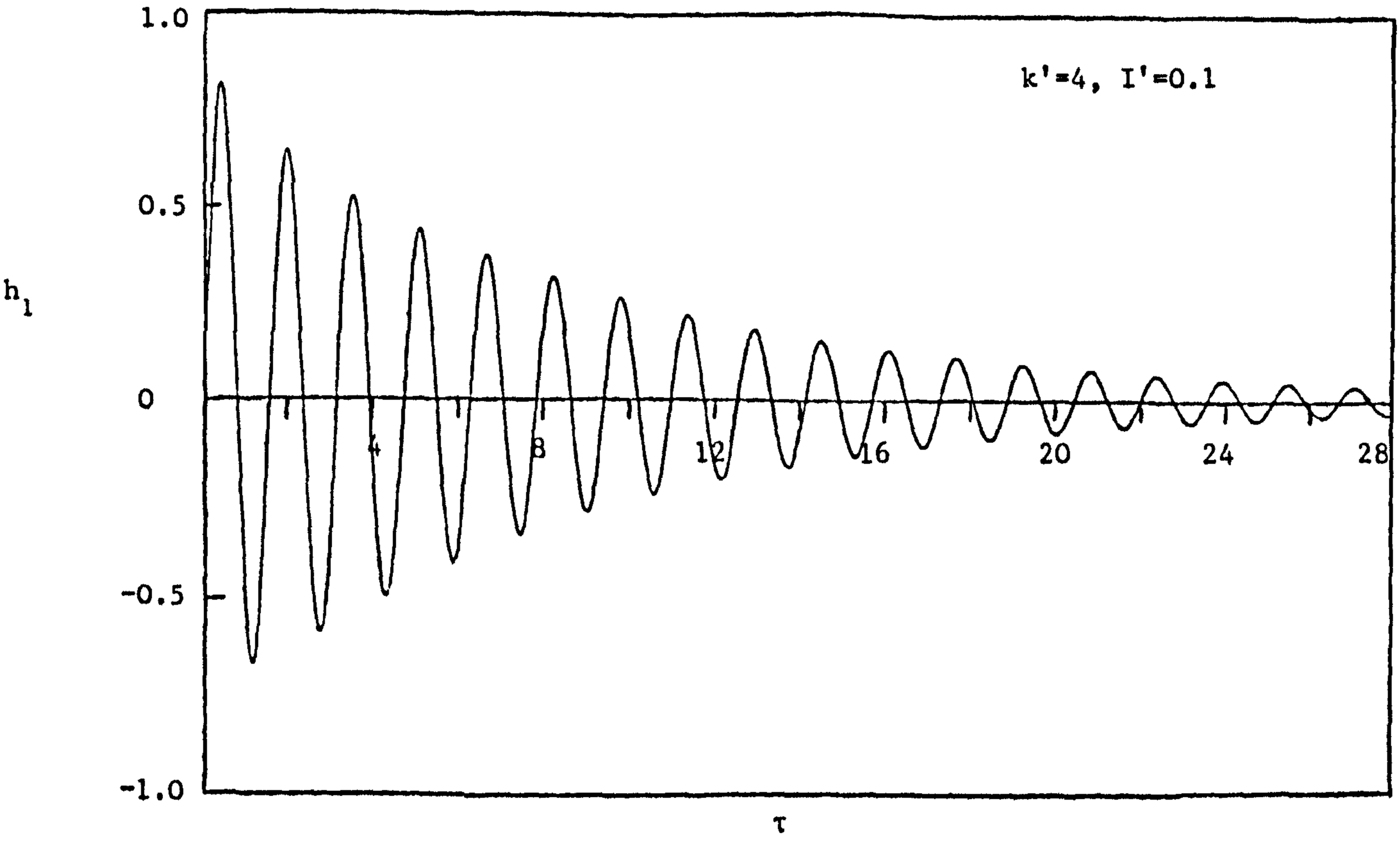
1.0
0.5
0
-0.5
-1.0
h_1
k'=4, I'=0.1
4
8
12
16
20
24
28
τ

FIG. (5.6)

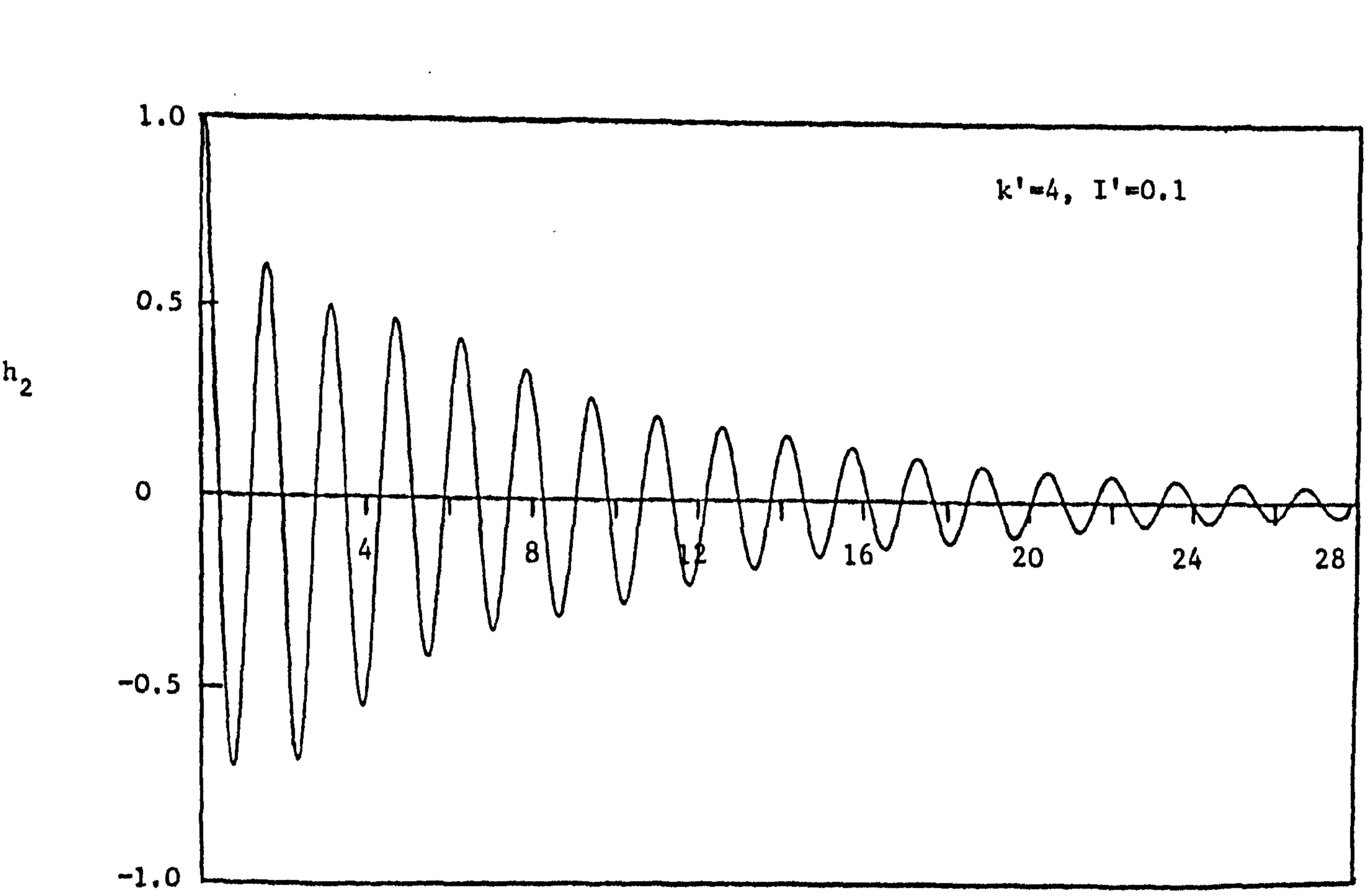
1.0
0.5
0
-0.5
-1.0
h_2
k'=4, I'=0.1
4
8
12
16
20
24
28
τ

FIG. (5.7)

dominant polar contribution, but similar comparison is not so good for $h_2(\tau)$ (figs. (5.10) and (5.11)). However, if consideration is taken of the other pole it is noticeable that for all τ there is a very good match between the behaviour of $h_i(\tau)$, $i = 1,2$, and the sum of these polar contributions. This is illustrated in the corresponding tables of results for $h_j(\tau)$, $j = 1,2$, where $h^p_{ji}(\tau)$ $i = 1,2$ represent the contribution from the poles. The undamped curves on these graphs display the motion of the system in air. They show that during the first cycle of $h_i(\tau)$, $h^v_i(\tau)$ undergoes approximately one and a half cycles for both $i = 1$ and 2.

The polar components eventually become exponentially small as τ gets large whilst the integral components remain algebraically small. In particular the integral component of $h_1(\tau)$ is dominant when

$$\frac{8}{k'^2}\left(\frac{1}{2} - \frac{2}{3\pi}\right)^2 \frac{6!}{\tau^7} > 2\rho_i e^{b_i\tau}$$

which gives, on using computed values from the dominant pole, $\tau \simeq 330$ for $k' = 4$, $I' = \cdot 1$ and $\tau \simeq 183$ when $k' = 3$ with $I' = \cdot 15$. Similarly $\hat{h}_2(\tau)$ is dominant when $\tau \simeq 256$ and $\tau \simeq 157$ respectively. It is therefore not surprising that we have not calculated how many oscillations occur before this behaviour takes place. In fact $\hat{h}_i(\tau)$ is virtually negligible for all values of τ, as seen in figs. (5.12) and (5.13).

We can therefore conclude that the motion of main interest is associated with the poles, in particular with the dominant polar contribution which is in known form and represents damped harmonic motion.

This is very similar to ship hydrodynamic theory where the motion of the ship is assumed to be damped harmonic, but governed by a second-order differential equation of the form

$$M_s\ddot{\theta} + D_s\dot{\theta} + K_s\theta = 0 ,$$

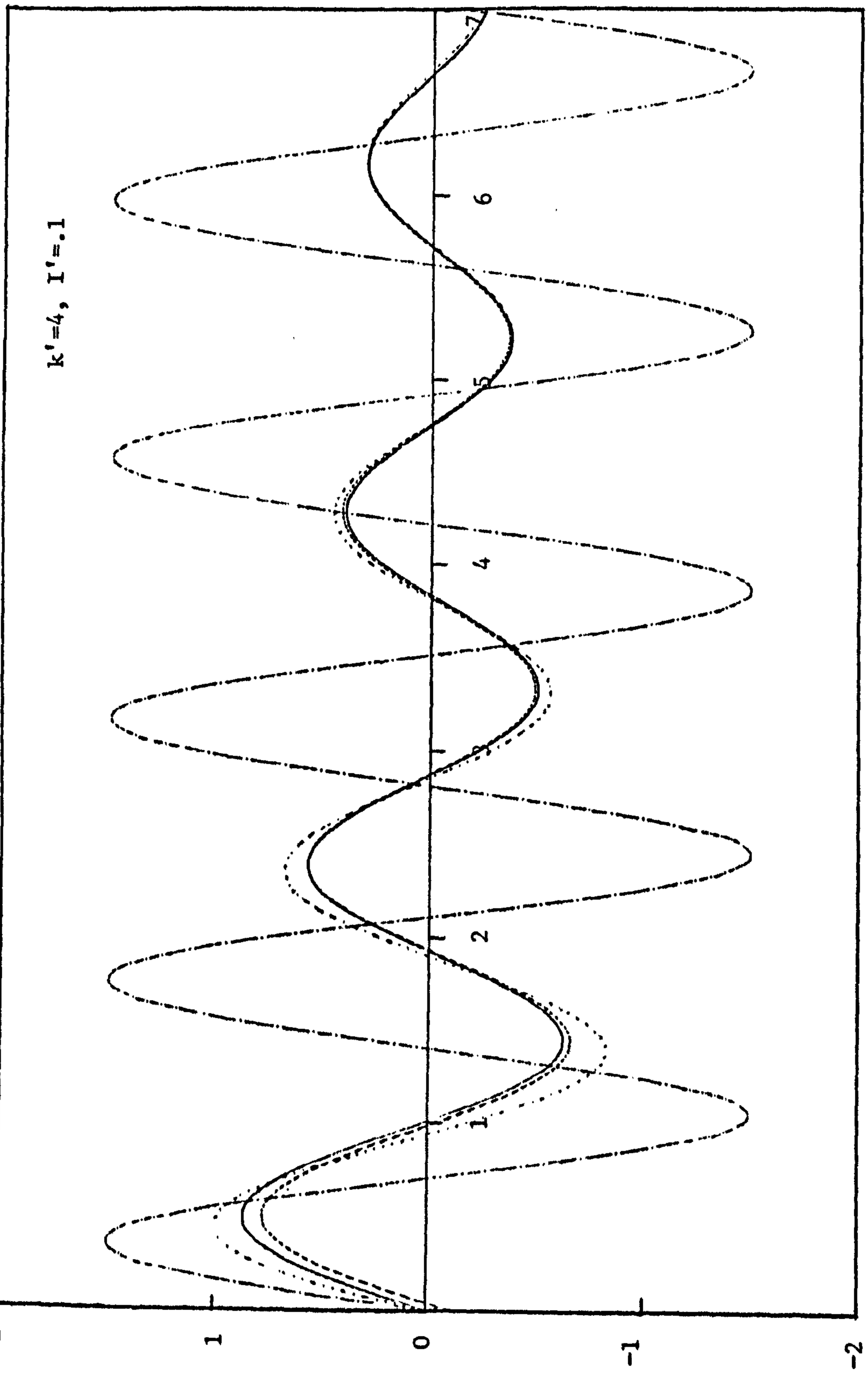

FIG. (5.8)

——— $h_1(\tau)$. ····· The approximation to $h_1(\tau)$ when the dominant pole. — · — · — · $h_1^{\vee}(\tau)$. ——— The contribution to $h_1(\tau)$ from the dominant pole.

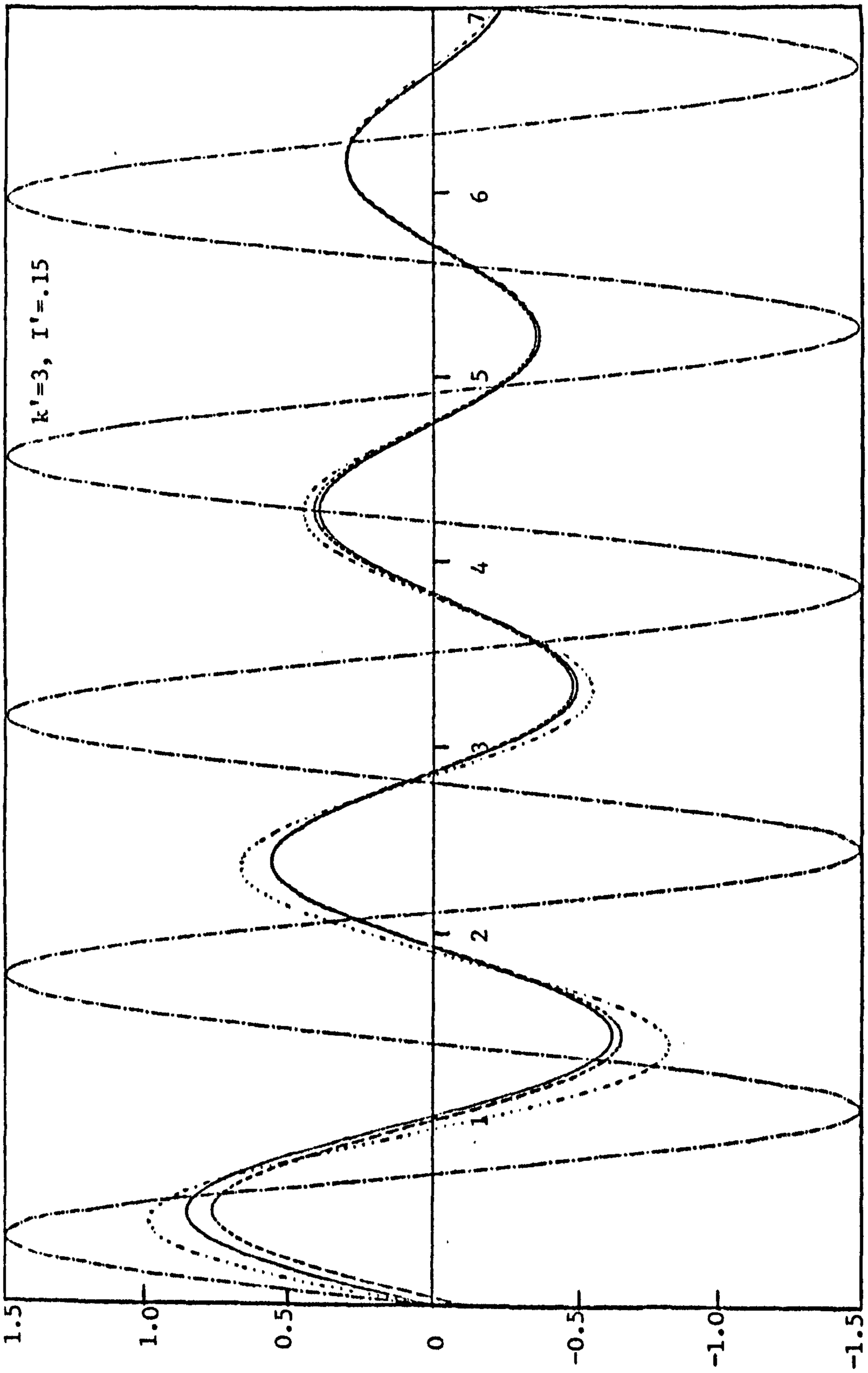

FIG. (5.9)

The contribution to $h_1(\tau)$ from the dominant pole.
The approximation to $h_1(\tau)$ when the real part of the force coefficient is fixed at the real part of the dominant pole.

——— $h_1(\tau)$. ·—·—· $h_1^v(\tau)$. ——— The approximation to $h_1(\tau)$ when the real part of the force coefficient is fixed at the real part of the dominant pole.

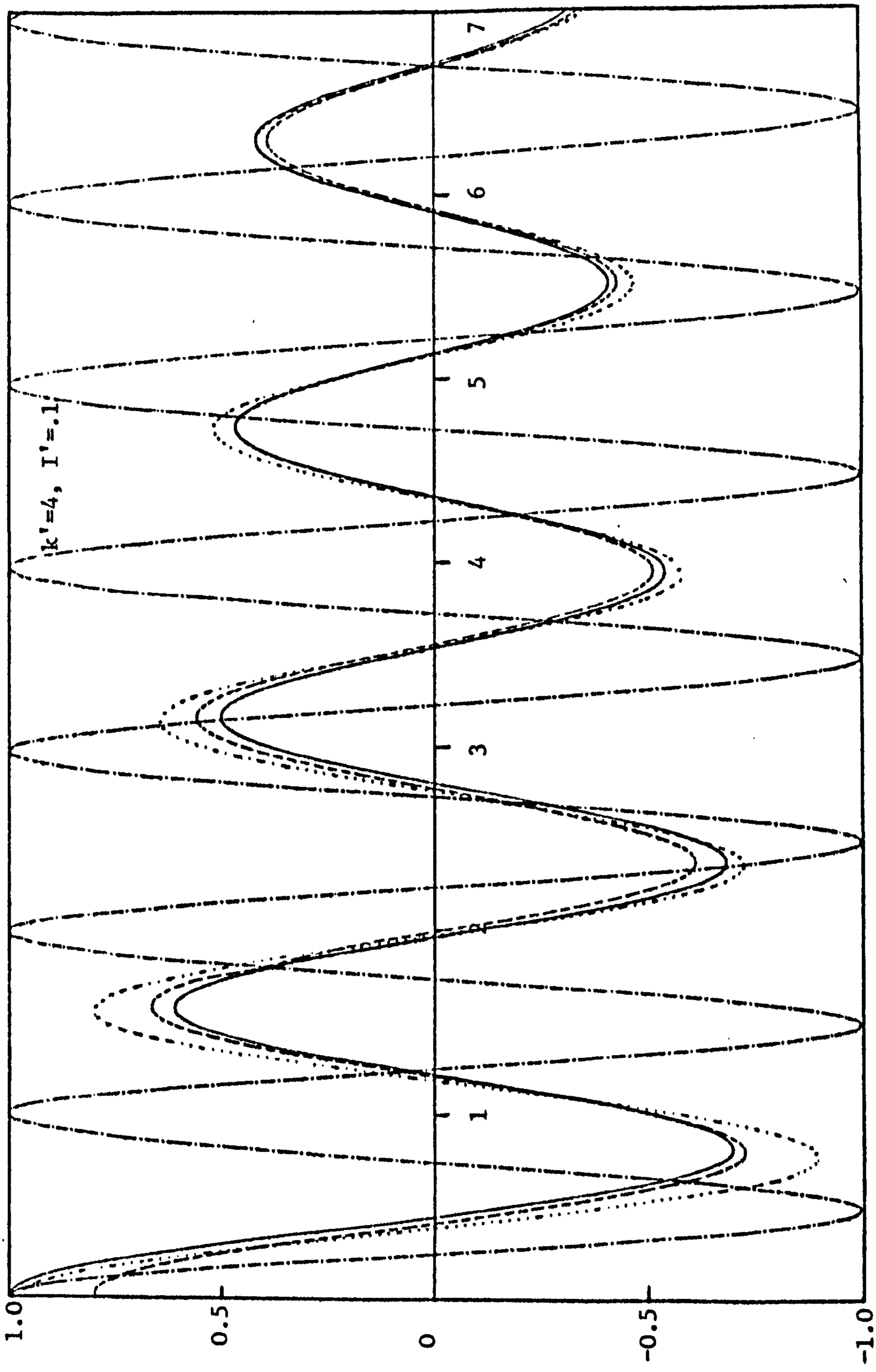

FIG. (5.10)

—·—·—·— $h_2(\tau)$. ——— The contribution to $h_2(\tau)$ from the dominant pole.

····· The approximation to $h_2(\tau)$ when the force coefficient is fixed at the real part of the dominant pole.

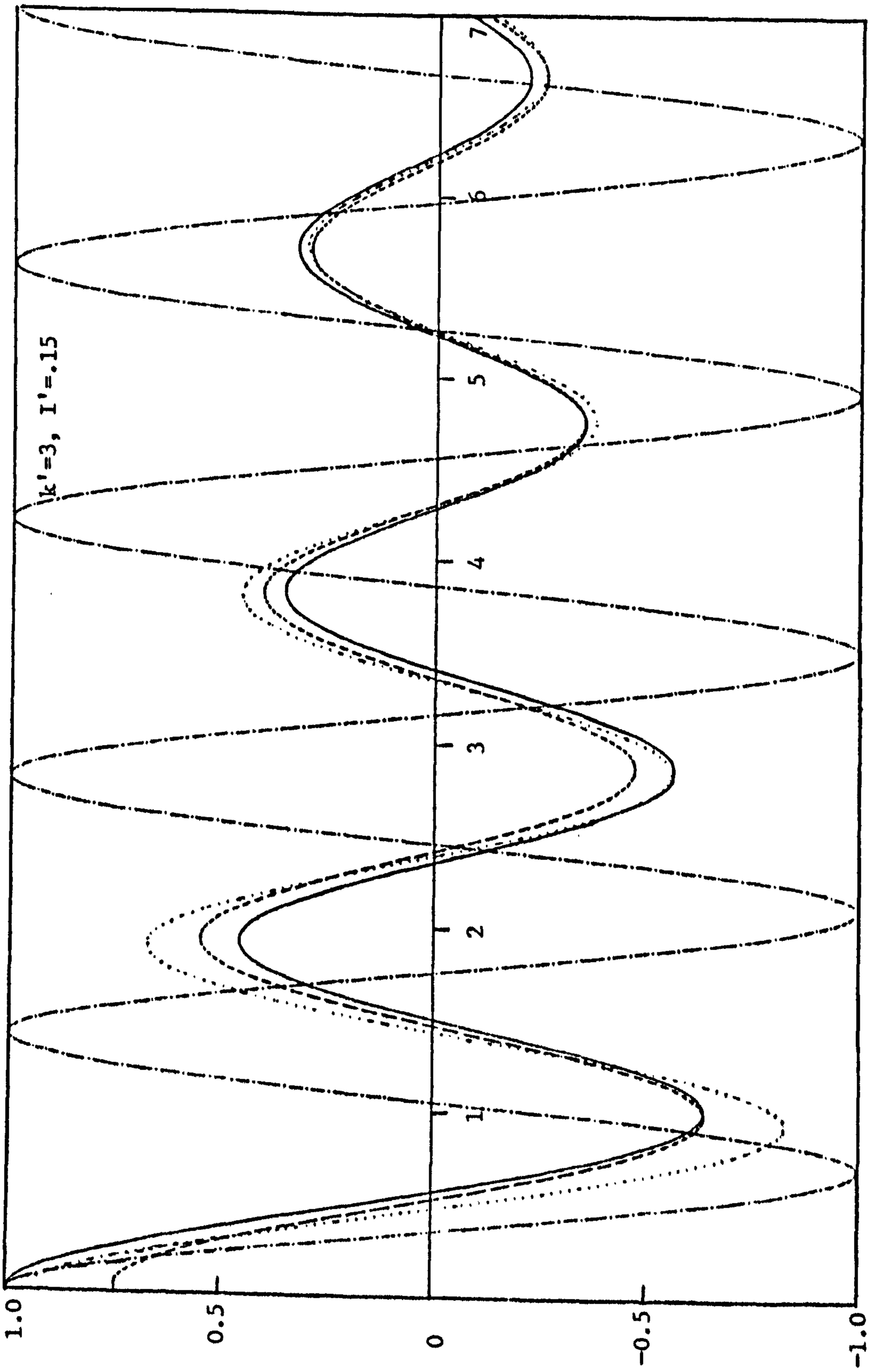

FIG. (5.1) —·—·—. $\dot{h}_2^{\nu}(\tau)$. ——— The contribution to $h_2(\tau)$ from the dominant pole.
—— $h_2(\tau)$. ..... The approximation to $h_2(\tau)$ when the force coefficient is fixed at the real part of the dominant pole.

τ	0.0	0.5	1.0	1.5	2.0	2.5	3.0	3.5	4.0	4.5
$h_1(\tau)$	0	.76149	-.46727	-.22361	.64062	-.28712	-.35165	.51630	-.11348	-.39660
$h_{11}^p(\tau)$	.02178	.02075	.01682	.01115	.00491	-.00085	-.00536	-.00820	-.00926	-.00873
$h_{12}^p(\tau)$	-.06182	.70810	-.50061	-.23996	.63586	-.28466	-.34491	.52521	-.10399	-.38784
$\Sigma h_{1i}^p(\tau)$	-.04004	.72885	-.48379	-.22881	.64077	-.28551	-.35027	.51701	-.11325	-.39657
$\hat{h}_1(\tau)$	.04004	.03265	.01651	.00522	-.00014	-.00162	-.00136	-.00072	-.00024	-.00002
$\hat{h}_1+\Sigma h_{1i}^p$	0	.76150	-.46728	-.22359	.64063	-.28713	-.35163	.51629	-.11349	-.39659
$h_2(\tau)$	1	-.15200	-.52120	.57422	-.09186	-.60940	.38242	.08842	-.52759	.26614
$h_{21}^p(\tau)$	.06482	.02172	-.01624	-.04440	-.06045	-.06436	-.05789	-.04403	-.02629	-.00807
$h_{22}^p(\tau)$	.79311	-.23897	-.52134	.62287	-.02295	-.53875	.44344	.13347	-.50116	.27411
$\Sigma h_{2i}^p(\tau)$	.85793	-.21725	-.53758	.57847	-.08340	-.60311	.38555	.08944	-.52745	.26604
$\hat{h}_2(\tau)$	.14208	.06524	.01640	-.00425	-.00847	-.00626	-.00313	-.00104	-.00012	.00010
$\hat{h}_2+\Sigma h_{2i}^p$	1.00001	-.15201	-.52118	.57422	-.09187	-.60937	.38242	.08840	-.52757	.26614

$k' = 4.0,\ I' = 0.1$

TABLE (5.1)

τ	0.0	0.5	1.0	1.5	2.0	2.5	3.0	3.5	4.0	4.5
$h_1(\tau)$	0	.85609	.02155	-.61723	.14835	.52505	-.21670	-.43080	.22693	.29579
$h^p_{11}(\tau)$	.03834	.03767	.03158	.02195	.01085	.00018	-.00858	-.01448	-.01717	-.01685
$h^p_{12}(\tau)$	-.10854	.76648	-.03551	-.64681	.13821	.52775	-.20579	-.41508	.24453	.31267
$\Sigma h^p_{1i}(\tau)$	-.07020	.80415	-.00393	-.62486	.14906	.52793	-.21437	-.42956	.22736	.29582
$\hat{h}_1(\tau)$	.07017	.05193	.02548	.00762	-.00070	-.00288	-.00235	-.00124	-.00042	-.00003
$\hat{h}_1+\Sigma h^p_{1i}$	-.00003	.85608	.02155	-.61724	.14836	.52505	-.21672	-.43080	.22694	.29579
$h_2(\tau)$	1	.17080	-.63883	-.01003	.44134	-.23369	-.52008	.12055	.29534	-.23167
$h^p_{21}(\tau)$	.09349	.03571	-.01680	-.05727	-.08193	-.09005	-.08344	-.06575	-.04162	-.01576
$h^p_{22}(\tau)$	.73764	.06127	-.63840	.05438	.53458	-.13554	-.43263	.18764	.33710	-.21607
$\Sigma h^p_{2i}(\tau)$	.83113	.09698	-.65520	-.00289	.45265	-.22559	-.51607	.12189	.29548	-.23183
$\hat{h}_2(\tau)$	.16886	.07381	.01637	-.00715	-.01132	-.00810	-.00401	-.00133	-.00014	.00015
$\hat{h}_2+\Sigma h^p_{2i}$	.99999	.17079	-.63883	-.01004	.44133	-.23369	-.52008	.12056	.29534	-.23168

$k' = 3.0,\ I' = 0.15$

TABLE (5.2)

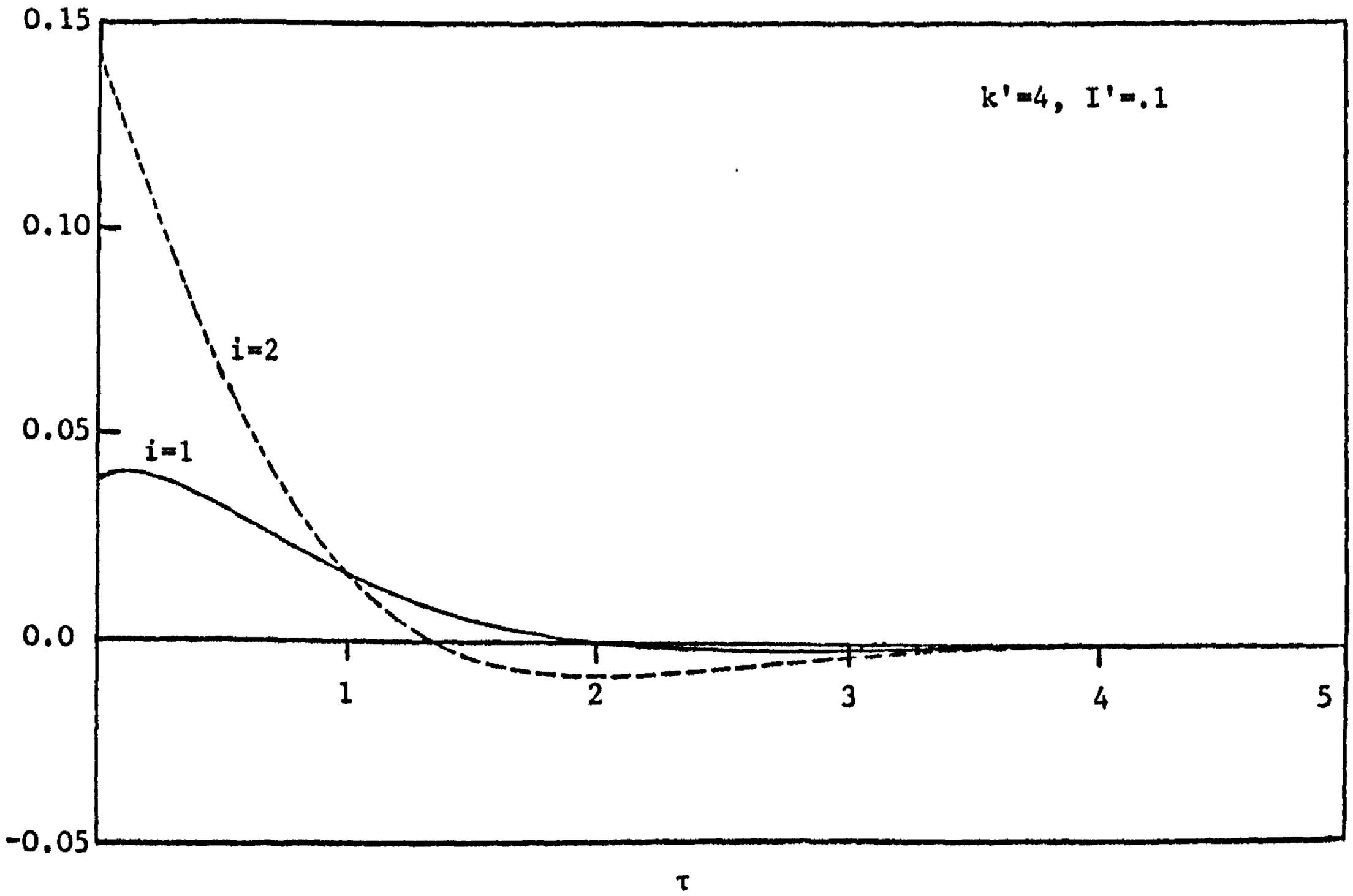

FIG. (5.12)

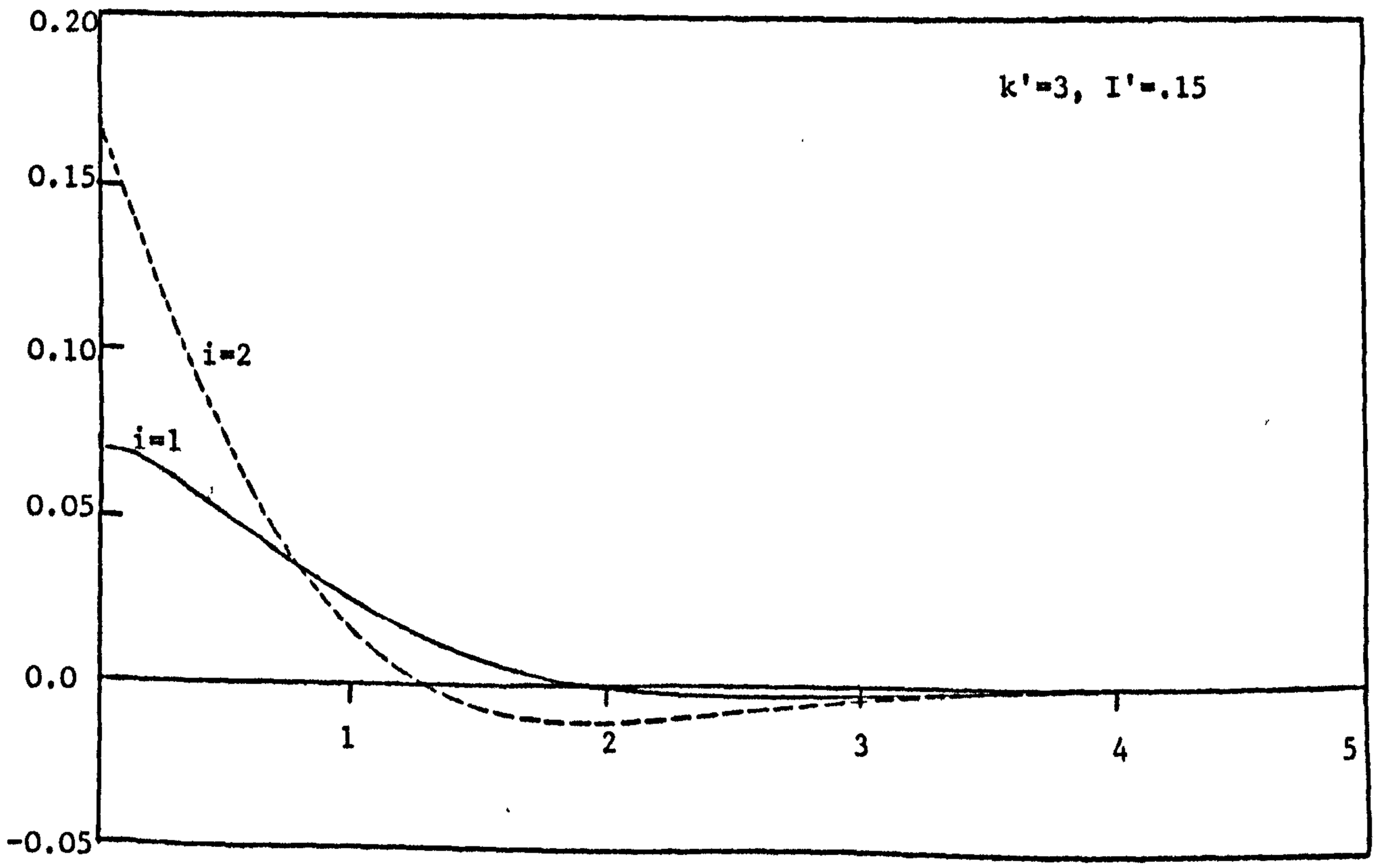

FIG. (5.13)

where M_s, D_s and K_s are constant coefficients. These are chosen by some physical or experimental argument in an attempt to characterise the true motion (see for example Havelock, 1942).

It has been attempted to relate M_s and D_s to the added inertia and damping coefficients, respectively, at a <u>particular</u> frequency so that the resulting motion corresponds to the known solution. This involves solving two simultaneous equations relating a_{33} and b_{33} for a fixed frequency, which cannot be done. However, for a crude approximation to the known solution, the frequency was fixed at that point on the real ω-axis closest to the pole, that is, the real part of the pole. The results are shown by the dotted curves on figs. (5.8)-(5.11). The significant conclusion is that the true motion of a rolling strip cannot be represented by a second-order differential equation with constant coefficients.

5.8 Conclusion

We have solved two initial-value problems in the form of Fourier integrals. In the case of impulsive motion, discussed at the end of §5.3, the first solution is related to the initial velocity, for from (5.16) and because

$$h_1'(\tau) \to \frac{1}{I'+a'} \quad \text{as} \quad \tau \to 0 \quad \text{(from (5.32))}$$

it follows that

$$\theta_1(t) = \left(\frac{a}{g}\right)^{\frac{1}{2}} \dot{\theta}_1(0)[I'+a']h_1\left(t\left(\frac{g}{a}\right)^{\frac{1}{2}}\right) \tag{5.41}$$

The second is related to the initial displacement.

For large time we know that the asymptotic behaviour of these solutions are

$$\Theta_1(t) \sim -\left(\frac{a}{g}\right)^4 \quad \dot{\Theta}_1(0)[I' + a']\left(\frac{1}{2} - \frac{2}{3\pi}\right)^2 \frac{8}{k'^2} \frac{6!}{\tau^7} , \tag{5.42}$$

and

$$\Theta_2(t) \sim -\left(\frac{a}{g}\right)^3 \quad \Theta_2(0) \frac{8}{k'} \left(\frac{1}{2} - \frac{2}{3\pi}\right)^2 \frac{5!}{\tau^6} . \tag{5.43}$$

The ultimate monotonic decaying motion is therefore slower when the body is initially displaced and then released than when the motion is generated by an applied force. As expected the asymptotic decay is faster than that obtained by Ursell for the heaving cylinder, since there is greater fluid reaction on the motion of a strip.

The work of this chapter has been published in Smith (1982).

CHAPTER 6

THE TRANSIENT MOTION OF A SUBMERGED PENDULUM BOB

6.1 Introduction

Consider a simple pendulum made up of a circular cylinder hanging, with its axis horizontal, from a fixed horizontal axis about which it is free to rotate by a system of equal length strings or rods. It is assumed that the motion is restricted to the surge mode only. Thus when the system is given a small angular displacement from its stable equilibrium position and then released, the pendulum will continue to oscillate in simple harmonic motion under the only external force caused by the mass of the bob and gravity.

If this device is then lowered into an infinitely deep fluid and set in motion as above, the fluid will produce an additional resistance force on the motion of the pendulum so that eventually both the fluid and the system will return to their equilibrium state of rest. It is with this motion that this chapter is concerned.

The problem is formulated and solved in §6.2 using the method of the previous chapter. Hence the subsequent angular displacement is described by a Fourier integral involving a force coefficient term. This coefficient has been examined by Ogilvie (1963) and Evans et al. (1979), and can also be obtained from Chapter 3 for the special case of $M = 0$. As discussed in §3.4 it is determined for any one value by solving an infinite system of equations. Thus numerical computations of the transient motion can be performed, and are presented in §6.3. However, unlike Chapter 5, a more detailed analysis of the motion to look for polar contributions has not been carried through.

A discussion of the investigation into the decaying transient motion of an arbitrary, totally submerged surging body is made in §6.4, before drawing final conclusions in §6.5

6.2 The pendulum motion

Suppose that the pendulum device described in §6.1 consists of a circular cylinder of radius a, mass m, attached to a light rod or string of length ℓ. When this system is set in motion by an angular displacement $\Theta_o(0)$, as illustrated in fig. (6.1), the subsequent

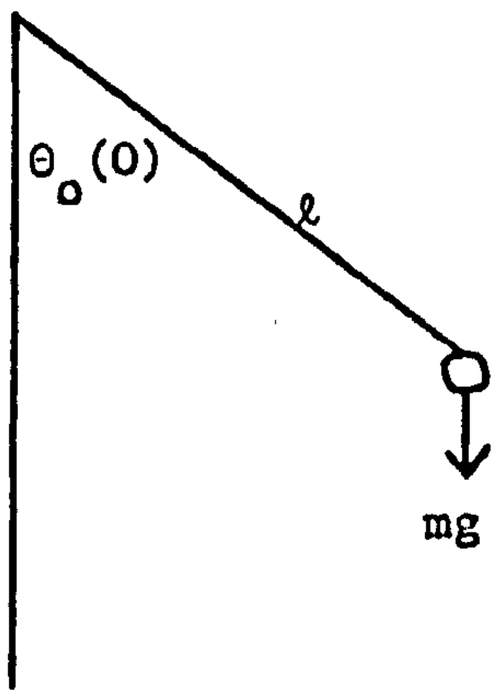

FIG. (6.1)

motion is described by the equation

$$m\ddot{\Theta}_o(t) = -\frac{mg}{\ell}\sin\Theta_o(t)$$

$$\simeq -\frac{mg}{\ell}\Theta_o(t) \quad , \tag{6.1}$$

if $\Theta_o(t)$ is assumed to be small. Therefore

$$\Theta_o(t) = \Theta_o(0)\cos\left[\left(\frac{g}{\ell}\right)^{\frac{1}{2}}t\right] . \tag{6.2}$$

The pendulum is now lowered into an infinitely deep fluid so that in its equilibrium position the string lies along the y-axis and the centre of the cylinder is at (0,h), h > a. It is further assumed that the pivot

remains above the free surface, thus giving $\ell > h + a$. As in Chapter 3 it is convenient to introduce polar co-ordinates (r,θ) defined by $x = r\sin\theta$, $y = h + r\cos\theta$.

The system is displaced by an angle $\Theta_o(0)$, and when the fluid has come to rest the bob is released with zero velocity at time $t = 0$. Thus under the usual assumptions of linearized flow, the fluid is described by a velocity potential $\Phi(x,y;t)$ which satisfies equations (2.1) in the region $x^2 + (y-h)^2 > a^2$, $y > 0$, (2.2b), (2.8), the radiation condition that at infinity waves are travelling outwards and

$$\frac{\partial\Phi}{\partial r} = \dot{\Theta}_o(t)\ \sin\theta \qquad \text{on } r = a\ . \tag{6.3}$$

Finally the equation of motion of the body can be obtained in the same way as equation (5.2), where, in contrast to (6.1), an additional force on the body is required to account for the body moving through the fluid. Hence

$$m\ddot{\theta}_o(t) = -\frac{mg}{\ell}\,\theta_o(t) + a\rho\int_{-\pi}^{\pi}\Phi_t(a\sin\theta,\ h + a\cos\theta,t)\sin\theta d\theta\ . \tag{6.4}$$

By applying the Fourier transform of Chapter 5 to these equations and supposing that there is no motion when $t < 0$, it follows that $\phi(x,y;\omega)$ satisfies the equations (5.7), (5.8) with

$$\frac{\partial\phi}{\partial r} = [-i\omega\theta_o(\omega) - \Theta_o(0)]\sin\theta\ , \qquad \text{on } r = a\ , \tag{6.5}$$

$$m[-\omega^2\theta_o(\omega) + i\omega\Theta_o(0)] = -\frac{mg}{\ell}\theta_o(\omega) - \rho ai\omega\int_{-\pi}^{\pi}\phi(a\sin\theta,h + a\cos\theta;\omega)\sin\theta d\theta\ , \tag{6.6}$$

and the radiation condition of outward travelling waves.

If simple harmonic motion of frequency ω is assumed, these equations describe the fluid motion due to a forced, periodic surging cylinder. Thus

$$\rho ai\omega\int_{-\pi}^{\pi}\phi(a\sin\theta,h + a\cos\theta;\omega)\sin\theta d\theta = [a_{11} \pm \frac{i}{\omega}\,b_{11}]i\omega[i\omega\theta_o(\omega) + \theta_o(0)],\ \omega \gtrless 0 \tag{6.7}$$

where a_{11}, b_{11} are the added mass and damping coefficients for a surging cylinder.

Substituting (6.7) in (6.6) and non-dimensionalizing by putting

$$a_{11} = M\mu \ , \quad b_{11} = M\omega\lambda \ , \quad \omega_o^2 = \frac{g}{\ell} \ ,$$

where $M = \pi\rho a^2$ is the mass per unit length of fluid displaced by a completely submerged circular cylinder, gives

$$\theta_o(\omega) = - \frac{i\Theta_o(0)\omega(m'+\Lambda)}{m'\omega_o^2-\omega^2(m'+\Lambda)} \tag{6.8}$$

where $m' = \frac{m}{M}$ and $\Lambda = \mu \pm i\lambda$, $\omega \gtrless 0$. Therefore by applying (5.6) to (6.8) yields

$$\Theta_o(t) = \Theta_o(0)h(\tau) \tag{6.9}$$

where

$$\begin{aligned} h(\tau) &= - \frac{i}{2\pi} \int_{-\infty}^{\infty} \frac{(m'+\Lambda)ue^{-iu\tau}}{m_o-u^2(m'+\Lambda)} \, du \ , && \tau > 0 \\ &= 0 \ , && \tau < 0 \end{aligned} \tag{6.10}$$

with

$$m_o = m'\omega_o^2 \frac{a}{g} = m' \frac{a}{\ell} \ , \quad u = \omega\left(\frac{a}{g}\right)^{\frac{1}{2}} \quad \text{and} \quad \tau = \left(\frac{g}{a}\right)^{\frac{1}{2}} t \ .$$

Equations (6.9) and (6.10) solve our problem in a form involving convergent integrals. In its present form it is not suitable for immediate computation, but by exploiting the conditions that $\Lambda(\bar{u}) = \overline{\Lambda(u)}$ and $h(\tau) = 0$ for $\tau < 0$, (6.10) reduces to

$$h(\tau) = \frac{2}{\pi} \int_o^{\infty} \frac{\lambda m_o u \cos u\tau}{[m_o-u^2(m'+\mu)]^2+u^4\lambda^2} \, du \ , \qquad \tau > 0 \ , \tag{6.11}$$

which is convenient for numerical computation.

An analytical examination of (6.10) for large τ can again proceed in the way described in §5.5. In Appendix B it is seen that Λ has a

logarithmic branch point at $\omega = 0$, and that near this point, Λ is a single-valued function in the u-plane cut along the negative imaginary axis. The contour of integration of (6.10) can therefore be deformed from along the real u-axis into the contour illustrated in fig. (5.1). The contribution to the integral from AC^-, C^+B requires the expansion of the integrand for large u, whilst the contribution from C^-OC^+ is determined by Watson's lemma. This latter contribution requires the leading terms in the expansion of the integrand near $u = 0$. Since single-valued terms make no contribution, only those terms containing $\ell n(Ka) - i\pi$ are of interest. It can be shown from the expressions obtained in Appendix B that for small values of u along OC^+ and OC^-,

$$[m_o - u^2(m' + \Lambda)]^{-1} = C_1^* + C_1^{**}u^6(\ell n|u| \mp i\pi)$$

where

$$C_1^{**} = \sum_{m=0}^{\infty} C_{1m}^{**} u^m \quad (\ell n|u| \mp i\pi)$$

such that $C_{10}^{**} \neq 0$. Therefore it is found that

$$\frac{1}{2\pi}\left(\int_{OC^+} - \int_{OC^-}\right) \sim -\frac{C}{\tau^6}$$

where C is a real constant.

It remains to determine the contribution to the integral from AC^-, C^+B. For this, we return to the notation and results of Chapter 3 for the special case when $M = 0$. Now, Davis (1974) has found that for large frequencies, or short waves, the radiated amplitude of a vertically oscillating cylinder is of the order of

$$\frac{A_2^+}{a} = O\left[(Ka)^{-\frac{1}{2}} e^{-K(h-a)}\right],$$

where (h-a) is not small compared with K^{-1}. Therefore using (3.56) in terms of non-dimensional quantities, it is found that

$$\lambda = \frac{|A_2^+|^2}{\pi a^2}$$

$$= O\left[(Ka)^{-1} e^{-2K(h-a)}\right] \quad \text{as } K \to \infty \ .$$

To determine the corresponding behaviour of the heave added mass coefficient, the asymptotic form of the Kramers-Kronig relation,

$$\mu(Ka) - \mu(\infty) \to -\frac{1}{\pi Ka} \int_0^\infty \lambda(z)dz < 0 \ , \quad \text{as } Ka \to \infty \ ,$$

given in Kotik and Mangulis (1962) is required. Since $\mu(\infty) = 1$, this enables the expression

$$\mu = 1 + O[(Ka)^{-1}] \qquad \text{as } Ka \to \infty$$

to be obtained.

From Chapter 3 it is known that these heave parameters are identical to the surge parameters. Hence it follows that the contribution to (6.10) from the curves AC^-, C^+B are negligible. Therefore the ultimate decay of the pendulum is algebraic, decaying like t^{-6}.

6.3 Results and discussion

The transient motion of an initially displaced pendulum bob when immersed in an infinitely deep fluid is given by equation (6.9) in terms of a Fourier integral (6.10) (or equivalently (6.11)). This integral involves the force coefficient term as a function of the integrating variable, and is computed for any one value by solving a truncated system of an infinite system of simultaneous equations. Therefore, in contrast to the previous chapter, this term is not known in explicit form and so the integral is evaluated using a third-order finite-difference formulae by a method due to Gill and Miller (1972).

The integral depends on three parameters: m', $\frac{h}{a}$ and $\frac{a}{\ell}$. The results of varying any one of these relative to the other two are presented in figs. (6.2)-(6.9) for $m' = 0.5,1,1.5$; $\frac{a}{\ell} = \frac{1}{4}, \frac{1}{8}, \frac{1}{10}$; and $\frac{h}{a} = 1.5,2,3$ as τ

goes from 0 to 100.

Figs. (6.2) and (6.3) show the effect of the relative mass when $a/\ell = \frac{1}{4}$ and $h/a = 2,3$ respectively. This corresponds to cylinders of different masses moving in the same fluid, or the same cylinder travelling through fluids of different densities. In either case it is seen that a lighter cylinder or a denser fluid produces motions with a greater amplitude and a longer period of oscillation. Therefore, as expected, the decay is slower for this situation than for a heavier cylinder or a less dense fluid.

The variation of a/ℓ is displayed in figs. (6.4) and (6.5). In fig. (6.4) $h/a = 2$ and $m' = 1.5$, wilst in fig. (6.5) $h/a = 1.5$ with $m' = 1$. Clearly, as the pivot point gets further away from the free surface (ℓ increases), the cylinder has greater freedom to move and therefore deviates further away from its equilibrium position. Since it travels further, it is not surprising that it has a longer period of oscillation. Indeed, as a/ℓ decreases, the motion becomes more regular.

Finally, the results obtained by setting a/ℓ and m', and allowing the immersion to cylinder radius ratio to change are exhibited in figs. (6.6)-(6.9). In addition to the curves for the h/a given above, the graphs for a deeply submerged cylinder, $h/a \to \infty$, and for the corresponding undamped pendulum motion in air are also plotted. Both these curves are periodic, for from equation (6.2) and the definition of τ, the latter has a period of $2\pi\left(\frac{\ell}{a}\right)^{\frac{1}{2}}$, whilst in the former the force coefficient tends to one and hence the period of oscillation is $2\pi\left(\frac{m'+1}{m_o}\right)^{\frac{1}{2}}$. As m' increases these periods get closer, but obviously the pendulumoscillating in air moves quicker than the one opposing the resistance of the fluid. This is in agreement with the displayed results. The diagrams also show that the decay of motion is more rapid, with a

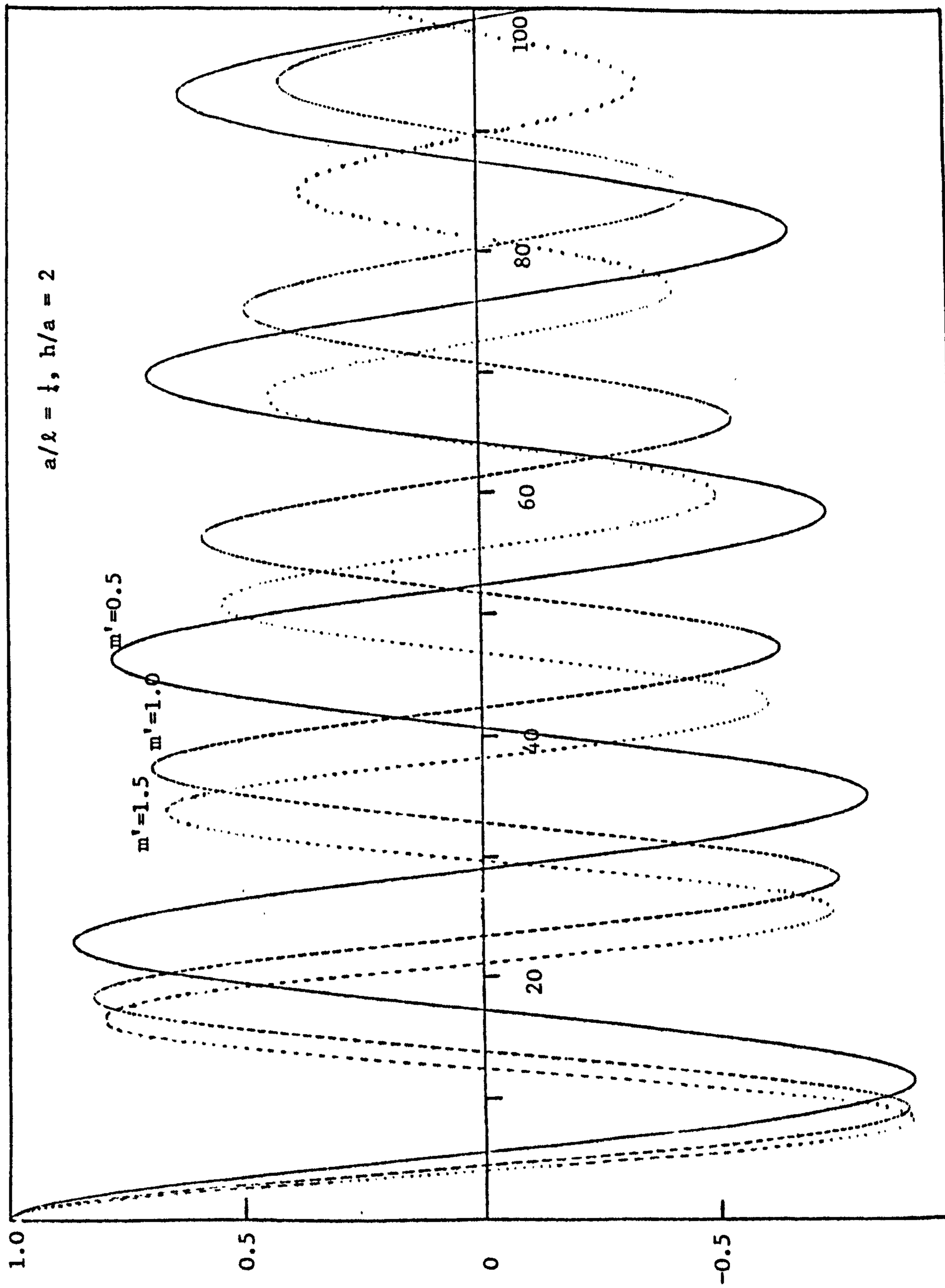

FIG. (6.2)

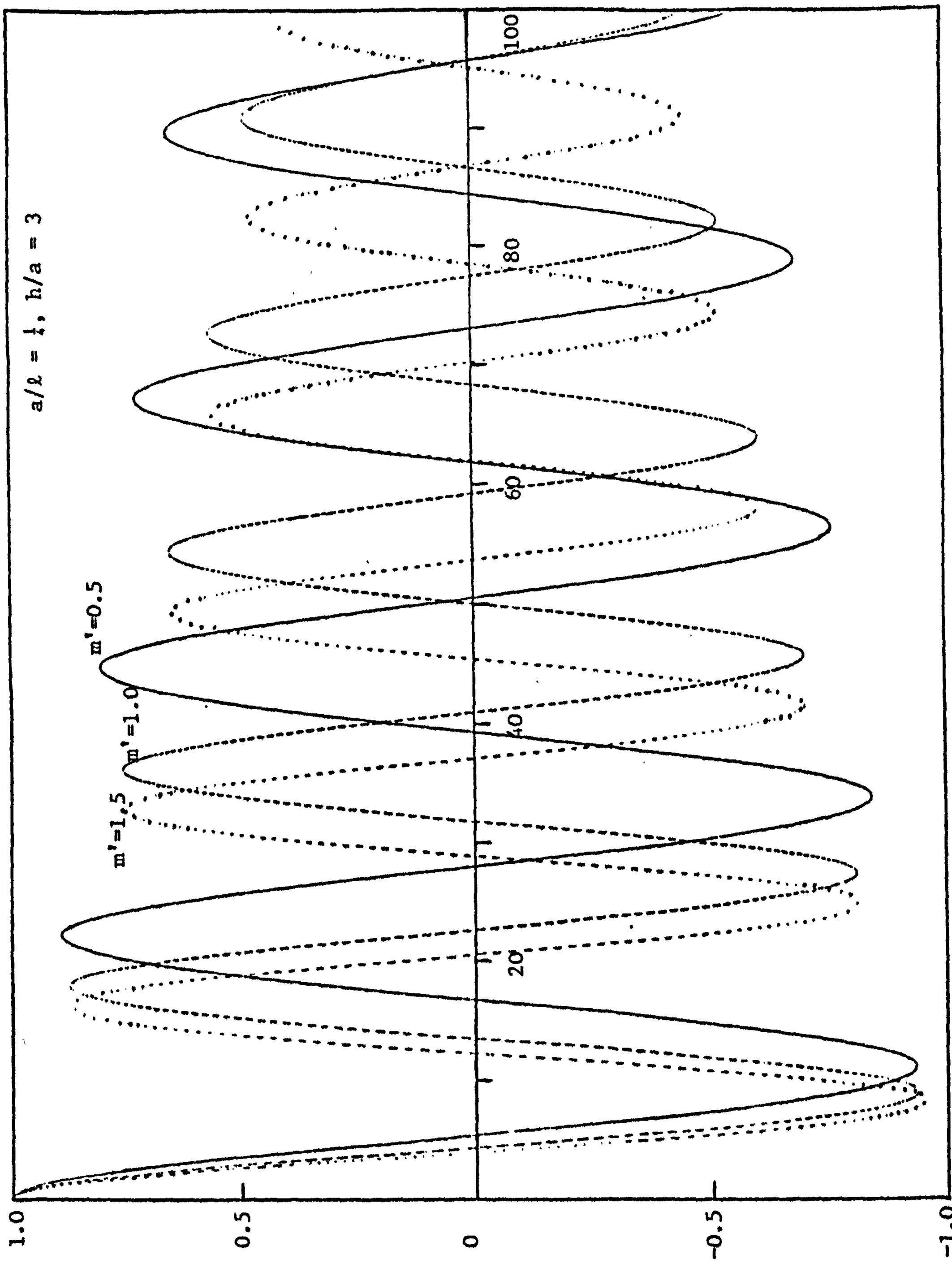

FIG. (6.3)

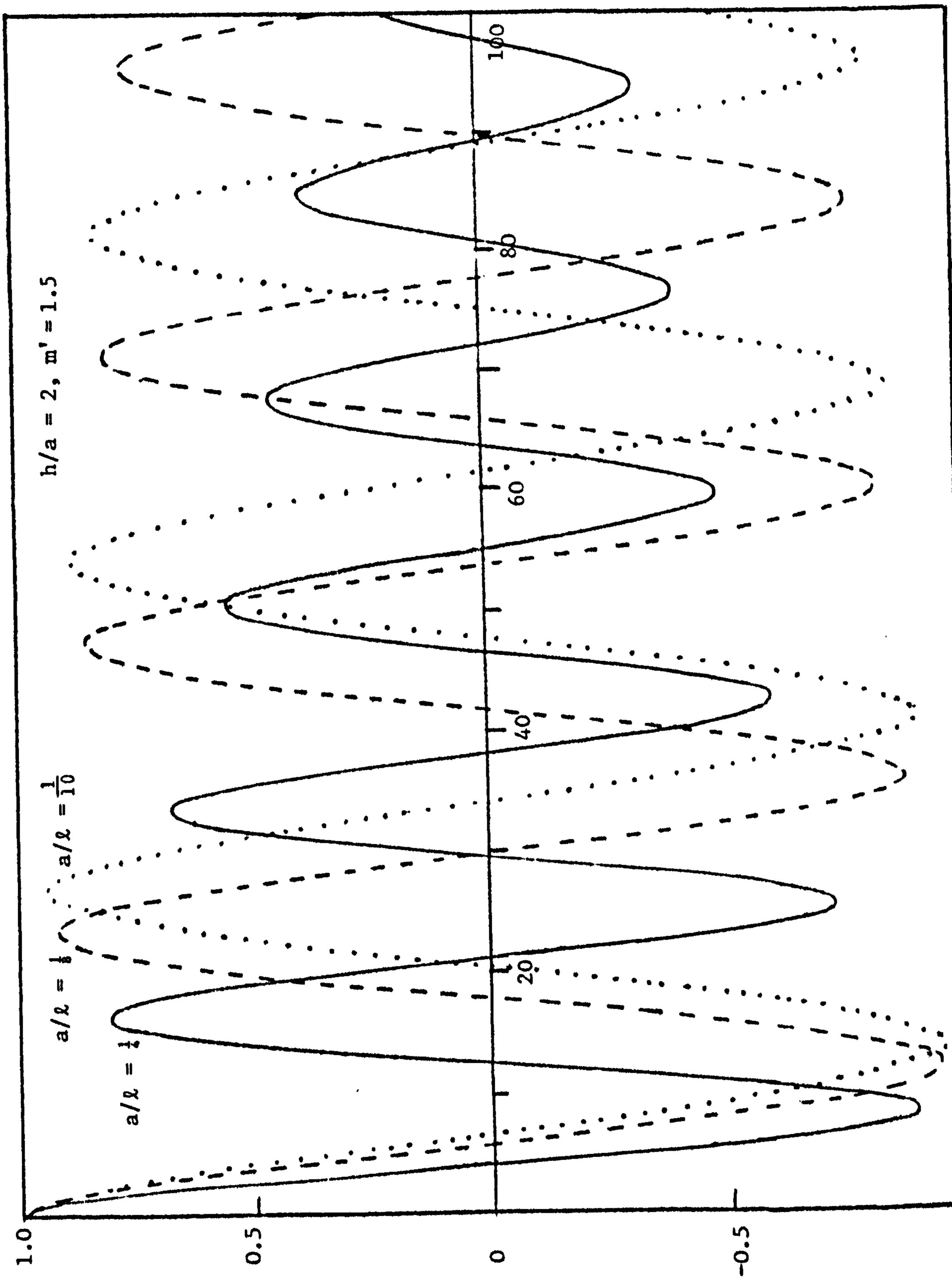

FIG. (6.4)

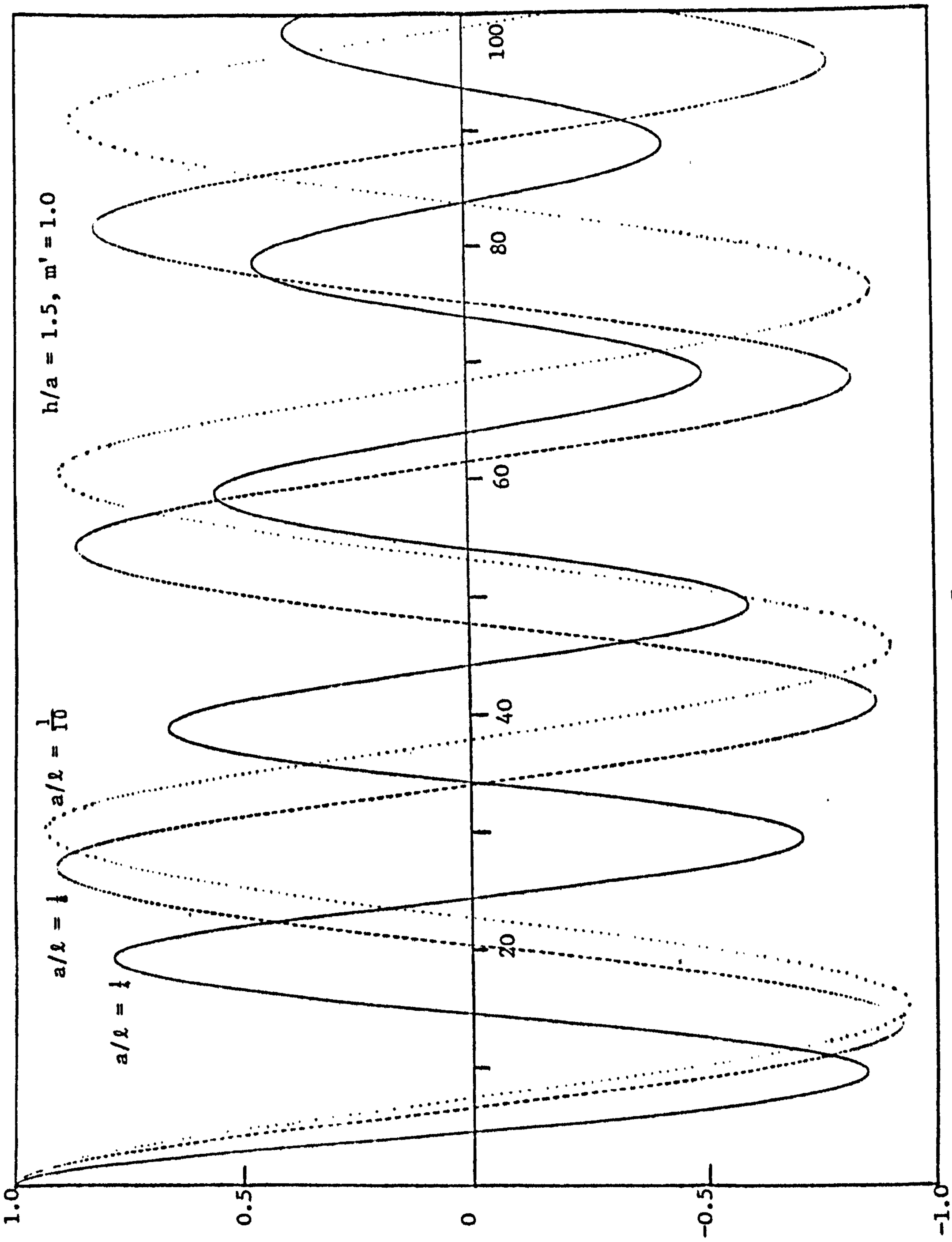

FIG. (6.5)

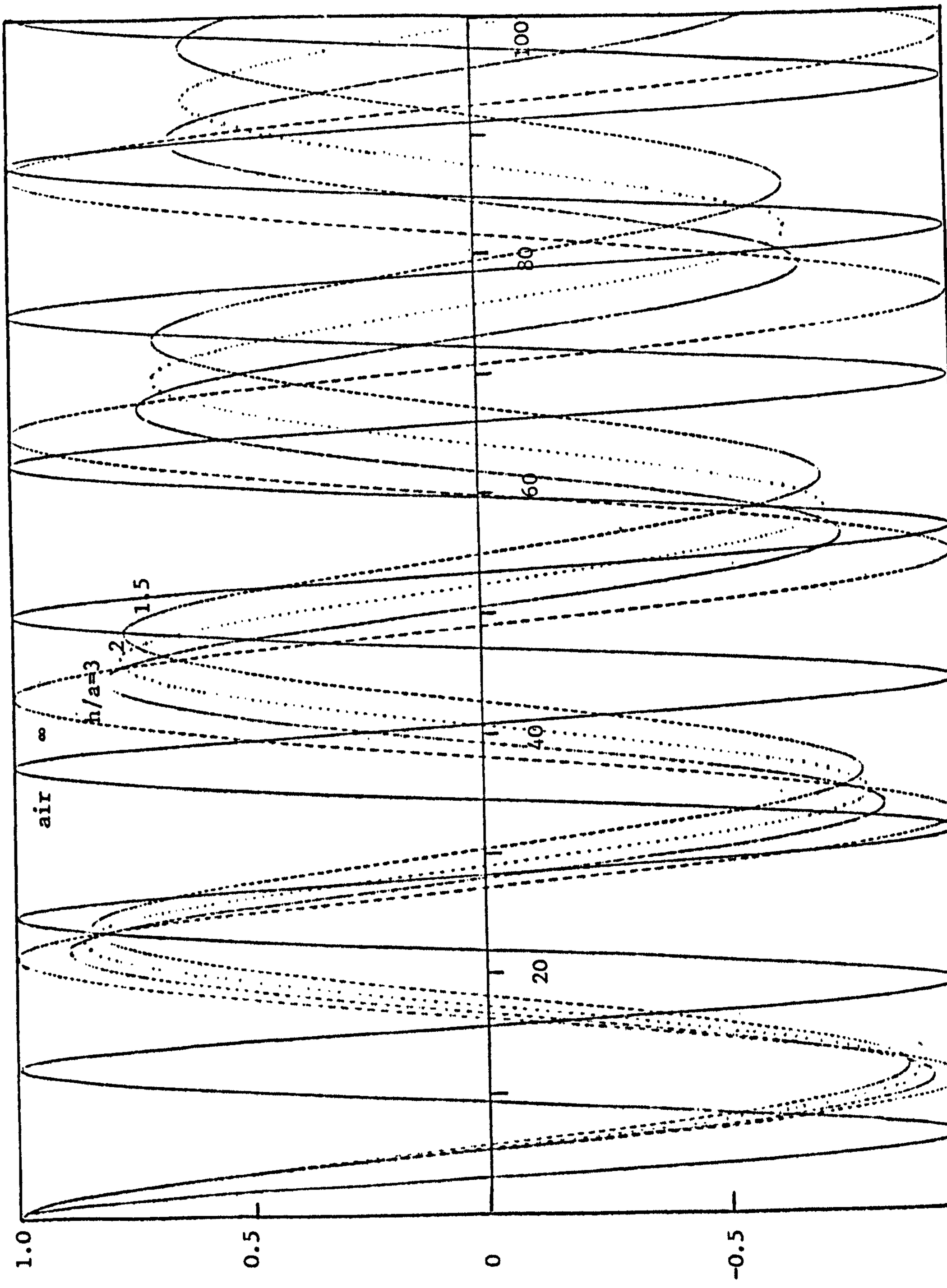

FIG. (6.6)

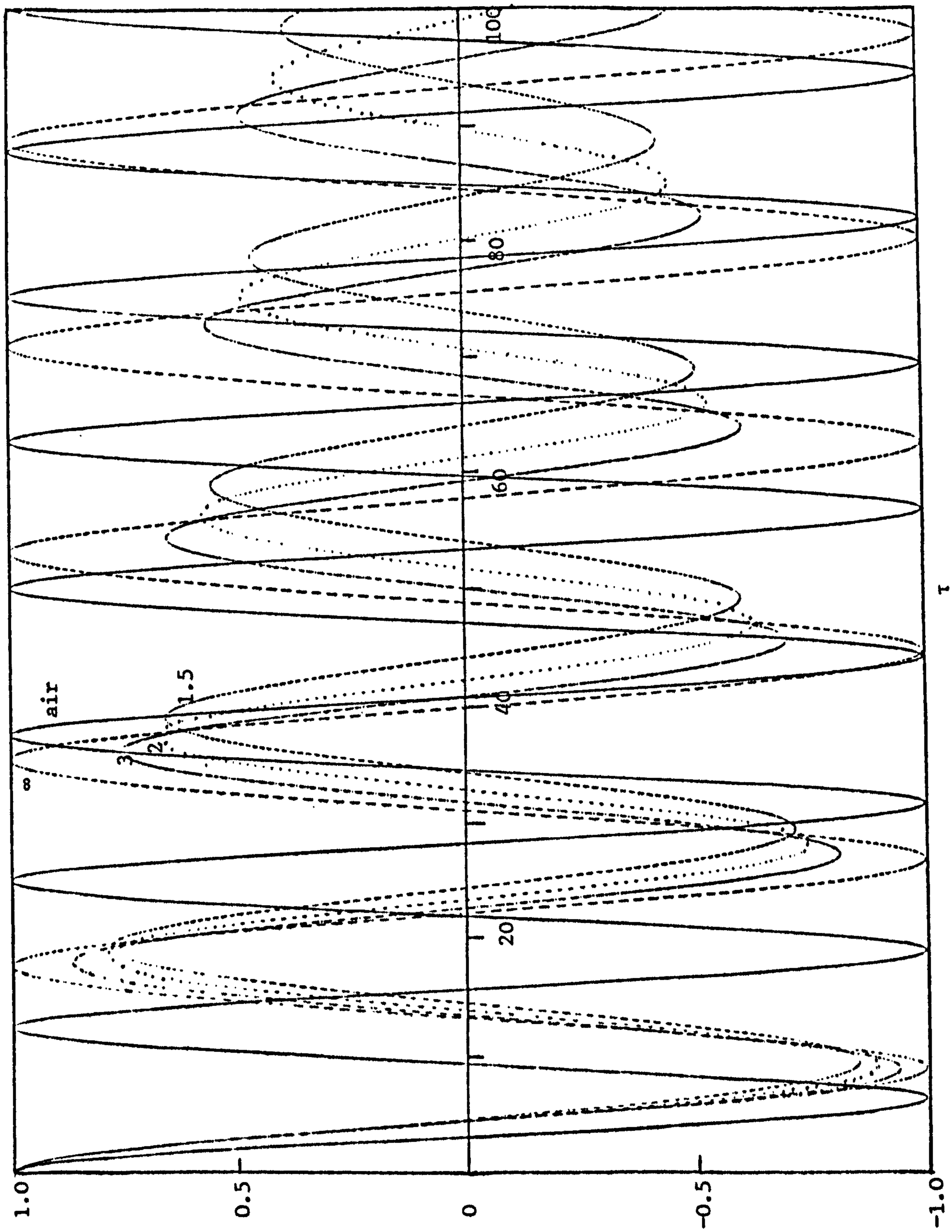

FIG. (6.7)

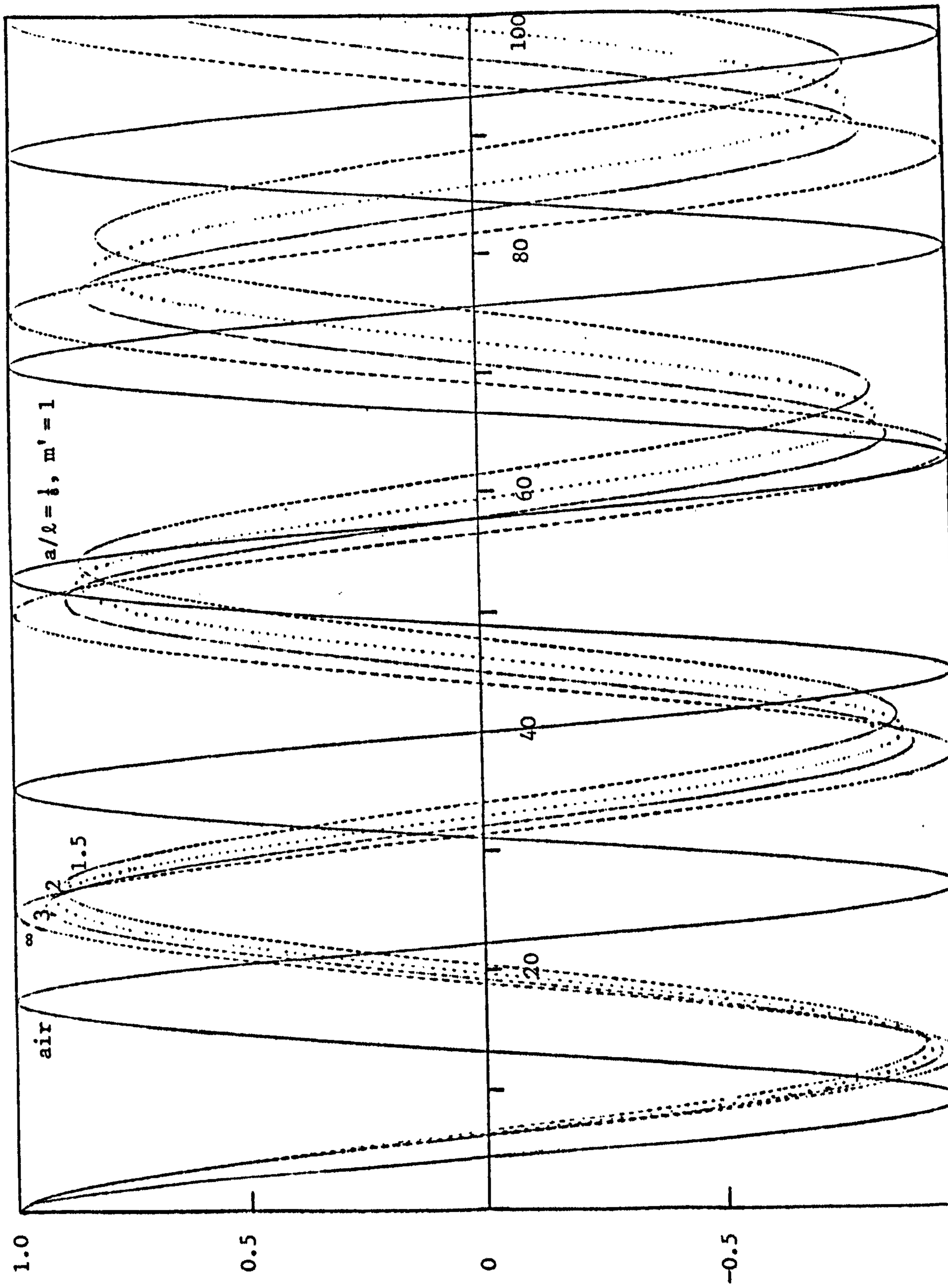

FIG. (6.8)

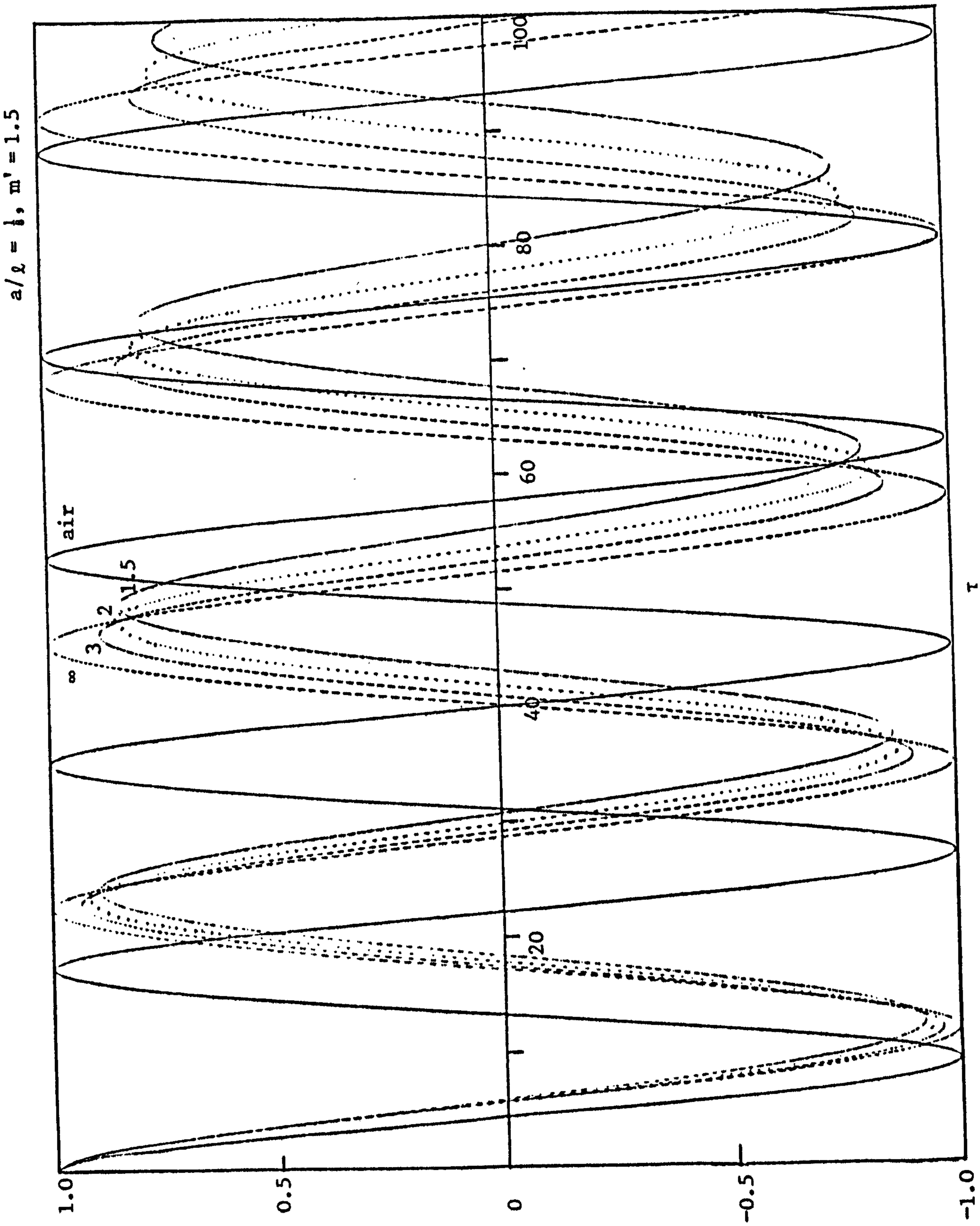

FIG. (6.9)

longer period of oscillation when the axis of the cylinder is nearer to the free surface.

6.4 The general case

In Kotik and Lurye (1964), the large time behaviour of the heave displacement of a cylinder of arbitrary cross-section released at zero velocity from a position of hydrostatic dis-equilibrium is obtained. The method they employ exploits the behaviour of the damping parameter at zero frequency, from which the corresponding, limiting value of the added mass coefficient is evaluated by use of the Kramers-Kronig relation, derived by Kotik and Mangulis (1962) for heave displacements.

In a similar manner, all that is required to calculate the asymptotic decaying behaviour of a totally submerged surging cylinder of arbitrary shape is the value of the added mass or damping parameter at zero frequency, since it is known that the Kramers-Kronig relations hold for all modes of oscillations (Ogilvie, 1964). For this situation the free surface condition (2.11) takes the form

$$\frac{\partial \phi}{\partial y} = 0 , \qquad \text{on } y = 0, \quad \omega \to 0 .$$

This is the rigid-wall boundary condition where the free surface is replaced by a fixed horizontal plane. The problem can therefore be solved by the method of images where the appropriate image is a body of the same geometrical form reflected about the plane $y = 0$. The phase of the image body motion must be such that the potential is an even function of y, and the normal velocity takes the same value at corresponding points on the body and its image.

In the case of a surging half-submerged body, the body plus its image forms a rigid double body moving in phase with the real body. Thus the velocity potential is related to the potential for a rigid body

in an unbounded fluid. This problem is discussed in Newman (1977b), together with a consideration of the other modes of oscillation, and classical methods may be applied.

The reflection of a totally submerged body follows through similarly, but in this instance it is not possible to get a closed form solution for the potential of the distinct rigid bodies in an unbounded fluid, in general.

6.5 Conclusion

The classical problem of a pendulum oscillating in air under the original disturbance of a small angular displacement has been extended to consider the damping effect that is produced when the pendulum is likewise set in motion in a very deep fluid. An analytic examination has shown that the ultimate decay is algebraic, like t^{-6}, although the computed transient motion results presented have not been continued far enough for this dominating behaviour to be seen.

CHAPTER 7

WAVE-POWER ABSORPTION BY OSCILLATING SURFACE PRESSURE DISTRIBUTIONS

7.1 Introduction

An area of international interest which has received much attention in the last decade is that of extracting energy from the sea. Over this period numerous wave-energy devices have been developed, a number of which are based on a common mode of operation - that of an oscillating column of water (OWC).

In its simplest form this consists of an open-ended, hollow structure, partially immersed with its open end downwards such that a volume of air is trapped above the internal free surface. In response to an incident wave train, a pressure fluctuation at the open lower end causes the water in the tube to oscillate, forcing the internal free surface to rise and fall. This in turn drives the volume of air back and forth at high speed through a constricted opening in the structure in which an air-turbine and generator set is housed which converts the energy into electricity.

This idea was successfully developed by Masuda as early as 1947 to self-power navigation buoys. Since then larger devices have been developed which operate on the same principle, examples of which include the CEGB "half-open matchbox" device, described in Count et al. (1981), the buoy of Queen's University, Belfast, and the Japanese Kaimei ship device. Full descriptions of the last two devices can be found in Quarrell (1978). A further device which is in its initial stages of

development is the Norwegian Kvœrner multiresonant OWC (KMOWC), described in Ambli et al. (1982). In contrast to the conventional designs this OWC has two parallel walls protruding from its main structure so that in addition to the basic resonance of the OWC, there are also "harbour" resonance effects.

It was originally assumed that the hydrodynamics of an OWC wave-energy device could be modelled by an adaption of the rigid body theory. This involved replacing the internal free surface by a weightless rigid piston to which a power take-off mechanism, consisting of a spring-damper system was attached. Evans (1978) provides an example of such an approach wherein the efficiency of two, closely spaced parallel plates, and the efficiency of a narrow tube of circular cross-section are determined.

A simpler but more accurate means of formulating the problem has since been developed by Evans (1982a) to correctly allow for the applied surface pressure distribution and the subsequent spatial variation of the internal free surface. This newly-developed theory has close analogies with the corresponding theory for rigid oscillating bodies, and many of the general results are identical. A few simple examples are given to illustrate this theory with the fuller problem of an axisymmetric duct being treated in Thomas (1981b). More recently Evans (1982b) has extended the theory to examine the wave-power absorption within a narrow resonant harbour.

A brief outline of the original surface pressure distribution theory is given in §7.2 for a single, two-dimensional device in a fluid of finite or infinite depth. Two simple examples are then considered in §7.3 and §7.4, assuming an impedance condition can be matched exactly. Results for these cases are presented before the more practical condition for resonance is applied to a two-dimensional model of a harbour with an

OWC at its closed end. Special, limiting cases of this problem are treated in §7.7 and §7.8 and comparisons with the full solution are made in §7.9. Finally concluding remarks are made in §7.10.

7.2 General theory

A fixed, open-ended, two-dimensional structure is immersed open end downwards in a fluid of finite or infinite depth such that it intersects the free surface, trapping a volume of air above the internal free surface. The structure enclosing this air column contains a small aperture to which a power mechanism in the form of a turbine is connected. In the presence of an incident wave train the internal free surface is forced to oscillate with the same frequency, ω, as the incoming wave, setting up a uniform pressure distribution over the internal free surface. If the compressibility of the air is small, this pressure is the same as that at the turbine, and assuming the turbine characteristics are linear, the pressure-drop across the turbine is proportional to the flow through it. Hence the mean power absorbed by the system is the time average of the pressure drop and volume flux, the volume flux being the product of the spatial average of the vertical velocity of the internal free surface and its length.

The velocity potential $\Phi(x,y,t)$ describing the fluid motion satisfies the equations (2.1) and (2.2), whilst the linearized free surface condition becomes

$$\left.\begin{aligned} g\eta - \frac{\partial \Phi}{\partial t} &= 0 \qquad \text{on the free surface} \\ \text{and} \\ g\eta - \frac{\partial \Phi}{\partial t} &= \frac{P(t)}{\rho} \qquad \text{on } S_i \text{ the internal free surface.} \end{aligned}\right\} \tag{7.1}$$

Here $P(t)$ is the uniformly distributed pressure on S_i. Finally there is the condition that on rigid boundaries

$$\frac{\partial \Phi}{\partial n} = 0 \,. \tag{7.2}$$

Again the radiation condition of outward travelling waves must be satisfied to account for the scattering of the incident wave from the structure.

Since it is assumed that all the motion is simple harmonic, it is convenient to define time-independent quantities ϕ,p by (2.9) and

$$P(t) = \mathrm{Re}\{pe^{-i\omega t}\} . \tag{7.3}$$

Therefore by using (7.1)-(7.3) and (2.9) with (2.3), it can be seen that ϕ must satisfy (2.10), (2.12),

$$\left.\begin{aligned} K\phi + \frac{\partial\phi}{\partial y} &= 0 \qquad \text{on the free surface,} \\ K\phi + \frac{\partial\phi}{\partial y} &= \frac{-i\omega p}{\rho g} \qquad \text{on } S_i , \end{aligned}\right\} \tag{7.4}$$

and

$$\frac{\partial\phi}{\partial n} = 0 \qquad \text{on a body.} \tag{7.5}$$

As for the rigid body problems described in Chapter 2, the potential ϕ can be decomposed into two parts such that

$$\phi = \phi_s - \frac{i\omega p}{\rho g}\psi \tag{7.6}$$

where ϕ_s is the solution of the scattering problem satisfying equations (2.10), (2.12), (7.4) with p = 0, and (7.5). This potential also includes an incident wave potential of the form described by (2.13) or (2.15) for a fluid of finite or infinite depth respectively. The power per unit frontage, that is, the mean energy flux per unit length across a vertical plane normal to the wave direction, contained in this incident wave is then

$$P_w = \frac{\rho g^2 A^2 kd\, N_o}{2\omega \cosh kd} , \tag{7.7a}$$

where N_o is given by (4.3). As $d \to \infty$

$$P_w \to \frac{\rho g^2 A^2}{4\omega} \quad . \tag{7.7b}$$

The other potential defined in (7.6), ψ, describes the radiation problem, representing outgoing waves at infinity. Indeed ψ satisfies equations (2.10), (2.12), (7.5) with

$$K\psi + \frac{\partial \psi}{\partial y} = 1 \qquad \text{on the internal free surface,} \tag{7.8}$$

$$K\psi + \frac{\partial \psi}{\partial y} = 0 \qquad \text{on the free surface,} \tag{7.9}$$

and is of the form

$$\psi \sim f^{\pm} \cosh k(d-y) e^{\pm ikx} \quad \text{as } x \to \pm\infty \text{ for a fluid of finite depth} \tag{7.10a}$$

or

$$\psi \sim f^{\pm} e^{-Ky \pm iKx} \quad \text{as } x \to \pm\infty \text{ for an infinitely deep fluid .} \tag{7.10b}$$

In keeping with the assumptions already made, the volume flow rate across S_i will also be simple harmonic. Therefore defining such a time-independent quantity by q gives

$$q = \int_{S_i} \frac{\partial \phi}{\partial y} \, dS$$

$$= q_s + q_r \tag{7.11}$$

where

$$q_s = \int_{S_i} \frac{\partial \phi_s}{\partial y} \, dS \tag{7.12}$$

and

$$q_r = -\frac{i\omega\rho}{\rho g} \int_{S_i} \frac{\partial \psi}{\partial y} \, dS \quad . \tag{7.13}$$

As an incident wave may approach from either direction let

$$q_s = q_s^+ \tag{7.14}$$

if the wave is from $x = +\infty$, and

$$q_s = q_s^- \tag{7.15}$$

when the wave is incident from $x = -\infty$.

In an analogous manner to the rigid body problem, the radiation flow rate can be decomposed into a damping component, $\tilde{B}$, in phase with the pressure, and a component $\tilde{A}$ in phase with the rate of change of pressure, such that

$$q_r = (\tilde{B} - i\omega\tilde{A})p = - Zp \quad . \tag{7.16}$$

By applying (2.30) to ψ and $\bar{\psi}$, and making use of (7.16), it follows that

$$\tilde{B} = \frac{Kkd\omega N_o}{\rho g} [|f^+|^2 + |f^-|^2] \quad \text{in a fluid of finite depth,} \tag{7.17a}$$

$$= \frac{K\omega}{2\rho g} [|f^+|^2 + |f^-|^2] \quad \text{as } d \to \infty \ . \tag{7.17b}$$

Similarly by applying (2.30) to ϕ_s and ψ ,

$$q_s^{\pm} = - \frac{2A\omega kdN_o f^{\pm}}{\text{coshkd}} \tag{7.18a}$$

$$= - \omega A f^{\pm} \quad \text{as } d \to \infty \ , \tag{7.18b}$$

showing that the far-field amplitude of the radiated problem is proportional to the induced volume flux across S_i. Clearly (7.17) and (7.18) combine to yield

$$\tilde{B} = \frac{1}{8P_w} [|q_s^+|^2 + |q_s^-|^2] \ . \tag{7.19}$$

The results (7.17)-(7.19) for an infinitely deep fluid are identical to those determined by use of the Kochin function in Evans (1982a).

The mean rate of working of the pressure force, or the mean power absorbed per unit width of pressure distribution, W, is the time average of the pressure and volume flux over a period of oscillation. Hence

$$W = \tfrac{1}{2}\,\mathrm{Re}\,\bar{p}q$$

$$= \tfrac{1}{2}\,\mathrm{Re}\,\bar{p}q_s - \tfrac{1}{2}|p|^2\tilde{B}\,, \qquad (7.20)$$

where a bar denotes complex conjugate. This has a maximum value

$$W_{max} = \tfrac{1}{8}\,|q_s|^2\tilde{B}^{-1} \qquad (7.21)$$

when

$$p = \tfrac{1}{2}\,\tilde{B}^{-1}\,q_s\,. \qquad (7.22)$$

Therefore the efficiency of power absorption, or the proportion of available power per unit frontage of the incident wave which is extracted from the body, is

$$\eta_{max} = \frac{W_{max}}{P_w}\,. \qquad (7.23)$$

When waves approach from $x = \pm\infty$ this becomes

$$\eta^{\pm}_{max} = \frac{|q^{\pm}_s|^2}{|q^{+}_s|^2 + |q^{-}_s|^2} \qquad (7.24)$$

$$= \frac{|f^{\pm}|^2}{|f^{+}|^2 + |f^{-}|^2}\,. \qquad (7.25)$$

Hence a good uni-directional wave generator is a good absorber. It also follows that when the pressure distribution is symmetric about the x-axis such that $f^{+} = f^{-}$, then the maximum efficiency is $\frac{1}{2}$.

These results for the maximum efficiency hold only if the pressure at the turbine is related to the induced volume flux across it in a manner

such that condition (7.22) is satisfied. In practice it is difficult to control this pressure drop across the turbine. However it may be easier to control the volume flow rate through the turbines. Thus, it is assumed that these quantities are related linearly and that the pump characteristics do not allow a phase lag between the pressure and volume flux to develop. Therefore

$$q = \Lambda p \tag{7.26}$$

where Λ is a positive constant, giving

$$W = \frac{|q_s|^2}{8\tilde{B}}\left\{1 - \frac{|\Lambda-\bar{Z}|^2}{|\Lambda+\bar{Z}|^2}\right\}. \tag{7.27}$$

This has a maximum value

$$W_{max} = \frac{|q_s|^2}{8\tilde{B}}\left\{1 - \left(\frac{\Lambda_{opt} - \tilde{B}}{\Lambda_{opt} + \tilde{B}}\right)\right\} \tag{7.28}$$

when

$$\Lambda = \Lambda_{opt}, \quad \text{say} \tag{7.29}$$

where

$$\Lambda_{opt} = (\tilde{B}^2 + \omega^2\tilde{A}^2)^{\frac{1}{2}} . \tag{7.30}$$

Hence the maximum efficiency is

$$\eta_{max} = \frac{|q_s|^2}{4P_w}\left(\frac{1}{\Lambda_{opt} + \tilde{B}}\right) . \tag{7.31}$$

In the next two sections the maximum theoretical efficiency given by (7.24), (7.25) is obtained for two simple problems, and then the resonance expression (7.31) is examined for an OWC formed by placing a thin barrier in front of a harbour wall.

(a) SIMPLE EXAMPLES

7.3 The theoretical maximum efficiency of a narrow duct with unequal length sides

Here we consider a column of water oscillating in a fluid of infinite depth between two, closely spaced vertical strips of differing lengths. The sides of the duct occupy the intervals $x = 0$, $0 < y < \ell$ and $x = a$, $0 < y < s$ where $s < \ell$. From equation (7.25) the quantity of interest, the theoretical maximum efficiency, can be computed from a knowledge of the far-field radiated amplitudes so only the radiation problem need be considered. Further, since it is assumed that the duct is narrow, this reduces to an examination of the "outer solution", a technique described in Chapter 4. In this instance an observer on the right-hand side and a long way from the fixed structure will see the two barriers as one of length ℓ, with flow issuing from a uni-directional source placed on the side of it at (0,s). This coincides with the end of the shorter barrier, as illustrated in fig. (7.1). Simultaneously an observer on the other side of the duct will see the consequence of this source as it flows underneath the barrier.

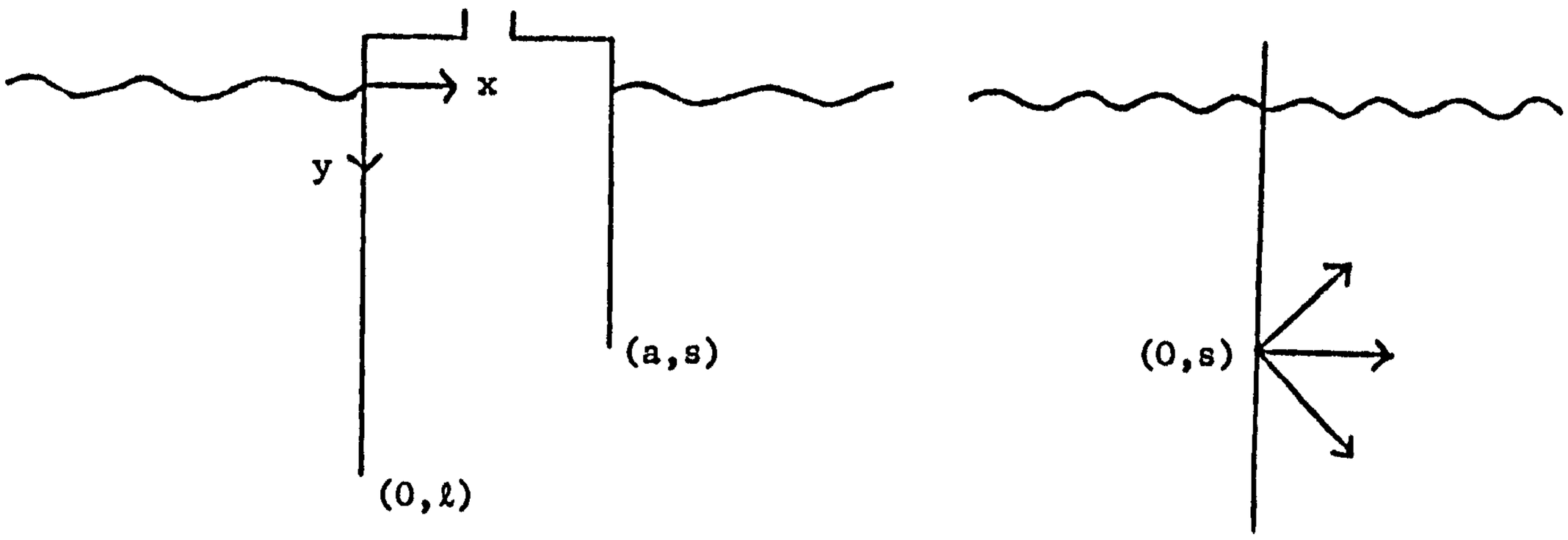

FIG. (7.1)

The more general far-field amplitudes due to a source placed anywhere in the presence of a fixed barrier have been obtained by Evans (1976). This resulted as a special case of his primary consideration of determining the behaviour of small oscillations of a vertical barrier. However, as Evans also pointed out in his paper, these results could more easily be obtained by a direct approach to the immediate problem. This alternative method is described below for the particular case when the source is on the side of the barrier. The general case for the source off the barrier follows through identically except that the position of the source must be excluded by a circle of small radius rather than a semi-circle.

Continuing with the notation already defined, the radiation potential $\psi(x,y)$ satisfies

$$\frac{\partial \psi}{\partial x} = 0 \qquad \text{on } x = 0,\ 0 < y < \ell \tag{7.32}$$

with the outward travelling waves of equation (7.10b) given by

$$\psi(x,y;0,s) = f^{\pm}(0,s)e^{-Ky \pm iKx} \qquad \text{as } x \to \pm\infty\ . \tag{7.33}$$

The required amplitudes are determined by introducing Ursell's (1947) explicit velocity potential solution for waves incident on a fixed plate. This is given by

$$\Phi_u(x,y,t) = \mathrm{Re}\{\phi_u(x,y)e^{-i\omega t}\}\ ,$$

where for $x > 0$

$$\phi_u(x,y) = \{\pi I_1(K\ell) + iK_1(K\ell)\}e^{-iKx-Ky} + \pi I_1(K\ell)e^{iKx-Ky} + \int_0^{\infty} \frac{J_1(k\ell)}{k^2+K^2}\,(k\cos ky - K\sin ky)e^{-kx}\,dk\ , \tag{7.34}$$

and for $x < 0$

$$\phi_u(x,y) = iK_1(K\ell)e^{-iKx-Ky} - \int_0^\infty \frac{J_1(k\ell)}{k^2+K^2}(k\cos ky - K\sin ky)e^{kx}\,dk \ . \quad (7.35)$$

The identity (2.30) is now applied to the harmonic functions ψ and $\phi_u(\pm x,y)$ within the region bounded by the lines:

$$0 < x < X\ , \quad y = 0\ ; \qquad x = X\ , \quad 0 < y < Y\ ;$$

$$-X < x < X\ , \quad y = Y\ ; \qquad x = -X\ , \quad 0 < y < Y\ ;$$

$$-X < x < 0\ , \quad y = 0\ ; \qquad x = 0^-, \quad 0 < y < \ell\ ;$$

$$x = 0^+\ , \quad 0 < y < \ell\ ; \qquad \text{with} \quad X,Y > 0\ ,$$

and where the point (0,s) is excluded by a semi-circle of small radius. As in Evans (1976) the only contribution to the integral in (2.30) arises from the integral around the plate, from the semi-circle around (0,s) and from the incoming wave combining with the outgoing wave of $\psi(x,y)$ at $x = +X$, $0 < y < Y$ as $X,Y \to \infty$. Thus

$$\int_0^Y \left[\psi(x,y)\,\frac{\partial\phi_u}{\partial x}\,(x,y) - \phi_u(x,y)\,\frac{\partial\psi}{\partial x}\,(x,y)\right] dy + \pi\phi_u(0,s) = 0\ ,$$

which reduces to yield

$$f^+(0,s) = \frac{-\pi i\phi_u(0^+,s)}{\pi I_1(K\ell)+iK_1(K\ell)} \quad (7.36)$$

on using (7.33), (7.34) and (7.35). Similarly

$$f^-(0,s) = \frac{-\pi i\phi_u(0^-,s)}{\pi I_1(K\ell)+iK_1(K\ell)}\ . \quad (7.37)$$

Therefore using (7.34) and (7.35),

$$f^\pm(0,s) = -\pi ie^{-Ks} \pm B \quad (7.38)$$

where

$$B = \frac{-i\pi}{\pi I_1(K\ell)+iK_1(K\ell)} \left\{ \int_0^\infty \frac{J_1(k\ell)}{k^2+K^2} (k\cos ks - K\sin ks)\,dk + \pi e^{-Ks} I_1(K\ell) \right\}. \tag{7.39}$$

From equation (7.25)

$$\eta^+_{max} = \frac{1}{1 + \left|\frac{1-\alpha}{1+\alpha}\right|^2} \tag{7.40}$$

where

$$\alpha = \frac{\alpha_{int}}{\pi I_1(K\ell)+iK_1(K\ell)}, \tag{7.41}$$

and

$$\alpha_{int} = \int_s^\ell \frac{te^{Kt}}{\ell(\ell^2-t^2)^{\frac{1}{2}}}\,dt .$$

Clearly, as $s \to 0$

$$\alpha \to \frac{1}{\pi I_1(K\ell)+iK_1(K\ell)} \left[1 + \frac{\pi}{2} \{I_1(K\ell)+L_1(K\ell)\} \right]. \tag{7.42}$$

Further, since

$$\alpha_{int} = \int_0^{\cos^{-1}(\frac{s}{\ell})} \cos\theta e^{K\ell\cos\theta}\,d\theta > 0 ,$$

$$\left|\frac{1-\alpha}{1+\alpha}\right|^2 = \frac{[\pi I_1(K\ell)-\alpha_{int}]^2 + K_1^2(K\ell)}{[\pi I_1(K\ell)+\alpha_{int}]^2 + K_1^2(K\ell)}$$

$$< 1$$

and therefore

$$\eta^+_{max} > \tfrac{1}{2} .$$

The alternate, complementary expression η^-_{max} is readily obtained from the relation

$$\eta^-_{max} = 1 - \eta^+_{max}$$

$$< \tfrac{1}{2} , \quad \text{from above.}$$

Hence the device is more efficient when the incident wave travels towards the shorter side.

Computational results for η^{+}_{max} alone are shown below, being tabulated in Table (7.1) as a function of $K\ell$. From the first few columns it can be seen that as the source moves closer to the free surface the expected value as $s \to 0$, given by (7.42) in (7.40), is approached. Further, as $\frac{s}{\ell}$ varies between 0.1 and 0.6, the value of the maximum possible efficiency for each $K\ell$ remains constant to within approximately 3%. Indeed for $K\ell > 0.8$, $\frac{s}{\ell} = 0.6$ is the desired ratio for achieving the greatest efficiency. For values of $\frac{s}{\ell}$ greater than 0.6, the maximum efficiency is very much lower. This is displayed more clearly in fig. (7.2) where it is seen that as $\frac{s}{\ell} \to 1$, the efficiency shows a reluctance to leave the value $\frac{1}{2}$. However, by applying Laplace's method to α_{int} for large $K\ell$, it is found that η^{+}_{max} does approach unity for all $\frac{s}{\ell} < 1$. Finally, when $\frac{s}{\ell} = 1$, $\eta^{+}_{max} = \frac{1}{2}$ as expected, for the device is then symmetric.

The corresponding curves for η^{+}_{max} as a function of Ks are plotted in fig. (7.3). Again, as ℓ approaches s it can be seen that the efficiency remains close to $\frac{1}{2}$ over the range considered, although ultimately it reaches unity.

To conclude graphs displaying the maximum efficiency against the ratio $\frac{s}{\ell}$ for constant $K\ell$ and Ks are given in figs. (7.4) and (7.5), respectively. It can be seen that the theoretical result of η^{+}_{max} tending to one as ℓ increases is obtained in both cases, and also that as the barriers become of equal length, the efficiency drops to $\frac{1}{2}$.

It would be of interest to do a fuller analysis of this problem by using the approximate method of matching, explained in Chapter 4. The problem would then reduce to a type studied by Newman (1974) and Evans (1978). However, as noted in the concluding paragraph of the

Kℓ	$s/\ell=0$	0.1	0.2	0.3	0.4	0.5	0.6	0.7	0.8	0.9
0.1	.5017	.5017	.5017	.5017	.5016	.5015	.5014	.5013	.5011	.5008
0.2	.5152	.5152	.5150	.5147	.5142	.5135	.5126	.5114	.5097	.5072
0.3	.5541	.5539	.5534	.5526	.5512	.5493	.5466	.5428	.5371	.5280
0.4	.6246	.6244	.6237	.6224	.6204	.6173	.6126	.6056	.5941	.5735
0.5	.7148	.7146	.7141	.7131	.7114	.7085	.7037	.6953	.6798	.6469
0.6	.8016	.8016	.8016	.8014	.8008	.7995	.7966	.7900	.7747	.7344
0.7	.8696	.8697	.8701	.8707	.8714	.8718	.8713	.8676	.8550	.8129
0.8	.9165	.9167	.9173	.9183	.9198	.9213	.9223	.9208	.9108	.8688
0.9	.9469	.9471	.9477	.9489	.9506	.9526	.9542	.9537	.9448	.9029
1.0	.9660	.9662	.9668	.9679	.9696	.9715	.9733	.9728	.9641	.9217
1.1	.9780	.9782	.9787	.9797	.9812	.9829	.9844	.9837	.9746	.9314
1.2	.9856	.9857	.9862	.9871	.9883	.9898	.9908	.9897	.9801	.9361
1.3	.9905	.9906	.9910	.9917	.9927	.9938	.9946	.9930	.9828	.9383
1.4	.9936	.9937	.9940	.9946	.9954	.9963	.9967	.9947	.9842	.9393
1.5	.9957	.9957	.9960	.9965	.9971	.9978	.9979	.9956	.9848	.9399
1.6	.9970	.9971	.9973	.9977	.9982	.9987	.9986	.9960	.9850	.9402
1.7	.9979	.9980	.9982	.9985	.9989	.9992	.9989	.9962	.9852	.9406
1.8	.9986	.9986	.9987	.9990	.9993	.9995	.9991	.9963	.9853	.9411
1.9	.9990	.9990	.9991	.9993	.9996	.9997	.9992	.9963	.9855	.9418
2.0	.9993	.9993	.9994	.9995	.9997	.9998	.9992	.9964	.9856	.9420

TABLE (7.1)

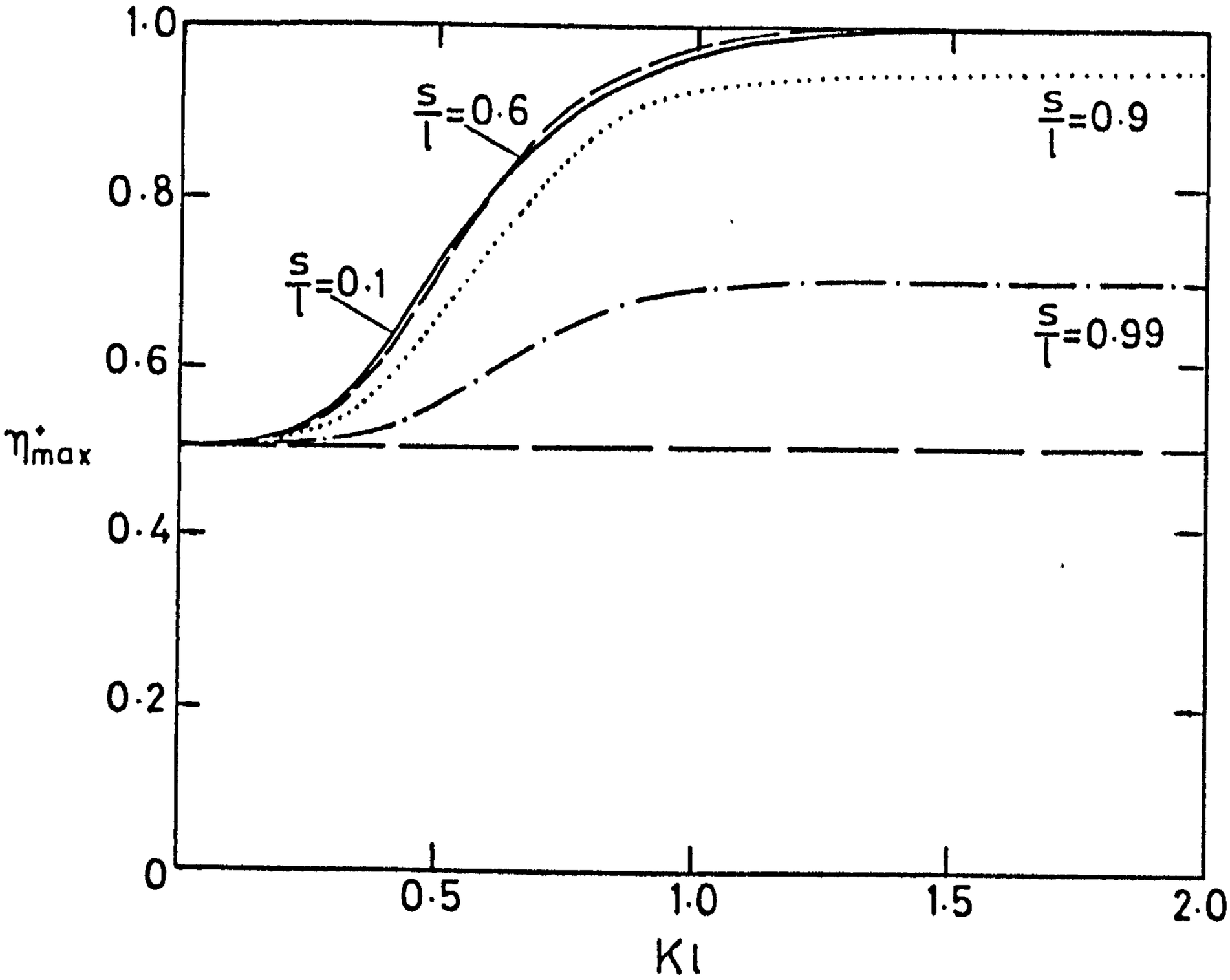
1·0
0·8
0·6
0·4
0·2
0
η^*_{max}
$\frac{s}{l}$=0·6
$\frac{s}{l}$=0·1
$\frac{s}{l}$=0·9
$\frac{s}{l}$=0·99
0·5
1·0
1·5
2·0
Kl

FIG. (7·2)

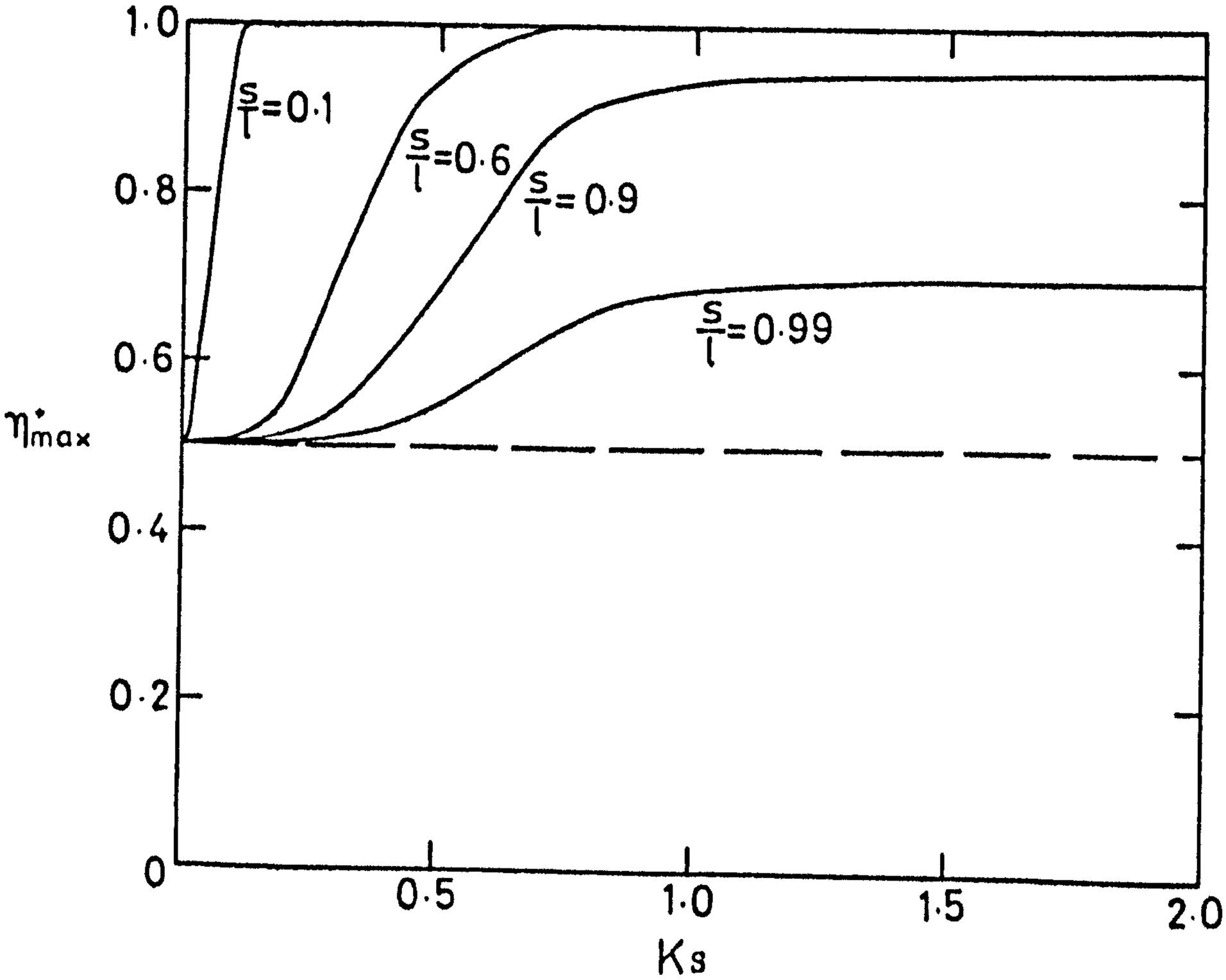
1·0
0·8
0·6
0·4
0·2
0
η^*_{max}
$\frac{s}{l}$=0·1
$\frac{s}{l}$=0·6
$\frac{s}{l}$=0·9
$\frac{s}{l}$=0·99
0·5
1·0
1·5
2·0
Ks

FIG. (7·3)

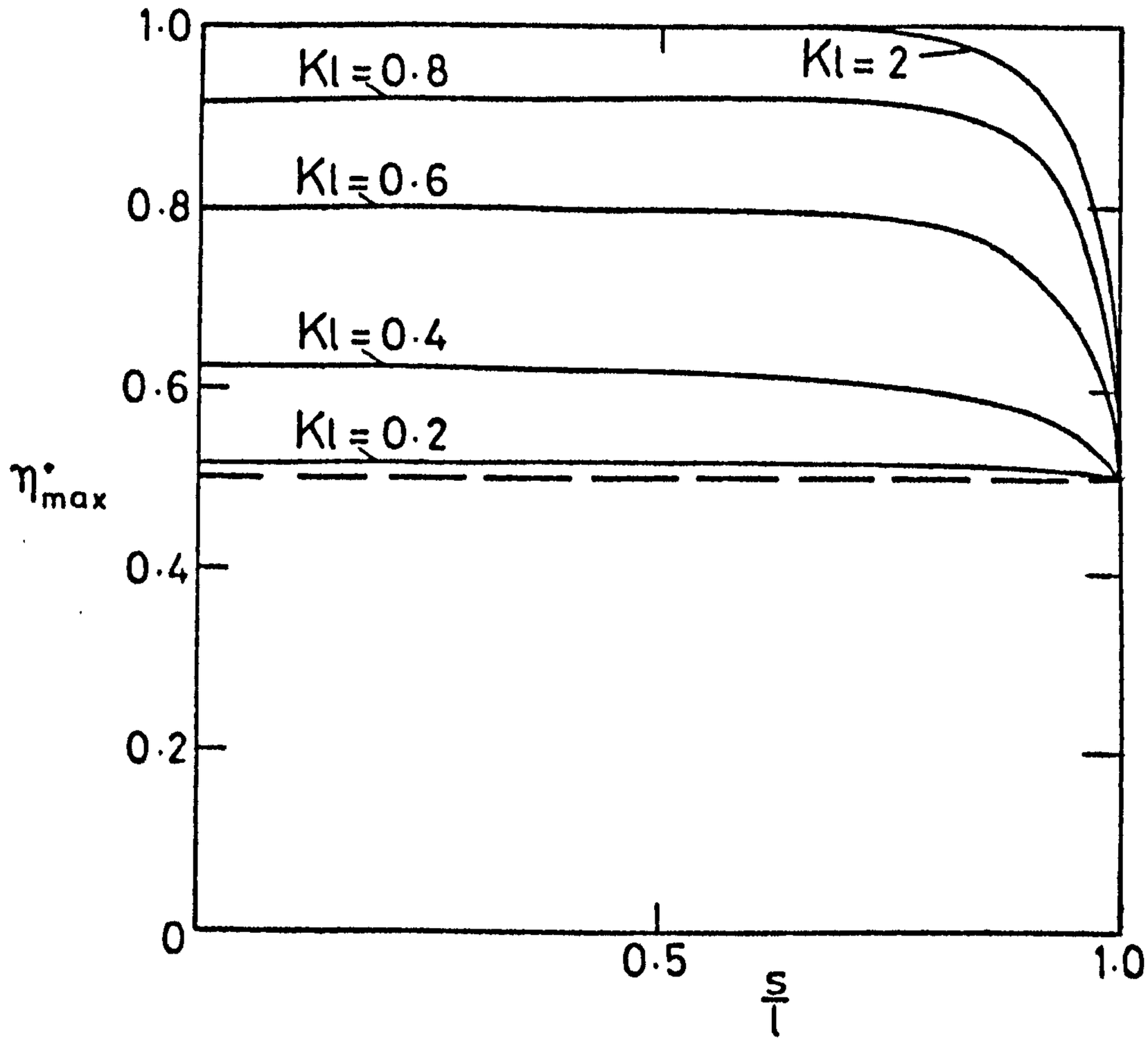
1·0
0·8
0·6
0·4
0·2
0
$\eta^{\bullet}_{max}$
Kl = 0·8
Kl = 0·6
Kl = 0·4
Kl = 0·2
Kl = 2
0·5
1·0
$\frac{s}{l}$

FIG. (7·4)

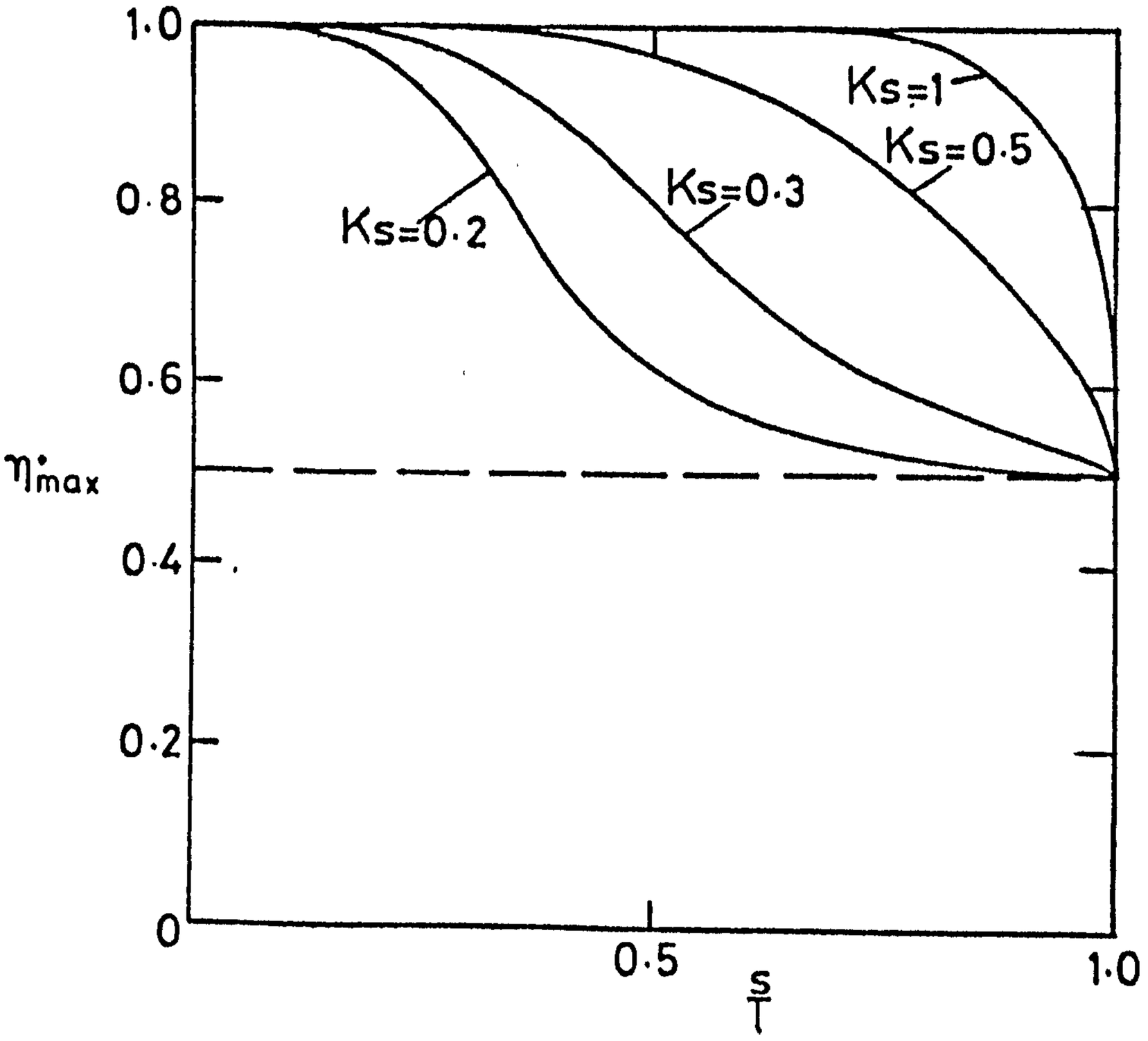
1·0
0·8
0·6
0·4
0·2
0
$\eta^{\bullet}_{max}$
Ks=0·2
Ks=0·3
Ks=0·5
Ks=1
0·5
1·0
$\frac{s}{l}$

FIG. (7·5)

latter paper, this requires the full solution of an oscillating source on the side of a barrier, which is not available in explicit form.

7.4 The theoretical maximum efficiency of a pressure patch adjacent to a vertical strip

Another easily examined, idealized device can be derived from the preceding problem where this time a is not necessarily small. Instead it is assumed that the immersed, shorter side of the duct is so shallow that it can be neglected. Consequently there is a pressure "patch" over the free surface adjoined at one end to a fixed vertical strip, as shown in fig. (7.6).

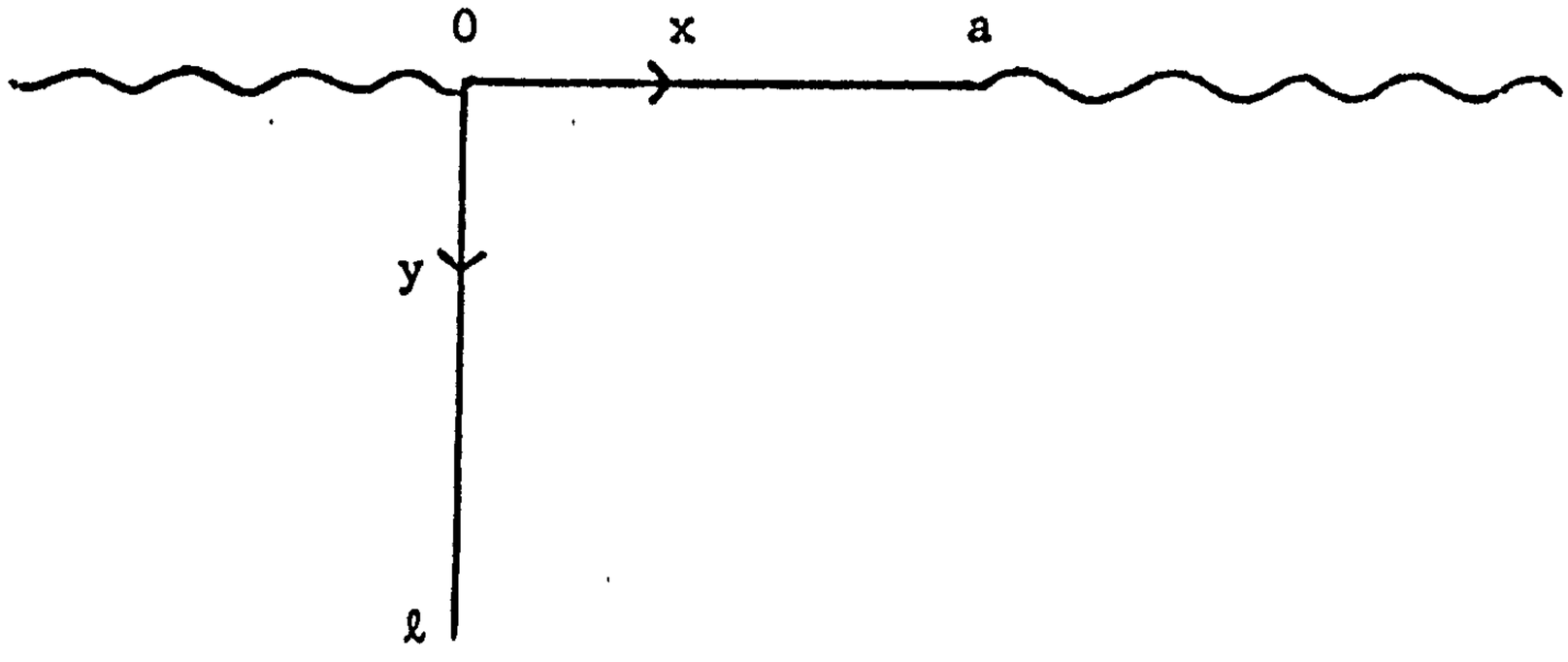

FIG. (7.6)

The advantage of this one-sided shallow draft assumption is that the volume flow rate, q_s, can be evaluated by integrating Ursell's (1947) explicit solution for an incident wave on a fixed barrier, given by (7.34) and (7.35), over the region $0 < x < a$, $y = 0$. Therefore (7.12) and (7.14) with (7.34) gives

$$q_s^+ = \int_0^a \frac{\partial \phi_u}{\partial y}(x,0)\, dx$$

$$= K_1(K\ell)[1 - e^{-iKa}] - 2\pi I_1(K\ell)\sin Ka - K\int_0^\infty \frac{J_1(k\ell)}{k^2+K^2}(1 - e^{-ka})\ dk\ . \tag{7.43}$$

Similarly, if the incident wave is from $x = -\infty$,

$$q_s^- = K_1(K\ell)[1 - e^{iKa}] + K\int_0^\infty \frac{J_1(k\ell)}{k^2+K^2}(1 - e^{-ka})\ dk\ . \tag{7.44}$$

Then substituting (7.43) and (7.44) in (7.24) yields

$$\eta_{max}^+ = \frac{1}{1 + \left|\frac{q^-}{q^+}\right|^2} \tag{7.45}$$

where

$$\left|\frac{q^-}{q^+}\right|^2 = \left|\frac{K_1(K\ell)[e^{iKa}-1]-K\mathscr{T}}{2\pi I_1(K\ell)\sin Ka+K_1(K\ell)[1-e^{-iKa}]+K\mathscr{T}}\right|^2 \tag{7.46}$$

with

$$\mathscr{T} = \int_0^\infty \frac{J_1(k\ell)}{k^2+K^2}\ (1 - e^{-ka})\ dk\ . \tag{7.47}$$

An alternative method is to apply equation (2.30) to the radiation potential ψ, and $\phi_u(\pm x,y)$. This gives

$$f^+ = \frac{1}{K}\ (1-e^{-iKa}) - \frac{\pi I_1(K\ell)(1-e^{iKa})}{K[\pi I_1(K\ell)+iK_1(K\ell)]} + \frac{i\mathscr{T}}{\pi I_1(K\ell)+iK_1(K\ell)}$$

and

$$f^- = \frac{K_1(K\ell)(1-e^{iKa})}{K[\pi I_1(K\ell)+iK_1(K\ell)]} - \frac{i\mathscr{T}}{\pi I_1(K\ell)+iK_1(K\ell)}\ .$$

Thus from (7.25) the efficiency is again given by (7.45).

If the incident waves were to approach from $x = -\infty$ the complementary expression can be obtained from the relation

$$\eta_{max}^- = 1 - \eta_{max}^+\ .$$

From (7.46),

$$\left|\frac{q^-}{q^+}\right|^2 = \left|1 + \frac{2\pi I_1(K\ell)\sin Ka}{K\mathcal{T}-K_1(K\ell)\left[e^{iKa}-1\right]}\right|^{-2}$$

$$= 1 \quad \text{when } Ka = n\pi,\ n = 0,1,2,.... \tag{7.48}$$

giving

$$\eta^+_{max} = \eta^-_{max} = \tfrac{1}{2}\ . \tag{7.49}$$

It can also be seen that as the pressure patch shrinks towards the barrier $(a \to 0)$,

$$\mathcal{T} \to \int_0^\infty \frac{J_1(k\ell)}{k^2+K^2}\,dk$$

$$= a\left\{1 + \frac{\pi}{2}\left[L_1(Ka) - I_1(Ka)\right]\right\},$$

yielding

$$\left|\frac{q^-}{q^+}\right|^2 \to \left|\frac{\pi I_1(K\ell)+iK_1(K\ell) - \frac{\pi}{2}\left[I_1(K\ell)+L_1(K\ell)\right]-1}{\pi I_1(K\ell)+iK_1(K\ell) + \frac{\pi}{2}\left[I_1(K\ell)+L_1(K\ell)\right]+1}\right|^2$$

$$= \left|\frac{1-\alpha_s}{1+\alpha_s}\right|^2$$

where

$$\alpha_s = \frac{1}{\pi I_1(K\ell)+iK_1(K\ell)}\left[1 + \frac{\pi}{2}\left\{I_1(K\ell)+L_1(K\ell)\right\}\right].$$

This is in agreement with the results obtained for the identical problem in §7.3, the equivalent α_s being given by (7.42).

Additional confirmation is illustrated in Table (7.2). Here numerical results of the theoretical maximum efficiency, η^+_{max}, as a function of $K\ell$ are presented for various values of a/ℓ. It is seen that as this ratio gets smaller the efficiency is in very good agreement with the results computed for the limiting case $a = 0$. Indeed there is little variation in the efficiency for $a/\ell < 1.0$.

Kℓ	$a/_{\ell=0}$	0.1	0.25	0.5	0.75	1.0	2.0	3.0	4.0	5.0
0.1	.5017	.5017	.5018	.5018	.5019	.5020	.5025	.5031	.5037	.5043
0.2	.5152	.5154	.5154	.5157	.5162	.5169	.5204	.5242	.5276	.5303
0.3	.5541	.5542	.5544	.5553	.5567	.5584	.5664	.5731	.5767	.5763
0.4	.6246	.6246	.6250	.6262	.6280	.6302	.6384	.6405	.6334	.6155
0.5	.7148	.7149	.7151	.7159	.7171	.7182	.7187	.7061	.6746	.6180
0.6	.8016	.8016	.8016	.8016	.8014	.8007	.7894	.7556	.6832	.5450
0.7	.8696	.8695	.8694	.8686	.8671	.8649	.8430	.7840	.6359	.3080
0.8	.9165	.9165	.9161	.9150	.9129	.9097	.8805	.7880	.4605	.1197
0.9	.9469	.9468	.9464	.9452	.9429	.9395	.9053	.7555	.0665	.6486
1.0	.9660	.9659	.9656	.9644	.9623	.9590	.9208	.6356	.4829	.8765
1.1	.9780	.9779	.9777	.9766	.9747	.9717	.9290	.2279	.8565	.9289
1.2	.9856	.9855	.9853	.9844	.9828	.9801	.9304	.3169	.9463	.8083
1.3	.9905	.9904	.9902	.9895	.9881	.9857	.9226	.8475	.9715	.9312
1.4	.9936	.9936	.9934	.9928	.9916	.9895	.8953	.9536	.9752	.9852
1.5	.9957	.9956	.9955	.9950	.9940	.9922	.7966	.9808	.9221	.9907
1.6	.9970	.9970	.9969	.9965	.9957	.9941	.2073	.9900	.9081	.9913
1.7	.9979	.9979	.9979	.9975	.9968	.9954	.7162	.9936	.9904	.9885
1.8	.9986	.9986	.9985	.9982	.9977	.9964	.9513	.9947	.9958	.9707
1.9	.9990	.9990	.9989	.9987	.9983	.9971	.9849	.9934	.9971	.4548
2.0	.9993	.9993	.9992	.9991	.9987	.9976	.9937	.9806	.9975	.9842

TABLE (7.2)

Further results for the efficiency η^+_{max} are shown in figs. (7.7)-(7.10). Firstly, in fig. (7.7) the variation is displayed as a function of $K\ell$ for different patch to barrier length ratios. The analytic limits as $K\ell \to 0$ and ∞, of $\eta^+_{max} \to \frac{1}{2}$ and 1 respectively are obtained, but more distinctive is the sudden fall and rise of the efficiency. As the efficiency drops, the value of $\frac{1}{2}$ is crossed at the points exemplified by (7.48) before reaching the minimum value of zero at the zeros of $|q^+|^2$. A closer examination of this quantity shows that $|q^+|^2 = 0$ at $Ka > n\pi$, with the number of zeros increasing as the ratio a/ℓ gets larger.

The corresponding curves for fixed a are shown in fig. (7.8). Here it is seen that $\eta^+_{max} = \frac{1}{2}$ at $Ka = \pi$ for all values of a/ℓ, whilst the zeros of $|q^+|^2$ depend upon both of these parameters. It is also seen that a greater efficiency is expected from a device when $a/\ell < 1$.

In figs. (7.9) and (7.10) the effect of varying $K\ell$ and Ka, respectively is presented for the maximum efficiency as a function of a/ℓ. Firstly as $K\ell$ increases for constant ℓ, the efficiency tends to one outside any zero value, although the number of zeros in a specified range of a/ℓ also increases. Similarly, when a is held fixed (fig.(7.10)) the efficiency tends to one as a/ℓ decreases. On the other hand, as ℓ moves towards the free surface, the expected maximum efficiency of $\frac{1}{2}$ is attained. In this situation of constant patch width, the efficiency decays monotonically from its maximum value to this limiting value when $Ka < \pi$. However, once the critical value of Ka has been passed, the efficiency tends to $\frac{1}{2}$ from below. From all these curves it can be deduced that the device is most efficient when waves first reach the pressure patch, and not the barrier.

The results just discussed, together with those of the previous section assume that the impedance condition (7.22) can be matched

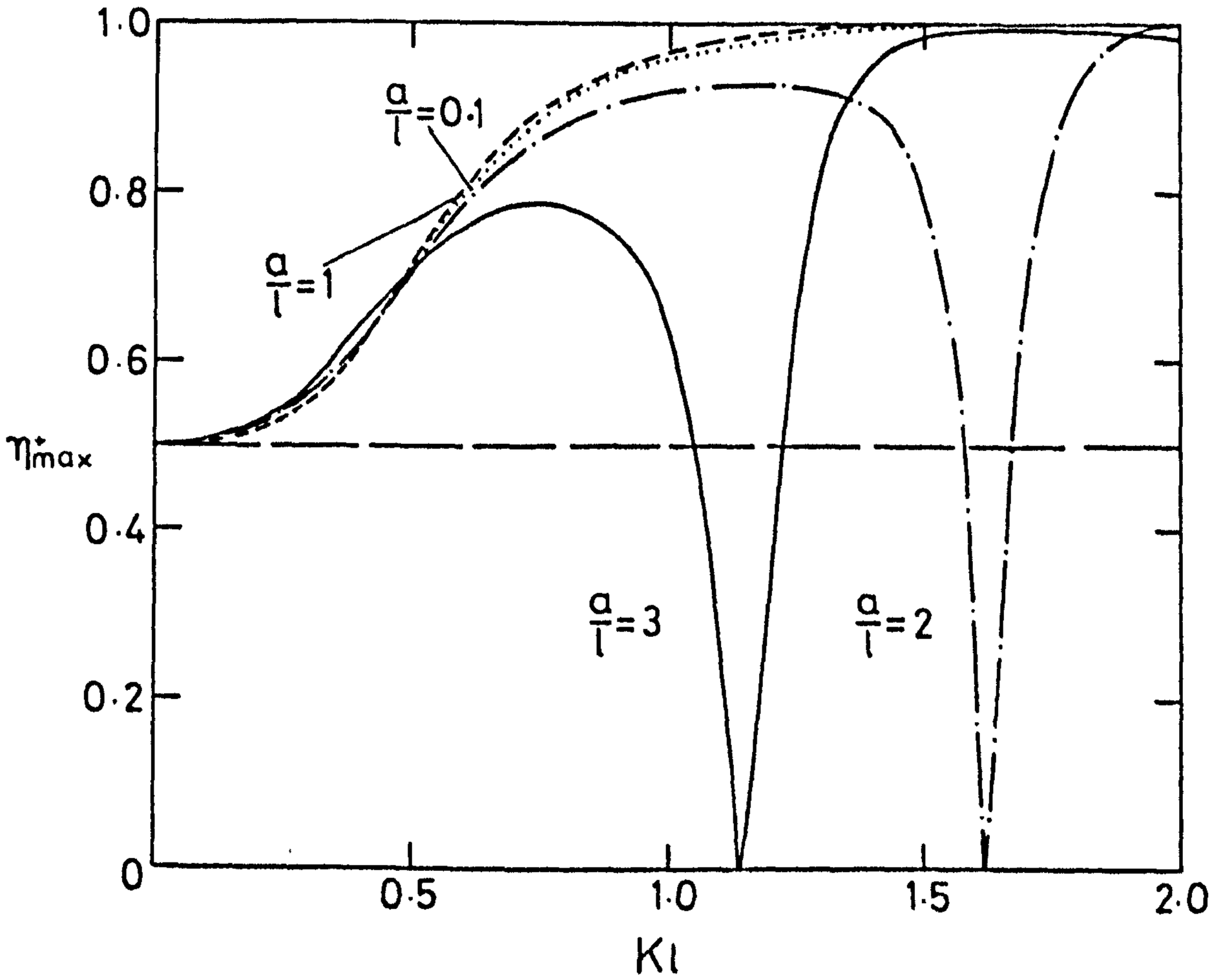
1·0
0·8
0·6
0·4
0·2
0
η^*_{max}
$\frac{a}{l}=0.1$
$\frac{a}{l}=1$
$\frac{a}{l}=3$
$\frac{a}{l}=2$
0·5
1·0
1·5
2·0
Kl

FIG. (7·7)

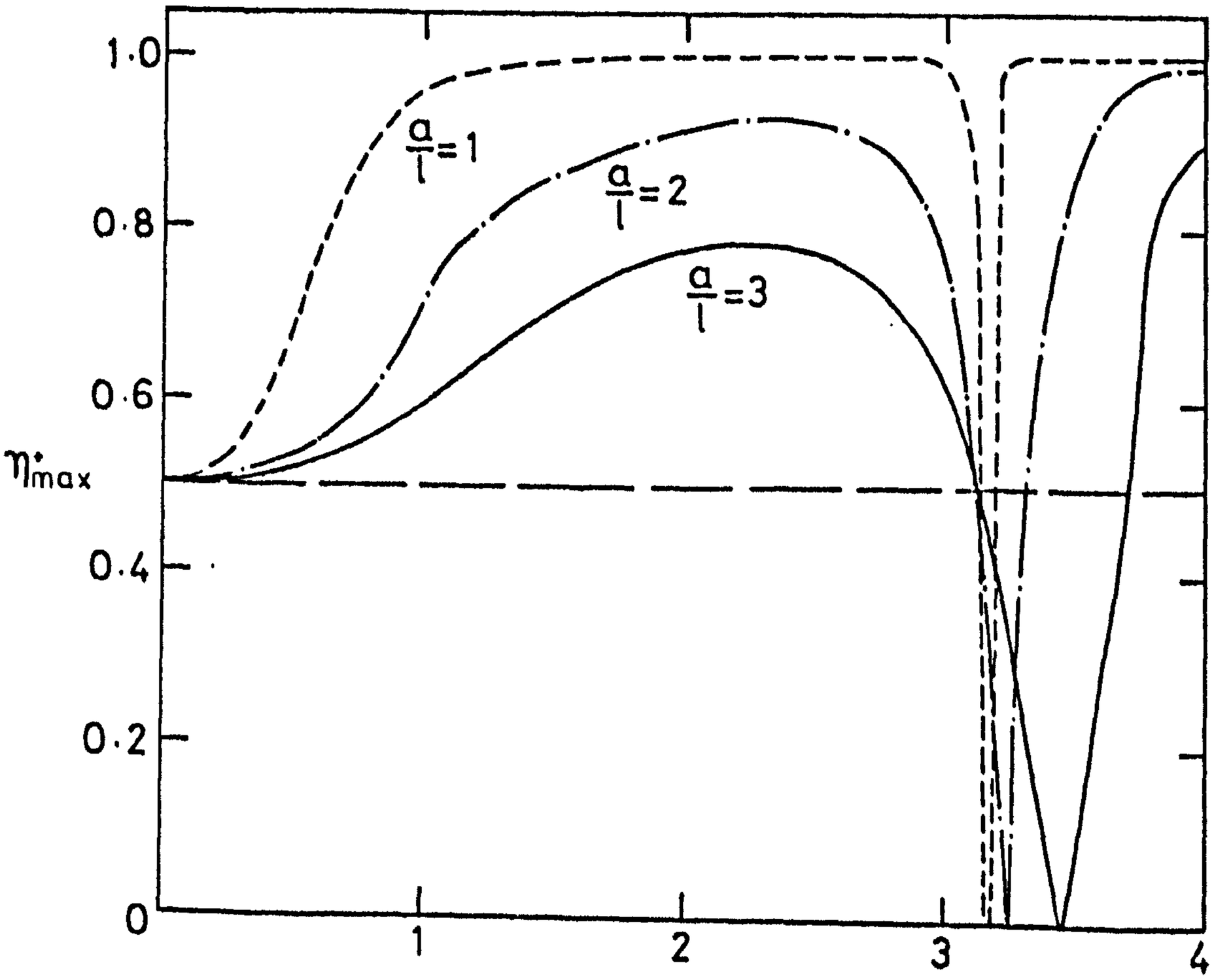
1·0
0·8
0·6
0·4
0·2
0
η^*_{max}
$\frac{a}{l}=1$
$\frac{a}{l}=2$
$\frac{a}{l}=3$
1
2
3
4
Ka

FIG. (7·8)

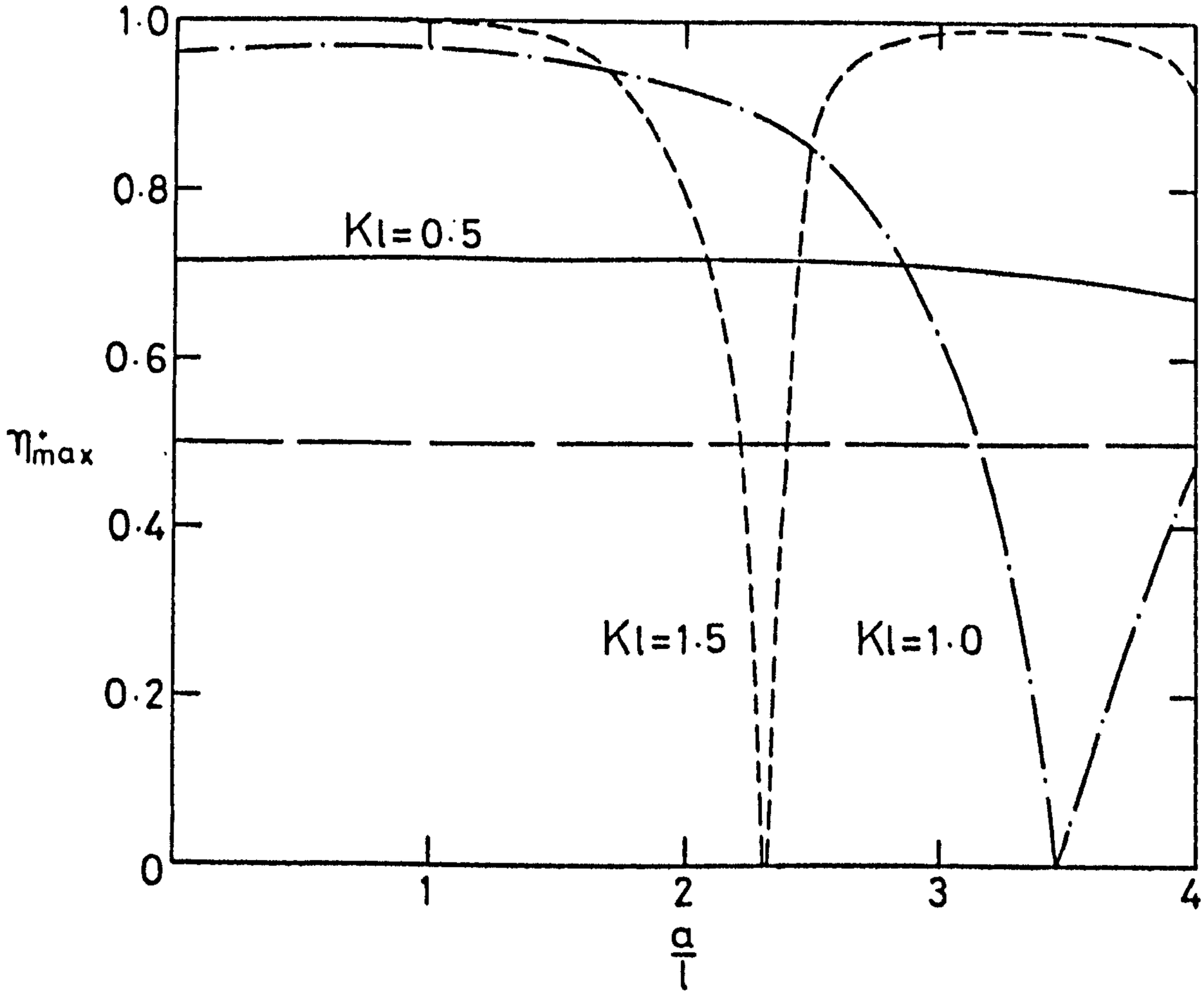

FIG. (7·9)

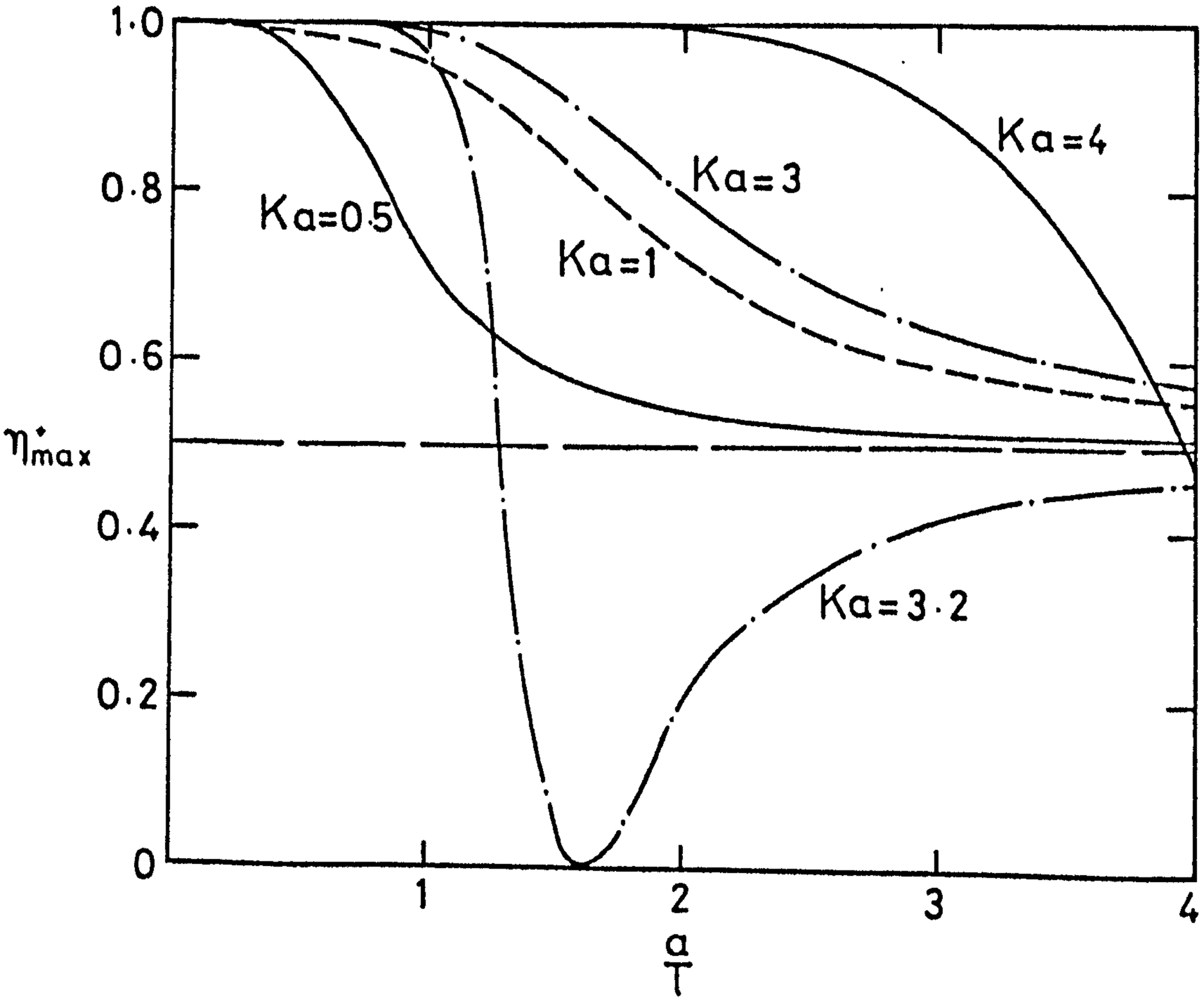

FIG. (7·10)

exactly. Therefore both problems have readily been determined by solving a linear wave diffraction problem without reference to pressure distributions. A more realistic problem assuming imperfect matching is treated in the following section.

(b) THE TWO-DIMENSIONAL HARBOUR

7.5 Formulation and solution

The theory of wave-power absorption by a pressure distribution is now applied to an OWC placed inside a two-dimensional harbour of constant depth d. The water column is formed by placing a fixed, thin, vertical barrier of length ℓ at a distance a away from the closed harbour end. An energy absorber is placed over the free surface between the barrier and the harbour wall, as illustrated in fig. (7.11). In fact this constitutes the side view of the KMOWC.

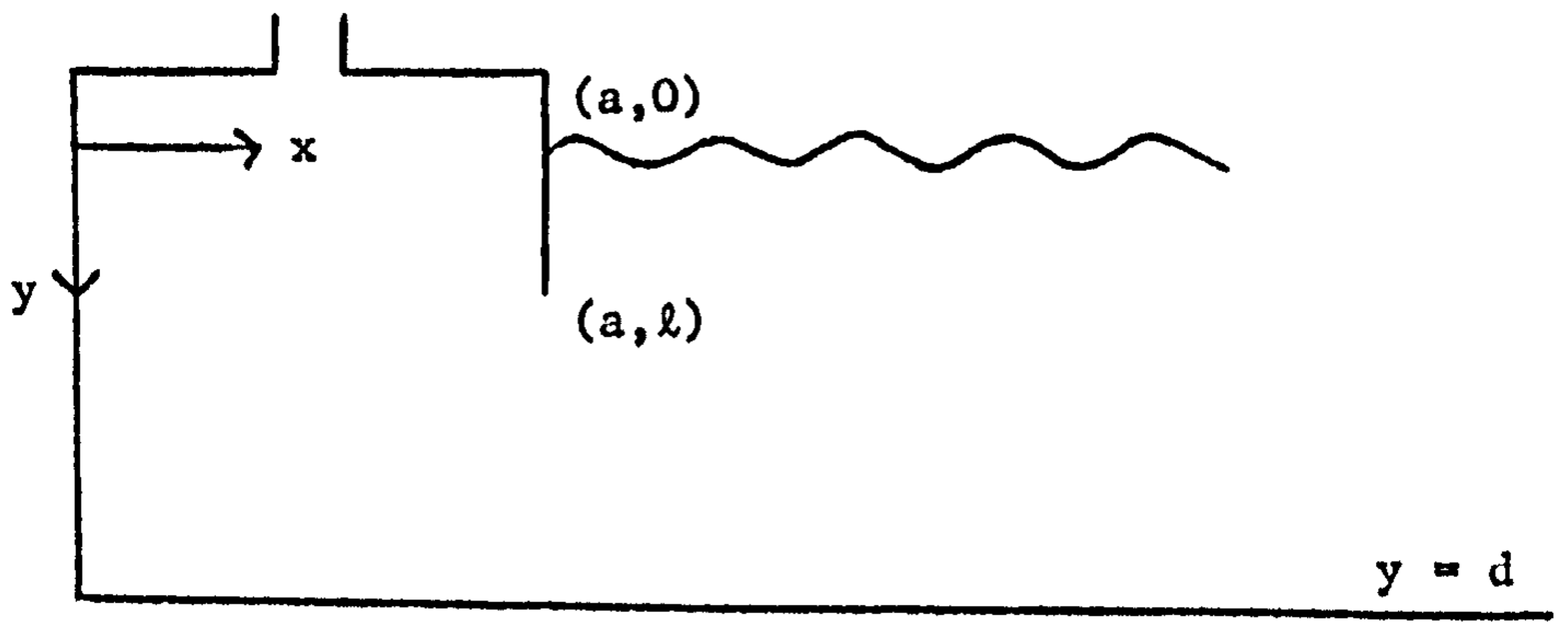

FIG. (7.11)

The theoretical maximum efficiency of the above device is clearly one provided that the condition (7.22) is satisfied. In the more practical case when there is no mechanism for introducing a phase difference between the volume flux and pressure drop through the turbine, the efficiency is given by (7.31) where the $\tilde{A},\tilde{B}$ coefficients

are determined from a consideration of the radiation problem.

Here the radiation potential $\psi(x,y)$ satisfies Laplace's equation (2.10) in the fluid, the sea-bed condition (2.12a), equation (7.8) on $y = 0$, $0 < x < a$ and (7.9) on $y = 0$, $x > a$,

$$\frac{\partial \psi}{\partial x}(0,y) = 0 \ , \quad \text{on} \quad 0 < y < d \ , \tag{7.50}$$

$$\frac{\partial \psi}{\partial x}(a,y) = 0 \ , \quad \text{on} \quad 0 < y < \ell \ , \tag{7.51}$$

and the radiation condition

$$\psi(x,y) \sim \frac{f^{\pm} e^{ikx}}{\text{coshkd}} \text{coshk}(d-y) \qquad \text{as } x \to \pm\infty \ . \tag{7.52}$$

Following Mei and Black (1969), and Black, Mei and Bray (1971), the potential ψ can be determined by solving Laplace's equation in the inner ($0 < x < a$) and outer ($x > a$) regions. In terms of the eigenfunctions, f_n, defined by equation (4.3), this yields

$$\psi(x,y) = \sum_{n=o}^{\infty} A_n e^{-k_n(x-a)} f_n(y) \ , \quad x > a \tag{7.53}$$

and

$$\psi(x,y) = \sum_{n=o}^{\infty} B_n \text{coshk}_n x f_n(y) + \frac{1}{K} \ , \quad 0 < x < a \tag{7.54}$$

where A_n, B_n are unknown constants and the particular solution in the inner region is included to satisfy the free surface condition (7.8). Clearly equations (7.53) and (7.54) satisfy all the boundary conditions for ψ with the exception of (7.51). As in Chapter 4 this is satisfied, and hence A_n, B_n are determined, by constructing a function $U_r(y)$ across the boundary line defined by

$$\frac{\partial \psi}{\partial x} = U_r(y) = \sum_{n=o}^{\infty} \mathcal{U}_{rn} f_n(y) \ , \quad x = a, \ 0 < y < d \ , \tag{7.55}$$

where $\mathcal{U}_{rn}$ is given by

$$\mathcal{U}_{rn} = \frac{1}{d}\int_{\ell}^{d} U_r(y)f(y)dy \ .$$

By employing (7.53) and (7.54) in (7.55), solutions for A_n, B_n in terms of $\mathcal{U}_{rn}$ are obtained, yielding

$$\psi = \sum_{n=o}^{\infty} -\frac{\mathcal{U}_{rn}}{k_n} e^{-k_n(x-a)} f_n(y) \ , \quad x > a \tag{7.56}$$

and

$$\psi = \sum_{n=o}^{\infty} \frac{\mathcal{U}_{rn} f_n(y)}{k_n \sinh k_n a} \cosh k_n x + \frac{1}{K} \ , \quad 0 < x < a \ . \tag{7.57}$$

Then since the pressure is continuous across the line $x = a$, $\ell < y < d$, (7.56) and (7.57) can be matched to give

$$\sum_{n=o}^{\infty} \mathcal{U}_{rn} f_n R_n = -\frac{1}{Ka} \ , \qquad \ell < y < d \ , \tag{7.58}$$

where

$$R_n = \frac{1 + \coth k_n a}{k_n a} \ . \tag{7.59}$$

Finally the boundary condition (7.51) gives

$$\sum_{n=o}^{\infty} \mathcal{U}_{rn} f_n(y) = 0 \ , \qquad 0 < y < \ell \ . \tag{7.60}$$

By multiplying (7.58) and (7.60) by $\frac{f_m}{d}$, integrating over the region of validity and adding, the expression

$$\sum_{n=o}^{\infty} E_{mn} \mathcal{U}_{rn} = C_m \tag{7.61}$$

is found where

$$E_{mn} = (R_n - 1)D_{mn} + \delta_{mn} \ , \tag{7.62}$$

D_{mn} is given by equations (4.17) and (4.19)

$$\text{and} \qquad C_m = \frac{1}{Kad}\int_{\ell}^{d} f_m(y)\, dy \ .$$

$$\left.\begin{aligned} \text{Hence} \qquad C_o &= -\frac{N_o^{-\frac{1}{2}}}{Kakd}\ \text{sinhkh}, \\ \text{and} \qquad C_m &= -\frac{N_m^{-\frac{1}{2}}}{Kak_m d}\ \text{sink}_m h\ , \qquad m > 1\ . \end{aligned}\right\} \tag{7.63}$$

As before R_n is real except for $n = 0$. Therefore the complex matrix equation (7.61) can be reduced to two real matrix equations by writing

$$\mathscr{U}_{rn} = a_n + ib_n \tag{7.64}$$

$$\text{and} \qquad E_{mo} = \alpha_m + i\beta_m \tag{7.65}$$

where $a_n, b_n, \alpha_m, \beta_m$ are real constants with

$$\alpha_m = \left(\frac{-\text{cotka}}{ka} - 1\right) D_{mo} + \delta_{mo} \tag{7.66}$$

$$\text{and} \qquad \beta_m = \frac{D_{mo}}{ka}\ . \tag{7.67}$$

Substituting the expressions (7.64)-(7.67) into (7.61) and equating the real and imaginary parts yields the systems

$$\alpha_m a_o + \sum_{n=1}^{\infty} E_{mn} a_n = C_m + b_o \beta_m\ , \tag{7.68}$$

$$\alpha_m b_o + \sum_{n=1}^{\infty} E_{mn} b_n = -a_o \beta_m\ . \tag{7.69}$$

Thus, if ε_n, δ_n are the solutions of

$$\alpha_m \varepsilon_o + \sum_{n=1}^{\infty} E_{mn} \varepsilon_n = C_m\ , \tag{7.70}$$

$$\alpha_m \delta_o + \sum_{n=1}^{\infty} E_{mn} \delta_n = \beta_m \tag{7.71}$$

for m = 0,1,2, ... , then

$$a_n = \varepsilon_n + b_o\delta_n \ , \tag{7.72}$$

$$b_n = - a_o\delta_n \ , \tag{7.73}$$

and it can be shown that

$$\mathscr{U}_{rn} = \left\{\varepsilon_n - \frac{\varepsilon_o\delta_o\delta_n}{1+\delta_o^2}\right\} - \frac{i\varepsilon_o\delta_n}{1+\delta_o^2} \ , \qquad n > 0 \ . \tag{7.74}$$

Hence once the systems of equations (7.70), (7.71) have been solved for n = 0,1,2, ... the solution of ψ is known via equations (7.56), (7.57) with (7.74).

The volume flux across the internal free surface is given by (7.13) as

$$q_r = - \frac{i\omega p}{\rho g} \int_o^a \frac{\partial\psi}{\partial y}\,(x,0)\ dx \ ,$$

which becomes with (7.57) and (4.3)

$$q_r = - \frac{i\omega p}{\rho g} \sum_{n=o}^{\infty} \frac{\mathscr{U}_{rn} N_n^{-\frac{1}{2}}}{k_n} \sin k_n d \ .$$

Substituting this in (7.16) gives

$$\tilde{A} = - \frac{a}{\rho g} \sum_{n=o}^{\infty} \mathrm{Re}(\mathscr{U}_{rn})\, \frac{N_n^{-\frac{1}{2}}}{k_n a} \sin k_n d \ , \tag{7.75}$$

and

$$\tilde{B} = - \frac{\omega a}{\rho g} \sum_{n=o}^{\infty} \mathrm{Im}(\mathscr{U}_{rn})\, \frac{N_n^{-\frac{1}{2}}}{k_n a} \sin k_n d \ . \tag{7.76}$$

Further, since no waves are radiated to x = $-\infty$ it follows from (7.19) that

$$\tilde{B} = \frac{|q_s|^2}{8P_w} \tag{7.77}$$

and therefore that the maximum efficiency, given by (7.31) is

$$\eta_{max} = \frac{2\tilde{B}}{\Lambda_{opt}+\tilde{B}} \ . \tag{7.78}$$

Clearly the maximum value of this efficiency is one, occurring when $\tilde{A} = 0$. This corresponds to the induced volume flux downwards across the internal free surface being exactly in phase with the applied pressure on the free surface.

Results for the $\tilde{A}$ and $\tilde{B}$ coefficients, together with curves for the maximum efficiency are presented and discussed in §7.9.

7.6 The diffraction problem

The full, interactive velocity potential describing this harbour problem is obtained by solving the complementary scattering problem. In contrast to the above work this potential includes the effect of an incident wave train. Thus the potential $\phi_s(x,y)$ satisfies the same governing equations as $\psi(x,y)$ when the internal free surface condition (7.8) is given by (7.9) and the radiation condition (7.52) allows for an approaching wave from $x = +\infty$.

Proceeding in a manner analogous to §4.3 and the previous section, the solution of Laplace's equation in an inner ($0 < x < a$) and outer ($x > a$) region is respectively

$$\phi_s = \sum_{n=o}^{\infty} B_n \cosh k_n x f_n(y) , \quad 0 < x < a \tag{7.79}$$

and

$$\phi_s = [e^{-ik(x-a)} + A_o e^{ik(x-a)}]\, \phi_o f_o(y) + \sum_{n=1}^{\infty} A_n e^{-k_n(x-a)} f_n(y), \quad x > a \tag{7.80}$$

where

$$\phi_o = \frac{-igAe^{-ika}}{\omega N_o^{-\frac{1}{2}} \cosh kd}$$

in order to satisfy the incident wave potential form given by equation (2.13). For explicitness the propagating mode has been separated from the evanescent modes in the latter equation (7.80).

If the $U_r, \mathcal{U}_{rn}$ of §7.5 are now replaced by $U_s, \mathcal{U}_{sn}$ so that the horizontal velocity potential is expanded across x = a in the normal fashion, it is found that

$$\phi_s = \sum_{n=o}^{\infty} \frac{\mathcal{U}_{sn} \cosh k_n x}{k_n \sinh k_n a} f_n(y) , \qquad 0 < x < a \tag{7.81}$$

and

$$\phi_s = [e^{-ik(x-a)} + e^{ik(x-a)}]\, \phi_o f_o(y) - \sum_{n=1}^{\infty} \frac{\mathcal{U}_{sn} f_n(y)}{k_n} e^{-k_n(x-a)} , \quad x > a . \tag{7.82}$$

Therefore matching the pressure across x = a yields

$$\sum_{n=o}^{\infty} \mathcal{U}_{sn} f_n(y) = 0 , \qquad 0 < y < \ell$$

and

$$\sum_{n=o}^{\infty} \mathcal{U}_{sn} R_n f_n(y) = \frac{2\phi_o}{a} f_o(y) , \quad \ell < y < d ,$$

where R_n is given by (7.59). These two systems combine to give

$$\sum_{n=o}^{\infty} E_{mn} \mathcal{U}_{sn} = C'_m \tag{7.83}$$

with E_{mn} defined by (7.62) and

$$C'_m = \frac{2\phi_o}{a} D_{mo}$$

$$= 2k\phi_o \beta_m \quad \text{from equation (7.67)}$$

$$= 2k\beta_m(\phi_{or} + i\phi_{oi}) \tag{7.84}$$

if $\phi_o = \phi_{or} + i\phi_{oi}$.

Using the decomposition of E_{mo} given in equation (7.65) with

$$\mathcal{U}_{sn} = c_n + id_n , \tag{7.85}$$

equation (7.83) reduces to the two real systems of equations,

$$c_o\alpha_m + \sum_{n=1}^{\infty} c_n E_{mn} = (2k\phi_{or} + d_o)\beta_m \tag{7.86}$$

and

$$d_o\alpha_m + \sum_{n=1}^{\infty} d_n E_{mn} = (2k\phi_{oi} - c_o)\beta_m \, . \tag{7.87}$$

Therefore, if δ_n is the solution of equation (7.71), then

$$c_n = (2k\phi_{or} + d_o)\delta_n \, , \tag{7.88}$$

$$d_n = (2k\phi_{oi} - c_o)\delta_n \, , \tag{7.89}$$

which finally gives

$$\mathscr{V}_{sn} = \frac{2k\phi_o\delta_n}{1+i\delta_o} \, . \tag{7.90}$$

Hence equations (7.12) and (7.81) give the induced flux as

$$\begin{aligned} q_s &= \int_o^a \frac{\partial\phi_s}{\partial y}(x,0)\, dx \\ &= \sum_{n=o}^{\infty} \frac{\mathscr{V}_{sn} N_n^{-\frac{1}{2}} \sin k_n d}{k_n} \, , \end{aligned}$$

enabling the coefficient $\tilde{B}$ to be evaluated from (7.77) with P_w defined by (7.7a). After some manipulation

$$\tilde{B} = \left(\frac{\omega a}{\rho g}\right) \frac{ka}{kd\tanh kd\,(1+\delta_o^2)} \left| \sum_{n=o}^{\infty} \frac{\delta_n N_n^{-\frac{1}{2}} \sin k_n d}{k_n a} \right|^2 ,$$

the computational results of which agree with those determined by the radiation problem.

7.7 Special case when $\ell = 0$

An interesting limiting case of this harbour problem is when the barrier forming the oscillating water column is of shallow draft so all

that remains is a pressure patch adjacent to the closed harbour end. In this instance the approach of §7.5 follows through identically with the necessary modifications when matching ψ across the whole fluid depth at $x = a$. Thus (7.58) becomes

$$\sum_{n=0}^{\infty} \mathcal{U}_{rn} f_n R_n = -\frac{1}{Ka}, \qquad 0 < y < d \tag{7.91}$$

which on multiplying by $\frac{f_m}{d}$ and integrating gives

$$\mathcal{U}_{rm} R_m = -\frac{1}{Kad} \int_0^d f_m(y)\, dy$$

$$= C_m, \quad \text{with} \quad \ell = 0. \tag{7.92}$$

Hence using (7.59), (7.63) and the dispersion relation (2.14),

$$\mathcal{U}_{ro} = N_o^{-\frac{1}{2}} \frac{\sinh kd \sin^2 ka}{Kd} (\cot ka + i) \tag{7.93}$$

and

$$\mathcal{U}_{rm} = \frac{-N_m^{-\frac{1}{2}} \sin k_m d}{Kd(1+\coth k_n a)}. \tag{7.94}$$

On substituting these in (7.75) and (7.76) it is found that

$$\tilde{A} = \frac{a}{\rho g} \left\{ -N_o^{-1} \frac{\sinh^2 kd \sin ka \cos ka}{Kdka} + \sum_{n=1}^{\infty} \frac{N_n^{-1} \sin^2 k_n d}{Kd\, k_n a (1 + \coth k_n a)} \right\} \tag{7.95}$$

and

$$\tilde{B} = -\frac{\omega a}{\rho g} N_o^{-1} \frac{\sinh kd \cosh kd \sin^2 ka}{kdka}. \tag{7.96}$$

Alternatively $\tilde{B}$ could be calculated from a consideration of the diffraction problem. This amounts to integrating the velocity potential representing a totally reflected incident wave, over $0 < x < a$. Again the expression (7.96) is obtained.

For frequencies where ka is equal to a multiple of π, the $\tilde{B}$ coefficient

is clearly zero. This corresponds to there being no outward propagating waves at large distances and consequently makes a poor wave-energy device at these frequencies.

As before results are displayed in §7.9.

7.8 The narrow duct approximation

An approximate solution to the harbour problem described in §7.5 can be derived when the water column is narrow. This involves a loose application of the method of matched asymptotic expansions, originally used by Newman (1974) to study the reflection and transmission coefficients of waves incident on an immersed narrow duct with vertical, equal length sides in a fluid of infinite depth. The same approach was adapted by Evans (1978) in examining the corresponding problem when there is a float-spring-dashpot system connected to the free surface of the duct, and then by Thomas (1981b) when the problem is formulated in terms of a surface pressure distribution.

The essential feature of this technique is to consider inner and outer regions as discussed in Chapter 4. In the far field the two sides are effectively collapsed into one, and the oscillatory flow will appear as an oscillating source on the side of a barrier, whilst in the thin column the fluid is in uniform, vertical oscillatory flow. Thus near the neighbourhood of the duct mouth where the free surface and fluid bottom have no effect, the flow will be as that depicted in fig. (7.12a). By the reflection principle (Lamb, 1932), the complex potential describing this flow is the same as that representing the flow shown in fig. (7.12b), which is also given in Lamb.

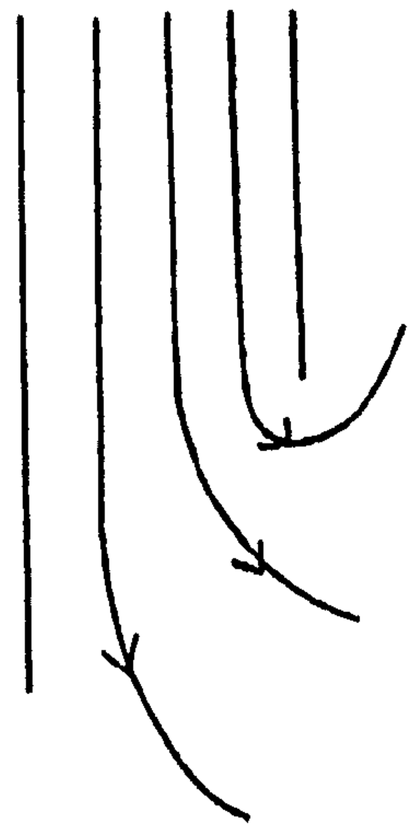

FIG. (7.12a)

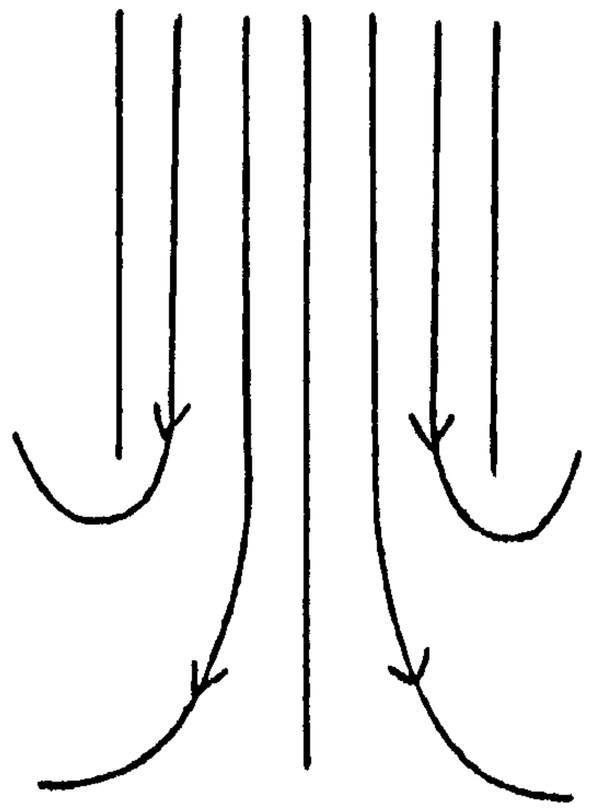

FIG. (7.12b)

The potential for a two-dimensional oscillating source at $(0,\ell)$ in a fluid of finite depth can be expressed from Thorne (1953) as

$$G(x,y;0,\ell) = \frac{1}{2\pi}\left\{\log\frac{r}{r'} + 2\int_0^\infty\left[\frac{\cosh t(d-\ell)\cosh t(d-y)}{\cosh td(K\cosh td - t\sinh td)} - e^{-td}\frac{\sinh t\ell \sinh ty}{t\cosh td}\right]\cos txdt\right.$$

$$\left. - 4\pi i\frac{\cosh k(d-\ell)\cosh k(d-y)}{2kd + \sinh 2kd}\cos kx\right\} \qquad (7.97)$$

with

$$r^2 = x^2 + (y-\ell)^2\ , \quad (r')^2 = x^2 + (y+\ell)^2$$

and where the integral takes its Cauchy principal value. If

$$G^*(x,y;0,\ell) = G(x,y;0,\ell) + G(-x,y;0,\ell)$$

$$= 2G(x,y;0,\ell) \qquad (7.98)$$

so that

$$\frac{\partial G^*}{\partial x}(0,y;0,\ell) = 0\ ,$$

then the outer solution takes the form,

$$\phi(x,y) = mG^*(x,y;0,\ell) \qquad (7.99)$$

where m is the unknown source strength. It follows that the inner limit of this outer solution valid for $r \to 0$ is given by

$$\psi(x,y) = \frac{m}{\pi}\left\{\log\frac{r}{2\ell} + 2\int_0^\infty\left[\frac{\cosh^2 th}{\cosh td(K\cosh td - t\sinh td)} - e^{-td}\frac{\sinh^2 t\ell}{t\cosh td}\right]dt\right.$$

$$\left. - \frac{4\pi i\cosh^2 kh}{2kd+\sinh 2kd}\right\} + O\left(\left(\frac{r}{\ell}\right)^{\frac{1}{2}}\right), \quad \frac{r}{\ell} \ll 1 , \tag{7.100}$$

where $h = d - \ell$.

It is necessary to match this solution with the inner solution in order to determine the unknown strength m. As in Newman (1974) the inner solution can be obtained from Lamb (1932) in terms of a stream function $\psi_s(x,y)$, being described by

$$x + i(y-\ell) = \frac{ia}{\pi}\{e^{-\alpha(\psi+i\psi_s)+\beta} - \alpha(\psi+i\psi_s) + 1 + \beta\} \tag{7.101}$$

where α,β are unknown constants. Thus the asymptotic solution for the flow between the barrier and the closed harbour end far above the lower edge $y = \ell$ is

$$x + i(y-\ell) \simeq \frac{ia}{\pi}[-\alpha(\psi+i\psi_s) + 1 + \beta] , \qquad \alpha\psi - \beta \gg 1 ,$$

yielding

$$\psi(x,y) \simeq \alpha^{-1}[1+\beta-\frac{\pi}{a}(y-\ell)] . \tag{7.102}$$

Applying the free surface boundary condition (7.8) to (7.102) defines the constant β as

$$\beta = \frac{1}{K}\left[\alpha + \frac{\pi}{a} - \frac{\pi K\ell}{a} - K\right]$$

so that

$$\psi(x,y) = \alpha^{-1}\left[\frac{\alpha}{K} + \frac{\pi}{aK} - \frac{\pi y}{a}\right] . \tag{7.103}$$

The outer approximation of (7.101) is

$$x+i(y-\ell) \simeq \frac{ia}{\pi} \exp\ [-\alpha(\psi+i\psi_s)+\beta],$$

which gives the outer limit of the inner solution as

$$\psi(x,y) \simeq -\frac{1}{\alpha} \log \frac{\pi r}{a} + \frac{\beta}{\alpha} + O\left(\left(\frac{a}{r}\right) \log^2\left(\frac{r}{a}\right)\right) , \quad \frac{r}{a} >> 1 . \tag{7.104}$$

Continuing as in Newman (1974) by matching in the overlap region $a << r << \ell$, it follows that

$$-\frac{1}{\alpha} = \frac{m}{\pi}$$

and, by matching the O(1) terms to eliminate α gives

$$m = \frac{\pi}{KD} \tag{7.105}$$

where

$$D = 2 \int_0^\infty \left[\frac{\cosh^2 th}{\cosh td(K\cosh td - t\sinh td)} - \frac{e^{-td}\sinh^2 t\ell}{t\cosh td}\right] dt$$

$$- \frac{4\pi i\cosh^2 kh}{2kd+\sinh 2kd} - \log \frac{2\pi\ell}{a} + \frac{\pi}{Ka}(1-K\ell) - 1 . \tag{7.106}$$

Thus all the unknown constants have been determined and so from (7.13) and (7.103),

$$q_r = \frac{i\omega p}{\rho g} \int_0^a \frac{\pi}{a\alpha}\, dx$$

$$= -\frac{i\omega p}{\rho g} m .$$

Substituting this in (7.16) gives, on equating the real and imaginary parts, the coefficients $\tilde{A}, \tilde{B}$ as

$$\tilde{A} = -\frac{Re(m)}{\rho g} \quad \text{and} \quad \tilde{B} = -Im(m)\frac{\omega}{\rho g} .$$

These coefficients along with the maximum efficiency curves are compared with the full harbour solution in the following section.

Before proceeding to present these results a comparison for this narrow duct situation is made with the original rigid body theory. This work models the internal free surface by a float or piston, so all that is required is to solve an identical radiation problem with the free surface condition (7.8) replaced by

$$\frac{\partial \psi}{\partial y} = 1 , \quad y = 0, \; 0 < x < a .$$

Then continuing in an identical manner it is found that the heave added mass and damping coefficients, a_2, b_2 satisfy

$$(a_2 + i\omega b_2)\rho a \ell = \frac{a}{\pi \ell}\left(\frac{\pi}{Ka} - D\right) ,$$

where D is given by (7.106).

This is comparable with the surface pressure distribution case, for by writing

$$a_2 = \rho a \ell \mu , \quad b_2 = \omega \rho a \ell \lambda$$

and

$$\tilde{A} = \frac{a}{\rho g}\mathscr{A}, \quad \tilde{B} = -\frac{\omega a}{\rho g}\mathscr{B}, \tag{7.107}$$

it can be shown that

$$\mathscr{A} = \frac{(\mu - \frac{1}{K\ell})}{K\ell[(\mu - \frac{1}{K\ell})^2 + \lambda^2]}$$

and

$$\mathscr{B} = \frac{\lambda}{K\ell[(\mu - \frac{1}{K\ell})^2 + \lambda^2]} .$$

Thus the $\tilde{A}$ and $\tilde{B}$ coefficients are related to the added mass and damping coefficients.

7.9 Results and discussion

Numerical computations for the $\tilde{A},\tilde{B}$ and maximum efficiency expressions derived in the last four sections are now presented. The results of §7.7 and §7.8 are readily calculated but the evaluation of the results in §7.5, and simultaneously that of §7.6, requires the solution of two infinite systems of real equations. Since both systems possess the same left-hand side, this matrix can be inverted once using the numerical procedure described in Chapter 3, with the same comments as for Chapter 4. In all sections the $\tilde{A}$ and $\tilde{B}$ coefficients are suitably non-dimensionalized by (7.107).

We commence with the narrow-duct approximation of §7.8 by illustrating respectively the variation of $\mathscr{A},\mathscr{B}$ and η_{max} as a function of $K\ell$ in figs. (7.13a), (7.13b) and (7.13c) for $a/\ell = \frac{1}{4}$ when $\ell/d = \frac{1}{4}, \frac{1}{2}$. The case of an infinitely deep fluid has also been considered, but there are no visible differences from the curves shown for $\ell/d = \frac{1}{4}$. From fig. (7.13a) it is seen that the $\tilde{A}$ coefficient possesses a zero at $K\ell \propto \cdot 819$ and $\cdot 822$ for $\ell/d = \frac{1}{4}$ and $\frac{1}{2}$ respectively, corresponding to the maximum value of both the $\tilde{B}$ coefficient and the maximum efficiency. However, in contrast to the $\tilde{A}$ coefficient which reaches a minimum and maximum value before decreasing monotonically to zero, the $\tilde{B}$ coefficient has a sharp resonance. For both the $\tilde{A}$ and $\tilde{B}$ coefficients the maximum value is slightly greater for infinite depth, occurring at a smaller value of $K\ell$. The efficiency curves are of a similar nature to the $\mathscr{B}$ coefficient, rising to a peak to attain its maximum value of unity. As a/ℓ decreases it is found that these efficiency bandwidths become narrower.

The accuracy of the approximate solution is tested against the results of the full solution in figs. (7.14a), (7.14b) and (7.14c), where curves are displayed for $a/\ell = \frac{1}{4}$ and $\ell/d = \frac{1}{2}$. The $\mathscr{A}$ coefficient is

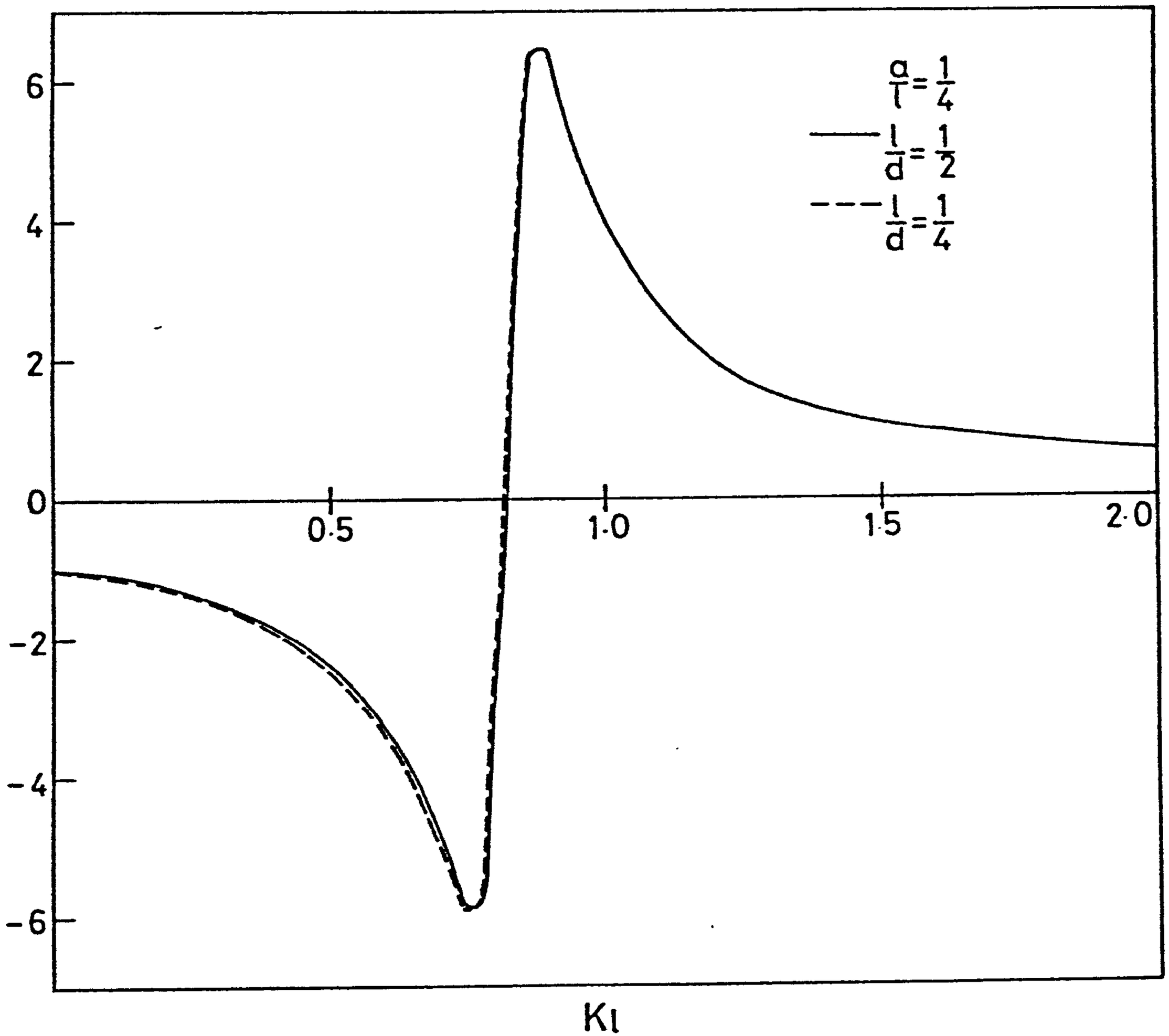
$\frac{a}{t}=\frac{1}{4}$
$\frac{l}{d}=\frac{1}{2}$
$\frac{l}{d}=\frac{1}{4}$
6
4
2
0
-2
-4
-6
0·5
1·0
1·5
2·0
$\mathscr{A}$
K_I

FIG. (7·13a)

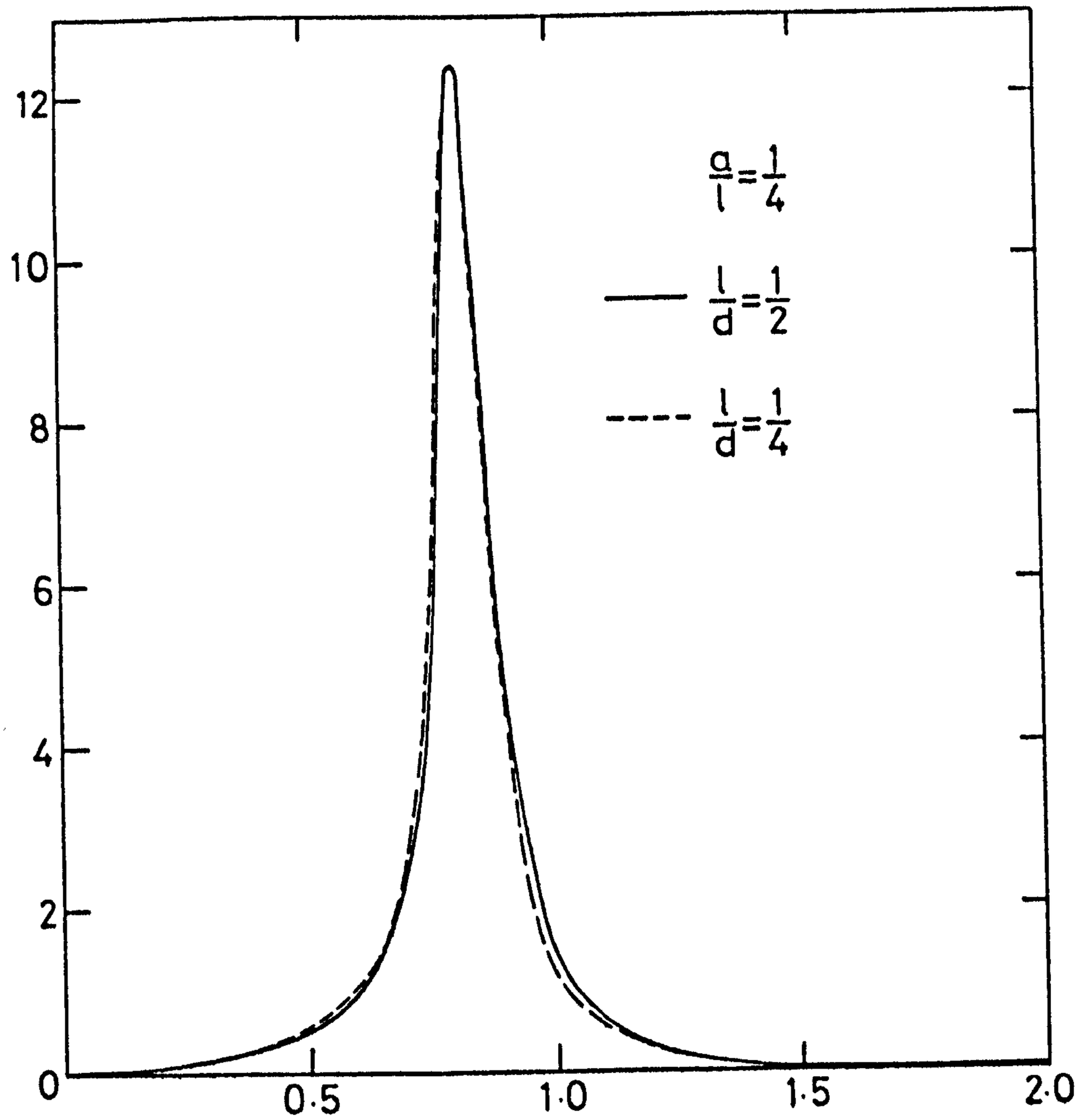

Kl

FIG. (7·13b)

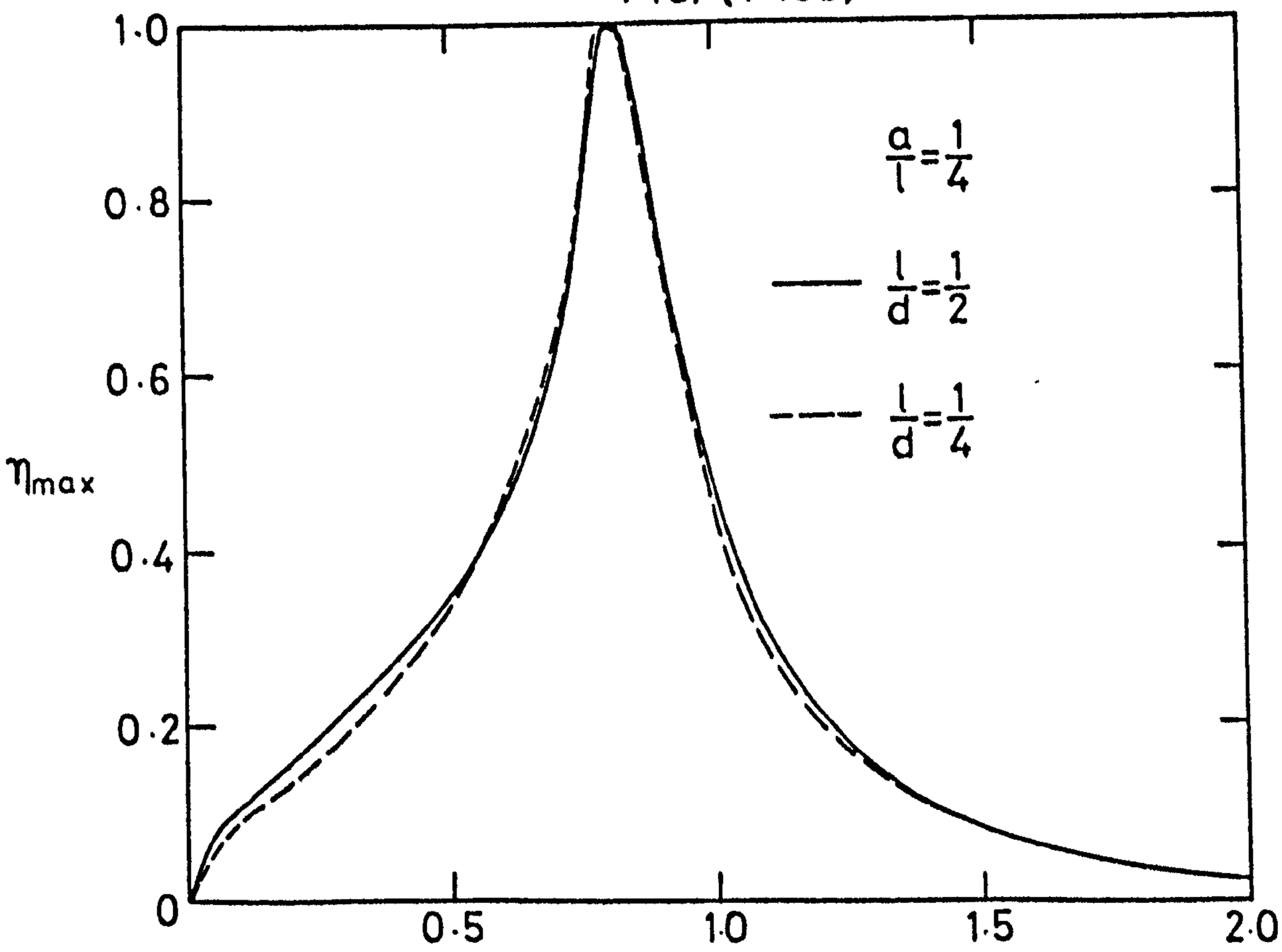

Kl

FIG. (7·13c)

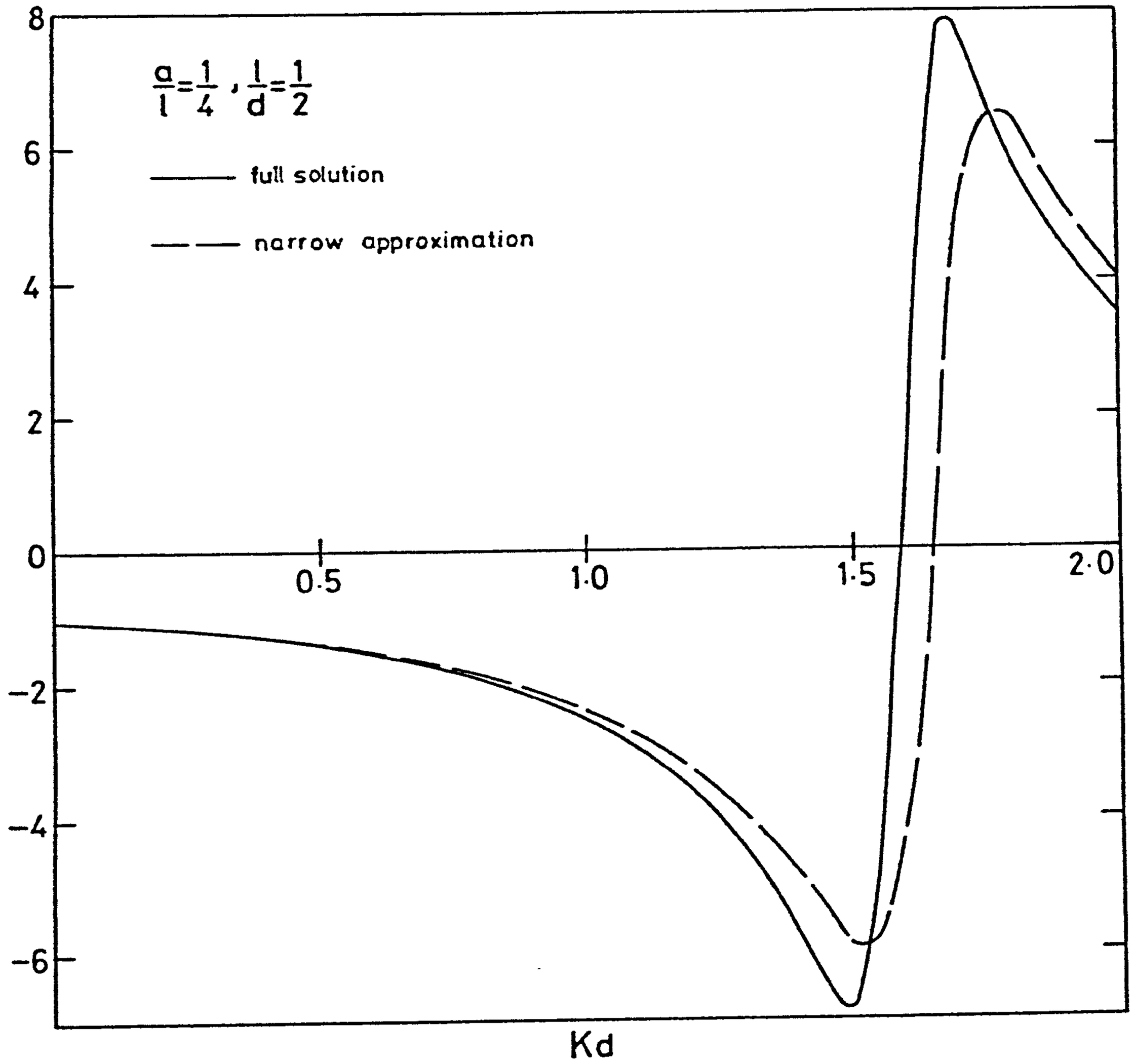
$\frac{a}{l}=\frac{1}{4}$, $\frac{l}{d}=\frac{1}{2}$
full solution
narrow approximation
8
6
4
2
0
-2
-4
-6
0·5
1·0
1·5
2·0
A
Kd

FIG. (7.14a)

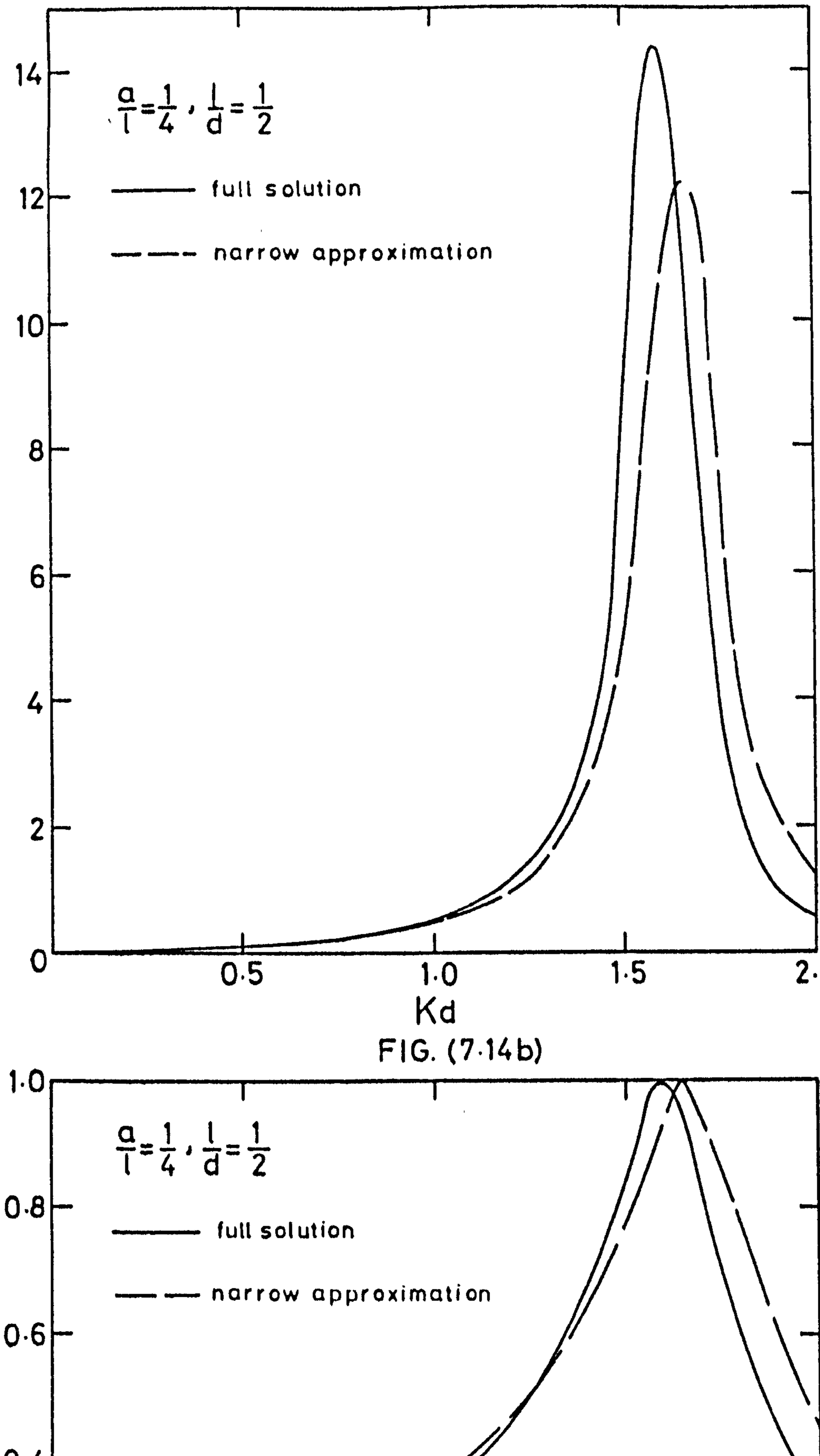

$\mathscr{B}$

FIG. (7·14b)

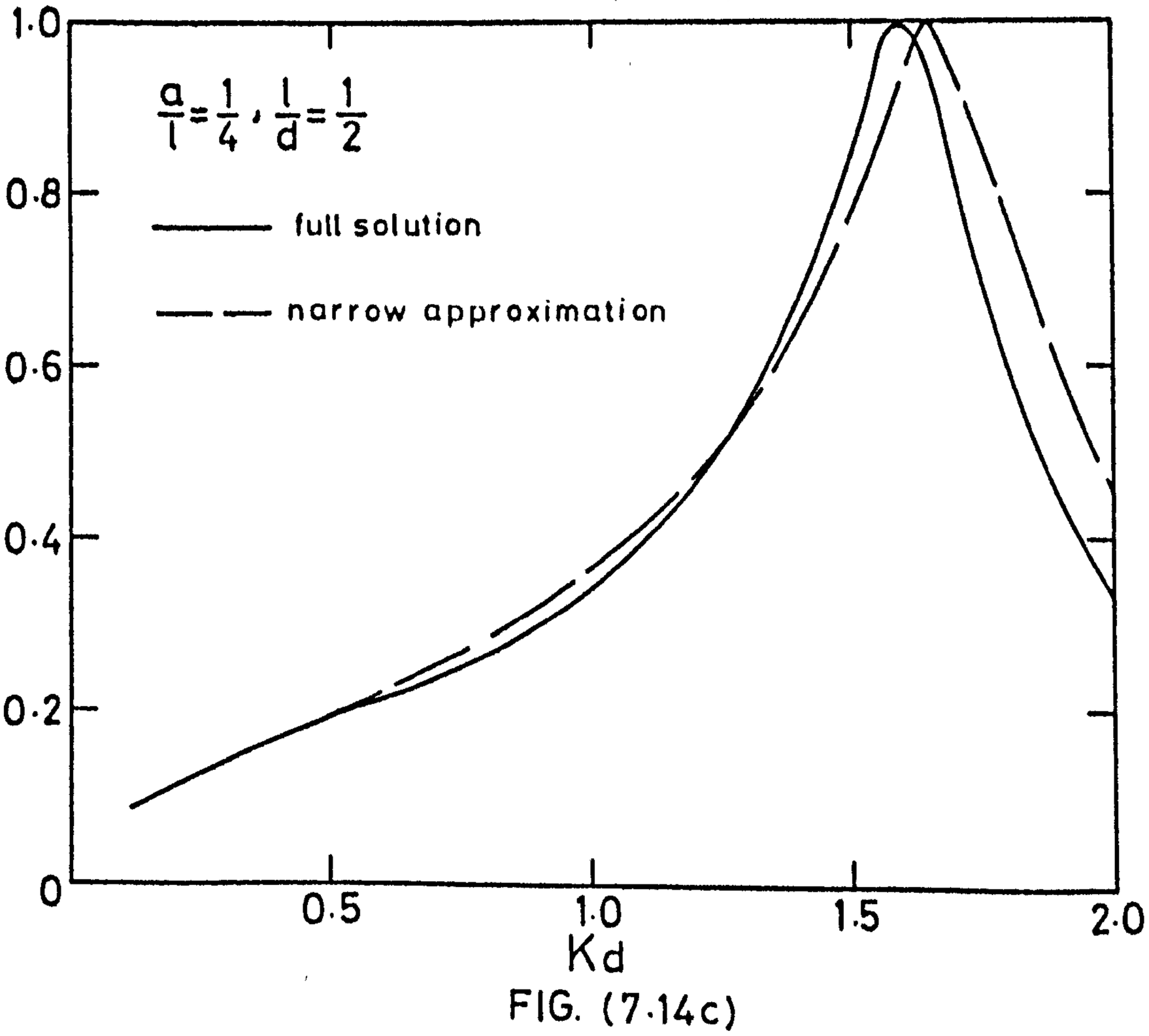

FIG. (7·14c)

in reasonable agreement apart from the region around the peak and trough, whilst the $\mathscr{B}$ coefficient shows a greater discrepancy. In both instances the shapes of the curves are very similar, and consequently the efficiency curves are in good agreement up to the maximum value. Thereafter the approximate solution over predicts the efficiency, this discrepancy increasing as Kd increases. As the duct gets narrower it is found that the agreement improves.

A thorough study of the full solution to the harbour problem is now made to examine the effect of various parameters. Firstly results for constant ℓ/d as the ratio a/d changes are presented in figs. (7.15). Here it can be seen that as a/d increases, that is, as the width of the oscillating water column gets broader, the amplitude of the maximum and minimum values of $\mathscr{A}$ decrease, occurring at smaller values of Kd. Therefore the first zero of $\mathscr{A}$ also occurs at a smaller value of Kd. Similarly, the maximum value of $\tilde{B}$ decreases as a/d increases whilst the bandwidth increases. These wider bandwidths for the narrower ducts are also a feature of the efficiency curves.

When the parameter a/d is kept constant at one, the effect of the barrier length ℓ is shown in figs. (7.16), including the case of §7.7 when ℓ shrinks into the free surface. As ℓ increases the first zero of $\tilde{A}$ (fig. 7.16a)) occurs at a smaller value of Kd. Meanwhile the turning points, which occur at greater amplitudes, move closer together. The maximum value of $\tilde{B}$ also increases as ℓ increases whilst the bandwidth decreases. The results of fig. (7.16c) show that when ℓ is small, the maximum efficiency graphs possess large bandwidths. Indeed, when $0 < \ell/d < \frac{1}{4}$, these curves do not alter greatly for $0 < Kd < 2$. However, as ℓ/d increases, the bandwidths decrease. In all of these figures (7.16), the pressure patch results justify the assertion that it is a shallow draft approximation.

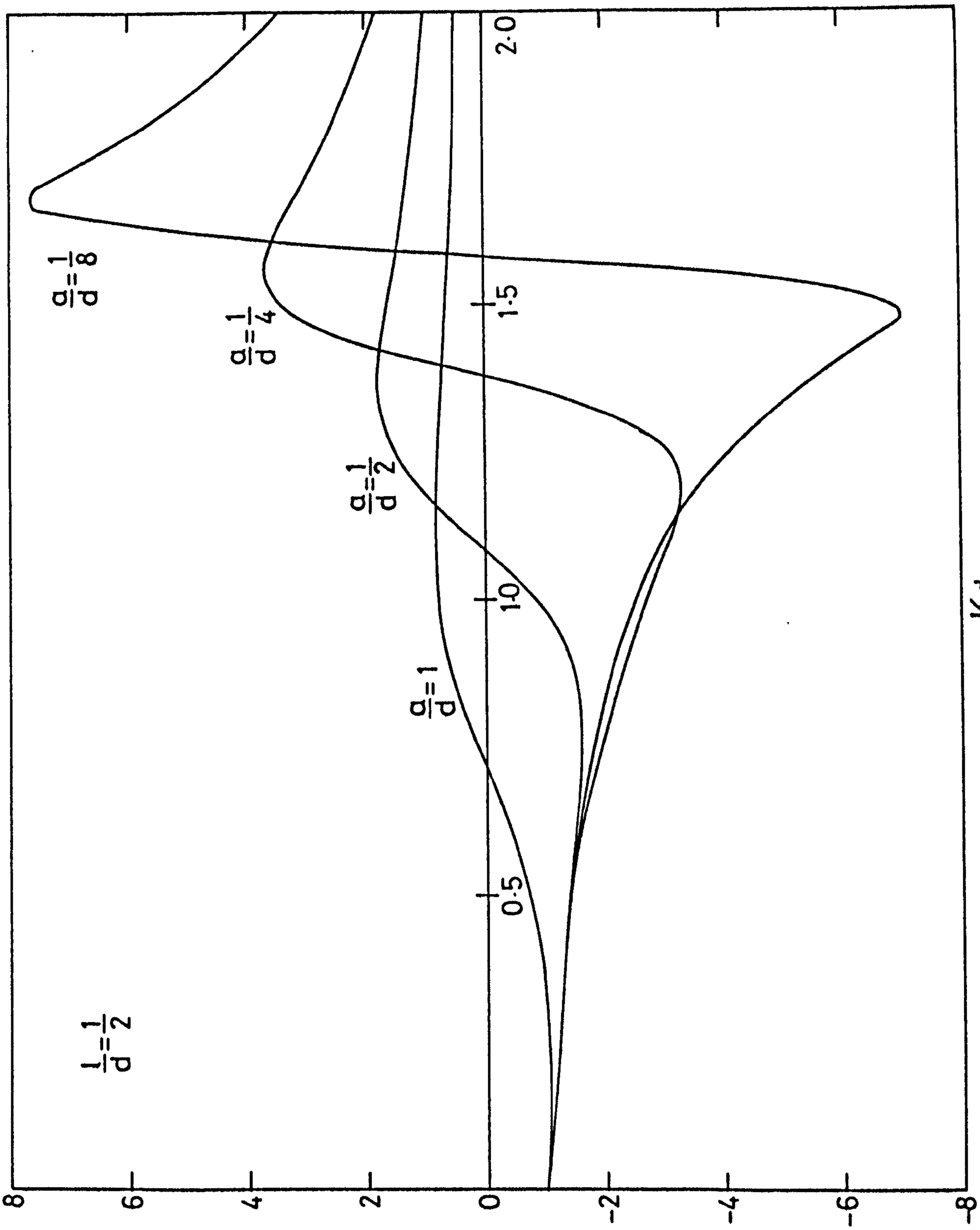

FIG. (7.15a)

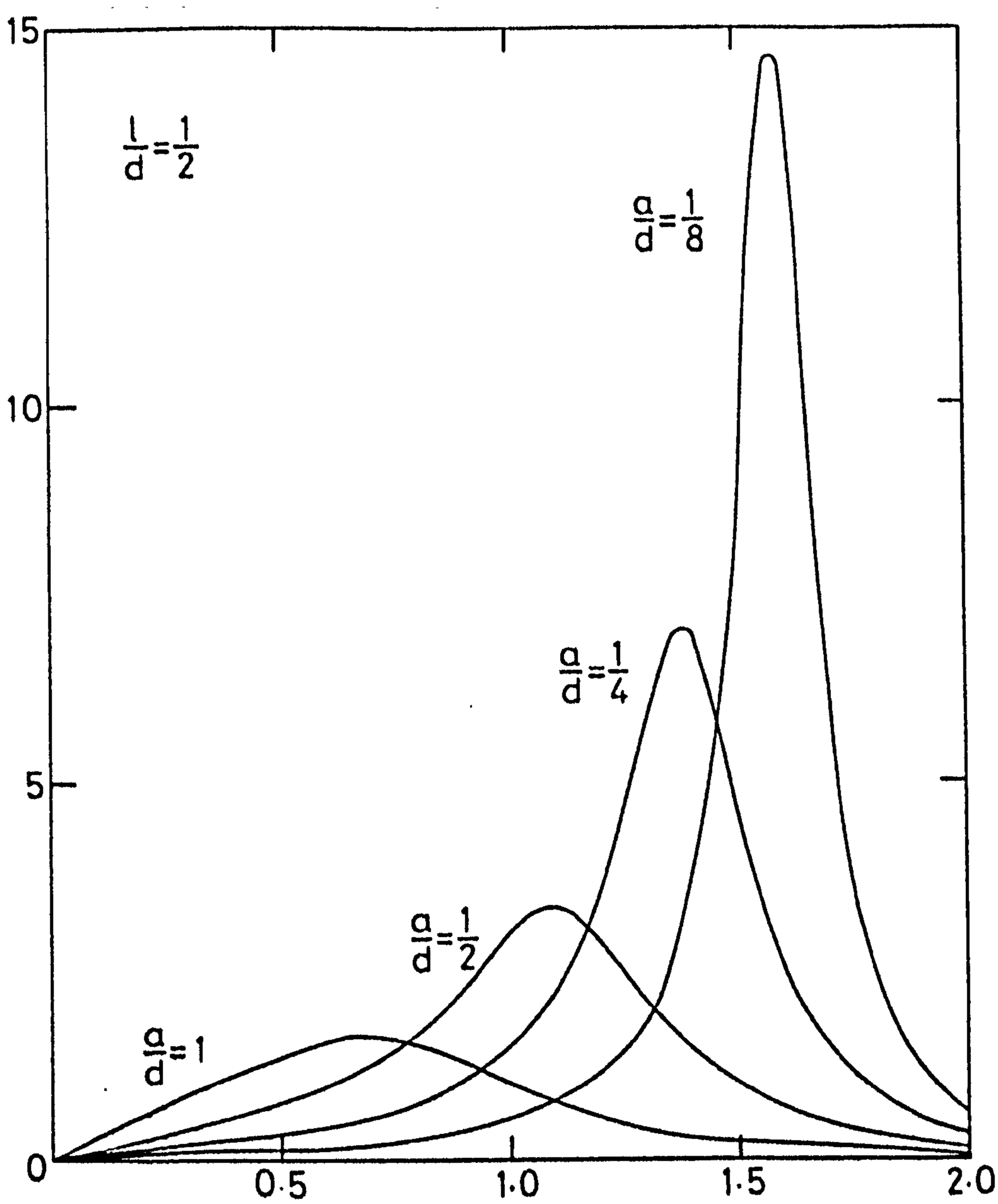

FIG. (7·15b)

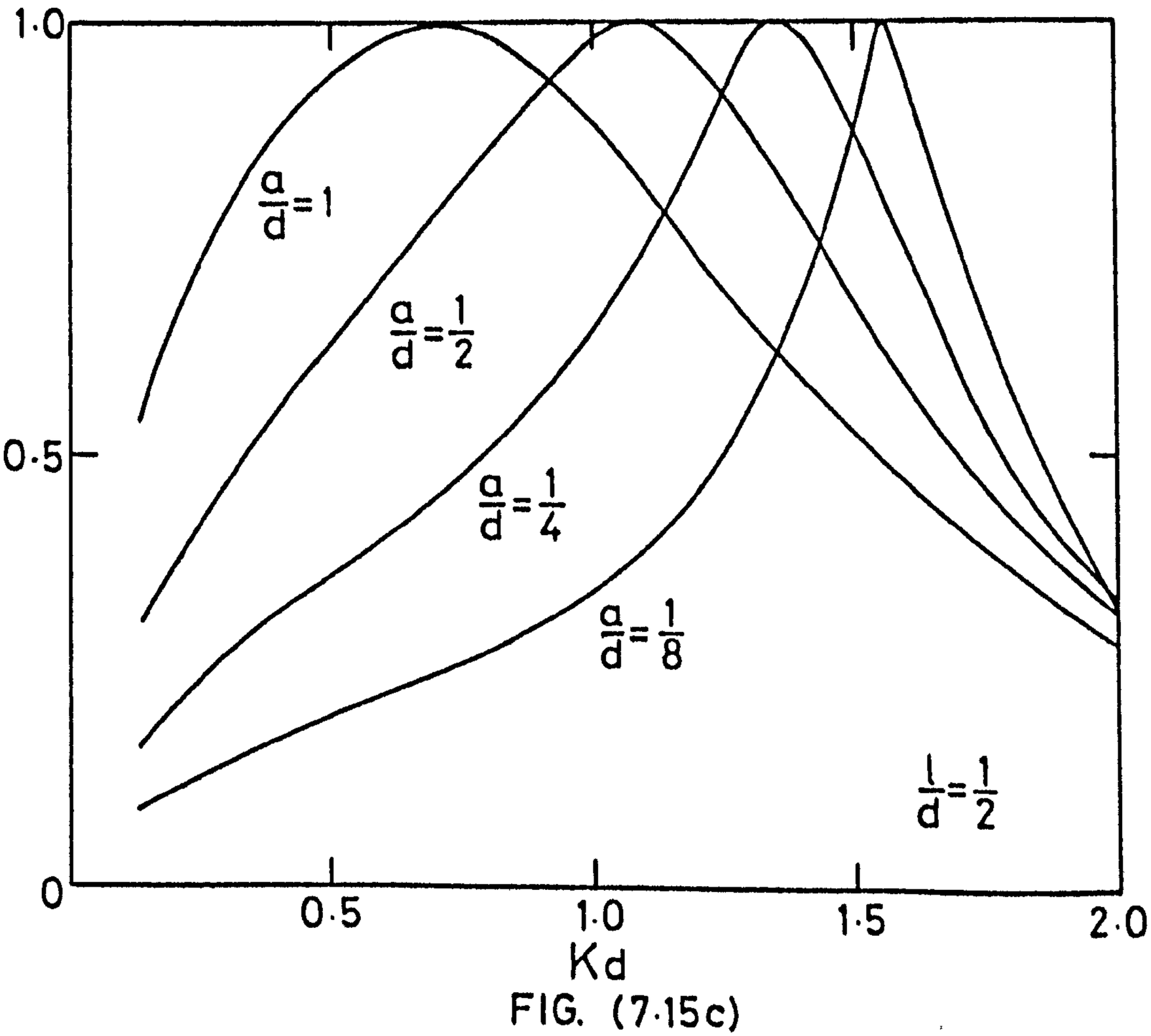

FIG. (7·15c)

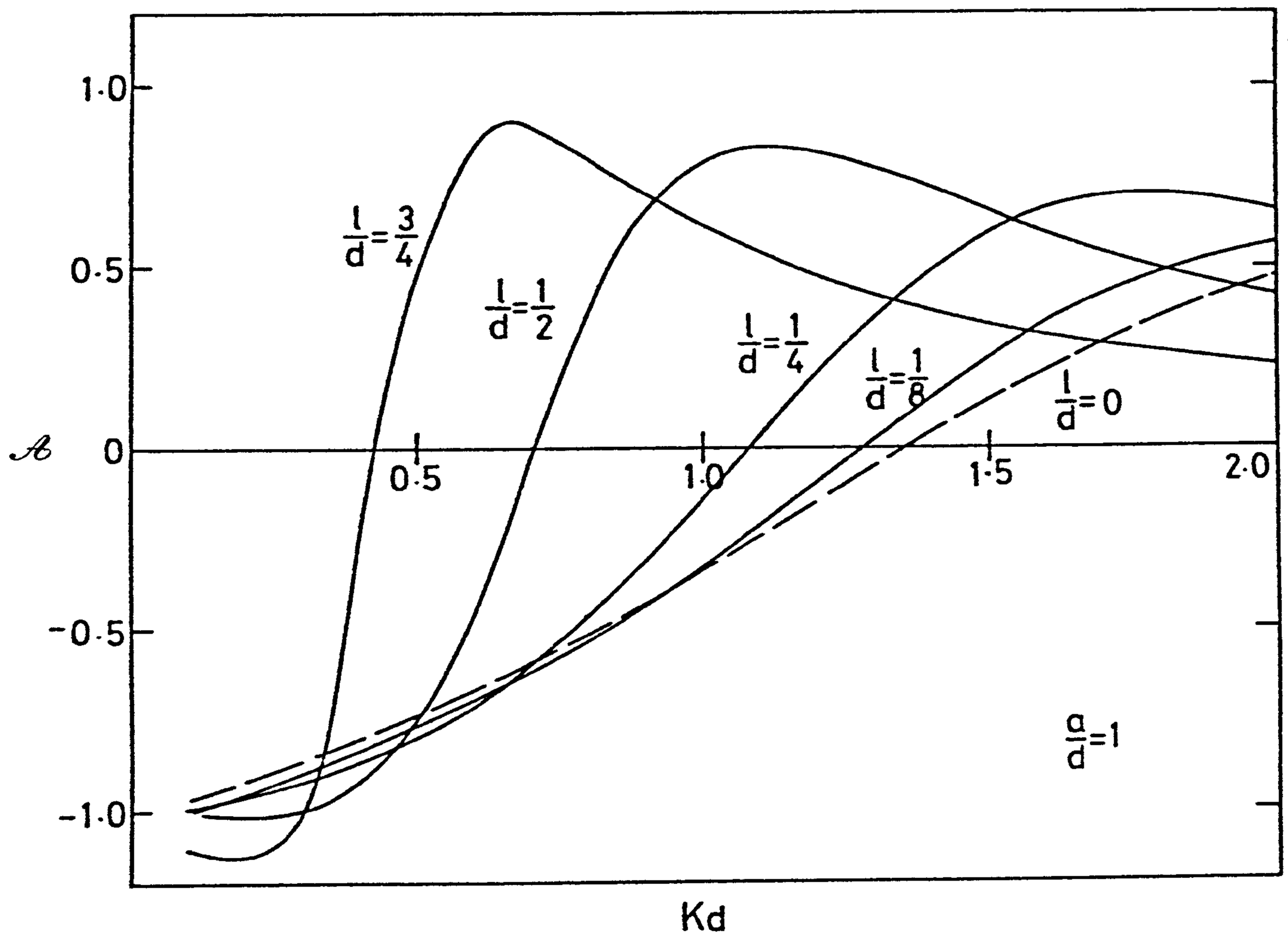
1·0
0·5
0
-0·5
-1·0
$\mathscr{A}$
$\frac{l}{d}=\frac{3}{4}$
$\frac{l}{d}=\frac{1}{2}$
$\frac{l}{d}=\frac{1}{4}$
$\frac{l}{d}=\frac{1}{8}$
$\frac{l}{d}=0$
0·5
1·0
1·5
2·0
$\frac{a}{d}=1$
Kd

FIG. (7·16a)

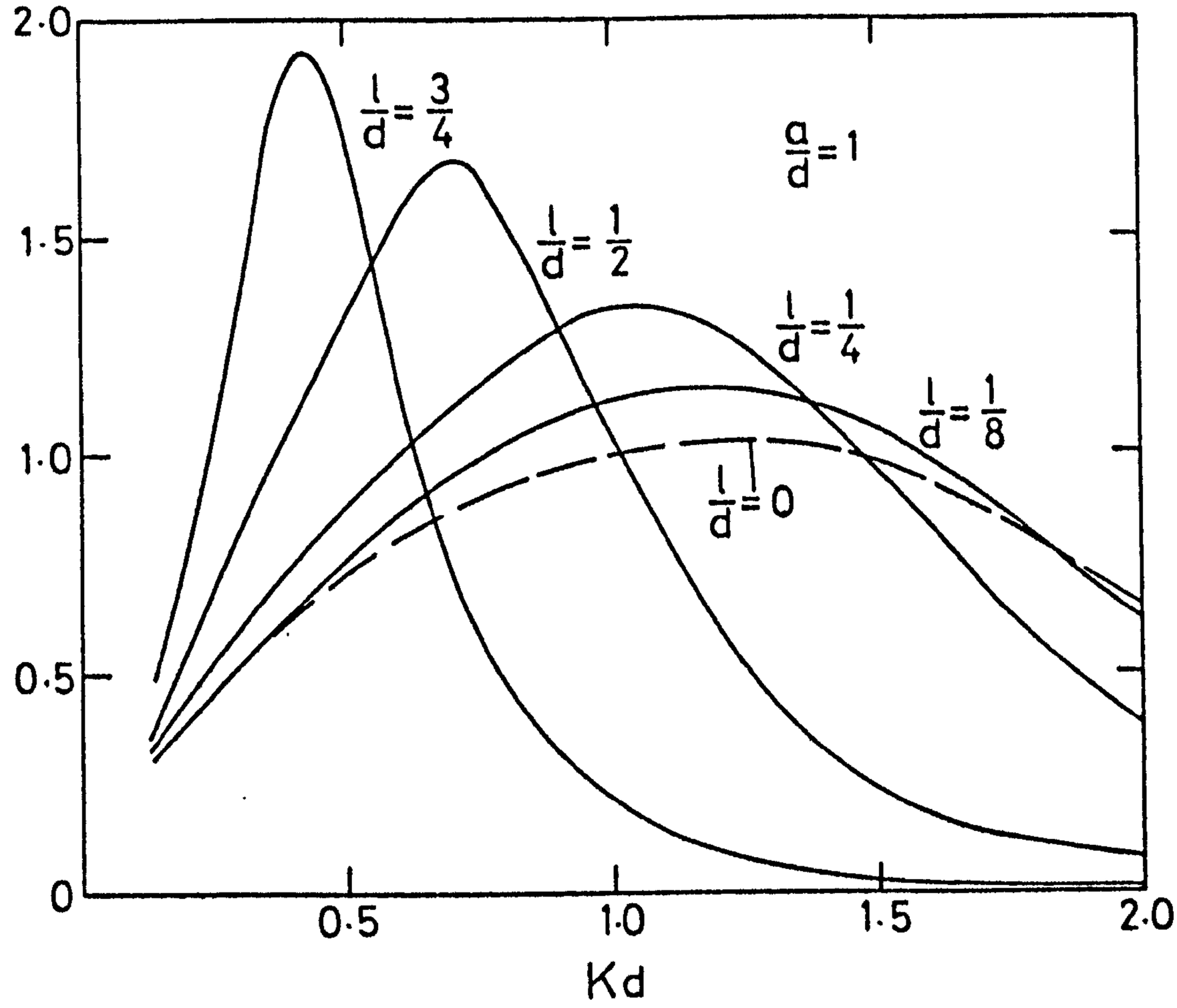

FIG. (7·16b)

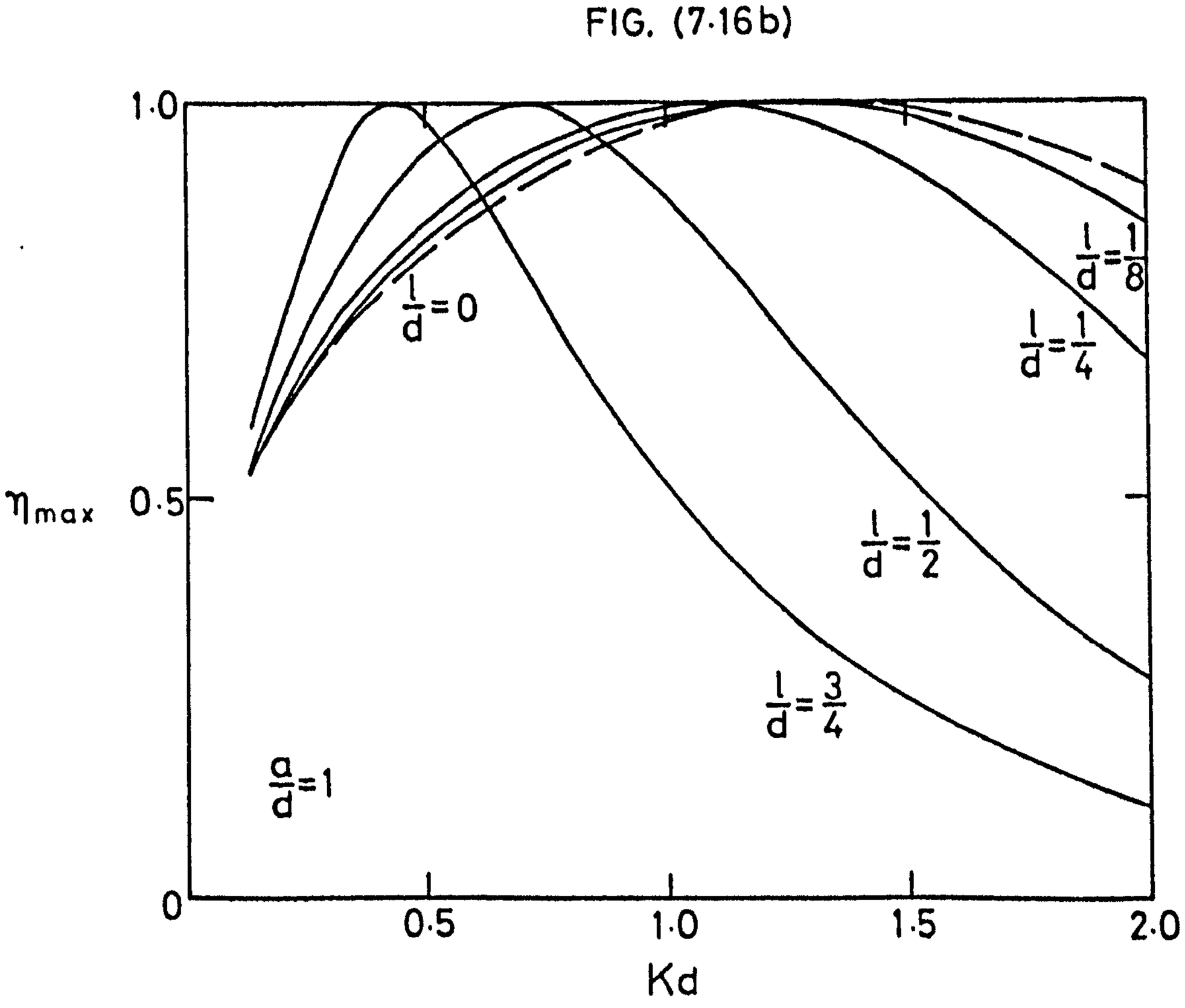

FIG. (7·16c)

Finally figs. (7.17a), (7.17b) and (7.17c) present further results for the case when $\ell = 0$ as a function of ka. For all values of a/d, $\mathscr{A}$ and $\mathscr{B}$ approach their respective analytic limits of -1 and 0 as ka → 0. The variation of $\mathscr{A}$ for different water depths is shown in fig. (7.17a). For all water depths there is a similar behaviour of damped oscillatory motion. After the first zero the different motions are in phase, with the amplitude for deeper fluid being greater than for shallow water. This continues for all ka, the negative values of $\tilde{A}$ diminishing more rapidly than the positive. Therefore the number of zeros decrease as the depth increases. In fact when a/d = ½ there are five zeros, and when a/d = 1, 1·6 and 2 there are seven, eleven and thirteen, respectively. The corresponding motion for $\mathscr{B}$ is displayed in fig. (7.17b). Again there is a similar behaviour for all water depths. As the depth increases the amplitude also increases, rising to a peak and then falling to a common zero when ka = nπ, n = 1,2,... The succession of peaks occur at decreasing values of $\tilde{B}$. These two sets of results combine to yield the maximum efficiency curves shown in fig. (7.17c). The maximum value of this quantity, occurs when $\tilde{A} = 0$ for all depths; and the zero value corresponds to $\tilde{B} = 0$.

This concludes our study of the two-dimensional KMOWC harbour problem. It would be interesting to compare the results with the three-dimensional device which utilises the resonant properties of the harbour to increase the efficiency of the absorber. However the disadvantage of the two-dimensional model is that a key parameter, the harbour length, is lost and so no direct comparison can be made.

7.10 Conclusion

Evans' (1982a) theory of wave-absorption by a surface pressure distribution has been applied to oscillatory water columns of different

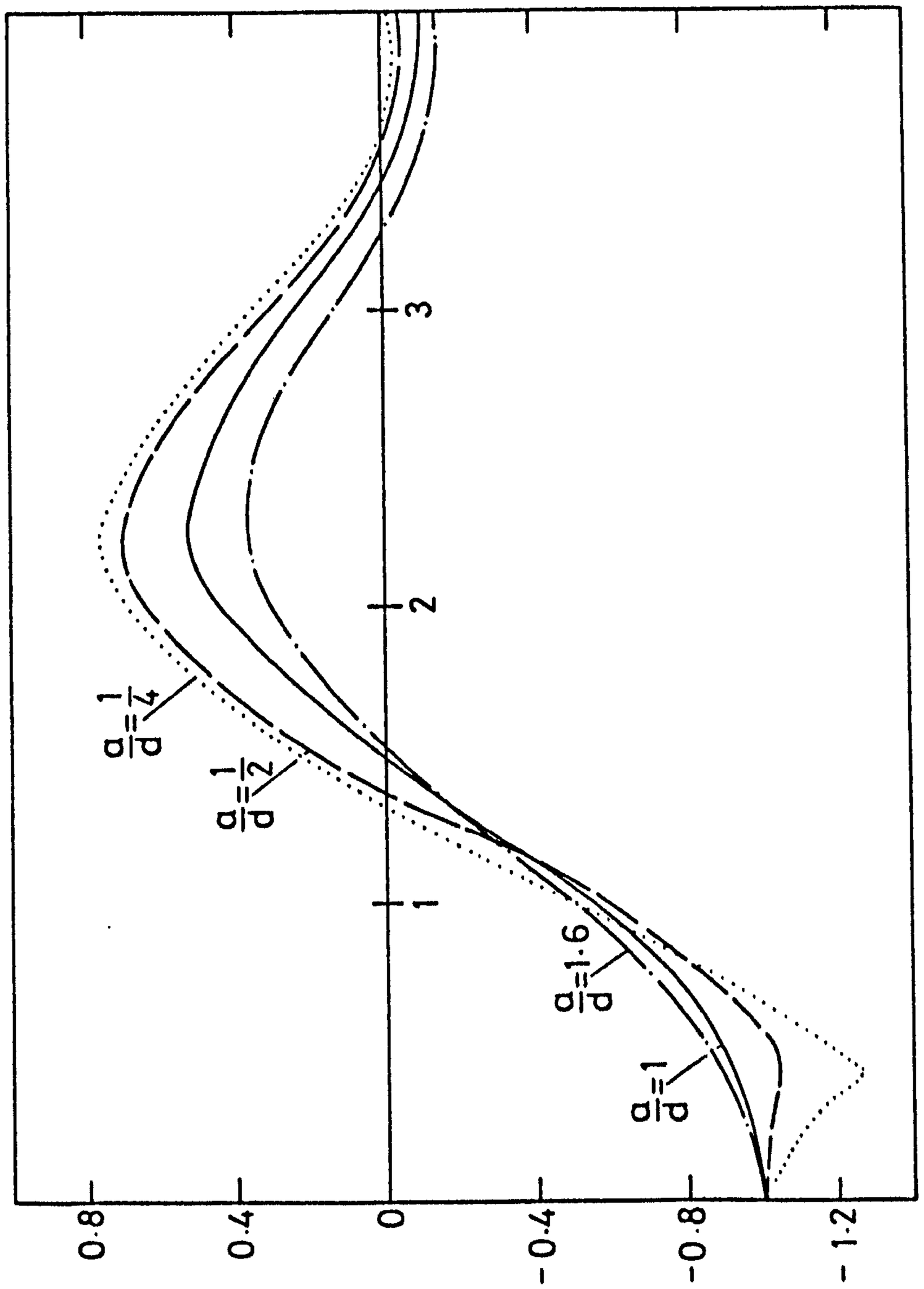

FIG. (7.17a)

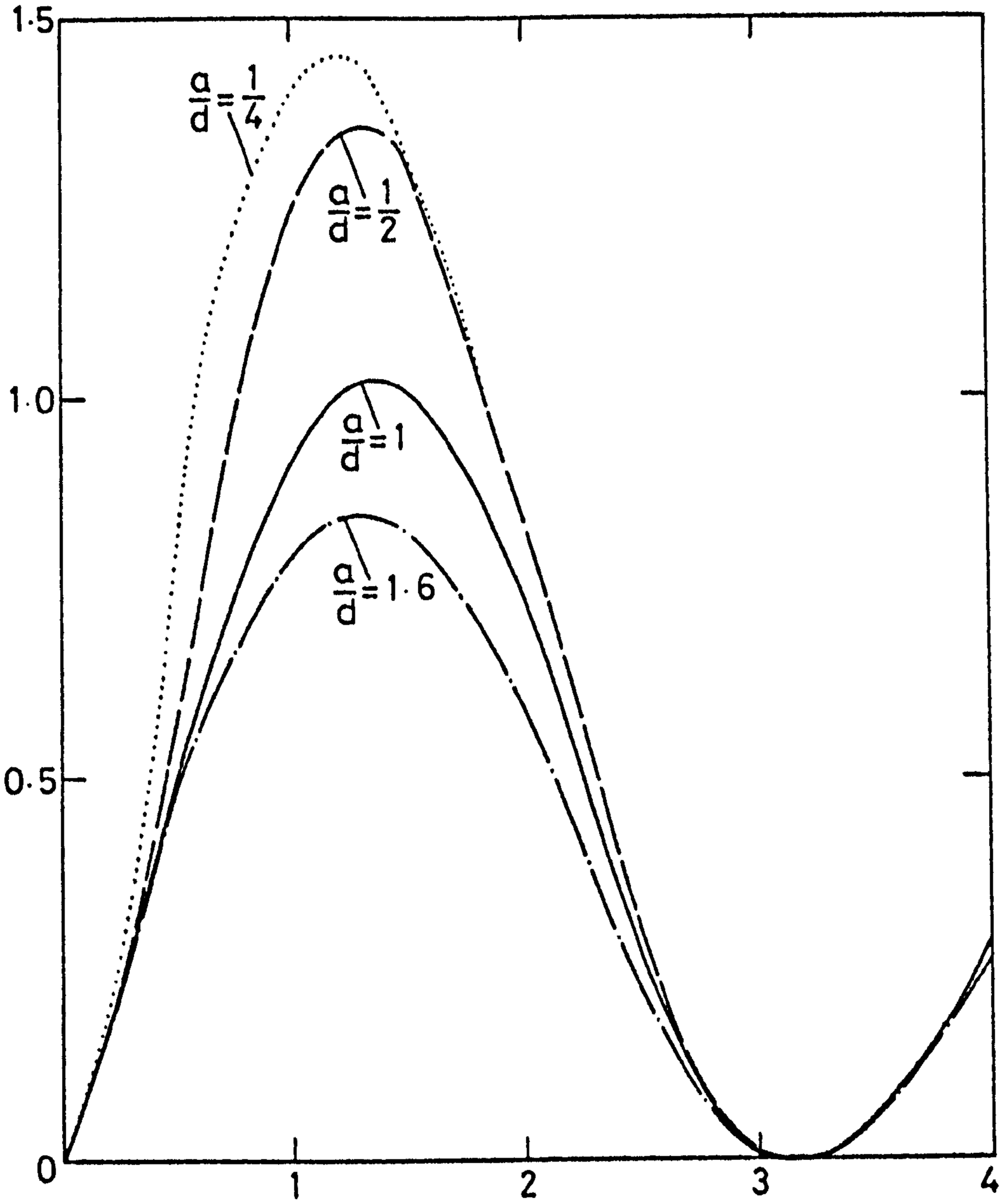

B

FIG. (7·17b)

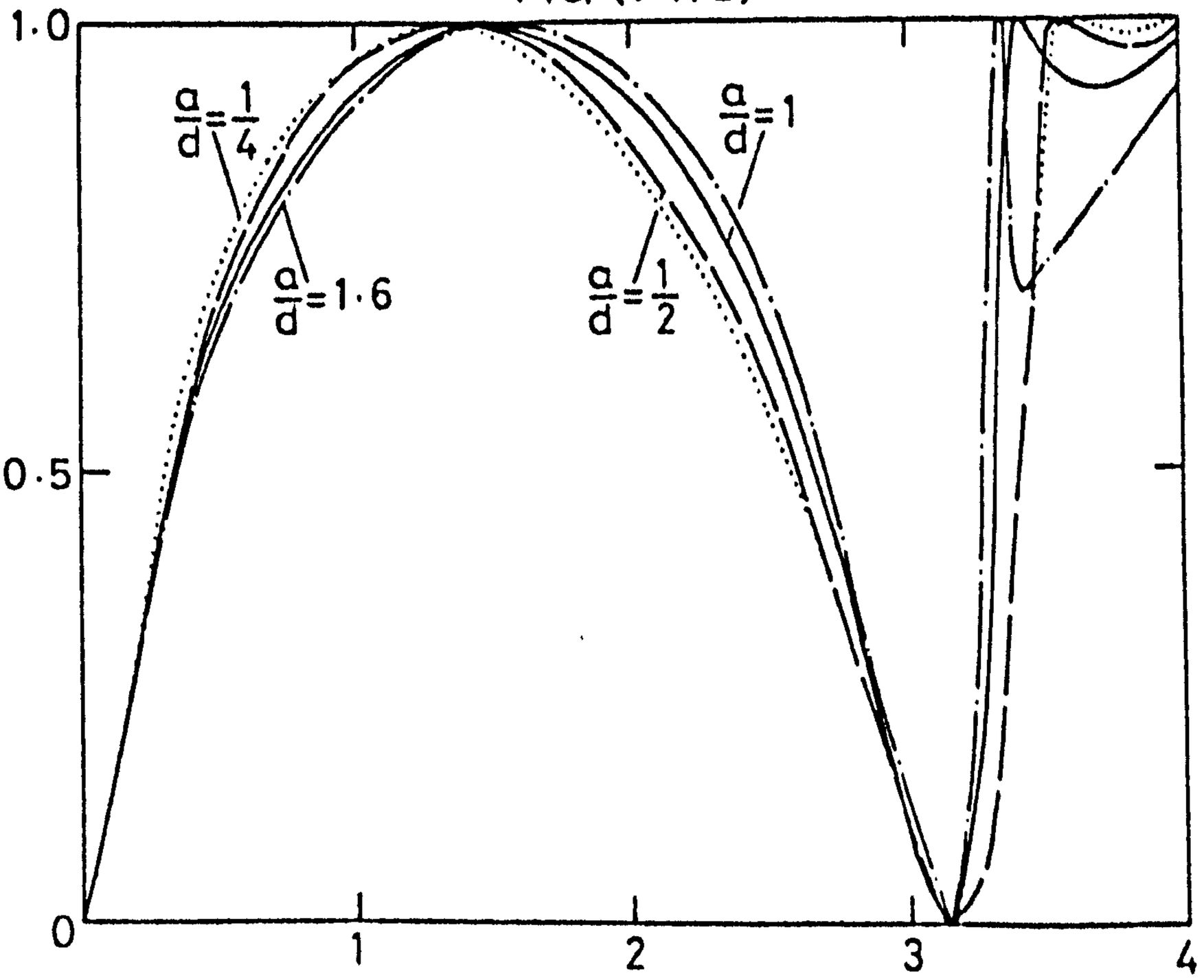

FIG (7·17c)

configurations. A study of the theoretical maximum efficiency for two simple devices has been made by solving the appropriate diffraction problems without specific reference to pressure distributions. In the more likely case when it is not possible to introduce a phase difference between the volume flow rate through the turbine and the pressure drop across it, the maximum effficiency for a realistic situation, the two-dimensional Kvœrner multiresonant OWC has been studied.

In this latter problem the maximum efficiency attains its theoretical maximum of one when $\tilde{A} = 0$ and $\tilde{B}$ reaches a local maximum value. It is also seen that a better, overall performance is achieved from an OWC which is neither of shallow draft nor narrow, for example when $a/d = \frac{1}{4}$, $\ell/d = \frac{1}{2}$. The examination of this problem is independent of the harbour length, a parameter of major importance in determining the efficiency of the full, three-dimensional device. However, by applying Evans' (1982b) surface pressure distribution theory within a resonant harbour, this work can be extended to include the omitted property, and therefore results appropriate to wave-tank models of the Norwegian device can be obtained.

CHAPTER 8

CONCLUDING REMARKS

The contents of the preceding chapters provide an indication of the great variety that is encompassed within the subject of linear wave theory, both in the types of physical problems that occur and in the mathematical methods needed to solve them. For even the handful of problems treated herein employ numerous techniques in solving various topics, ranging from submerged bodies in the presence of surface tension, to the transient motion of bodies, to oscillating water column wave-energy devices.

The work begins by showing that the classical theorems of Haskind and Newman continue to hold for a totally submerged body when the effect of surface tension is accounted for. Under these identical conditions it is also seen that Dean's (1948) result of an incident wave being totally transmitted from a fixed cylinder when surface tension is negligible, is again obtained, and that a cylinder moving uniformly in a circle of small radius radiates outward travelling waves in one direction only. The method of solution utilizes the appropriate multipole expansions and is justified by introducing a complex analysis approach.

In contrast to this, the problem of a fixed vertical barrier intersecting the free surface of a fluid of finite depth is solved by matching eigenfunction expansions across the fluid beneath the end of the barrier. This solution is comparable with the explicit results of Ursell (1947) and Haskind (1959) when the fluid is very deep; and with the approximate, matched asymptotic results evaluated for the special case of a long barrier. This latter approach requires both the tools of conformal mapping and complex methods in general.

The main technique utilized in solving the transient motion problems is that of the Fourier transform. Complex methods are also exploited, which require the asymptotic expansions of the force coefficient for large and small waves. Together these approaches unite to show that the ultimate decaying motion of a rolling barrier is monotonic, like t^{-7} when an initial force is applied, and like t^{-6} when there is an initial displacement. Similarly, the decaying motion of a surging cylinder following an initial displacement is like t^{-6}.

Finally the work concludes by combining a selection of some of these approaches in treating a recently developed field within the area of oscillating water column wave-energy devices. In particular, specific attention is focussed on the two-dimensional side view of the Norwegian, Kvaerner multiresonant device. The full solution is determined from an application of the method of matched eigenfunction expansions, which can be compared with the shallow draft solution and the approximate, narrow duct solution.

In spite of the different techniques that have been employed, all the problems culminate with some degree of numerical computation. This is a characteristic of many current investigations in linear wave theory, for exact, analytic solutions are not usually obtained. Indeed, such solutions are primarily a feature of the original works which now form the basis of the well established results and theories. Thus throughout this thesis, reference has not only been made to several of these results, but also to more recent developments and theories.

APPENDIX A

The added inertia and damping coefficients for a rolling barrier

As mentioned in the introduction to Chapter 5, these coefficients can be found using Porter's paper (1974), referred to as P in this section. Here he gives a method for solving a normally incident train of small amplitude waves on an arbitrary arrangement of n vertical barriers. The barriers lie in deep water in a vertical line and each is allowed to perform small rolling or swaying oscillations of the same frequency as the incident wave. The solution is in the form of a singular integral with a certain solvability condition to be satisfied. Porter mentions that the wave forces and moments on the barrier can be calculated but gives no examples to illustrate this.

For our purpose we examine the case of a single barrier intersecting the free surface in its equilibrium position. It is hinged at its submerged end point and in the absence of any incident wave is forced to oscillate in the roll mode (that is, the radiation problem). In P this is an example of Case 2 with $n = 1$, $I = 0$, $a_1 = 0$, $b_1 = c_1 = a$ and $e^{-i\varepsilon_1} = -i$ (to agree with Ursell (1948)), but for completeness the theory is repeated for this specific problem.

The barrier is hinged at the point (0,a) and makes small rolling oscillations of amplitude θ and frequency ω about its vertical equilibrium position $x = 0$, $0 < y < a$. Under the usual assumptions of linear theory the fluid motion is described by a time-independent velocity potential $\phi(x,y)$ given by equation (2.9), where ϕ must satisfy equations (2.10), (2.11) and (2.12b). To first-order the normal velocity of the barrier is given by

$$\frac{\partial \phi}{\partial x} = \omega\theta i(a-y) \quad , \qquad x = 0,\ 0 < y < a \qquad \text{(A1)}$$

where for rolling motion it follows that ϕ is odd in x. Thus

$$\phi(0,y) = 0 \quad , \qquad y > a \ . \tag{A2}$$

For large values of x we assume waves are moving away from the origin and therefore

$$\phi(x,y) \sim C \ \mathrm{sgn}\ x \ e^{-Ky \pm iKx} \qquad \text{as } x \to \pm\infty \tag{A3}$$

where C is a constant to be determined. Finally the fluid velocity possesses a singularity at the edge of the plate represented by

$$\frac{\partial\phi}{\partial r} \sim r^{-\gamma} \qquad \text{as } r \to 0 \ , \quad 0 < \gamma < 1 \ , \tag{A4}$$

where r denotes the distance from a point in the fluid to the edges.

Following P a function $\psi(x,y)$ defined by

$$\frac{\partial\psi}{\partial y} - K\psi = \phi(x,y) + Ce^{-Ky-iKx} \quad , \qquad x < 0 \ , \tag{A5}$$

is introduced. Then (A3) is satisfied if

$$\psi \ , \frac{\partial\psi}{\partial y} \to 0 \qquad \text{as } x \to -\infty \ , \tag{A6}$$

and to satisfy (2.12b) the condition

$$|\nabla\psi| \to 0 \qquad \text{as } y \to \infty \tag{A7}$$

is imposed. From (A4) and (A6) the derivatives of ψ must be bounded at (0,0).

If $\nabla^2\psi = 0$ for $x < 0$, $y > 0$, then using this with (2.11) and (A6) gives

$$\psi(x,0) = 0 \ , \quad x < 0 \ . \tag{A8}$$

Equation (A1) with (A8) and (A2) with (A7) then yields

$$\frac{\partial\psi}{\partial x}(0,y) = f(y) = -\frac{i\omega\theta e^{Ky}}{K^2}(1-Ka) + \frac{\omega\theta i}{K^2}[1-K(a-y)] - iC\sinh Ky, \quad 0 < y < a \tag{A9}$$

and

$$\psi(0,y) = h(y) = -\frac{Ce^{-Ky}}{2K} \quad , \qquad y > a \ . \tag{A10}$$

It now remains to determine $\psi(x,y)$. To do this the Green's function

$$G(x,y;\xi,\eta) = \hat{G}(x,y;\xi,\eta) + \hat{G}(x,y;-\xi,-\eta) - \hat{G}(x,y;-\xi,\eta) - \hat{G}(x,y;\xi,-\eta)$$

where

$$\hat{G}(x,y;\xi,\eta) = -\frac{1}{2\pi} \log \{(x-\xi)^2 + (y-\eta)^2\}^{\frac{1}{2}}$$

is introduced. Applying the identity (2.30) to G and ψ in $x < 0$, $y > 0$ we obtain

$$\psi(x,y) = -\int_0^\infty \frac{\partial G}{\partial \xi}(x,y;0,\eta)\psi(0,\eta)\, d\eta.$$

Differentiating, and then integrating by parts using (A8) and (A10) gives

$$\frac{\partial \psi}{\partial x}(0,y) = \frac{1}{\pi}\int_0^\infty \frac{2y}{y^2-\eta^2} \frac{\partial \psi}{\partial \eta}(0,\eta)\, d\eta ,$$

where the integral is taken as the Cauchy principal value. Therefore

$$\frac{1}{\pi}\int_0^a \frac{2y}{\eta^2-y^2} \frac{\partial \psi}{\partial \eta}(0,\eta)\, d\eta = \frac{1}{\pi}\int_a^\infty \frac{2yh'(\eta)}{y^2-\eta^2} d\eta - f(y) , \qquad 0 < y < a$$

$$= F(y) , \qquad \text{(A11)}$$

a singular integral equation which can be solved for $\frac{\partial \psi}{\partial n}(0,\eta)$, bounded at (0,0) and (0,a) by introducing an appropriate Carleman function and using the Plemelj formulae to derive an equivalent Riemann-Hilbert problem. The solution to this can be determined from Muskhelishvili (1963), the details involved being similar to Porter (1972). This then gives

$$\frac{\partial \psi}{\partial y}(0,y) = \frac{2}{\pi}\sqrt{y^2-a^2}\left\{\int_a^\infty \frac{i\eta h'(\eta)}{\sqrt{\eta^2-a^2}(y^2-\eta^2)} d\eta - \int_0^a \frac{\eta f(\eta)}{\sqrt{\eta^2-a^2}(y^2-\eta^2)} d\eta\right\}, \quad 0 < y < a \qquad \text{(A12)}$$

provided that

$$\int_a^\infty \frac{\eta h'(\eta)}{\sqrt{\eta^2-a^2}} d\eta + \int_0^a \frac{\eta f(\eta)}{\sqrt{a^2-\eta^2}} d\eta = 0 . \qquad \text{(A13)}$$

Solving (A13) using Gradshteyn and Ryzhik (1980) gives

$$C = \frac{\omega\theta\pi a}{K[\pi I_1(Ka)+iK_1(Ka)]}\left[\frac{1}{2} - \frac{(1-Ka)}{Ka}[I_1(Ka)+L_1(Ka)]\right] . \qquad (A14)$$

Having obtained a unique expression for $\frac{\partial\psi}{\partial y}(0,y)$ on the barrier it is possible to proceed to calculate the desired coefficients by considering the first-order moment acting on the barrier about its hinged point. Making use of the axi-symmetric motion of roll it follows from (2.37) and (A1) that

$$2\rho i\omega \int_0^a \phi(0,y)(a-y)dy = \theta[a_{33}\omega^2 + i\omega b_{33}] \qquad (A15)$$

where a_{33}, b_{33} are the required added inertia and damping coefficients respectively. The integral in this equation can be evaluated by substituting the expression

$$\int_0^a \psi(0,y)(a-y)dy = -\frac{a^2 Ce^{-Ka}}{4K} + \int_0^a \left(\frac{y^2}{2} - ay\right)\frac{\partial\psi}{\partial y}(0,y)\,dy , \qquad (A16)$$

obtained by integrating by parts and using $\psi(0,a) = \frac{-Te^{-Ka}}{2K}$, into (A5). Then with (A6) this becomes

$$\int_0^a \phi(0,y)(a-y)dy = \int_0^a \frac{\partial\psi}{\partial y}(0,y)\left\{a-y(1-Ka)-\frac{Ky^2}{2}\right\}dy + Ce^{-Ka}\left[\frac{a^2}{4} - \frac{1}{K^2}\right] + C\left[\frac{1}{K^2} - \frac{a}{K}\right] . \qquad (A17)$$

Inserting (A12), (A9) and (A10) into the first term on the right-hand side of this equation results in a repeated integral, the order of which can be reversed. Evaluating these integrals, using (A14), and making use of the identities (Abramowitz and Stegun, 1970)

$$I_o(\mu)K_1(\mu) + K_o(\mu)I_1(\mu) = \frac{1}{\mu} ,$$

$$\frac{\pi^2 I_o(\mu)I_1(\mu) - K_o(\mu)K_1(\mu)}{\pi^2 I_1^2(\mu) + K_1^2(\mu)} = \frac{I_o(\mu)}{I_1(\mu)} - \frac{K_1(\mu)}{\mu I_1(\mu)[\pi^2 I_1^2(\mu) + K_1^2(\mu)]} ,$$

an explicit solution for the right-hand side of (A17) is obtained.

Substituting this in (A15) gives, on equating the real and imaginary parts, the expressions

$$a_{33} = \frac{\rho\pi a^4}{(Ka)^4 I_1}\left\{\frac{K_1}{I_1(\pi^2 I_1^2+K_1^2)}\left[\frac{Ka}{2} - (1-Ka)(I_1+L_1)\right]^2 - \frac{(Ka)^3}{4} I_o\right.$$

$$+ Ka(1-Ka)\left[(1-Ka)L_1-Ka\right]\left[I_1L_o-I_oL_1\right] - \frac{2}{\pi} I_1(1-Ka)\int_0^{Ka} xL_1(x)dx$$

$$\left. + (Ka)^2 I_1\left[\frac{1}{2} + \frac{2Ka}{3\pi}(1-Ka) + \frac{(Ka)^2}{16}\right]\right\}$$

and

$$b_{33} = \frac{\pi^2\rho\omega a^4}{(Ka)^2(\pi^2 I_1^2+K_1^2)}\left[\frac{1}{2} - \frac{(1-Ka)}{Ka}(I_1+L_1)\right],$$

where the modified Bessel functions and Struve functions are of argument Ka. These coefficients are in agreement with those given by Mei (1976). On non-dimensionalizing the force coefficient $\Lambda(\omega)$ is obtained.

Now I_o, I_1, L_o, L_1 can be represented by the convergent power series

$$I_\nu(z) = \sum_{k=o}^{\infty} \frac{1}{k!\Gamma(\nu+k+1)}\left(\frac{z}{2}\right)^{\nu+2k} \tag{A18}$$

$$L_\nu(z) = \sum_{k=o}^{\infty} \frac{1}{\Gamma(\nu+k+3/2)\Gamma(k+3/2)}\left(\frac{z}{2}\right)^{\nu+2k+1} \tag{A19}$$

and

$$K_1(z) = I_1(z)\left[\ell n\ \frac{z}{2} + \gamma\right] + \frac{1}{2}\sum_{k=o}^{\infty}\frac{(z/2)^{1+2k}}{k!(k+1)!}\left[\sum_{m=1}^{k+1} m^{-1} + \sum_{m=1}^{k} m^{-1}\right] + \frac{1}{z} \tag{A20}$$

where γ is Euler's constant. Thus $\Lambda(\omega)$ can be represented by

$$\Lambda(\omega) = \frac{C_1(Ka)}{C_3(Ka)(\ell nKa - i\pi)+C_4(Ka)} + C_2(Ka)$$

$$= \frac{C_1^*(Ka)(\ell nKa - i\pi)+C_2^*(Ka)}{C_3^*(Ka)(\ell nKa - i\pi)+C_4^*(Ka)}$$

where the C_i's are convergent power series in Ka with real coefficients.

When $\omega < 0$ then $\ell nKa - i\pi$ must be replaced by $\ell nKa + i\pi$. Since $Ka = u^2$ and ℓnz is defined for $-\pi < \arg z \leq \pi$, it follows that the definition of $\Lambda(u)$ can be extended to the whole complex u-plane cut along the negative imaginary u-axis. Thus $\Lambda(u)$ has a logarithmic branch point at $u = 0$.

To conclude, using the above expansions (A18)-(A20),

$$\Lambda(u) = 8\left(\frac{1}{4} - \frac{2}{3\pi}\right) + \frac{4}{\pi^2} - 4u^4\left(\frac{1}{2} - \frac{2}{3\pi}\right)^2\left(\ell n\,\frac{u^2}{2} - i\pi\right) + c_1(u^2) + c_2\left(u^4\left(\ell n\frac{u^2}{2} - i\pi\right)\right) \qquad \text{(A21)}$$

for small u where

$$c_1 = \sum_{i=0}^{\infty} c_{1i}\, u^{2(i+1)} \quad , \qquad c_2 = \sum_{i=0}^{\infty} c_{2i}\, u^{2(i+2)} \quad (2\ell nu - i\pi) \ ,$$

are convergent power series with real coefficients.

APPENDIX B

The force coefficient $\Lambda(u)$ near $u = 0$ for a submerged, surging, circular cylinder

The analytic form of $\Lambda(u)$ for small u is needed in Chapter 6, equation (6.10). This is derived by following closely the method of infinite processes used by Ursell (unpublished work, and 1964).

In a manner similar to that of Chapter 3, it can be shown that when $M = 0$, the velocity potential $\phi_1(x,y;\omega)$ for a surging submerged circular cylinder can be expanded in the form

$$\frac{1}{a^2}\phi_1 = D(Ka)\phi_{11} + \sum_{n=1}^{\infty} \frac{\alpha_n(Ka)}{n} a^n \phi_{1n}^F \tag{B1}$$

where D, α_n are power series in Ka, ϕ_{11} is the first multipole expansion and ϕ_{1n}^F are the wave-free potentials. These potentials are given by

$$\phi_{11} = \frac{\sin\theta}{r} + \int_0^{\infty} \frac{k+K}{k-K} e^{-k(y+h)} \sin kx\,dk + 2\pi i K e^{-K(y+h)} \sin Kx \tag{B2}$$

$$= \frac{\sin\theta}{r} + \sum_{m=0}^{\infty} B_{m1} r^m \sin m\theta \tag{B3}$$

where

$$B_{m1} = \frac{(-1)^m}{m!} K^{m+1} \left\{ - \frac{m!}{(2Kh)^{m+1}} + 2\left[e^{-2Kh} Ei(2Kh) - \sum_{k=0}^{m+n-2} \frac{k!}{(2Kh)^{k+1}} \right] - 2\pi i e^{-2Kh} \right\} \tag{B4}$$

and

$$\phi_{1n}^F = I_s + K\frac{\sin n\theta}{r^n} + n\frac{\sin(n+1)\theta}{r^{n+1}} + Mn(n+1)(n+2)\frac{\sin(n+3)\theta}{r^{n+3}} \tag{B5}$$

where

$$I_s = \frac{(-1)^n}{(n-1)!} \int_0^{\infty} k^{n-1} [K+k] e^{-k(y+h)} \sin kx\,dk \tag{B6}$$

$$= \mathrm{Re}\left[\frac{(-1)^n}{(2h+re^{-i\theta})^n} \left\{ K + \frac{n}{2h+re^{-i\theta}} \right\} \right] . \tag{B7}$$

Let

$$\Theta = -i\omega\theta_o(\omega) - \Theta_o(0)$$

and define angular brackets $\langle\ \rangle$ to indicate that r is to be put equal to a.

Then the normal velocity condition on the cylinder (6.5)

$$\left\langle \frac{\partial \phi_1}{\partial r} \right\rangle = \Theta \sin\theta \qquad \text{(B8)}$$

is also satisfied if

$$a^2 D\left\langle \frac{\partial \phi_{11}}{\partial r} \right\rangle + \sum_{n=1}^{\infty} \frac{\alpha_n}{n} a^{n+1} \left\{ \left\langle \frac{\partial I_s}{\partial r} \right\rangle - Kn \frac{\sin n\theta}{a^{n+1}} - n(n+1) \frac{\sin(n+1)\theta}{a^{n+2}} \right\} = \Theta \sin\theta \ . \qquad \text{(B9)}$$

Integrating (B9) over $0 < \theta < \pi$ gives

$$2\Theta = Da^2 \int_o^{\pi} \left\langle \frac{\partial \phi_1}{\partial r}\ (r,\theta') \right\rangle d\theta' + \sum_{n=1}^{\infty} \alpha_n \left\{ \frac{a^{n+2}}{n} \int_o^{\pi} \left\langle \frac{\partial I_s}{\partial r}\ (r,\theta') \right\rangle d\theta' - Ka\left(\frac{1-\cos n\pi}{n}\right) \right.$$

$$\left. - [1-\cos(n+1)\pi] \right\} , \qquad \text{(B10)}$$

which with (B9) enables Θ to be eliminated, and yields

$$Da^2 \left[2\left\langle \frac{\partial \phi_{11}}{\partial r} \right\rangle - \sin\theta \int_o^{\pi} \left\langle \frac{\partial \phi_{11}}{\partial r} \right\rangle d\theta' \right] = \sum_{n=1}^{\infty} \alpha_n \left\{ \frac{a^{n+2}}{n} \left[\sin\theta \int_o^{\pi} \left\langle \frac{\partial I_s}{\partial r} \right\rangle d\theta' - 2\left\langle \frac{\partial I_s}{\partial r} \right\rangle \right] \right.$$

$$- Ka\sin\theta\left(\frac{1-\cos n\pi}{n}\right) + 2Ka\sin n\theta$$

$$\left. - \sin\theta[1-\cos(n+1)\pi] + 2(n+1)\sin(n+1)\theta \right\} . \qquad \text{(B11)}$$

The function on the right-hand side of this equation involves Ka as a linear factor only, whilst the left-hand side includes terms like $(Ka)^m$ and $(Ka)^m(\ell nKa - i\pi)$. This is readily seen from (B4) and the expansion of Ei given by equation (3.40). In particular,

$$\left\langle a^2 \frac{\partial \phi_{11}}{\partial r} \right\rangle = - \sin\theta + \sum_{m=o}^{\infty} (Ka)^{m+1} \frac{(-1)^m}{(m-1)!} \left\{ - \frac{m!}{(2Kh)^{m+1}} + 2e^{-2Kh}[\ell n(Ka) - i\pi] \right.$$

$$\left. + 2e^{-2Kh} \left[\ell n\left(\frac{2h}{a}\right) + \gamma + \sum_{n=1}^{\infty} \frac{(2Kh)^n}{n.n!} - \sum_{k=o}^{m+n-2} \frac{k!}{(2Kh)^{k+1}} \right] \right\} . \qquad \text{(B12)}$$

Therefore, by applying the integral operators

$$\int_o^\pi \sin n\theta \ldots d\theta , \qquad n = 1,2,\ldots.$$

to (B11), an infinite system of equations is obtained for the infinite number of unknowns α_n. It follows from the above analytic forms that

$$\frac{\alpha_n(Ka)}{D(Ka)} = (\ell n\ Ka - i\pi)\alpha_n^*(Ka) + \alpha_n^{**}(Ka) \tag{B13}$$

where α_n^*, α_n^{**} are power series in Ka with real coefficients. Substitution in (B11) gives

$$\frac{1}{a^2}\int_{-\pi}^{\pi} \langle \phi \rangle \sin\theta d\theta = D(Ka)\left\{(\ell nKa - i\pi)Y_o^*(Ka) + Y_o^{**}(Ka)\right\} \tag{B14}$$

and in (B10) gives

$$\Theta = D(Ka)\left\{(\ell nKa - i\pi)Z_o^*(Ka) + Z_o^{**}(Ka)\right\} \tag{B15}$$

where Y_o^*, Y_o^{**}, Z_o^*, and Z_o^{**} are real power series in Ka. Hence it follows from (B7) that for $\omega > 0$,

$$\Lambda = \frac{\int_{-\pi}^{\pi} \langle \phi \rangle \sin\theta\ d\theta}{-\pi a\Theta}$$

$$= \frac{(\ell nKa - i\pi)A_1^*(Ka) + A_1^{**}(Ka)}{(\ell nKa - i\pi)A_2^*(Ka) + A_2^{**}(Ka)} . \tag{B16}$$

When $\omega < 0$, then $\ell nKa - i\pi$ must be replaced by $\ell nKa + i\pi$, and since $Ka = u^2 = \frac{\omega^2 a}{g}$, it follows that near $u = 0$, the function Λ is single-valued in the u-plane cut along the negative imaginary u-axis.

More specifically, we require the leading terms of this expression for small Ka. Using (B12) in (B11) and applying the above integral operators yields

$$\frac{\alpha_n}{D} = \frac{n a^{n+1} B_{n1} \pi\delta_{nm} - \sum_{m=o}^{\infty} \frac{\pi}{2} a^{m+1} B_{m1}[1-\cos(m\pi)]\delta_{n1}}{\frac{\pi}{2}\delta_{n1}\left[\frac{a^{n+2}}{n}\int_o^\pi \left\langle \frac{\partial I_s}{\partial r}\right\rangle d\theta' - \{1-\cos(n+1)\pi\}\right] - \frac{2}{n} a^{n+2}\int_o^\pi \left\langle \frac{\partial I_s}{\partial r}\right\rangle \sin\theta' d\theta'} + O(Ka).$$

(B17)

Similarly, from (B14), (B15) and (B16) for small Ka,

$$\Lambda = \frac{a\pi + a^3\pi B_{11} + \sum_{n=1}^{\infty} \frac{\alpha_n}{D} \frac{a^{n+2}}{n} \int_{-\pi}^{\pi} \langle I_s \rangle \sin\theta' d\theta'}{-\pi a\left[-1 + \sum_{m=o}^{\infty} a^{m+1} B_{m1}\left\{\frac{1-\cos(m\pi)}{2}\right\} + \sum_{n=1}^{\infty} \frac{\alpha_n}{2D}\left\{\frac{a^{n+2}}{n}\int_{o}^{\pi}\left\langle\frac{\partial I_s}{\partial r}\right\rangle d\theta' - [1-\cos(n+1)\pi]\right\}\right]} + O(Ka) \quad . \tag{B18}$$

Now for small Ka,

$$a^{m+1} B_{m1} = B_1^*(Ka) + B_1^{**}(Ka)(Ka)^{m+1}[\ell nKa - i\pi]$$

and hence

$$\frac{\alpha_n}{D} = Y_1^*(Ka) + Y_1^{**}(Ka)(Ka)^{n+1}[\ell n(Ka) - i\pi]$$

where B_1^*, B_1^{**}, Y_1^* and Y_1^{**} are real power series in Ka. Therefore from (B18)

$$\Lambda = Z_1^*(Ka) + Z_1^{**}(Ka)(Ka)^2[\ell n(Ka) - i\pi] \tag{B19}$$

where Z_1^*, Z_1^{**} are power series such that

$$Z_1^{**}(Ka) = \sum_{m=o}^{\infty} z_{1m}^{**} (Ka)^m \quad [\ell n(Ka) - i\pi]$$

and $z_{1m}^{**} \neq 0$.

REFERENCES

Abramowitz, M. & Stegun, I.A. 1970 Handbook of Mathematical Functions. New York: Dover Publications (9th edition).

Ambli, N., Bϕnke, K., Malmo, O. & Reitan, A. 1982 The Kvaerner multiresonant oscillating water column. Proc. 2nd International Symposium on Wave Energy Utilization, Trondheim.

Bach, H. 1969 Complex root finding. Collected algorithms from C.A.C.M., algorithm 365.

Bailey, D.J., Griffiths, D.J. & Maskell, S.J. 1976 On the experimental observation of a heaving sphere. Schiffstechnik Bd., 23, pp 31-45.

Black, J.L., Mei, C.C. & Bray, M.C.G. 1971 Radiation and scattering of water waves by rigid bodies. J. Fluid Mech., 46, pp 151-164.

Carslaw, H.S. & Jaegar, J.C. 1947 Operational Methods in Applied Mathematics. Oxford University Press (2nd edition).

Count, B.M., Fry, R., Haskell, J. & Jackson, N. 1981 The M.E.L. oscillating water column. C.E.G.B. Rep. no. RD/M/1157N81.

Davis, A.M.J. 1974 Short surface waves in the presence of a submerged circular cylinder. SIAM J. Appl. Math., 27, pp 464-491.

Dean, W.R. 1945 On the reflection of surface waves by a flat plate floating vertically. Proc. Camb. Phil. Soc., 41, pp 231-238.

Dean, W.R. 1948 On the reflection of surface waves by a submerged circular cylinder. Proc. Camb. Phil. Soc., 44, pp 483-491.

Erdélyi, A. 1956 Asymptotic Expansions. New York: Dover.

Evans, D.V. 1968a The influence of surface tension on the reflection of water waves by a plane vertical barrier. Proc. Camb. Phil. Soc., 64, pp 795-810.

Evans, D.V. 1968b The effect of surface tension on the waves produced by a heaving circular cylinder. Proc. Camb. Phil. Soc., 64, pp 833-847.

Evans, D.V. 1970 Diffraction of water waves by a submerged vertical plate. J. Fluid Mech., 40, pp 433-451.

Evans, D.V. 1975 A note on the total reflection or transmission of surface waves in the presence of parallel obstacles. J. Fluid Mech., 67, pp 465-472.

Evans, D.V. 1976 A note on the waves produced by the small oscillations of a partially immersed vertical plate. J. Inst. Math. Applic., 17, pp 135-140.

Evans, D.V. 1977 Water-wave transmission through barriers with small gaps. J. Engineering Maths., 11, pp 1-10.

Evans, D.V. 1978 The oscillating water column wave-energy device. J. Inst. Math. Applic., 22, pp 423-433.

Evans, D.V. 1981 Power from water waves. Ann. Rev. Fluid Mech., 13, pp 157-187.

Evans, D.V. 1982a Wave-power absorption by systems of oscillating surface pressure distributions. J. Fluid Mech., 114, pp 481-499.

Evans, D.V. 1982b Wave-power absorption within a resonant harbour. Proc. 2nd International Symposium on Wave Energy Utilization, Trondheim, pp 371-378.

Evans, D.V., Jeffrey, D.C., Salter, S.H. & Taylor, J.R.M. 1979 Submerged cylinder wave energy device: theory and experiment. Appl. Ocean Research, 1, pp 3-12.

Garrett, C.J.R. 1970 Bottomless harbours. J. Fluid Mech., 43, pp 433-449.

Garrett, C.J.R. 1971 Wave forces on a circular dock. J. Fluid Mech., 46, pp 129-139.

Gill, P.E. & Miller, G.F. 1972 An algorithm for the integration of unequally spaced data. Comp. Journal, 15, pp 80-83.

Gradshteyn, I.S. & Ryzhik, I.M. 1980 Tables of Integrals, Series and Products. Academic Press (4th edition).

Guiney, D.C., Noye, B.J. & Tuck, E.O. 1972 Transmission of water waves through small apertures. J. Fluid Mech., 55, pp 149-161.

Haskind, M.D. 1948 The pressure of waves on a barrier. Inzhenernyi Sbornik, 4, pp 147-160.

Haskind, M.D. 1959 The radiation and diffraction of surface waves from a vertically floating plate. Appl. Math. Mech., 23, pp 770-783.

Havelock, T.H. 1929 Forced surface waves on water. Phil. Mag., 8, pp 569-576.

Havelock, T.H. 1942 The damping of the heaving and pitching motion of a ship. Phil. Mag.(7), 33, pp 666-673.

Kotik, J. 1963 Damping and inertia coefficients for a rolling or swaying vertical strip. J. Ship Research, 7, pp 19-23.

Kotik, J. & Lurye, J.R. 1964 Some topics in the theory of coupled ship motions. Fifth Naval Hydrodynamics Symposium, Bergen, pp 407-424.

Kotik, J. & Lurye, J.R. 1967 Heave oscillations of a floating cylinder or sphere. Paper presented to S.N.A.M.E. H-5 Panel, 19th Jan. See also Schiffstechnik, 15, pp 37-38.

Kotik, J. & Mangulis, V. 1962 On the Kramers-Kronig relations for ship motions. International Shipbuilding Progress, 9, pp 3-10.

Lamb, H. 1932 Hydrodynamics. Cambridge University Press (6th edition).

Levine, H. & Rodemich, E. 1958 Scattering of surface waves on an ideal fluid. Stanford University Technical Report No. 78.

Lewin, M. 1963 The effect of vertical barriers on progressing waves. J. Maths. Phys., 42, pp 287-300.

Lighthill, M.J. 1979 Waves In Fluids. Cambridge University Press.

Longuet-Higgins, M.S. 1977 The mean forces exerted by waves on floating or submerged bodies with applications to sand-bars and wave-power devices. Proc. Roy. Soc. Lond., A 352, pp 463-480.

Maskell, S.J. & Ursell, F. 1970 The transient motion of a floating body. J. Fluid Mech., 44, pp 303-313.

Mei, C.C. 1966 Radiation and scattering of transient gravity waves by vertical plates. Quart. J. Mech. Appl. Math., 19, pp 417-440.

Mei, C.C. 1976 Power extraction from water waves. J. Ship Research, 20, pp 63-66.

Mei, C.C. & Black, J.L. 1969 Scattering of surface waves by rectangular obstacles in waters of finite depth. J. Fluid Mech., 38, pp 499-511.

Miles, J.W. & Gilbert, F. 1968 Scattering of gravity waves by a circular dock. J. Fluid Mech., 34, pp 783-793.

Morris, C.A.N. 1970 Diffraction of water waves by vertical barriers. M.Sc. Thesis, Bristol University.

Muskhelishvili, N.I. 1963 Singular Integral Equations. Groningen, Holland: Noordhoff.

Newman, J.N. 1974 Interaction of water waves with two closely spaced vertical obstacles. J. Fluid Mech., 66, pp 97-106.

Newman, J.N. 1977a The motions of a floating slender torus. J. Fluid Mech., 83, pp 721-735.

Newman, J.N. 1977b Marine Hydrodynamics. M.I.T. Press.

Ogilvie, T.F. 1960 Propagation of waves over an obstacle in water of finite depth. University of California, Institute of Eng. Research, Report Series No.82, Issue No.14 (Ph.D. thesis).

Ogilvie, T.F. 1963 First- and second-order forces on a cylinder submerged under the free surface. J. Fluid Mech., 16, pp 451-472.

Ogilvie, T.F. 1964 Recent progress towards the understanding and prediction of ship motions. Fifth O.N.R. Symposium on Naval Hydrodynamics, pp 3-80.

Oliver, J. 1972 A doubly-adaptive Clenshaw-Curtis quadrature method. Comput. J., 15, pp 141-147.

Packham, B.A. & Williams, W.E. 1972 A note on the transmission of water waves through small apertures. J. Inst. Math. Applic., 10, pp 176-184.

Porter, D. 1972 The transmission of surface waves through a gap in a vertical barrier. Proc. Camb. Phil. Soc., 71, pp 411-421.

Porter, D. 1974 The radiation and scattering of surface waves by vertical barriers. J. Fluid Mech., 63, pp 625-634.

Porter, W.R. 1965 Damping and inertia coefficients for a rolling or swaying vertical strip. J. Ship Research, 9, pp 11-12.

Quarrell, P. 1978 Proc. Wave Energy Conf. London-Heathrow. H.M.S.O.

Rabinowitz, P. 1970 Numerical Methods for Non-Linear Algebraic Equations. London: Gordon and Breach.

Rhodes-Robinson, P.F. 1970 Fundamental singularities in the theory of water waves with surface tension. Bull. Austral. Math. Soc., 2, pp 317-333.

Rhodes-Robinson, P.F. 1971 On the forced surface waves due to a vertical wave-maker in the presence of surface tension. Proc. Camb. Phil. Soc., 70, pp 323-337.

Rhodes-Robinson, P.F. 1974 On forced three-dimensional surface waves in a channel in the presence of surface tension. Proc. Camb. Phil. Soc., 75, pp 405-426.

Rhodes-Robinson, P.F. 1979 On surface waves in the presence of immersed vertical boundaries I. Quart. J. Mech. Appl. Math., 32, pp 109-124.

Rhodes-Robinson, P.F. The effect of surface tension on the reflection of surface waves by a vertical wall. Dept. of Mathematics, Victoria University of Wellington, New Zealand, Internal Report.

Smith, C.M. 1982 The transient motion of a partially immersed rolling strip in water. I.M.A. J. Appl. Math., 29, pp 59-77.

Sretenskii, L.N. 1937 On damping of the vertical oscillations of the centre of gravity of floating bodies (in Russian). Trudy Tsentral Aero-Gidrodinam Inst. no. 330.

Srokosz, M.A. 1979 The submerged sphere as an absorber of wave power. J. Fluid Mech., 95, pp 717-741.

Srokosz, M.A. & Evans, D.V. 1979 A theory for wave-power absorption by two independently oscillating bodies. J. Fluid Mech., 90, pp 337-362.

Stahl, A.W. 1892 The utilization of the power of ocean waves. Trans. A.S.M.E., 13, pp 438-506.

Stiassnie, M. & Dagan, G. 1973 Wave forces on a submerged vertical plate. J. Eng. Maths., 7, pp 235-247.

Thomas, J.R. 1981a The absorption of wave energy by a three-dimensional submerged duct. J. Fluid Mech., 104, pp 189-215.

Thomas, J.R. 1981b Hydrodynamics of certain wave-energy absorbers. Ph.D. thesis, University of Bristol.

Thorne, R.C. 1953 Multipole expansions in the theory of surface waves. Proc. Camb. Phil. Soc., 49, pp 707-716.

Tuck, E.O. 1971 Transmission of water waves through small apertures. J. Fluid Mech., 49, pp 65-74.

Tuck, E.O. 1975 Matching problems involving flow through small holes. Adv. App. Mech., 15, pp 89-158.

Ursell, F. 1947 The effect of a fixed vertical barrier on surface waves in deep water. Proc. Camb. Phil. Soc., 43, pp 374-382.

Ursell, F. 1948 On the waves due to the rolling of a ship. Quart. J. Mech. Appl. Math., 1, pp 246-252.

Ursell, F. 1950a,b Surface waves on deep water in the presence of a submerged circular cylinder I, II. Proc. Camb. Phil. Soc., 46, pp 141-152, 153-158.

Ursell, F. 1964 The decay of the free motion of a floating body. J. Fluid Mech., 19, pp 305-319.

Ursell, F. (unpublished work) The periodic heaving motion of a half-immersed sphere: The analytic form of the velocity potential. Long-wave asymptotics of the virtual-mass coefficient.

Warren, F.W.G. 1968 Gravity wave damping of hydrostatic oscillations for a buoyant disk. J. Fluid Mech., 31, pp 309-319.

Watson, G.N. 1940 Theory of Bessel Functions. Cambridge University Press (2nd edition).

Wehausen, J.V. 1971 The motion of floating bodies. Ann. Rev. Fluid Mech., 3, pp 237-268.

Wehausen, J.V. & Laitone, E.V. 1960 Surface waves. Handbuch der Physik, IX, pt. III, pp 446-814. Berlin: Springer.

Whitham, G.B. 1974 Linear and Non-Linear Waves. Wiley-Interscience.